GROUNDWATER DROUGHT PROPAGATION AND DISTRIBUTION IN TEMPERATE AND SEMI-ARID CLIMATES

Buruk Kitachew WOSSENYELEH

Promoter:
Prof. Dr. ir. M. Huysmans
Prof. Dr. B.Verbeiren

Members of the Examination Committee:

Prof. Dr. Ph. Muchez
Prof. Dr. ir. J. Diels
Prof. Dr. G.J. Weltje
Prof. Dr. A.F.van Loon (VU Amsterdam,NL)
Prof. Dr. ir. P.Goderniaux (UMONS, BE)

Dissertation presented in partial fulfilment of the requirements for the degree of Doctor of Science

August 2021

© 2021 Buruk Kitachew Wossenyeleh
Uitgegeven in eigen beheer, Buruk Kitachew Wossenyeleh, Leuven

Alle rechten voorbehouden. Niets uit deze uitgave mag worden vermenigvuldigd en/of openbaar gemaakt worden door middel van druk, fotokopie, microfilm, elektronisch of op welke andere wijze ook zonder voorafgaandelijke schriftelijke toestemming van de uitgever.

All rights reserved. No part of the publication may be reproduced in any form by print, photoprint, microfilm, electronic or any other means without written permission from the publisher.

Acknowledgments

All praise and glory to God, who gave me the courage and patience to carry out this work. Without Him, I can do nothing.

Undertaking this PhD research has been a truly life-changing experience for me, and it would not have been possible to do without the support and guidance that I received from many wonderful people that contributed directly or indirectly to this work.

This PhD research was financed by Interfaculty Council for Development Co-operation (IRO) within the framework of the contributions to development co-operation of KULeuven University. I acknowledge this generous financial support.

First of all, I would like to express my sincere and deep gratitude to my promotor, Prof. Dr. Ir. Marijke Huysmans for the continuous support of my PhD study and related research, for her patience, motivation, and immense knowledge. Her guidance helped me in all the time of research and writing of this thesis. I am thankful for her confidence in me, the freedom I got to think independently, and for allowing me to participate in the conference, seminar, and teaching. I could not have imagined having a better advisor and mentor for my PhD study. Thanks a lot, Prof. Marijke, for being most helpful and for all guidance during my research.

Many thanks also goes to my co-promotor, Prof. Dr. Boud Verbeiren, for his continued guidance and technical support, shared research ideas, and data arrangement. I enjoyed our long meetings, and I learned a lot from them. Thank you, Prof. Boud, for your guidance, time, and comprehensive feedback on our research papers.

I would also like to thank all the jury members: Prof. Dr. Philippe Muchez, Prof. Dr. Ir. Jan Diels, Prof. Dr. Gert Jan Weltje, Prof. Dr. Anne F.van Loon and Prof. Dr. Ir. Pascal Goderniaux for their time, for reviewing my PhD manuscript, and for their interesting and constructive comments. I also gratefully recognize the help of Prof. Dr. Ir. Jan Diels for his idea and guidance during the model development of the groundwater recharge delay estimation in the vadose zone.

I am also indebted to all the people I have met along the way and have contributed to the development of the research idea and data arrangement. In particular, I would like to show my gratitude to Dr. Gert Ghysels, Dr. Ir. Mustafa Syed Md, Bram Pardis, and Ayalew Shura for their support during python coding, groundwater modeling, and data collection.

I am fortunate to have been a part of the Geology Division of KULeuven. Thank you for the fun and the talks I had during my research stay. Special thanks to Alex, Anne, Bram, Dominique, Reiko, Rik, Robin, and Sofie for sharing their ideas and the fun I had in the office, during PhD midweek, ping-pong games. I also extend my special thanks to my colleagues Gert, Cas, Annable, Inne, Sebastian, and Kaoutar from the Department of Hydrology and Hydraulics engineering (HYDR) at VUB for your time and support during my stay at HYDR and the international conference.

I really appreciate and thank Ethiopian friends and community in Leuven, Friday soccer teammates, and Friday De Spuye fun group members, as they have furnished a good environment in Leuven to feel at home and shared many insights with me. Prof. Dr. Mulugeta and Wase also deserve enormous acknowledgments for being by our side during happiness and sad moments. Thank you all.

My sincere thanks goes to Bereketab Wondesen (Beki), who, as a good friend, was always willing to help and give his best support during difficult periods. Many thanks to my best friends Beki, Dr. Kelem, Gecho, Eyoba, Nebrshi, Eskie S., Tesfeshi, and Wase for all the chats and beautiful moments I shared during my study.

Finally, I would like to thank my beloved parents (አባቴ ና እናቴ), my sisters (Z-sis, Hili), my brother (Jose), those closest to me, whose presence and love helped to make the completion of my study possible. Yet importantly, I express my thanks to my parents-in-law (ገላኔ ና ወላንስ), sisters-in-law (Helu and Sife), and brothers-in-law (Wudie, Heny, Dawit, Addis, and Mehari) for their love, prayers, and caring. Last but not least, I would also like to thank my beautiful wife and my bestie, Mehret Gelan (Mercy), who has made this arduous journey much more pleasant. Mercy (my bestie), thank you for always unconditionally sticking by my side; you have shown me pure, deep, and relentless love and support in every step. You are a phenomenal best friend and a gorgeous lover, all in one!

Abstract

Droughts are mainly caused by a reduction in precipitation and affect both surface and groundwater resources. This drought propagates through the hydrological cycle. Meteorological drought propagates to surface water and the unsaturated soil zone then to groundwater. When drought occurs in groundwater, it is called groundwater drought. Groundwater drought can be defined as a temporary decrease in groundwater availability over a significant period of time. It can be identified when the water table in an aquifer falls below a critical level over a certain period resulting in several adverse effects.

Water security during meteorological, hydrological (only surface water), and agricultural drought is highly dependent on groundwater availability, access to groundwater, and demand for groundwater. Consequently, studies related to groundwater drought are essential for the sustainable use and management of groundwater. This research aims to develop and apply a method and supporting tools for groundwater drought propagation and distribution in temperate (Dijle catchment and parts of the Demer and Zenne basins , Belgium) and semi-arid (Bilate River Catchment, Ethiopia) climate regions.

In this research, a series of methodologies were developed to assess drought propagation in the hydrological cycle. An unsaturated flow model, a groundwater flow model, and a water balance model are combined in the developed method. Using this methodology, this Ph.D. research (1) developed a model to estimate spatially distributed groundwater recharge delay in the vadose zone and its effect on groundwater drought, (2) assessed drought propagation from meteorological drought to groundwater drought, (3) investigated groundwater drought propagation in the aquifer and its impact on wetlands and rivers, and (4) analyzed the influence of land use/ land cover and climate factors on groundwater recharge and drought.

An essential factor in the propagation of drought from meteorological drought to groundwater drought is the delay between a precipitation event and the groundwater recharge reaching the groundwater table. This research therefore started by analyzing the groundwater recharge delay in the vadose zone. A method for estimating spatially distributed delay in the vadose zone using the kinematic wave approximation of Richards' equation combined with the van Genuchten-Burdine and Brooks-Corey parametric model was developed. The result shows that the vadose zone delay influences groundwater drought characterization features such as the number, duration, and intensity of drought events.

Vulnerable ecosystems such as rivers and wetlands fed by groundwater might be impacted during droughts propagation through the hydrological cycle. In this study, a series of methods were used to investigate meteorological and groundwater drought. A standardized precipitation index (SPI) and a standardized groundwater drought index (SGI) were used to investigate meteorological drought severity and groundwater drought, respectively. In addition, a variable threshold method was also used to investigate and characterize groundwater drought. For groundwater drought analysis, time series of groundwater recharge (R) and groundwater discharge (Q) with a high spatial and temporal resolution were simulated using a water balance model (WetSpass-M) and groundwater flow model (MODFLOW). The results indicate that drought propagates from meteorological drought to groundwater drought, but not all meteorological droughts result in groundwater drought. Moreover, as drought is attenuated in the subsurface, groundwater discharge droughts affecting groundwater flow to rivers and wetlands have a lower frequency and severity than groundwater recharge droughts.

Both meteorological variations and human-induced factors, such as land use/land cover changes, play a role in causing or worsening drought events. In this research, natural meteorological variation and land use/ land cover change impact on groundwater recharge and drought were distinguished using a water balance model. The result indicates that groundwater recharge decreases between 1980 to 2013 because of land use/land cover change and a shift of the meteorological variables from the long-term "normal" conditions.

The methodology developed in this research is applicable in analyzing different drought types in the hydrological cycle and can be used to understand the nature of drought propagation through the hydrological cycle and the aquifers for temperate and semi-arid climate regions.

List of abbreviations and symbols

a.s.l.	Above sea level
BC	Brooks-Corey model
BELSPO	Belgian Federal Science Policy Office
c	Celerity or kinematic wave velocity (mm/month)
C_{riv}	Riverbed conductance (m^2/d)
C_{drn}	Drain conductance (m^2/d)
D	Drought deficit (mm)
DEM	Digital Elevation Model
DOV	“Databank Ondergrond Vlaanderen”
EBK	Empirical Bayesian Kriging
FAO	Food and Agriculture Organization of the United Nations
GroWaDRISK	Drought-related vulnerability and risk assessment of groundwater resources in Belgium
h	Matric potential head (m)
h_b	Bubbling pressure (m)
h_s	Simulated head (m)
HCOV	“Hydrogeologische Codering van de Ondergrond van Vlaanderen”
HK	Horizontal hydraulic conductivity (m/d)
I	Drought intensity (mm)
IDW	Inverse Distance Weighting
K(h)	Unsaturated hydraulic conductivity in the function of the matric potential head (m/d)

$K(\theta)$	Unsaturated hydraulic conductivity in the function of the soil moisture content (m/d)
K_r	Relative hydraulic conductivity (--)
Ks	Saturated hydraulic conductivity (m/d)
L	Drought duration (day)
LULC	Land use/ Land cover
NGI	National Geographic Institute
NSE	Nash-Sutcliffe Efficiency (--)
OK	Ordinary Kriging
OLS	Ordinary Least Squares
PBIAS	Percent of bias (%)
PET	Potential evapotranspiration (mm)
q_f	Filtered base flow from observed river discharge (m/d)
q_s	Simulated base flow from groundwater recharge (m/d)
Q(t)	Groundwater discharge (m^3/d)
r^2	Coefficient of determination (--)
RMSE	Root Mean Square Error (m)
R(t)	Groundwater recharge (mm)
S-N	South-North
Se	Relative soil moisture content or effective saturation (--)
SGI	Standardized Groundwater Index (--)
SPI	Standardized Precipitation Index (--)
S_r	Relative sensitivity (--)
S_y	Specific yield (-)

t_d	Groundwater recharge delay (day)
T_{vz}	Thickness of vadose zone (m)
USDA	United States Department of Agriculture
VGM	van Genuchten-Mualem model
VGB	van Genuchten-Burdine model
VITO	Flemish Institute for Technological Research
VMM	Flemish Environment Agency
WetSpass	Water, Energy, Transfer between Soil, Plant and Atmosphere under quasi Steady State
WetSpass-M	Monthly time step WetSpass Version
WETSPRO	Water engineering time series processing tool
3D	Three dimensional
1D	One dimensional
^oC	Degree Celsius
W-E	West-East
θ	Soil moisture content (mm/mm)
θ_s	Saturation soil moisture content (mm/mm)
θ_r	Residual soil moisture content (mm/mm)
σ^2	Variance (m^2)

Table of contents

Acknowledgments i

Abstract iii

List of abbreviations and symbols v

Table of contents viii

List of figures xiii

List of tables xix

Chapter 1 1

1 Introduction 1

1.1 Groundwater drought 2

1.2 Meteorological and groundwater drought quantification 3

1.3 Groundwater drought propagation 4

1.4 Drought in temperate and semi-arid climatic regions 6

1.5 Research objectives 7

1.6 Dissertation outline 7

1.7 References 9

Chapter 2 13

2 Vadose zone lag time effect on groundwater drought in a temperate climate 13

2.1 Abstract 14

2.2 Introduction 14

2.3 Study site and data 17

2.4 Mathematical model development 21

2.4.1 Kinematic wave approximation theories 21

2.4.2 Parameterization of the kinematic wave model 22

2.5 Methods 25
2.5.1 Modeling approaches 25
2.5.2 Comparison with other methods 26
2.5.3 Delay effect on groundwater drought 27
2.6 Results and discussion 28
2.6.1 Detailed physical parametrization of geological layers 28
2.6.2 Lumped parametrization of geological layers 32
2.6.3 Comparison of groundwater recharge delay to physically based conceptual flow model 35
2.6.4 Delay effect on groundwater drought 36
2.7 Conclusion 39
2.8 References 40
Chapter 3 45
3 Groundwater drought propagation in the hydrological cycle in temperate climate regions 45
3.1 Abstract 46
3.2 Introduction 46
3.3 Methodology 48
3.3.1 Study area and data 48
3.3.2 Methods 52
3.4 Results and discussion 58
3.4.1 Meteorological drought 58
3.4.2 Groundwater modeling 59
3.4.3 Groundwater drought 64
3.4.4 Drought propagation from meteorological drought to groundwater recharge 66
3.4.5 Drought propagation and its impact on groundwater hydrology of wetlands 68

3.5 Conclusions 74
3.6 References 75
Chapter 4 79
4 Differentiating between land use and climate as influencing factors on groundwater recharge drought 79
4.1 Abstract 80
4.2 Introduction 80
4.3 Methodology 82
4.3.1 Groundwater recharge estimation 83
4.3.2 Identifying the influence of land use and climate factors on recharge 86
4.3.3 Model calibration 88
4.4 Results and Discussion 90
4.4.1 Model calibration 90
4.4.2 Groundwater recharge 90
4.4.3 Influence of land use/land cover change on groundwater recharge 92
4.4.4 Influence of climate factor on groundwater recharge 98
4.4.5 Discussion 100
4.5 Conclusion 101
4.6 References 102
Chapter 5 107
5 Drought propagation in the hydrological cycle in a semi-arid region: a case study in the Bilate Catchment (Ethiopia) 107
5.1 Abstract 108
5.2 Introduction 108
5.3 Study area and data 110
5.3.1 Meteorological Data 111

5.3.2 Soil and land use/ land cover 113
5.3.3 Slope 114
5.3.4 Hydrogeology 115
5.4 Methodology 116
5.4.1 Meteorological drought analysis 117
5.4.2 Groundwater drought estimation 117
5.4.3 Groundwater drought analysis and drought propagation 119
5.5 Results and discussion 120
5.5.1 Model calibration 120
5.5.2 Meteorological drought 120
5.5.3 Groundwater recharge 122
5.5.4 Groundwater drought 125
5.5.5 Drought propagation in the hydrological cycle 126
5.6 Conclusion 129
5.7 References 130
6 General conclusions and future perspectives 135
6.1 Introduction 136
6.2 Contribution of the vadose zone on drought propagation 136
6.3 Drought propagation in temperate and semi-arid climatic regions 138
6.4 Land use/ land cover and climate factors as influencing factor on groundwater drought 139
6.5 Limitations 140
6.6 Concluding remarks and future research perspectives 141
6.7 References 142
Appendices 143
Appendix A: Vadose zone groundwater recharge delay 144

Appendix B: Meteorological drought, groundwater recharge and discharge thresholds values for Dijle and parts of the Demer and Zenne basin 152

Appendix C: Steady-state groundwater model calibration result 156

Appendix D: Estimated groundwater recharge of the Static runs 158

Appendix E: Meteorological drought and groundwater recharge threshold value for Bilate river catchment 160

List of publications during the PhD 163

List of figures

Figure 1.1: Characterizing features of drought propagation in hydrological cycle: pooling, lag, attenuation and lengthening (adopted from van Loon, 2013) 5
Figure 2.1: Location of the study area, Digital Elevation Model (DEM) and lithology profile boreholes in Belgium. 17
Figure 2.2: Hydrogeological S-N cross-section through the study area. The location of the cross-section is indicated in Figure 2.1 A-'A'. Descriptions of HCOV codes can be found in Table 2.1. The elevation is measured from a Belgian referencing system for elevation called TAW ("Tweede Algemene Waterpassing") 18
Figure 2.3: Thickness of the vadose zone (m) in the study area, estimated as the difference between 100-m digital elevation model data and averaged water table data. (obtained from GroWaDRISK project) 19
Figure 2.4: Yearly averaged groundwater recharge from 1980 to 2013, estimated using WetSpass (the result of GroWaDRISK project) 20
Figure 2.5: Average soil moisture content for 168 locations found in Dijle and Demer catchment, ordered from low to high soil moisture content. 29
Figure 2.6: van Genuchten-Burdine and Brooks-Corey model soil moisture content and celerity estimation difference using the same groundwater recharge input for 168 sample boreholes. The clustering on the graph corresponds to the type of lithology of the boreholes. 29
Figure 2.7: Celerity of soil moisture in the vadose zone estimated by van Genuchten Burdine (left) and Brooks_Corey model (right) 30
Figure 2.8: Spatially distributed groundwater recharge delay in the vadose zone using the Brooks-Corey parametric model (left) and van Genuchten-Burdine parametric model (right) 31
Figure 2.9: Groundwater recharge delay difference between the delay estimated by the Brooks-Corey model and van Genuchten-Burdine model. 31
Figure 2.10: Groundwater recharge delay relation with the thickness of the vadose zone ... 32
Figure 2.11: Van Genuchten-Burdine and Brooks-Corey model celerity estimation difference using the same groundwater recharge input for eight geological layers found in the vadose zone. The result is ordered layer 1 to layer 8. 33

Figure 2.12: Box plots showing the distribution of groundwater recharge delay in each geological layer of the vadose zone using the Brooks-Corey parametric model. See Table 1 for the description of layers. 34
Figure 2.13: Box plots showing the distribution of groundwater recharge delay in each geological layer of the vadose zone using the van Genuchten-Burdine Parametric model. See Table 1 for the description of layers. 34
Figure 2.14: Comparison of HYDRUS-1D output with groundwater recharge delay estimated using Brooks Corey and van Genuchten-Burdine method for both detailed parametrization and lumped approaches 35
Figure 2.15: Deviation from the threshold value of spatially average monthly groundwater recharge (top) and delayed recharge (bottom) for the whole study area based on 6-month moving average. The red color represents groundwater drought. 36
Figure 2.16: Deviation from the threshold value of monthly groundwater recharge (top) and delayed groundwater recharge(bottom) based on 6-month moving average aggregation. The red color represents a groundwater drought. This drought analysis is for the deep groundwater table area with groundwater depth greater than 48m..... 37
Figure 2.17: Deviation of monthly groundwater recharge (top) and delayed groundwater recharge(bottom) based on 6-month moving average aggregation from the threshold value. The red color represents a groundwater drought. This drought analysis is for shallow groundwater table area with maximum groundwater depth of 5m..... 38
Figure 3.1: Location of the study area, the digital elevation model (DEM) in Belgium 49
Figure 3.2: Hydrogeological S-N (top) and W-E (bottom) cross-sections through the study area. The location of the cross-section is indicated in Figure 3.1 A-A' and B-B', respectively. The elevation is measured from a Belgian referencing system for elevation called TAW ("Tweede Algemene Waterpassing") 50
Figure 3.3: Monthly averaged delayed groundwater recharge from 1980 to 2013 of the study area, estimated using WetSpass (left) and land cover class (right) 51
Figure 3.4: Conceptual framework of the study 52
Figure 3.5: Conceptual model setup, showing boundary conditions and aquifer bottom elevation 54
Figure 3.6: Average monthly delayed groundwater recharge 56

Figure 3.7: Meteorological drought severity for the Uccle station based on (A) SPI-1 value and (B) SPI-12 value between the hydrological year of 1980 and 2011.....58
Figure 3.8: Spatially distributed Meteorological drought severity for Dijle catchment and parts of the Demer and Zenne basin based on (A) SPI-3 (Trimester) value, (B) SPI-6 (Semester) value, and (C) SPI-12 (Annual) value for the hydrological year of 2008-09.....59
Figure 3.9: Spatial groundwater depth distribution after steady-state groundwater model calibration 60
Figure 3.10: Steady state groundwater model water balance 61
Figure 3.11: Spatially distributed hydraulic conductivity before (left) and after (right) calibration 62
Figure 3.12: Observed and simulated groundwater head at observation well DYLP081 between Oct-2002 and Sep-2011.....63
Figure 3.13: Average simulated groundwater head time series and groundwater recharge time series 63
Figure 3.14: Simulated total groundwater discharge and monthly average groundwater recharge.....64
Figure 3.15: Deviation from the threshold value of monthly groundwater recharge. The red color represents the groundwater recharge drought events.....64
Figure 3.16: Deviation from the threshold value of monthly groundwater discharge to rivers. The red color represents groundwater drought events on discharge. 65
Figure 3.17: Comparison of recharge and discharge drought events as percent deviation from the threshold 66
Figure 3.18: Groundwater recharge deviation from the threshold between 1981 to 2011. The red color represents recharge drought events. 66
Figure 3.19: Comparison of meteorological drought severity and groundwater recharge drought (A) Monthly SPI value and (B) Groundwater recharge drought using monthly SGI. 68
Figure 3.20: Doode Bemde nature reserve with delineated wetland 69
Figure 3.21: Deviation from the threshold value of monthly averaged modelled groundwater recharge of Doode Bemde wetland (top) and monthly total modelled groundwater discharge to wetland (bottom). The red color represents groundwater recharge drought events.....70

Figure 3.22: Comparison of groundwater recharge and groundwater discharge drought events using the percent deviation from the threshold for the Doode Bemde wetland 70
Figure 3.23: Groundwater recharge deviation from the threshold between 1981 to 2011. The red color represents recharge drought events. 71
Figure 3.24: Comparison of meteorological drought severity and groundwater recharge drought (A) Monthly SPI value and (B) Groundwater recharge drought using monthly SGI. 72
Figure 3.25: Observed groundwater head distribution collected from 14 observation wells (boxplot with monthly timestep), long-term (2003-2013) average monthly observed groundwater head (dotted-green line), and groundwater recharge deviation from threshold value (dotted-blue line) between 2006 and 2008. These observation wells are mainly found in the delineated wetland area (Figure 3.20). 73
Figure 4.1: Location of the study area, the digital elevation model (DEM) in Belgium 84
Figure 4.2: Integrated land use map of 2013 (obtained from GroWaDRISk project) 85
Figure 4.3: Conceptual figure that demonstrates how LULC effects on recharge are assessed, using two static and one dynamic run. 88
Figure 4.4: Simulated baseflow calculated from dynamic run (run 3) recharge of Sint-Joris-Weert sub-catchment vs. monthly filtered base-flow from flow measurement at Sint-Joris-Weert station. 90
Figure 4.5: Monthly averaged groundwater recharge from 1980 to 2013 of the study area for the four different model runs, estimated using WetSpass-M. 91
Figure 4.6: Estimated groundwater recharge of the dynamic run (run 3) to show the temporal variation. The dark blue line is the median curve (50th percentile) and shows the median groundwater recharge value for each month. The green shadow area represents the interquartile range (IQR). The light green shaded area represents the lowest and highest 5 % of each month's groundwater recharge values. 92
Figure 4.7: Monthly averaged groundwater recharge difference between run 2 and run 1 (left) (run2-run1), and LULC changed places between static land use/cover map of 1990 and 2013 (right). 92
Figure 4.8: Spatially monthly averaged groundwater recharge for the first three runs with their linear regression line. 93

Figure 4.9: Static land use/land cover map of 1990 (left) and 2013 (right) for the places where simulated groundwater recharge has decreased 94
Figure 4.10: Area of each land use/land cover for the places where simulated groundwater recharge has decreased.....94
Figure 4.11: Spatially monthly averaged groundwater recharge for the first three runs with their linear regression line, for the places where simulated groundwater recharge has decreased. 95
Figure 4.12: Static land use/land cover map of 1990 (left) and 2013 (right) for the places where simulated groundwater recharge has increased. 96
Figure 4.13: Area of each land use/land cover for the places where simulated groundwater recharge has increased.....96
Figure 4.14: Spatially monthly averaged groundwater recharge for the first three runs with their linear regression line, for the places where simulated groundwater recharge has increased.....97
Figure 4.15: Deviation from a threshold value of monthly groundwater recharge based on a 6-month moving average aggregation based on the static LULC of 2013 (run 2, red) and the dynamic run (run 3 lime). The shaded areas represent groundwater drought.....97
Figure 4.16: Monthly averaged simulated groundwater recharge difference between dynamic (run 3) and long-term average (run 4) meteorological input.....98
Figure 4.17: Spatially monthly averaged groundwater recharge for dynamic (run 3) and long-term "normal" (run 4) meteorological conditions with their linear regression line.....99
Figure 4.18: Deviation from a threshold value of monthly groundwater recharge based on a 6-month moving average aggregation based on the dynamic run (run 3 lime) and long-term "normal" meteorological conditions (run 4 blue). The shaded areas represent groundwater drought. 99
Figure 4.19: Spatial pattern of estimated monthly averaged groundwater recharge difference at pixel scale for run 2 minus run 1 (left); run 3 minus run 4 (right). 100
Figure 5.1: Location and Digital Elevation Model (DEM) of the study area 111
Figure 5.2: Average monthly total rainfall distribution of Bilate catchment using 11 meteorological stations.....112
Figure 5.3: Spatial average monthly total rainfall distribution of Bilate catchment using 11 meteorological stations.....113

Figure 5.4: Soil texture distribution (left) and land use/land cover classification (right). 114
Figure 5.5: Slope distribution of the Bilate river catchment. 115
Figure 5.6: Conceptual framework of the study 116
Figure 5.7: Simulated baseflow based on WetSpass output groundwater recharge vs. monthly filtered baseflow from flow measurements at the Bilate -Tena gauging station. 120
Figure 5.8: Meteorological drought occurrence and severity based on (A) Monthly SPI value and (B) Annual SPI value for 1980 – 2013. The SPI is calculated using the average rainfall of the 11 stations found in the study area. 121
Figure 5.9: Spatially distributed meteorological drought severity based on (A) SPI-4 (Quarter) value, (B) SPI-6 (Semester) value, and (C) SPI-12 (Annual) value for the hydrological year of 2008-09 122
Figure 5.10: Average monthly groundwater recharge distribution and average monthly total rainfall 123
Figure 5.11: Temporal variation of estimated groundwater recharge. The dark blue line is the 50th percentile curve (median) and shows the median groundwater recharge value for each month. The green shadow area represents the interquartile range (IQR). Moreover, the light green shaded area represents the lowest and highest 10 % of each month's groundwater recharge values. 123
Figure 5.12: Spatial monthly averaged groundwater recharge distribution from 1980 to 2013 in the Bilate river catchment, estimated using WetSpass. 124
Figure 5.13: Monthly groundwater recharge deviation from the threshold value. The red color indicates groundwater recharge drought events. 126
Figure 5.14: Comparison of meteorological drought severity and groundwater recharge drought (A) Monthly SPI value and (B) Groundwater recharge drought using monthly SGI. 127

List of tables

Table 2.1: Geological layers found in the vadose zone of the study area 18
Table 2.2: Prediction error of Empirical Bayesian Kriging 29
Table 3.1: Drought intensity categories based on SPI values (McKee et al., 1993) 53
Table 3.2: Model evaluation statistics for calibration and validation period 62
Table 3.3: Groundwater recharge drought characteristics (onset, number events, duration, and deficit volume) between Oct-1981 and Sep-2011 66
Table 3.4: Onset of SGI groundwater recharge drought between Oct-1981 and Sep-2011 and number of meteorological droughts (SPI-1) ranging from moderate to extreme severity before the onset of groundwater recharge drought with lag time. 67
Table 3.5: Groundwater recharge drought characteristics (onset, number events, duration, and deficit volume) between 1981 and 2010, calculated using variable threshold method. 71
Table 3.5: Onset of SGI groundwater recharge drought between Oct-1981 and Sep-2011 and number of meteorological droughts (SPI-1) ranging from moderate to extreme severity before the onset of groundwater recharge drought with lag time. 72
Table 4.1: Period-specific use of land-use maps, urban masks, and sealed surface proportion maps. 86
Table 4.2: WetSpass model runs with varying inputs, enabling to assess the separate effects of the factor' LULC change' and 'climate variability.' 87
Table 4.3: Calibrated parameter values after calibration.....90
Table 5.1: Drought severity categories based on SPI values (McKee et al., 1993) 117
Table 5.2: Average monthly groundwater recharge based on the land use classes.....124
Table 5.3: Groundwater recharge drought characteristics (onset, number events, duration, and deficit volume) between Jan-1980 and Dec-2013. 125
Table 5.4: Onset of SGI groundwater recharge drought between Jan-1980 and Sep-2013 and number of meteorological droughts (SPI-1) ranging from moderate to extreme severity before the onset of groundwater recharge drought with lag time. 127

Chapter 1

1 Introduction

Groundwater is defined as water, which occurs in the subsurface saturated zone (Kebede, 2013). Since groundwater represents 99% of earth's liquid freshwater, has comparatively good quality and the capacity to buffer short-term climate variability, it is an important source of water supply; over two billion people rely on it as their primary water source (Calow and MacDonald, 2009; Famiglietti, 2014; MacDonald et al., 2009). However, these natural resources are under pressure due to natural climate variations and human-induced factors. Overexploitation and urbanization are the most common human-induced threats to groundwater resources. Moreover, in many regions in the world, climate change also contributes to reducing precipitation and/or increasing evapotranspiration, ultimately reducing groundwater recharge (Panwar and Chakrapani, 2012) . Currently, because of these pressures, many of the world's major groundwater reservoirs are experiencing groundwater depletion (Eltahir and Yeh, 1999). Therefore, in recent years, studying and mitigating groundwater drought has become increasingly important in groundwater resources management. These studies cover different aspects: the effect of groundwater drought on availability of water resources, the role of groundwater-surface water interaction, its connection to storage properties, the regional character of groundwater drought, propagation of drought in groundwater storage, and its relations to climate change (Chang and Teoh, 1995; Eltahir and Yeh, 1999; Panwar and Chakrapani, 2012; Peters, 2003a; White et al., 1999).

1.1 Groundwater drought

Drought can be described as a temporary decrease in water availability over a significant period. It can have severe socio-economic, agricultural, and environmental impacts and threaten environmental resources' sustainability (Bloomfield and Marchant, 2013; Calow et al., 1997; Mishra and Singh, 2010; Wilhite, 2000). Drought is a direct result of deficient precipitation, and as such, it is mainly a meteorological-related hazard. Typically, three definitions of drought are used: meteorological, agricultural, and hydrological drought. The first refers to a period without or with little precipitation; the second refers to a shortage of water in the soil and as such for natural vegetation and crops; the third is describing an impact on hydrological water bodies. It can affect both surface and groundwater resources. In case it concerns groundwater bodies, the term groundwater drought is used. Groundwater drought can be defined as a temporary decrease in groundwater availability over a significant period. This drought results in decreased groundwater levels and discharges to the surface water system, such as streams, springs, and wetlands (Peters and van Lanen, 2003). Subsequently, a decrease in groundwater levels can have many adverse effects, such as increased costs of

pumping for abstractions, drying up wells, loss of crop yield or increased stress for natural vegetation because of decreased transpiration, increased land subsidence, changes in water quality, and thus damage to terrestrial or aquatic ecosystems.

Groundwater drought mainly occurs because of natural meteorological variations, i.e., low groundwater recharge caused by low precipitation and/or high evapotranspiration. However, human-induced factors also play a role in creating or making an existing one worse (Van Lanen and Peters, 2000). Van Loon et al. (2016a) reported anthropogenic change plays a significant role in recent droughts in different parts of the world. Anthropogenic changes, such as land-use change and increasing water demand because of population growth, alter groundwater drought (Jin et al., 2015; Van Lanen and Peters, 2002; Van Loon et al., 2016a, 2016b; Mustafa et al., 2017; Schwartz and Ibaraki, 2011). Therefore, there is a need for an improved understanding of groundwater drought and the human-induced factors influencing the groundwater balance. This should form the basis for an integrated approach that allows tackling adverse effects and safeguarding groundwater resources' sustainability.

Groundwater drought has garnered attention only in recent times (Verbeiren et al., 2013). Groundwater drought has not received as much attention in the scientific literature as meteorological and hydrological drought. Peters (2003) showed how the drought propagates through the groundwater system. Van Lanen & Peters (2000) have developed definitions, effects, and assessment of groundwater droughts. Adhikary et al. (2013) have emphasized groundwater drought assessment related to irrigation water requirements. These studies show that understanding drought propagation and its impacts are crucial for long-term water management, even more, because many groundwater systems are slowly responding systems with very long recovery periods after drought (Calow et al., 1997).

1.2 Meteorological and groundwater drought quantification

Quantification of both meteorological and groundwater drought is essential for the assessment and management of drought severity in all climatic regions. In the quantification of drought, the hydrological variable anomalies are identified in time and space. Different drought indices and drought assessment methods have been used to predict and monitor drought (Tsakiris et al., 2013; Tsakiris and Nalbantis, 2008).

To analyze meteorological drought severity and its spatial and temporal extent, different drought indices are used: standardized precipitation index (SPI), reconnaissance drought index (RDI), Palmer drought severity index (PDSI), etc. These indices are calculated using

precipitation as only an input variable or in combination with other meteorological variables, such as potential evapotranspiration.

Groundwater drought can be identified when the water table in an aquifer falls below a critical level over a certain period, resulting in several adverse effects. This groundwater drought is often the result of the combination of different drought events occurring in the hydrological time series. For groundwater drought analysis, the time-series of the three main groundwater variables need to be available with a high spatial and temporal resolution: groundwater recharge (R), groundwater level (H), and groundwater discharge (Q). The annual minimum approach and threshold approach are two well-known methods to derive drought events (Peters, 2003a; Yevjevich, 1967). The annual minimum approach considers the minimum value from each annual period, and the drought severity is expressed relatively by comparing the minimum values of the time series in each period. In this approach, it is not possible to define a multi-year drought event as one event. The threshold level approach uses a critical level, which is used as a reference to indicate drought. In this method, the drought severity is defined by the drought deficit (D), drought duration (L), or drought intensity (I). An advantage of the threshold approach over the annual minimum method is the possibility of identifying a multi-year drought. Thus, this approach is mostly used for groundwater drought analysis. A threshold value derived from exceedance probabilities is used frequently for defining drought (Peters, 2003a; Yevjevich, 1967).

1.3 Groundwater drought propagation

Drought can propagate in the hydrological cycle, e.g. meteorological drought resulting in hydrological drought (Tallaksen et al., 2006; Van Loon and Van Lanen, 2012; van Loon, 2013). This means that prolonged precipitation deficits cause less input for the hydrological system like streams, soil moisture storages, and groundwater. Van Loon et al. (2011), in their technical report of "WATCH water and global change," emphasized this propagation of drought in different hydro-climatic regions and physical catchment structures. Each type of drought occurring in the hydrological cycle has a link to other types of drought. Wang, Ertsen, Svoboda, & Hafeez (2016) showed the linkage between meteorological drought, agricultural drought, and hydrological drought and their influence on each other. There can be a time lag between each type of drought, for example, months or even years between a meteorological and groundwater drought (Machlica and Stojkovova, 2008).

During drought propagation, meteorological drought may cause hydrological drought, but every meteorological drought event may result in hydrological drought. Conversely, a series of minor meteorological droughts may can turn into a severe hydrological drought (Van Lanen, 2006; van Loon et al., 2011). Several features characterize drought: pooling, lag, attenuation, and lengthening, mainly controlled by climate and catchment factors (Eltahir and Yeh, 1999; van Loon, 2013; Peters et al., 2003). These features are used to show how drought characteristics (e.g., duration, onset, severity) are behaving in different drought types and how the early drought contributes to the next drought during its propagation. According to Van Loon and Van Lanen (2012) and Van Loon (2013), catchment characteristics such as storage capacity and response time of the catchment affect all drought propagation features. In contrast, the nature and seasonality of the climate only influenced the pooling and lengthening features. Therefore, these controlling factors play a significant role in developing and recovering of drought in the hydrological cycle.

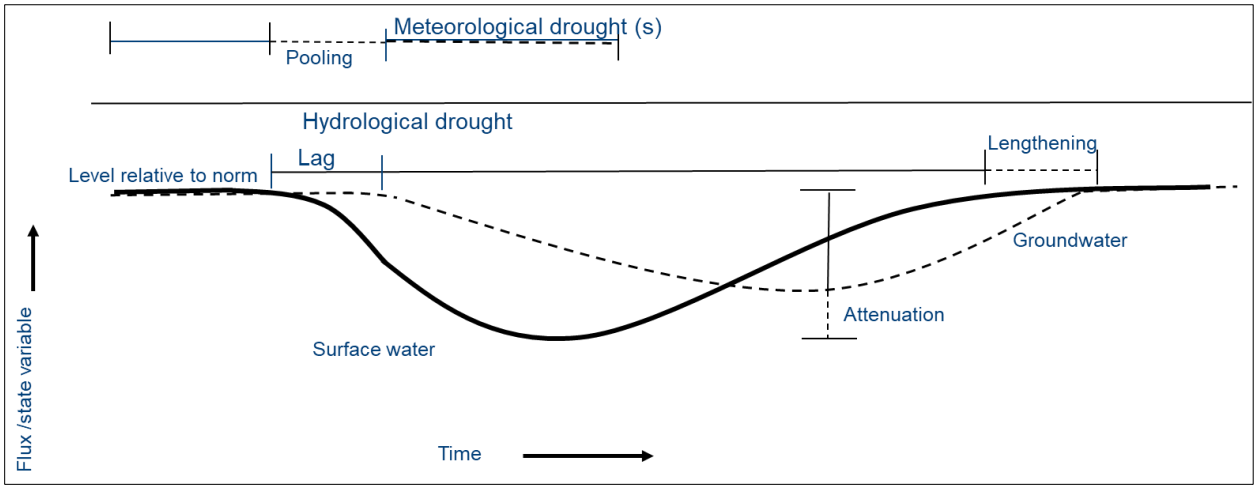


Figure 1.1: Characterizing features of drought propagation in hydrological cycle: pooling, lag, attenuation and lengthening (adopted from van Loon, 2013)

Groundwater is the final component to react to a drought situation in drought propagation, except when the surface water is mainly fed by baseflow. In a groundwater system, both aquifer characteristics and climate significantly influence groundwater drought development and recovery (Van Loon, 2015). This propagation of groundwater drought can be analyzed by focusing on the recharge increment/decrement or the relationship between recharge, groundwater level, and discharge in the aquifer system. Groundwater drought directly affects groundwater level and discharge. This effect is very complex. Peters (2003b) used a linear reservoir model to show the propagation of drought from groundwater recharge to discharge

and the aquifer characteristics' influence on propagation. In this propagation, the groundwater level depends on the amount of recharge, the baseflow to the stream, the aquifer's storage characteristics, and the pre-event conditions and rate of decline of the level (Van Loon, 2015). In this thesis, propagation of drought from meteorological drought to groundwater recharge and to groundwater discharge/level is investigated.

1.4 Drought in temperate and semi-arid climatic regions

Droughts occur in all climatic regions in the world: temperate, arid, semi-arid, and semi-humid. Since mean annual precipitation and potential evapotranspiration are different in different climatic regions, drought development and recovery are also different (Pandey and Ramasastri, 2002; Stahl and Hisdal, 2004). Moreover, drought characteristics, causes, and consequences in the environment also vary over climatic regions. The climatic variables are dependent on the topographical and atmospheric conditions of the region (Pandey and Ramasastri, 2002; Ponce et al., 2000). For example, precipitation depends on latitude, season, proximity to oceans, mesoscale atmospheric circulation, atmospheric pressure, and earth's surface; potential evapotranspiration depends on net solar radiation, vapor pressure deficit, surface roughness, and leaf area index (Ponce et al., 2000).

In semi-arid climatic regions, mean annual potential evapotranspiration is two to five times the mean annual precipitation. However, in a humid climate, total mean annual precipitation is higher than 75% of the mean annual potential evapotranspiration. Therefore, meteorological drought are more frequent in semi-arid climatic regions than in humid climatic regions (Pandey and Ramasastri, 2002; Ponce et al., 2000; Schwabe et al., 2013a; Stahl and Hisdal, 2004; WMO, 1975).

According to Peters and van Lanen (2003), climate and hydrogeology of a region highly determine the development of groundwater recharge and discharge drought. Besides the above factors, groundwater drought is influenced by overexploitation of groundwater resources for irrigation in semi-arid regions and for industrial and domestic water supply in temperate regions (Van Lanen and Peters, 2000a).

Therefore, understanding the region's climate is a crucial step towards assessing and managing meteorological drought. However, for groundwater drought, also the hydrogeology of the region should be considered to understand development and recovery of drought in aquifers.

1.5 Research objectives

The general objective of this study is to develop and apply a methodology for quantifying groundwater drought propagation and distribution in temperate (Dijle catchment and parts of the Demer and Zenne basins , Belgium) and semi-arid (Bilate River Catchment, Ethiopia) climate regions. An unsaturated flow model, groundwater model, and water balance model are combined in the developed method. Moreover, drought quantification indices and methods are incorporated to investigate drought propagation and distribution for both climatic regions.

The specific objectives of this study are:

- to estimate spatially distributed lag time of groundwater recharge in the vadose zone. The groundwater recharge is the output of the water balance model below the root zone. This part of the research objective helps to:
    i. identify the main factors for the estimation of lag time in the vadose zone,
    ii. propose a simplified approach for lag time estimation in the vadose zone,
    iii. get insight into the contribution of the vadose zone to groundwater drought propagation,
    iv. obtain time series of delayed groundwater recharge to the groundwater table.
- to investigate drought propagation in the hydrological cycle by developing and applying a methodology for simulating meteorological drought, groundwater drought, and its propagation in the aquifer in a temperate climate region.
- to differentiate in space and time between the effects of the land-use and climate on groundwater drought in a temperate climate context.
- to investigate drought propagation in the hydrological cycle, focusing on assessing its impact on groundwater recharge in a semi-arid climate context.
- to compare the processes and techniques for quantifying drought propagation and distribution in temperate and semi-arid climate regions.

1.6 Dissertation outline

In order to address the research objectives, the first part of this research estimates spatially distributed groundwater recharge delay in the unsaturated soil zone. Then, the propagation of drought in the hydrological cycle is analyzed by focusing on the relationship between rainfall, recharge, groundwater level, and discharge. A combined water balance and groundwater modeling strategy with consideration of a threshold level approach is used to simulate groundwater drought. Finally, a comparison is made between the processes and

techniques for quantifying groundwater drought propagation and distribution in temperate and semiarid climate region case studies. These research methodologies are discussed in different chapters. The chapters are based on peer-reviewed journal articles that are either published, accepted, under review, or in preparation to submit.

In Chapter 2, spatially distributed lag time between precipitation and groundwater recharge in the vadose zone is estimated and its effect on groundwater drought is investigated. In the first part of this chapter, a mathematical model is developed based on the kinematic wave approximation of the Richards' equation under the assumption of deep drainage occurring in response to rainfall infiltration, steady vertical flow (no flow barriers or artificial drainage), and isotropic and homogenous soil hydraulic properties. In the second part of this chapter, the estimated lag time is combined with groundwater recharge time series to investigate its impact on groundwater drought.

In Chapter 3, drought propagation in the hydrological cycle is investigated using a combined water balance and groundwater model. The meteorological drought and groundwater drought are quantified using drought indices and a threshold method, respectively. Drought propagation, specifically from meteorological to groundwater recharge and from groundwater recharge to discharge, is investigated. The research is implemented in a temperate climate context.

In Chapter 4, the effect of human-induced and climate factors on groundwater drought is investigated. First, groundwater recharge is estimated using a water balance model, and then the effects of the land-use and the climate factor on groundwater recharge are assessed. Finally, the potential contribution of land-use and climate effect on groundwater recharge drought is identified.

In Chapter 5, drought propagation in the hydrological cycle is investigated using a water balance model and meteorological drought indices. Groundwater recharge drought is quantified using the threshold method. Drought propagation from meteorological to groundwater recharge is investigated. The research is implemented in a semi-arid climate context.

In chapter 6, the conclusions and future perspectives of this study are summarized. First, studying drought propagation in humid and semiarid climates is compared. Then, the conclusions of the study answering the research objectives are summarized. Finally, some future perspectives are given.

1.7 References

Calow, R., MacDonald, A., 2009. What will climate change mean for groundwater supply in Africa?, Background Note of the Water Science and Policy work stream.

Calow, R.C., Robins, N.S., MacDonald, A.M., Macdonald, D.M.J., Gibbs, B.R., Orpen, W.R., Mtembezeka, P., Andrews, A.J., Appiah, S.O., 1997. Groundwater management in drought-prone areas of Africa. Int. J. Water Resour. Dev. 13, 241–262. doi:10.1080/07900629749863

Chang, T.J., Teoh, CBB, 1995. Use of the Kriging Method for Studying Characteristics of Groundwater Droughts. WATER Resour. Bull. 31, 1001–1007.

Eltahir, E.A.B., Yeh, P.J.F., 1999. On the asymmetric response of aquifer water level to floods and droughts in Illinois. Water Resour. Res. 35, 1199–1217. doi:10.1029/1998WR900071

Famiglietti, J.S., 2014. The global groundwater crisis. Nat. Clim. Chang. 4, 945–948. doi:10.1038/nclimate2425

Jin, G., Shimizu, Y., Onodera, S., Saito, M., Matsumori, K., 2015. Evaluation of drought impact on groundwater recharge rate using SWAT and Hydrus models on an agricultural island in western Japan. IAHS-AISH Proc. Reports 371, 143–148. doi:10.5194/piahs-371-143-2015

Kebede, S., 2013. Groundwater in Ethiopia Features, Numbers and Opportunities. Springer-Verlag Berlin Heidelberg, Addis Ababa. doi:10.1007/978-3-642-30391-3

MacDonald, A.M., Carlow, R.C., MacDonald, D.M.J., Darling, W.G., Dochartaigh, B.É.Ó., 2009. What impact will climate change have on rural groundwater supplies in Africa? Hydrol. Sci. J. 54, 690–703. doi:10.1623/hysj.54.4.690

Machlica, a, Stojkovova, M., 2008. Groundwater drought in different geological conditions. IOP Conf. Ser. Earth Environ. Sci. 4, 012010. doi:10.1088/1755-1307/4/1/012010

Mustafa, S.M.T., Abdollahi, K., Verbeiren, B., Huysmans, M., 2017. Identification des facteurs influençant la sécheresse et le rabattement des eaux souterraines au nord-ouest du Bangladesh. Hydrogeol. J. 25, 1357–1375. doi:10.1007/s10040-017-1547-7

Pandey, R.P., Ramasastri, K.S., 2002. Incidence of droughts in different climatic regions. Hydrol. Sci. J. 47, S31–S40. doi:10.1080/02626660209493020

Panwar, S., Chakrapani, G.J., 2012. Climate change and its influence on groundwater resources. Res. Inven. Int. J. Eng. Sci. 1, 43–60.

Peters, E., 2003. Propagation of drought through groundwater systems, Ph.D. thesis. Wageningen Universiteit, The Netherlands. 221 pp.

Peters, E., Torfs, P.J.J.F., van Lanen, H.A.J., Bier, G., 2003. Propagation of drought through groundwater - A new approach using linear reservoir theory. Hydrol. Process. 17, 3023–3040. doi:10.1002/hyp.1274

Peters, E., van Lanen, H.A.J., 2003. Propagation of drought in groundwater in semi-arid and sub-humid climatic regimes. In Proceedings of the International Symposium of Hydrology of the Mediterranean and Semi-Arid Regions, Montpellier, France, 278, pp. 312–317.

Ponce, V.M., Pandey, R.P., Ercan, S., 2000. Characterzation of Drought across Climatic Spectrum. Hydrol. Eng. 5, 222–224. doi:10.1061/(ASCE)1084-0699(2000)5:2(222)

Schwabe, K., Albiac, J., Connor, J.D., Rashid Hassan, González, L.M., 2013. Drought in Arid and Semi-Arid Regions, A Multi-Disciplinary and Cross-Country Perspective. Springer Netherlands, Dordrecht. doi:10.1007/978-94-007-6636-5_20

Schwartz, F.W., Ibaraki, M., 2011. Groundwater: A resource in decline. Elements 7, 175–179. doi:10.2113/gselements.7.3.175

Stahl, K., Hisdal, H., 2004. Hydroclimatology, in: Tallaksen, L.M., Van Lanen, HAJ (Eds.), Hydrological Drought: Processes and Estimation Methods for Streamflow and Groundwater. Elsevier Ltd, pp. 19–51. doi:10.1007/1-4020-3266-8_103

Tallaksen, L.M., Hisdal, H., Van Lanen, H.A.J., 2006. Propagation of drought in a groundwater fed catchment, the Pang in the UK. IAHS-AISH Publ. 128–133.

Tsakiris, G., Nalbantis, I., 2008. Drought meteorological monitoring network design for the reconnaissance drought index (RDI). Drought Manag. Sci. Technol. Innov. Zaragoza 62, 57–62.

Tsakiris, G., Nalbantis, I., Vangelis, H., Verbeiren, B., Huysmans, M., Tychon, B., Jacquemin, I., Canters, F., Vanderhaegen, S., Engelen, G., Poelmans, L., De Becker, P., Batelaan, O., 2013. A System-based Paradigm of Drought Analysis for Operational Management. Water Resour. Manag. 27, 5281–5297. doi:10.1007/s11269-013-0471-4

Van Lanen, HAJ, 2006. Drought propagation through the hydrological cycle, in: Climate Variability and Change—Hydrological Impacts. IASH, pp. 122–127.

Van Lanen, H.A.J., Peters, E., 2002. Temporal variability of recharge as an indicator for natural groundwater droughts in two climatically contrasting basins, in: FRIEND 2002 - Regional Hydrology: Bridging the Gap between Research and Practice. Fourth International Conference on FRIEND (Flow Regimes from International Network Data). Cape Town, South Africa, pp. 101–106.

Van Lanen, H.A.J., Peters, E., 2000. Definition, Effects and Assessment of Groundwater Droughts, in: VOGT, J. V., SOMMA, F. (Eds.), Drought and Drought Mitigation in Europe. Elsevier Ltd, pp. 49–61. doi:10.1007/978-94-015-9472-1_4

Van Loon, A.F., 2015. Hydrological drought explained. Wiley Interdiscip. Rev. Water 2, 359–392. doi:10.1002/wat2.1085

Van Loon, A.F., Gleeson, T., Clark, J., Van Dijk, A.I.J.M., Stahl, K., Hannaford, J., Di Baldassarre, G., Teuling, A.J., Tallaksen, L.M., Uijlenhoet, R., Hannah, D.M., Sheffield, J., Svoboda, M., Verbeiren, B., Wagener, T., Rangecroft, S., Wanders, N., Van Lanen, H.A.J., 2016a. Drought in the Anthropocene. Nat. Geosci. 9, 89–91. doi:10.1038/ngeo2646

Van Loon, A.F., Stahl, K., Di Baldassarre, G., Clark, J., Rangecroft, S., Wanders, N., Gleeson, T., Van Dijk, A.I.J.M., Tallaksen, L.M., Hannaford, J., Uijlenhoet, R., Teuling, A.J., Hannah, D.M., Sheffield, J., Svoboda, M., Verbeiren, B., Wagener, T., Van Lanen, H.A.J., 2016b. Drought in a human-modified world: Reframing drought definitions, understanding, and analysis approaches. Hydrol. Earth Syst. Sci. 20, 3631–3650. doi:10.5194/hess-20-3631-2016

Van Loon, A.F., Van Lanen, H.A.J., 2012. A process-based typology of hydrological drought. Hydrol. Earth Syst. Sci. 16, 1915–1946. doi:10.5194/hess-16-1915-2012

van Loon, A.F., van Lanen, H.A.J., Tallaksen, L.M., Hanel, M., Sapriza, G., Koutroulis, A., vam Huijgevoort, M., Hisdal, H., 2011. Propagation of drought through the hydrological cycle. Watch Tech. Rep.

van Loon, A.F. Van, 2013. On the propagation of drought How climate and catchment characteristics influence hydrological drought development and recovery, Ph.D. thesis. Wageningen University, The Netherlands. 210 pp.

Verbeiren, B., Huysmans, M., Tychon, B., Jacquemin, I., Canters, F., Vanderhaegen, S., Engelen, G., Poelmans, L., De Becker, P., Tsakiris, G., Vangelis, H., Batelaan, O., 2013. Drought-related vulnerability and risk assessment of groundwater resources under temperate conditions, in: 13th International Conference on Environmental Science and Technology. Athens, Greece, p. 10.

Wang, W., Ertsen, M.W., Svoboda, M.D., Hafeez, M., 2016. Propagation of drought: From meteorological drought to agricultural and hydrological drought. Adv. Meteorol. 2016. doi:10.1155/2016/6547209

White, I., Falkland, T., Scott, D., 1999. Droughts in Small Coral Islands : Case study, South tarawa, Kiribati.

WMO, 1975. Drought and Agriculture.

Yevjevich, V., 1967. An objective approach to definitions and investigations of continental hydrologic droughts. Hydrol. Pap. Color. State Univ. Fort Collins CO 23.

Chapter 2

2 Vadose zone lag time effect on groundwater drought in a temperate climate

Based on: Wossenyeleh, B. K., Verbeiren, B., Diels J., and Huysmans, M Vadose zone lag time effect on groundwater drought in a temperate climate. Water 12, 2123, doi:10.3390/w12082123, 2020.

2.1 Abstract

An essential factor in the propagation of drought from meteorological drought to groundwater drought is the delay between a precipitation event and the groundwater recharge reaching the groundwater table. This delay, which mainly occurs in the vadose zone of the hydrological cycle, is often poorly studied. Therefore, this paper proposes a method for estimating spatially distributed delay in the vadose zone using the kinematic wave approximation of 'Richards' equation combined with the van Genuchten-Burdine and Brooks-Corey parametric model. The modeling was approached: (1) using a detailed parametrization of soil and geological layers and (2) using lumped hydraulic and physical properties of geological layers. The results of both approaches were compared against the physically-based flow model Hydrus-1D. This analysis shows that using a detailed parametrization of soil and geological layers results in good comparison with a Nash-Sutcliffe Efficiency of 0.89 for Brooks-Corey and 0.79 for van Genuchten-Burdine. The delay result of the Brooks-Corey model was incorporated into the groundwater recharge time series from 1980 to 2013 to analyze the effect of this delay on groundwater drought. The result shows that the delay in the vadose zone influences groundwater drought characterization features such as the number, duration, and intensity of drought events.

2.2 Introduction

Drought can be described as a temporary decrease in water availability over a significant period of time. Drought is a direct result of deficient precipitation and as such, it is mainly a meteorological-related hazard. Typically, three definitions of drought are used: meteorological, agricultural and hydrological drought. The first is referring to a period without or with little precipitation; the second is referring to a shortage of water in the soil and as such for vegetation; the third is describing an impact on hydrological water bodies. It can affect both surface and groundwater resources. In case it concerns groundwater bodies, the term groundwater drought is used. Groundwater drought can be defined as a temporary decrease in groundwater availability over a significant period of time. This drought causes decreased groundwater levels and discharge to the surface water system (Peters and van Lanen, 2003).

In Belgium, Tricot et al., 2015 have shown that drought periods have not intensified during the last century. The meteorological drought periods were defined as the number of consecutive days without significant precipitation (less than 0.5 mm) for the six hottest months of the year. However, the study area experienced long periods of drought and low groundwater levels in

the past four years. According to Verbeiren et al., 2013, the main influencing factors for groundwater drought are climate, land use/land cover (LULC), and groundwater demand for human activities.

An essential factor in the propagation of drought from meteorological drought to groundwater drought is the delay between a precipitation event and the resulting groundwater recharge reaching the groundwater table. The spatial and temporal distribution of this delay determines how fast and how significant groundwater is affected after periods of meteorological drought. This delay mainly occurs in the unsaturated soil zone of the hydrological cycle. However, studies of drought propagation (Van Lanen, 2006; Peters, 2003b; Peters et al., 2003, 2006) in the hydrological cycle often give less attention to lag effects caused by the vadose zone. Additionally, this effect is often not considered in groundwater modeling, analysis of climate change impact on groundwater, and effective management and sustainability of future water resources.

Estimation of the time for groundwater recharge below root zone to reach the groundwater table needs critical understanding and estimating of hydraulic properties and flow in the vadose zone. Therefore, unsaturated soil flow equations and modeling can be used to estimate this delay. This flow is controlled by the spatial and temporal heterogeneity of the vadose zone and hydrological perturbations at the surface and within the subsurface.

The groundwater recharge delay is mainly influenced by changes in soil moisture and pressure in the vadose zone. These factors are a result of small hydrological perturbations at the surface (Rasmussen et al., 2000). Kinematic wave approximation theory can be used to predict these small changes of pressure in the vadose zone (Beven, 2012; Charbeneau, 1984; Germann and Beven, 1985; Rasmussen et al., 2000; Scaini et al., 2017; Sisson and Ferguson, 1980; Smith, 1983). According to Lighthill and Whitham (1955), a one-dimensional pressure wave in the hydrological system can be described using kinematic wave theory. Therefore, soil moisture content, unsaturated hydraulic conductivity and vertical soil moisture velocity in the vadose zone can be described using this theory. However, hydraulic properties of the vadose zone should be defined continuously over the spatial and temporal scale of the working domain (Germann and Beven, 1985).

This study considers one-dimensional vertical soil moisture movement in the unsaturated soil zone. This vertical flow is governed by capillary and gravity forces. Gravity dominant flow can be applied in the case of deep drainage in response to rainfall and soil with larger soil moisture

content than field capacity (Smith, 1983). For gravity dominated flow, kinematic wave velocity is used to analyze the vertical soil moisture movement of small changes of pressure perturbations in the unsaturated soil zone (Rasmussen et al., 2000). That means that this velocity controls the travel time of pressure distributions in the unsaturated soil zone (Scaini et al., 2017).

Numerical simulations are used for the quantification of small changes in pressure distribution in the vadose zone in time and space scale. Some studies have used numerical simulations of the vadose zone by solving the 3D Richards equation to determine the travel time of soil moisture (Kollet et al., 2010; Kollet and Maxwell, 2008). However, numerical simulation using the 3D equation leads to complex models and model calibration issues and needs long calculation times as well as extensive data. Therefore, the 1D gravity-driven kinematic wave approximation approach is used for a simplified treatment of flow processes in the vadose zone (Grismer, 2013; Rossman et al., 2014).

Estimation of groundwater recharge delay in the vadose zone can be handled at a point or spatially distributed scale. Hocking and Kelly's (2016) and Mattern and Vanclooster's (2010) studies estimate groundwater recharge delay in the vadose zone at the point scale. However, other studies such as Rossman et al. (2014) estimate lag time using a kinematic wave approximation of the Richards equation in a spatially distributed way based on the Van Genuchten-Mualem parametric model. Rossman et al. (2014) mainly focus on the effect of the vadose zone thickness and climate change on the groundwater recharge delay.

This chapter aims to estimate the spatially distributed vadose zone lag time in relation to groundwater drought using the kinematic wave approximation of the Richards equation under the assumption of deep drainage occurring in response to rainfall infiltration, steady vertical flow (no flow barriers or artificial drainage), and isotropic and homogenous soil hydraulic properties. This theory is combined with the van Genuchten-Burdine and Brooks-Corey parametric models. Besides, the best-validated model resulting lag time will be incorporated to obtain delayed groundwater recharge time series to the groundwater table. This delayed groundwater recharge is then used as input for the groundwater modeling, drought propagation in the aquifer and hydrological cycle study, and investigation of the effects of the land-use and climate effect on groundwater drought. Finally, the research will also propose a simplified approach for lag time estimation in the vadose zone.

2.3 Study site and data

The study area consists of the Dijle and Demer catchments in central Belgium, underlain by the Brulandtkrijt and Central Campine groundwater systems (Figure 2.1). The aquifer has a surface area of 5800 km^2. The land surface elevation ranges between 10 m and 100 m. Belgium has a temperate climate with a long-term average annual rainfall around 800 mm and an average temperature of around 10 ^{o}C (Verbeiren et al., 2013). This high and frequent rainfall is the main factor to initiate the subsurface drainage in the study area. The vadose zone in the study area vertically extends from the Quaternary and Campine Aquifer Systems (HCOV 0100 & 0200) to the Cretaceous Aquifer System (HCOV 1100) shown in Figure 2.2. However, more than 65 percent of the vadose zone contains geological layers from the Quaternary and Campine Aquifer Systems. The Quaternary deposits are mostly sandy in the northern part of the study area. In contrast, loamy deposits characterize the hilly regions in the south. Moreover, the central part of the river valleys (Dijle, Demer, and smaller tributaries) are covered with alluvial deposits, typically loamy or clayey (Vandersteen and Gedeon, 2013).

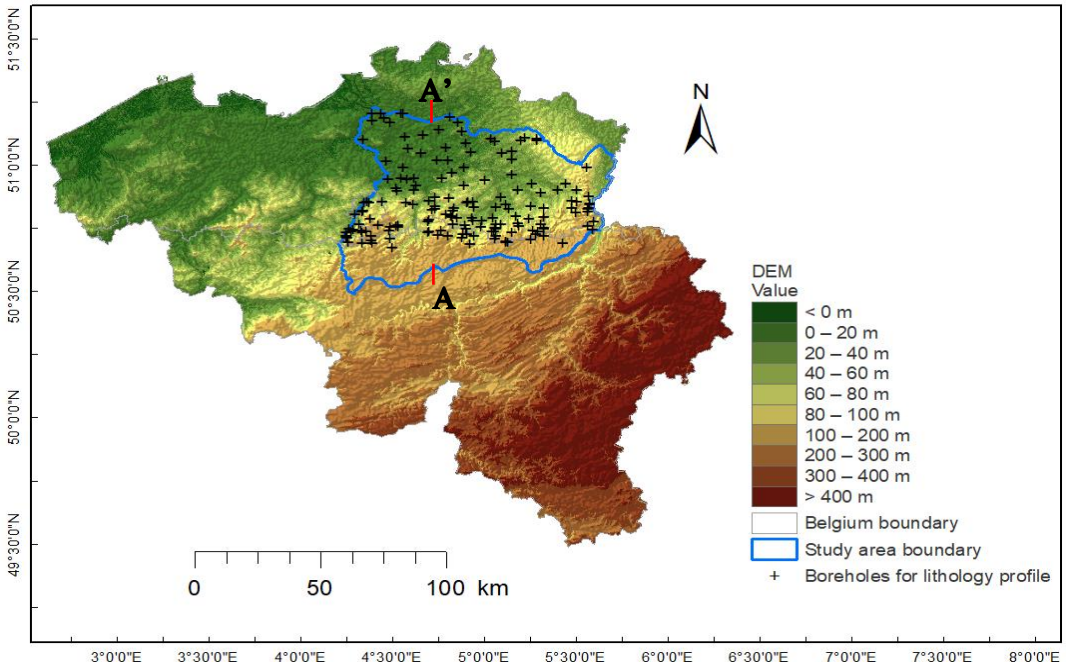


Figure 2.1: Location of the study area, Digital Elevation Model (DEM) and lithology profile boreholes in Belgium.

Geological, hydrogeological and groundwater data such as borehole information on geology, hydraulic properties, groundwater monitoring wells, etc., is available from the DOV database (Databank Ondergrond Vlaanderen – dov.vlaanderen.be), the Flemish Groundwater Model (Ministerie Vlaamse Gemeenschap, 2004a and 2004b) and the Service Public Wallonie

(SPW). Detailed characterization of soil texture, i.e., proportions of sand, silt, and clay, in the vadose zone was taken from 168 soil boreholes (Figure 2.1). Soil physical properties such as porosity n, saturated hydraulic conductivity K_s and pore size distribution index λ are depending on soil texture (Fernandez-Illescas and Rodriguez-Iturbe, 2001). The USDA soil texture classification and the univariate regression equation by Cosby, Hornberger, Clapp, & Ginn (1984) were used for deriving soil parameter values.

HCOV is a hydrogeological code developed in the framework of the Flemish Groundwater Model (Cools et al., 2002) giving a unique code to every aquifer and aquitard in Flanders.

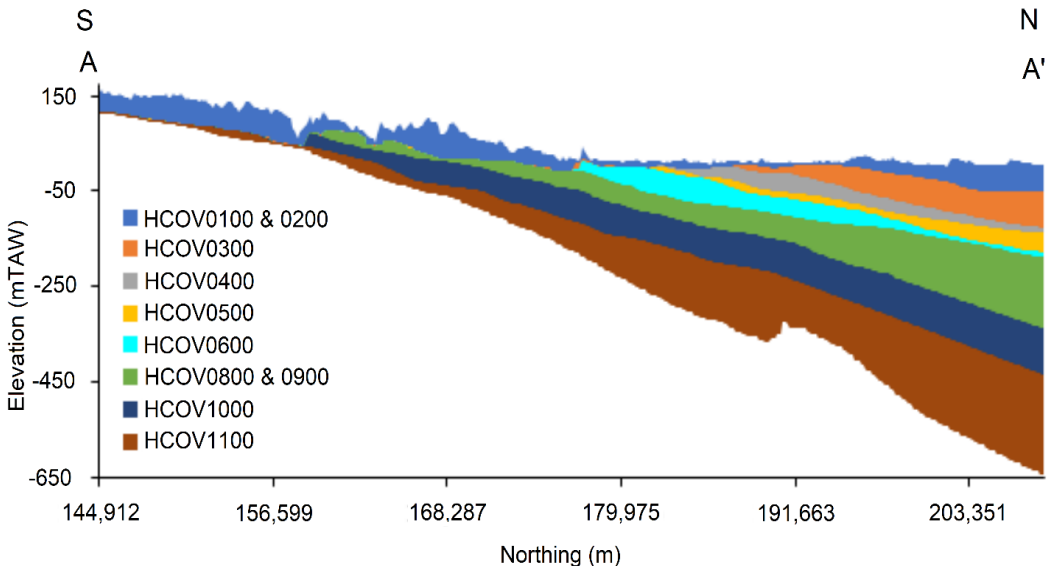


Figure 2.2: Hydrogeological S-N cross-section through the study area. The location of the cross-section is indicated in Figure 2.1 A-'A'. Descriptions of HCOV codes can be found in Table 2.1. The elevation is measured from a Belgian referencing system for elevation called TAW ("Tweede Algemene Waterpassing")

Table 2.1: Geological layers found in the vadose zone of the study area

LAYER	GROUNDWATER UNIT	HCOV Codes	Range of Layer Thickness [m]
1	Top of the Quaternary aquifer Systems Local deposits of the Campine aquifer System	HCOV 0100 HCOV 0200	0-87
2	Deposits of the Boom aquitard	HCOV 0300	0-14.5
3	Oligocene aquifer System	HCOV 0400	0-32.5
4	Bartoon Aquitard system	HCOV 0500	0-6
5	Ledo Panselian Brusselean aquifer System	HCOV 0600	0-35
6	Ypresian Aquifer System Ypresian Aquitard system	HCOV 0800 HCOV 0900	0-36
7	Paleocene Aquifer System	HCOV 1000	0-24
8	Cretaceous Aquifer System	HCOV 1100	0-29

The vadose zone thickness was estimated as a difference between land surface elevation and groundwater level (Figure 2.3). A groundwater table map was generated based on monthly groundwater level readings from 1980 to 2013 in observation wells found in the study area. The northern part of the study area has a shallow groundwater table (less than 10 m), while a thicker vadose zone characterizes the southern part of the study area.

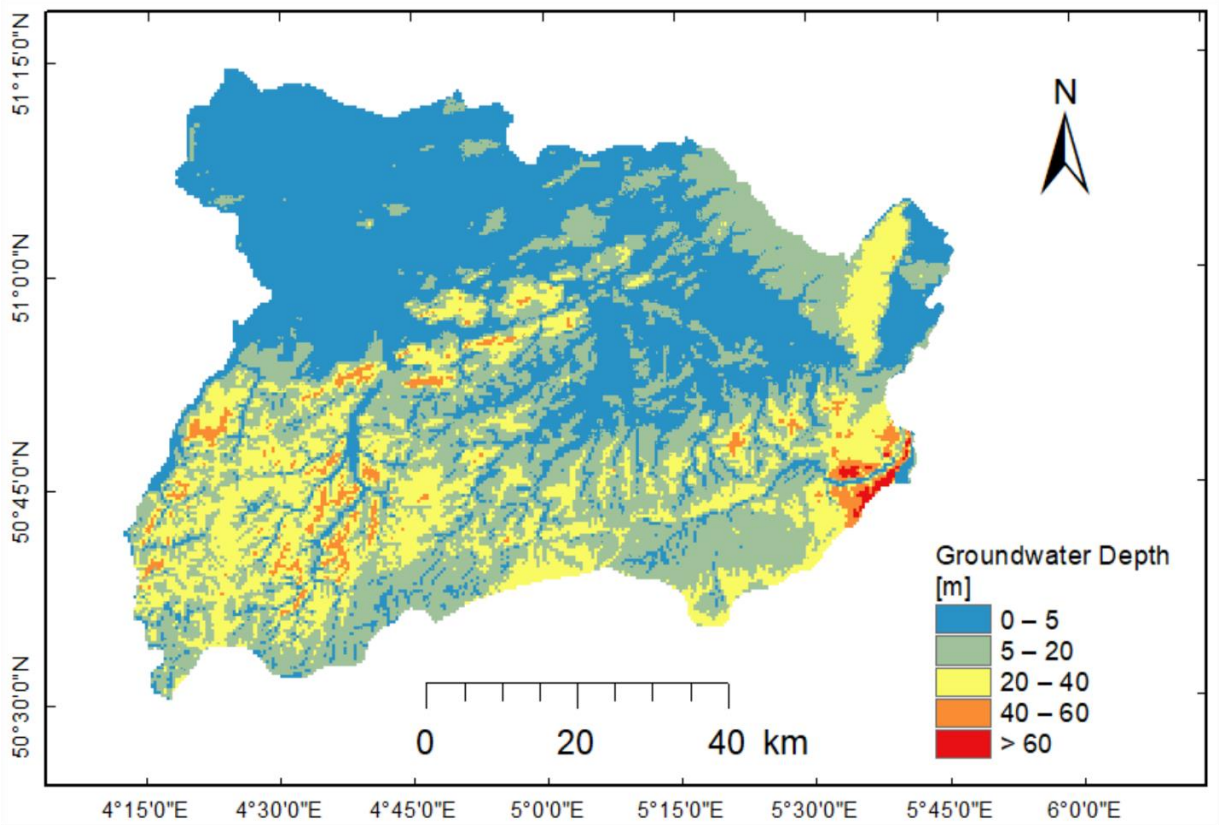


Figure 2.3: Thickness of the vadose zone (m) in the study area, estimated as the difference between 100-m digital elevation model data and averaged water table data. (obtained from GroWaDRISK project)

Spatially distributed groundwater recharge below root zone (*R(t)*) generated in the GroWaDRISK project was used. This project was aiming for the development of a drought-related vulnerability and risk assessment strategy for sustainable management of groundwater resources under temperate conditions (Verbeiren et al., 2013). In this project, a monthly averaged spatially distributed groundwater recharge was estimated using the WetSpass model from 1980 to 2013. WetSpass is a physically-based model for the estimation of spatially distributed surface runoff, actual evapotranspiration, and groundwater recharge (Batelaan and DeSmedt, 2001). This model accounts for spatially distributed landuse, soil type, slope, elevation, monthly average groundwater depth, and meteorological conditions as

an input and calculate the water balance up to the root zone (Abdollahi et al., 2017; Batelaan and De Smedt, 2007). Therefore, the groundwater recharge computed using this model has to pass through the vadose zone to reach the groundwater table. Figure 2.4 shows groundwater recharge is higher than 300 mm/year in the north, which is characterized by sandy soil and gentle slope. Moreover, in river valleys characterized by loamy soil and steep slope, groundwater recharge ranges between 100 and 300 mm/year. In the urbanized areas, groundwater recharge is often lower than 100 mm/year because of impervious surfaces. In general, the estimated groundwater recharge is larger than 150 mm/year in most of the study area. These high rates of groundwater recharge, along with the presence of the thick permeable aquifers, make the area valuable for its groundwater reserves and drinking water supply.

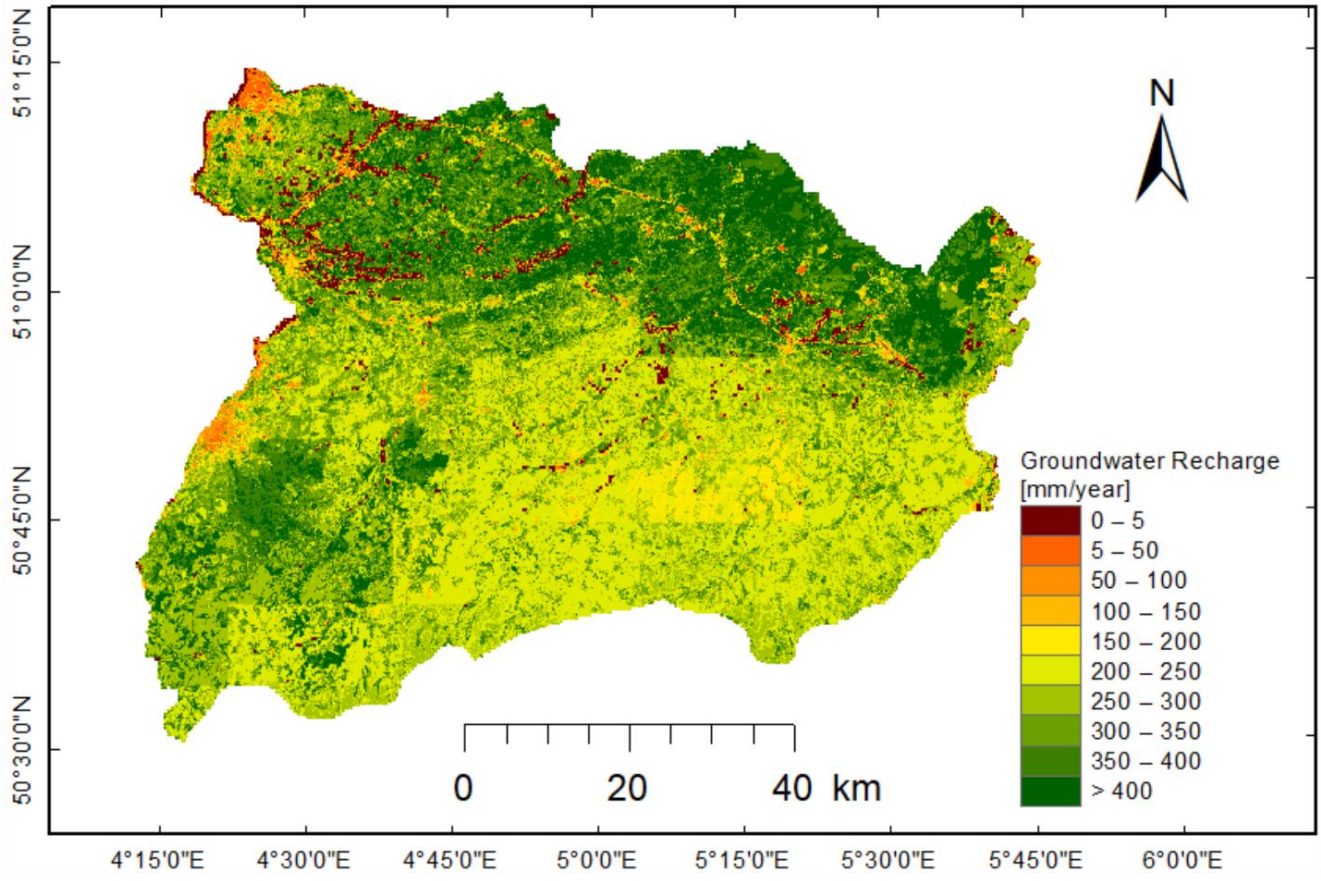


Figure 2.4: Yearly averaged groundwater recharge from 1980 to 2013, estimated using WetSpass (the result of GroWaDRISK project)

2.4 Mathematical model development

2.4.1 Kinematic wave approximation theories

In this section, the derivation of kinematic velocity from the kinematic-wave approximation model in the vadose zone will be presented. The kinematic wave model is primarily based on the continuity equation and only approximates the dynamic equation with uniform-flow (Miller, 1984). As stated in Lighthill and Whitham (1955), kinematic waves only propagate in the vertical direction; thus, kinematic waves have one wave speed, which is called celerity or kinematic velocity. The 1D flow of the kinematic wave model in the vadose zone is a functional relationship between the flow (q) and head (h) or soil moisture content (θ).

Smith (1983) stated that if the steady gravity-driven vertical porous media flow passing down through the vadose zone, the kinematic wave velocity or celerity (c) can be expressed as:

$$c = \frac{dq}{d\theta} \qquad (2.1)$$

In porous media flow, celerity can be expressed in terms of soil moisture (θ) and unsaturated hydraulic conductivity. Therefore, the Buckingham-Darcy flux law under the assumption of gravity dominant unsaturated flow (Nimmo, 2005) was used to express this celerity.

The flow in the vadose zone of soil is often assumed as one-dimensional steady gravity dominant flow because the hydrological changes at the surface are often minimal, and subsurface drainage mainly occurs under frequent rainfall. For gravity dominant flow in the vadose zone with water flowing downward at a constant rate, matric potential gradient (*dh/dz*) approaches zero and water flows under the influence of gravity alone. Therefore, the Buckingham-Darcy flux law for gravity-driven flow can be approximated as follows:

$$q \approx -K(h) \approx -K(\theta) \qquad (2.2)$$

Unsaturated hydraulic conductivity is a function of the matric potential head (h) K(h), and soil moisture content (θ) K(θ). Therefore, K may be written directly as a function of θ.

Celerity or kinematic wave velocity in the vadose zone for steady gravity dominate flow can be derived based on *Equations 2.1* and *2.2*.

$$c = \frac{dK(\theta)}{d\theta} \qquad (2.3)$$

Equation 2.3 is used to indicate that a small change of soil moisture or capillary pressure at a water table resulting from a small change of hydrological conditions at the land surface. This

velocity is the most relevant when calculating the delay of groundwater recharge in the vadose zone (Rossman et al., 2014).

2.4.2 Parameterization of the kinematic wave model

For conditions where the moisture flux is only a function of the moisture content, kinematic wave models are applied to describe the moisture flow behavior in the vadose zone (Charbeneau, 1984). Unsaturated hydraulic conductivity, porosity, residual soil moisture, and pore size distributions of the vadose zone are used to parametrize the soil moisture content and celerity. In this study, the relationships formulated by Brooks-Corey and van Genuchten-Burdine are used to express soil moisture and celerity(c) in a parametric form based on their unsaturated hydraulic conductivity function.

2.4.2.1 Unsaturated hydraulic conductivity function

Water flow and solute transport in the subsurface are strongly influenced by hydraulic conductivity. Parameters of the vadose zone like pore size distribution of the medium, and the tortuosity, shape, roughness, and degree of interconnectedness of the pores are affecting the value of hydraulic conductivity in the subsurface (van Genuchten and Pachepsky, 2011).

In this study, the closed-form analytical expression based on ' 'Burdine's theory for predicting unsaturated hydraulic conductivities is used. Since the Burdine theory is applicable for isotropic media (Brooks and Corey, 1964, 1966), the flow is assumed to be in isotropic media. The following equation was derived by Burdine (1953) for predicting relative hydraulic conductivity from pore size distribution data and basic laws of fluid flow in a porous medium.

$$K_r = {S_e}^2 \int_0^{S_e} \frac{1}{h^2(x)}\,dx \Big/ \int_0^1 \frac{1}{h^2(x)}\,dx \qquad (2.4)$$

where h is the pressure head, which is a function of relative soil moisture content or effective saturation, S_e:

$$S_e = \frac{\theta - \theta_r}{\theta_s - \theta_r} \qquad (2.5)$$

In *Equation (2.5)* θ_s and θ_r indicate the saturation and residual soil moisture content in the vadose zone, respectively. Both Brooks-Corey and Van Genuchten express the relative soil moisture content in the form of pressure head to solve the Burdine relative hydraulic conductivity equation.

Based on the observation of a large number of experimental data, Brooks and Corey (1964, 1966) express relative soil moisture content in the function of pressure head, as follows,

$$S_e = \left(\frac{h}{h_b}\right)^{-\lambda} \qquad (2.6)$$

where h_b is the bubbling pressure (approximately equal to the air entry value), and λ a number to characterize pore size distribution. Then, the closed-form expression of relative hydraulic conductivity can be derived by solving *Equation (2.4)* using *Equation (2.6) (*Brooks and Corey 1964, 1966) . Therefore, relative hydraulic conductivity using Brooks-Corey is as follows:

$$K_r = S_e^{(3\lambda+2)/\lambda} \qquad (2.7)$$

van Genuchten (1980) also express the effective saturation in the function of pressure head:

$$S_e = \left[\frac{1}{1+|\alpha h|^n}\right]^m \qquad (2.8)$$

where α and n are van Genuchten empirical coefficients which depend on the air bubbling pressure and pore size distribution respectively, *m* = 1-2/n (with n>2), and h is pressure head assumed to be positive below the root zone or during deep drainage. Then, a closed-form expression for van Genuchten relative hydraulic conductivity can be derived by solving *Equation (2.4)* of Burdine theory using *Equation* (2.*8) (*van Genuchten 1980):

$$K_r = S_e^{\,2}\left[1-(1-S_e^{\frac{1}{m}})^m\right] \qquad (2.9)$$

Relative hydraulic conductivity in *Equations (2.7)* and (2.*9)* is equal to the ratio of unsaturated K(θ) and saturated hydraulic conductivity K_s.

$$K_r = K(\theta)/K_s \qquad (2.10)$$

Using relative hydraulic conductivity *equations (2.7, 2.9 & 2.10)*, parametric models can be developed to estimate unsaturated hydraulic conductivity, K(θ), from vadose zone properties. Therefore, unsaturated hydraulic conductivity for the two parametric models can be expressed as follows:

- ✓ Brooks-Corey model (BC):

$$K(\theta) = K_s(S_e)^{\frac{3\lambda+2}{\lambda}} \qquad (2.11)$$

- ✓ van Genuchten-Burdine model (VGB):

$$K(\theta) = K_s S_e^{\,2}\left[1-\left(1-S_e^{\frac{1}{m}}\right)^m\right] \qquad (2.12)$$

According to the soil retention curve resulting from van Genuchten (1980), the above two parametric models become identical for a sufficiently low value of soil moisture, θ, under the same parameter values of α & n and λ (which is equal to n-1) (Mualem, 1978).

2.4.2.2 Soil moisture content

Due to the relatively large size of the catchment, the difficulty of measuring soil moisture content values in the subsurface, and its variability in space and time, soil moisture content was estimated using the Brooks–Corey and van Genuchten–Burdine parametric models.

During the soil moisture transport in the vadose zone, when the moisture content reaches field capacity, hydraulic conductivity is sufficient to pass the volumetric flux q in the downward direction under the force of gravity, so that water content θ can be inferred from knowledge of q and K(θ) (Charbeneau, 1999). The assumption hereby is that under these conditions, the hydraulic gradient is equal to one (flow is only driven by gravity), and hence the water content of the vadose zone must be the water content at which K(θ)=q. By setting K(θ)=q in the Brooks-Corey model (*Equation 2.11*), and rearranging, the average soil moisture content in the vadose zone can be calculated as follows:

$$\theta = \theta_r + (\theta_s + \theta_r)\left(\frac{q}{K_s}\right)^{\frac{\lambda}{3\lambda+2}} \qquad (2.13)$$

By similarly setting K(θ)=q in the van Genuchten-Burdine equation (*Equation 2.12*), the average soil moisture content can be calculated from the recharge flux as follows:

$$\frac{q}{K_s} = {S_e}^2\left[1 - \left(1 - S_e^{\frac{1}{m}}\right)^m\right] \qquad (2.14)$$

2.4.2.3 Kinematic wave velocity or celerity

A parametric expression of celerity can be obtained by derivation of the unsaturated hydraulic conductivity formulation of Brooks-Corey and van Genuchten-Burdine with respect to the soil moisture content in the vadose zone.

According to *Equation 2.3,* the celerity for the Brooks-Corey equation is obtained by taking the derivative of unsaturated hydraulic conductivity (*Equation 2.11)* with respect to the water content θ, which yields the following:

$$c = \frac{K_s(3\lambda+2){S_e}^{\frac{3\lambda+2}{\lambda}}}{\lambda(\theta-\theta_r)} \qquad (2.15)$$

Similarly, the celerity in case of the van Genuchten Burdine equation is obtained by taking the derivative of *Equation 2.12* with respect to the water content θ, which yields the following:

$$c = \frac{K_S S_e}{(\theta_S - \theta_r)}\left[2(1 - {S_f}^m) + S_e^{\frac{1}{m}} S_f^{m-1}\right] \quad (2.16)$$

where S_f is equal to $1\text{-}S_e^{1/m}$.

2.5 Methods

In this study, groundwater recharge is assumed as the only vertical water flow in the vadose zone. Thus, groundwater recharging passing through the vadose zone is approximated by the Darcy flow driven by gravity. Therefore, Darcy flux (q) mentioned in all the above equations can be substituted by groundwater recharge.

The parametric models of Brooks-Corey (BC) and van Genuchten-Burdine (VGB) directly address moisture content as the variable of interest and assume gravity as the driving force for water flow. These models were used to estimate soil moisture content and celerity in the vadose zone.

Groundwater recharge delay was calculated from celerity using the following expression:

$$t_d = \frac{T_{vz}}{c} \quad (2.17)$$

where t_d is groundwater recharge delay (d) in the unsaturated zone, T_{vz} is the thickness of vadose zone (m) which is equal to the mean of groundwater table depth described in Figure 2.3, and c is the celerity (m/day) calculated with *equation 2.15* or 2.*16*, thereby calculating the moisture content θ with *equation 2.13* or 2.*14*, respectively.

The methods used here to estimate t_d may lead to a small potential error because the capillary fringe near the water table is not taken to account.

2.5.1 Modeling approaches

In this study, two modeling approaches were applied: (1) using a detailed physical parametrization of the geological layers and (2) using lumped geological layers.

2.5.1.1 Detailed physical parametrization of geological layers

Detailed soil characterization of the geological layers was taken from 168 soil boreholes found in the Demer and Dijle catchments (Figure 1.1).

In these soil boreholes, soil texture is aggregated using a soil texture triangle, and homogeneous soil texture within the thickness of each borehole was considered. For each soil texture group, parameter values of physical properties were determined using the USDA

soil texture classification and the univariate regression equation by Cosby et al. (1984). Yearly average soil moisture content was estimated for each borehole using Brooks-Corey and Van Genuchten-Burdine parametric models. After estimating point scale kinematic velocity, Empirical Bayesian Kriging (EBK) was used to interpolate celerity throughout the study area. Empirical Bayesian kriging requires minimal interactive modeling, and spatial relationships are modeled automatically and account for the error introduced by estimating the underlying semivariogram. Mirzaei and Sakizadeh (2016) and Yao et al. (2013) shows high interpolation performance of Empirical Bayesian kriging compared to ordinary kriging (OK) and inverse distance weighting (IDW). During the interpolation of celerity, 80% of the point scale values were used as training data while the rest was used for validation of interpolation.

2.5.1.2 Lumped parametrization of geological layer

In the second modeling method, groundwater recharge delay was estimated by lumping the different geological layers found in the vadose zone. The thickness of each geological layer was computed from its top surface elevation, the bottom elevation of each layer, and water table elevation. The data for the elevations of each geological layer was taken from VMM (2008). Hydraulic and physical properties of the geological layers were taken from the hydrogeology study of North-East Belgium by Vandersteen & Gedeon (2013).

Spatially distributed, yearly averaged soil moisture content was estimated for each geological layer using the Brooks–Corey and van Genuchten–Burdine parametric models. Moreover, celerity was estimated in each geological layer based on the result of the soil moisture content and yearly averaged groundwater recharge. The groundwater recharge delay in the vadose zone was estimated using the relationship of celerity and vadose zone thickness shown in *Equation (2.17).*

2.5.2 Comparison with other methods

Direct measurement of the delay time in the unsaturated zone is not possible, and validation is very challenging, especially for the size of the study area. As direct validation of the resulting delay time is not possible, the model results were compared to results from different models (Sargent, 2011). The results of the above parametric models are compared to a physically based flow model, HYDRUS-1D, which solves the 1-D Richards flow equation numerically.

$$\frac{\partial \theta}{\partial t} = \frac{\partial}{\partial z}\left[K(h)\left(\frac{\partial h}{\partial z} + 1\right)\right] - S \qquad (2.18)$$

where *z* is the vertical coordinate (positive upward), t is time (d), *S* is a sink term (d^{-1}), h is the pressure head (m), θ is the volumetric moisture content (mm/mm), and K is the unsaturated hydraulic conductivity function (m/d).

The results of both the van Genuchten-Burdine and Brooks-Corey parametric models were compared to the HYDRUS-1D model for 15 selected locations varying in the thickness of the vadose zone. For those locations, the lithological information could be inferred from borehole data. The soil physical properties were parametrized based on USDA default soil texture parameter value mentioned in Cosby et al. (1984).

A variable flux condition was imposed on the soil surface, considering the same inputs of groundwater recharge below root zone (*R(t))* as those used in the parametric models. Since the bottom of the flow domain is the groundwater table, a constant soil moisture content equal to the saturated soil moisture content was imposed there. Field capacity soil moisture content throughout the vadose zone was defined as the initial condition. The soil hydraulic property model was set as Brooks-Corey and van Genuchten-Mualem for different simulations.

Groundwater recharge delay was calculated by comparing the timing of the peak flow daily timeseries at the soil surface and the groundwater table.

2.5.3 Delay effect on groundwater drought

To assess the effect of the delay in the vadose zone on groundwater drought, the groundwater recharge delay output was implemented on the spatially distributed monthly recharge timeseries between 1980 and 2013 obtained from the GroWaDRISK project resulting in a delayed recharge time series ($R(t)_d = R(t-t_d)$).

A groundwater drought analysis was performed on the original groundwater recharge (R(t)) and the delayed groundwater recharge $R(t)_d$ time series of 34 years. The threshold level method introduced by Yevjevich (1967), with a variable threshold value (Beyene and Loon, 2014), was used to determine the occurrence of groundwater recharge drought events.

To do so, a separate frequency analysis was conducted for each of the 12 months. The threshold level for each month was determined as the 70^{th} percentile of the probability of exceedance of monthly recharge in that month in the 34-year series (1980-2013). This threshold level is within the 70^{th}-95^{th} percentile of the probability of exceedance range used for most drought studies (van Loon, 2013). For each month of the year, the monthly recharge

values in the time series were ranked from highest to lowest. For each month, percentiles were calculated using the formula from (Hazen, 1914):

$$P_i = 100\frac{i-0.5}{n} \qquad (2.19)$$

where P_i is the percentile of the data set; *i* is the rank number, and n is the total number of data points. The formula was rearranged to calculate the rank for the 70th percentile recharge for each month, and the corresponding threshold value of recharge value was obtained using linear interpolation between successive ranks. Finally, the comparison of drought events of groundwater recharge and delayed groundwater recharge were made in terms of numbers of drought events, the severity of drought, and their duration and timing. The results were analyzed for the whole study area and also separately for the subareas with deep and shallow groundwater tables, defined as areas with the average groundwater depth higher than 40 m and lower than 10 m, respectively.

2.6 Results and discussion

2.6.1 Detailed physical parametrization of geological layers

2.6.1.1 Soil moisture and celerity

Estimated soil moisture content in the study area varies from 0.03 mm/mm to 0.25 mm/mm (Figure 2.5). The van Genuchten-Burdine model gives a higher estimation of soil moisture than the Brooks-Corey model. Soils with low hydraulic conductivity and high deep percolation have higher soil moisture content.

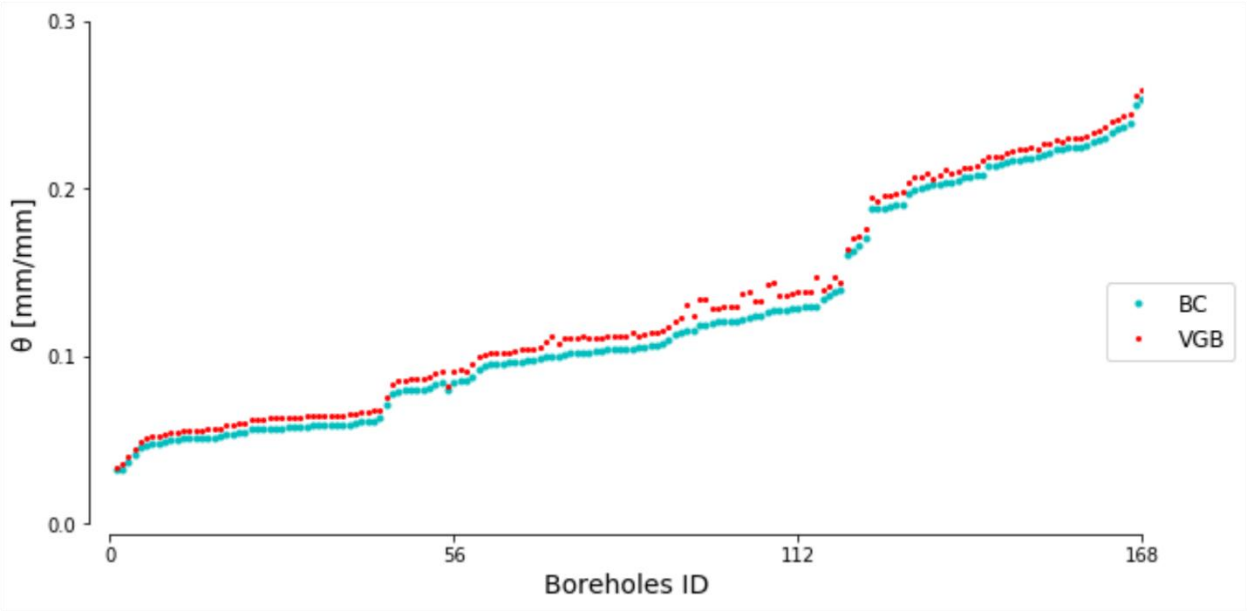


Figure 2.5: Average soil moisture content for 168 locations found in Dijle and Demer catchment, ordered from low to high soil moisture content.

Celerity estimated using the van Genuchten-Burdine model ranges from 179 mm/month to 6367 mm/month, while the Brooks-Corey model estimates values from 148 mm/month to 3597 mm/month (Figure 2.6). Because of the different estimates of soil moisture in the two models, the celerity estimated by the Brooks-Corey model has lower values compared to the van Genuchten-Burdine model.

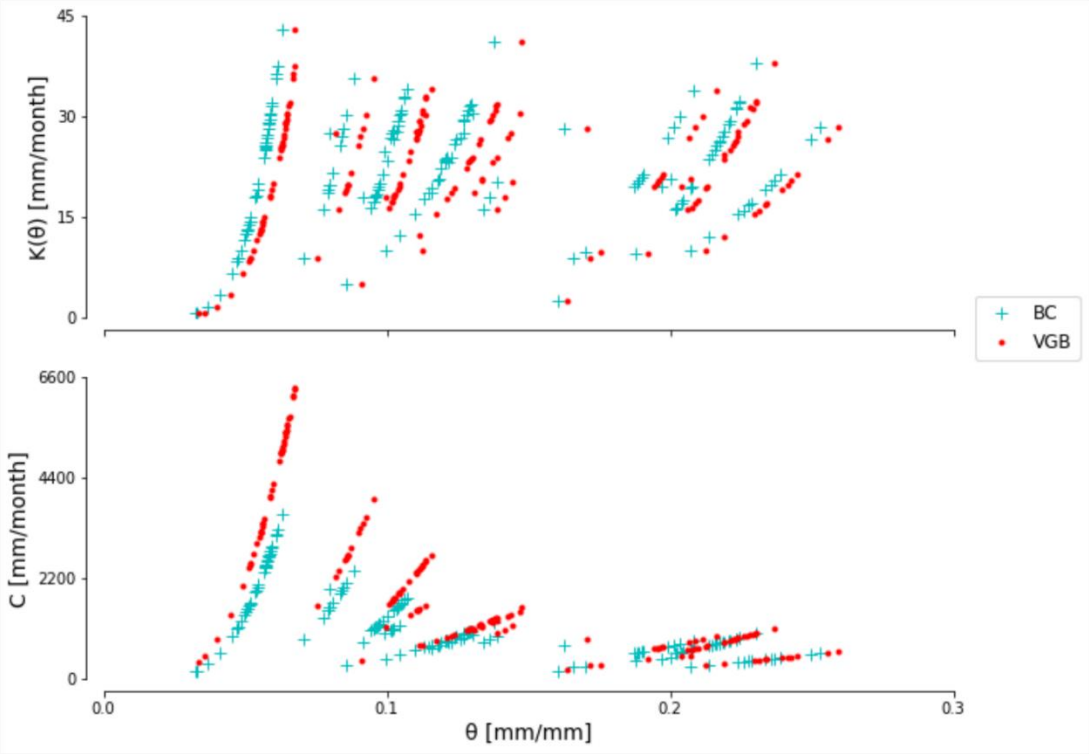


Figure 2.6: van Genuchten-Burdine and Brooks-Corey model soil moisture content and celerity estimation difference using the same groundwater recharge input for 168 sample boreholes. The clustering on the graph corresponds to the type of lithology of the boreholes.

The spatially distributed celerity using Empirical Bayesian Kriging is shown in Figure 2.7. The performance of the interpolation method is indicated in Table 2.2.

Table 2.2: Prediction error of Empirical Bayesian Kriging

Prediction Error	VGB	BC
Root-Mean-Square [mm/month]	1461	691
Mean Standardized [--]	-0.0109	-0.0034
Root-mean-Square Standardized [--]	0.994	0.989
Average standard Error [mm/month]	1452	686

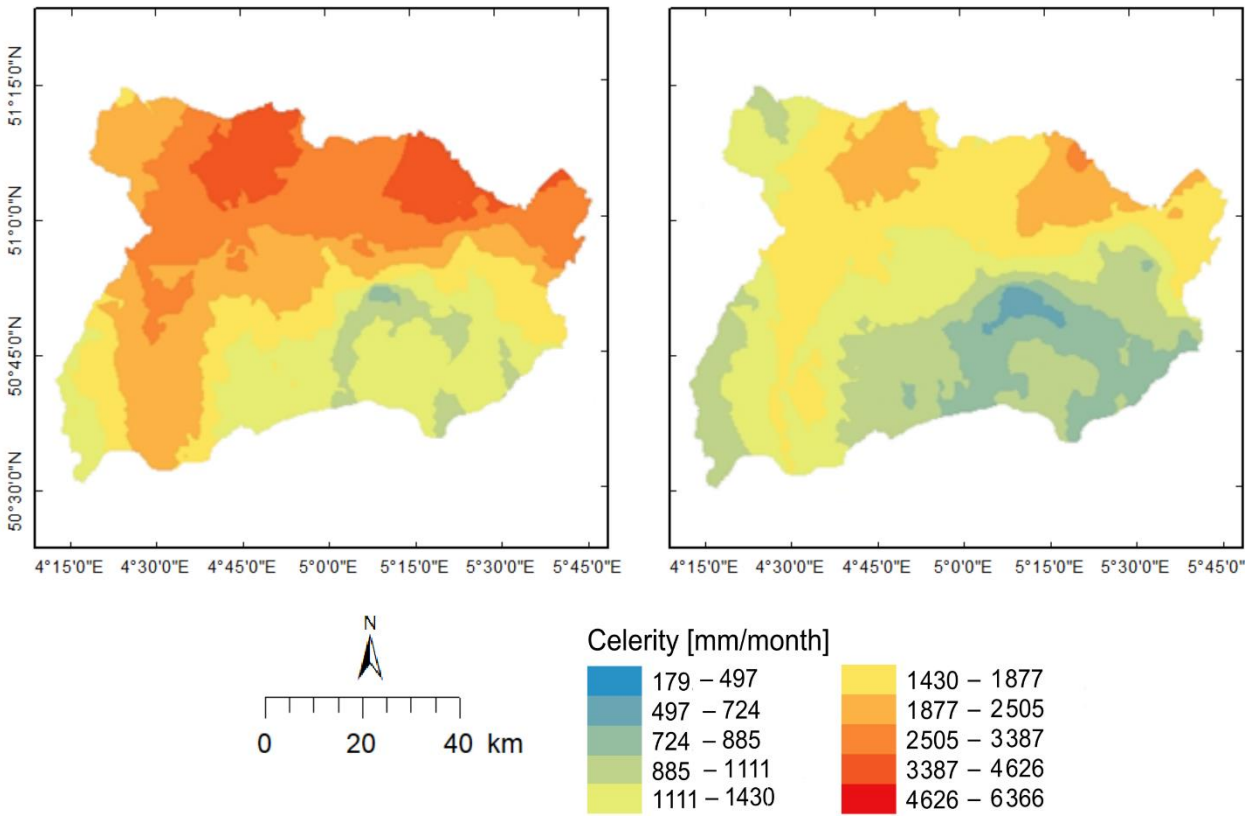


Figure 2.7: Celerity of soil moisture in the vadose zone estimated by van Genuchten Burdine (left) and Brooks_Corey model (right)

2.6.1.2 Groundwater recharge delay

Figure 2.8 shows the distribution of groundwater recharge delay. The estimated groundwater recharge delay in the vadose zone using the Brooks-Corey model ranges from 0 to 110 months, with a spatial mean of 10.32 months, whereas, under the van Genuchten-Burdine model, the delay ranges from 0 to 73 months, with the spatial mean of 6.65 months. The difference map shown in Figure 2.9 shows the spatial distribution of the difference in delay between the Brooks-Corey and van Genuchten-Burdine models. The spatially averaged mean difference is 3.6 months.

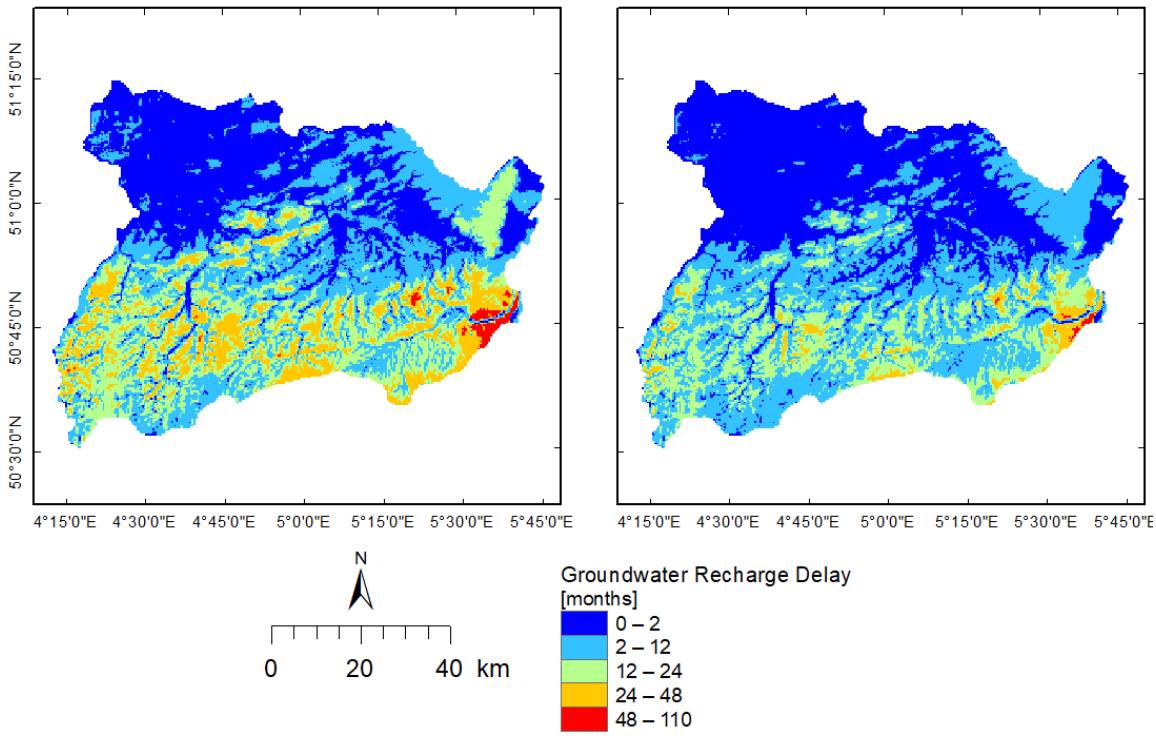


Figure 2.8: Spatially distributed groundwater recharge delay in the vadose zone using the Brooks-Corey parametric model (left) and van Genuchten-Burdine parametric model (right)

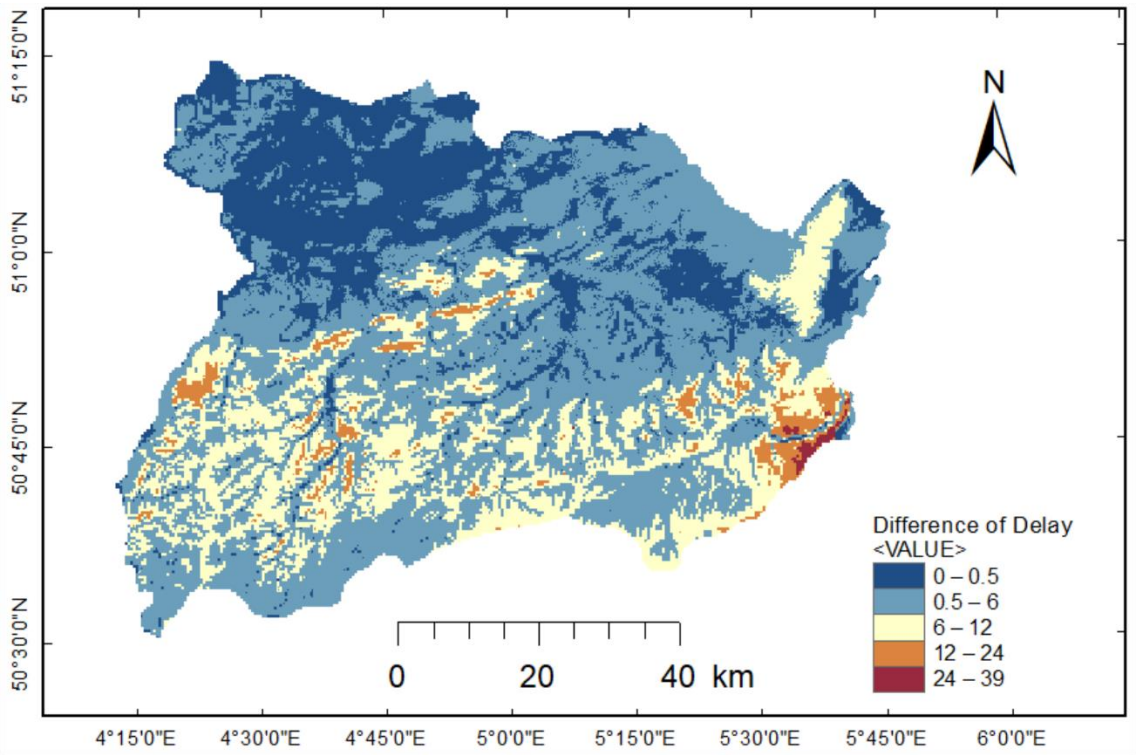


Figure 2.9: Groundwater recharge delay difference between the delay estimated by the Brooks-Corey model and van Genuchten-Burdine model.

Comparing the spatial distribution of recharge delay and Figure 2.3, it is clear that the distribution of the vadose zone thickness and delay have the same pattern. This indicates that the thickness of the vadose zone is the main factor influencing groundwater recharge delay (Figure 2.10). In the northern part of the study area with shallow groundwater, groundwater recharge delay is below 2 months while delay goes up to 110 months in the area found in the southeast with a deep water table.

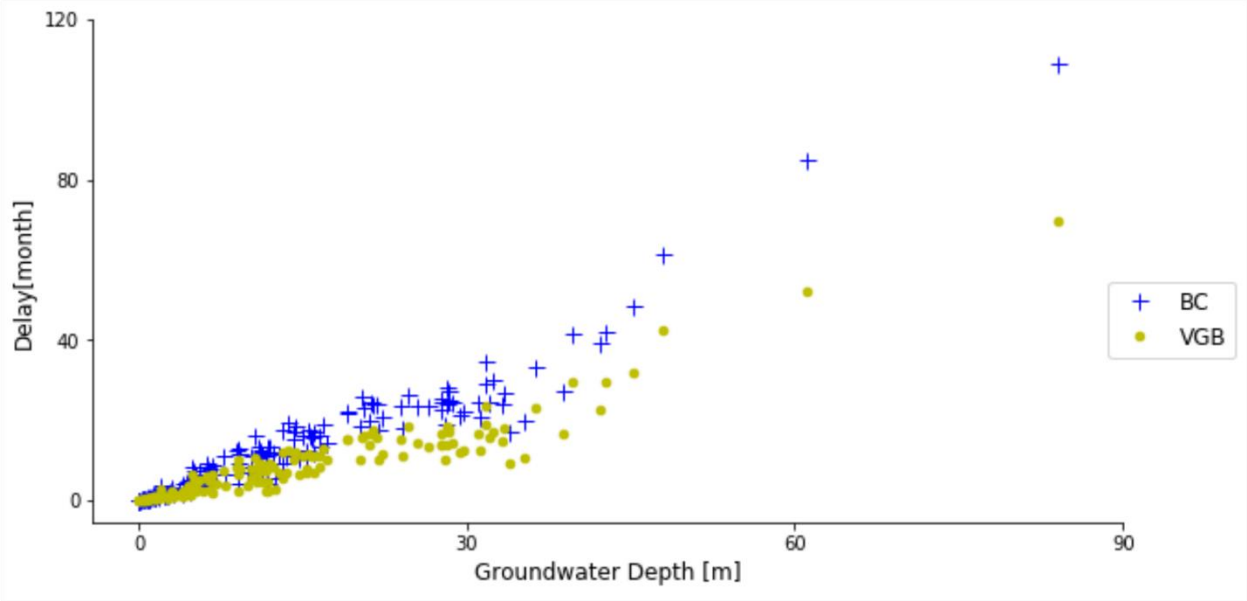


Figure 2.10: Groundwater recharge delay relation with the thickness of the vadose zone

2.6.2 Lumped parametrization of geological layers

2.6.2.1 Soil moisture and celerity

The van Genuchten–Burdine and Brooks–Corey models were also used to estimate soil moisture

content and celerity for each geological layer found in the vadose zone of the study area. Figure 2.11 shows that soil moisture and celerity in the vadose zone are mainly influenced by the hydrogeologic properties of the geological layers (mainly saturated hydraulic conductivity) and groundwater recharge. As in the detailed parameterization approach, for a given groundwater recharge, the van Genuchten-Burdine model gives a higher estimation of celerity than the Brooks-Corey model.

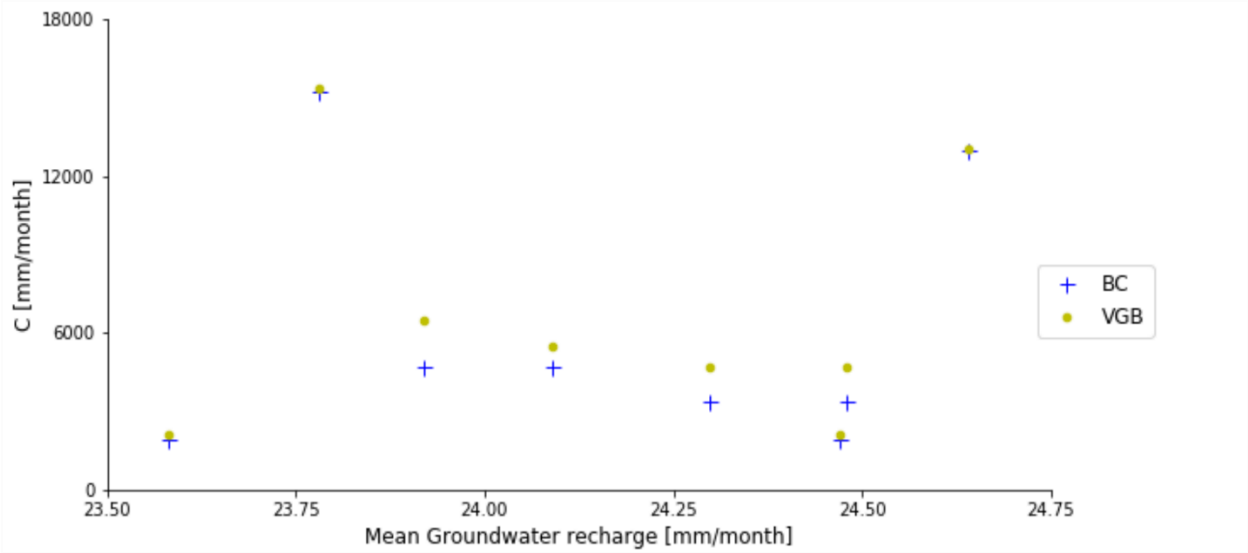


Figure 2.11: Van Genuchten-Burdine and Brooks-Corey model celerity estimation difference using the same groundwater recharge input for eight geological layers found in the vadose zone. The result is ordered layer 1 to layer 8.

2.6.2.2 Groundwater recharge delay

Figure 2.12 and Figure 2.13 show the distribution of the groundwater recharge delay. The estimated groundwater recharge delay in the vadose zone using the Brooks-Corey model ranges from 0 to 26 months. Under the van Genuchten-Burdine model, the delay ranges from 0 to 18 months.

The comparison of the delay estimated in each geological layer using both models allows examination of the contribution of each layer. As most of the vadose zone is found in Quaternary (HCOV 0100) and deposits of the Kempen (HCOV 0200) aquifer systems, the most delay occurs in layer 1.

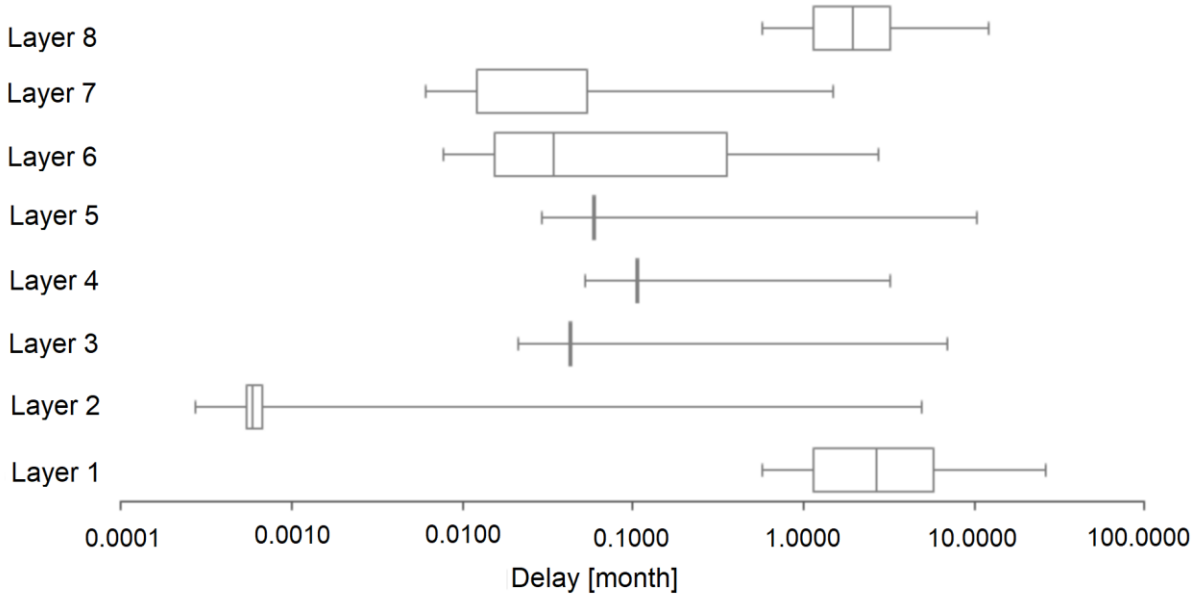


Figure 2.12: Box plots showing the distribution of groundwater recharge delay in each geological layer of the vadose zone using the Brooks-Corey parametric model. See Table 1 for the description of layers.

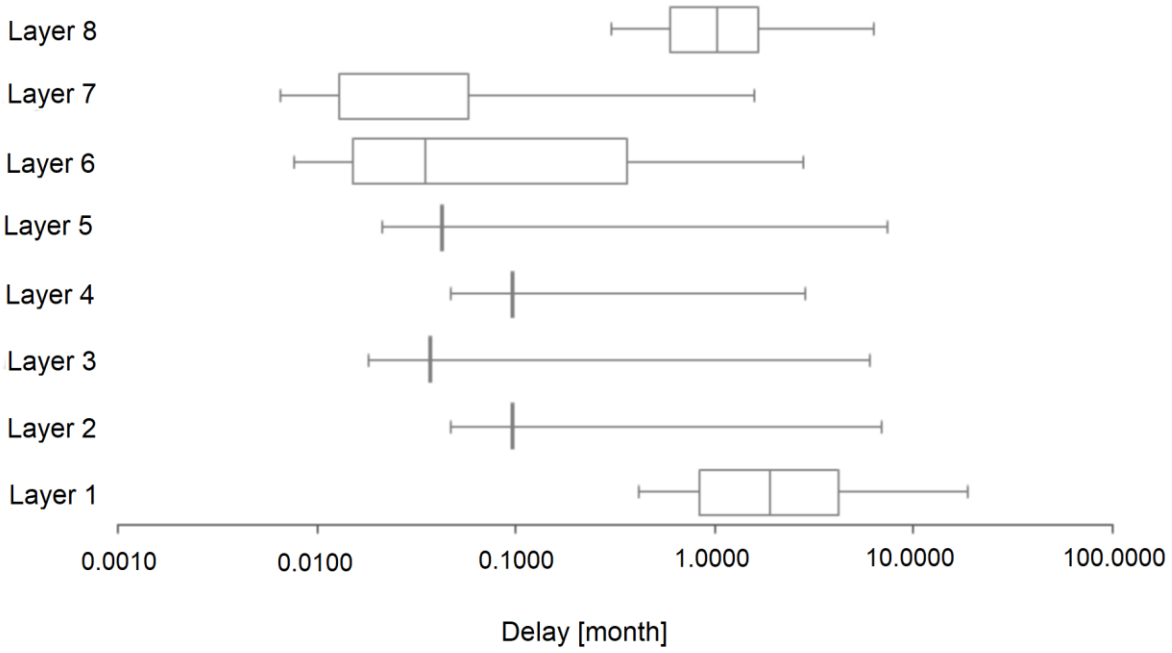


Figure 2.13: Box plots showing the distribution of groundwater recharge delay in each geological layer of the vadose zone using the van Genuchten-Burdine Parametric model. See Table 1 for the description of layers.

2.6.3 Comparison of groundwater recharge delay to physically based conceptual flow model

The delay estimated using the above parametric models from both modeling approaches was compared to output from a physically based flow model (i.e., HYDRUS-1D). Figure 2.14 shows, the approach using a detailed parametrization of the geological layers compares better to the HYDRUS-1D output with a Nash-Sutcliffe Efficiency of 0.89 for Brooks-Corey and 0.79 for van Genuchten-Burdine.

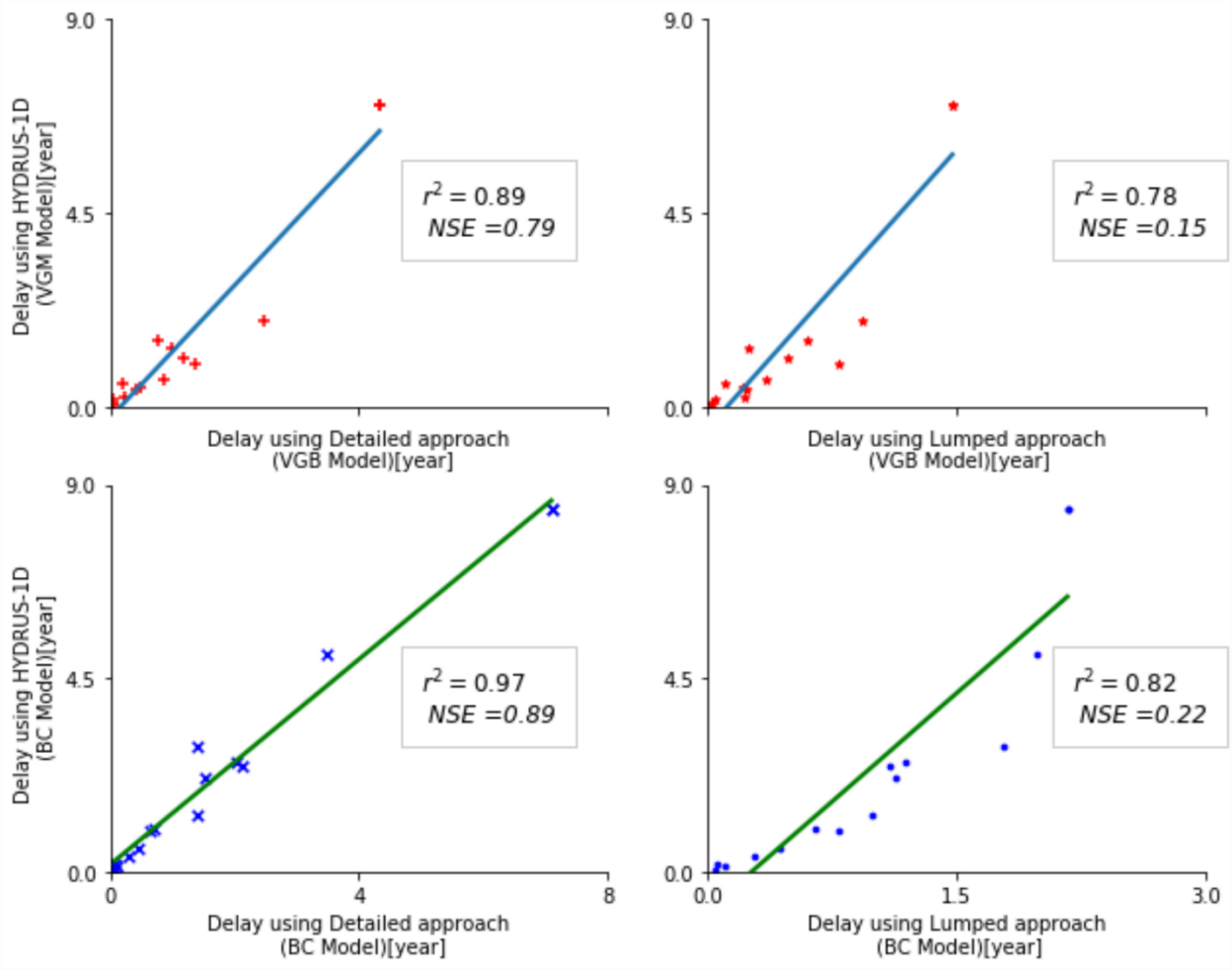


Figure 2.14: Comparison of HYDRUS-1D output with groundwater recharge delay estimated using Brooks Corey and van Genuchten-Burdine method for both detailed parametrization and lumped approaches

The 'models' output from the lumped geological layer approach compares poorly to HYDRUS-1D with a Nash-Sutcliffe Efficiency of 0.22 for Brooks-Corey and 0.15 for van Genuchten-Burdine. However, as a result of the systematical underestimation of the groundwater

recharge delay regarding the output of HYDRUS-1D model output, the coefficient of determination (r^2) is larger than 75%.

2.6.4 Delay effect on groundwater drought

The effect of the recharge delay on the occurrence and timing of groundwater drought was analyzed using a variable threshold method, where the threshold value was calculated as the 70th percentile of the probability of exceedance for the original and delayed recharge time series, for the whole study area and the subareas with deep and shallow groundwater tables.

2.6.4.1 Delay effect on groundwater drought for the whole study area

Figure 2.15 shows the deviation of groundwater recharge from the threshold value in time. Negative anomalies indicate groundwater drought. The result indicates that considering the delay in the vadose zone decreases the number of drought events from 10 to 4 events and the cumulative deficit volume from 49.51 mm to 46.87 mm. However, the average duration of drought events increases from 3 months to 8 months.

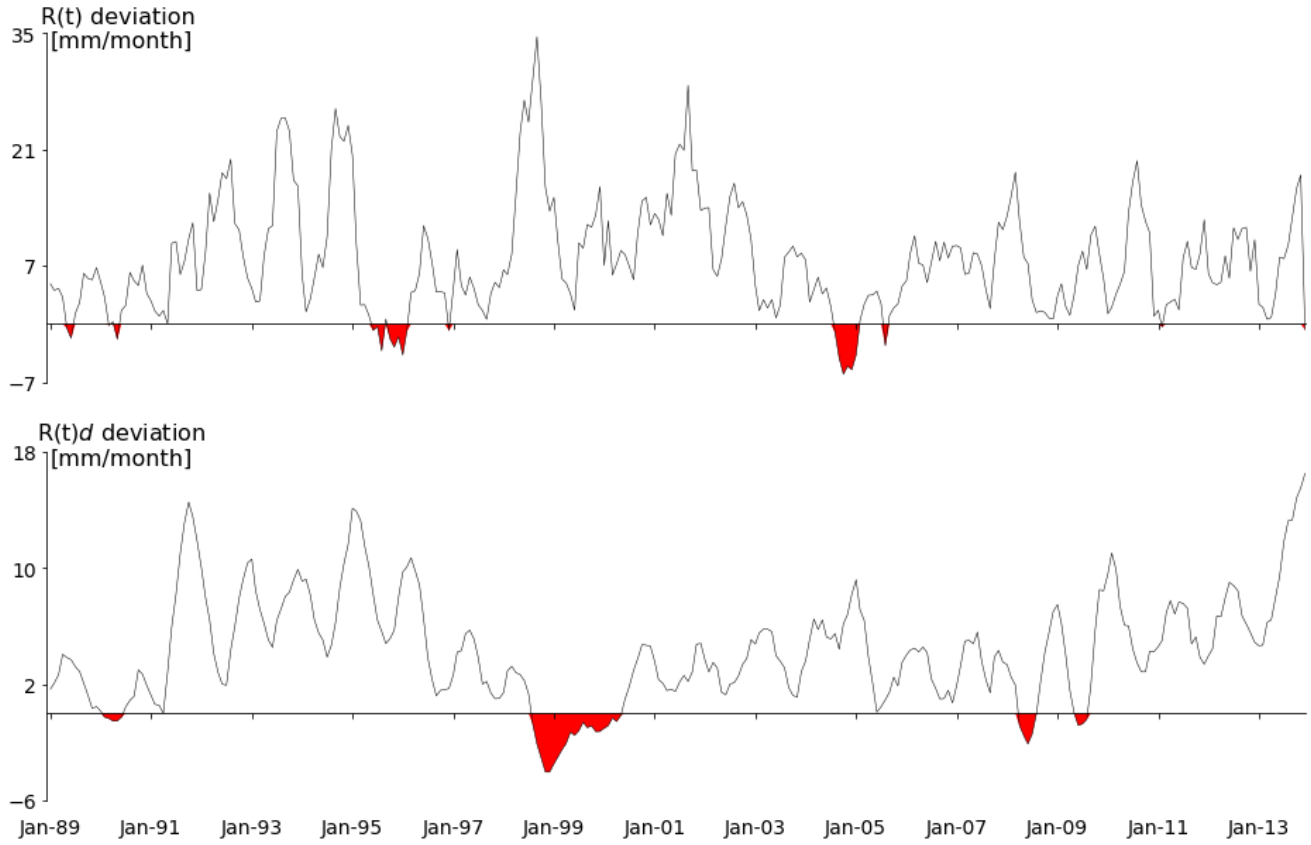


Figure 2.15: Deviation from the threshold value of spatially average monthly groundwater recharge (top) and delayed recharge (bottom) for the whole study area based on 6-month moving average. The red color represents groundwater drought.

This shows that including recharge delay in the unsaturated zone results in fewer but longer groundwater drought events with a lower cumulative deficit volume. Passage of recharge through the unsaturated zone has a smoothing and delaying effect on the occurrence of groundwater drought.

2.6.4.2 Delay effect on groundwater drought for deep water table area

Monthly groundwater recharge and delayed groundwater recharge for deep groundwater area with average groundwater depth of 48 m and delay of 61 months was used to estimate groundwater drought events. Figure 2.16 shows the deviation of both recharges from the threshold value. The result indicates that the first groundwater drought happened on delayed groundwater recharge in July 1994, 61 months later than the first drought event in the original groundwater recharge timeseries. The cumulative deficit of delayed groundwater recharge is 4.8 mm lower. Moreover, considering the delay in the vadose zone, the number of events decreased from 11 to 9 events. This could be because of the larger attenuation in this deep vadose zone and the storage properties of the vadose zone.

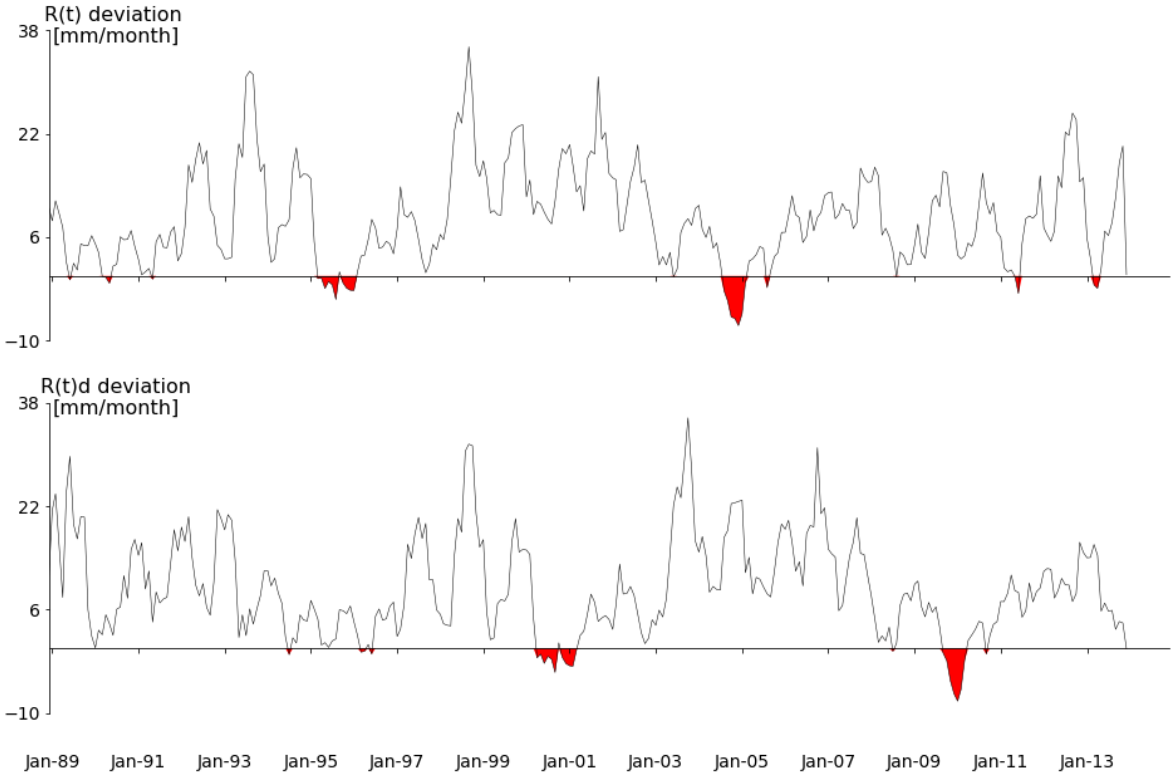


Figure 2.16: Deviation from the threshold value of monthly groundwater recharge (top) and delayed groundwater recharge(bottom) based on 6-month moving average aggregation. The red color represents a groundwater drought. This drought analysis is for the deep groundwater table area with groundwater depth greater than 48m.

The result also shows that the average duration of drought events for delayed recharge and original recharge is 2.6 months and 2.5 months, respectively. Therefore, considering the delay in areas with deep groundwater tables would mainly affect the onset of drought events.

2.6.4.3 Delay effect on groundwater drought for shallow water table area

In the shallow groundwater area, a cumulative deficit of 91.56 mm was calculated versus 92.92 mm for the recharge time series without delay. This small difference in cumulative deficit could be explained by the smaller attenuation in the thin vadose zone and smaller delay time.

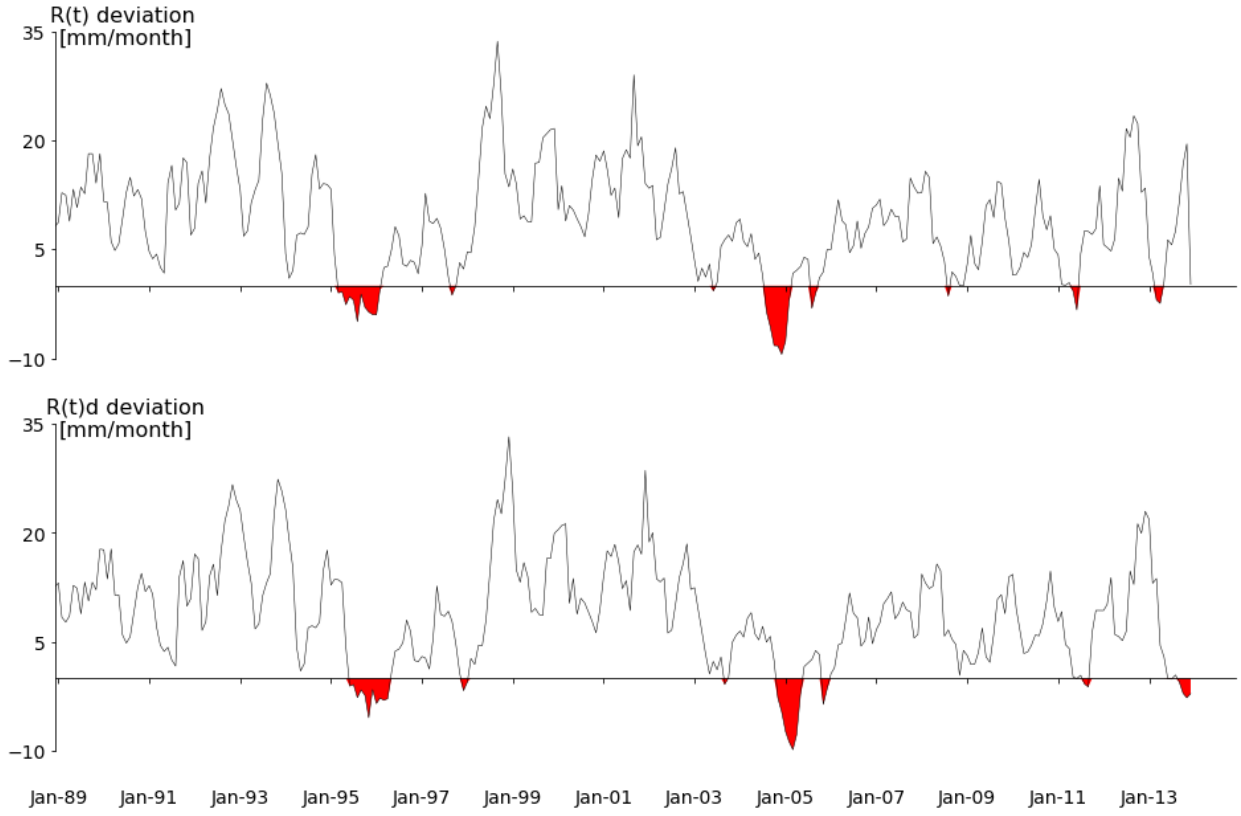


Figure 2.17: Deviation of monthly groundwater recharge (top) and delayed groundwater recharge(bottom) based on 6-month moving average aggregation from the threshold value. The red color represents a groundwater drought. This drought analysis is for shallow groundwater table area with maximum groundwater depth of 5m.

The number of drought events estimated using both recharge time series is the same, i.e., ten events. However, Figure 2.17 shows that the first groundwater drought with delayed recharge happened in Oct 1983, 3 months after the first drought event in the undelayed groundwater recharge time series.

2.7 Conclusion

In this study, spatially distributed groundwater recharge delay through the vadose zone was estimated in the Dijle and Demer catchments in Central Belgium. This estimation was conducted using two mathematical models developed by combining the kinematic wave approximation of 'Richards' equation with two parametric models describing the soil hydraulic properties, i.e., the Brooks–Corey and van Genuchten–Burdine models.

The vertical soil moisture velocity or celerity was influenced by saturated hydraulic conductivity and soil moisture content in the vadose zone for both models. The Brooks–Corey model estimated lower celerity compared to the van Genuchten–Burdine model.

The calculated delay was compared to the physically based flow model HYDRUS-1D. Delays calculated based on a detailed parametrization of the soil and geological layers are very similar to the HYDRUS-1D results, with a Nash–Sutcliffe efficiency of 0.89 for Brooks–Corey and 0.80 for van Genuchten–Burdine. However, in both models, there is a slightly systematic underestimation of the delay compared to the HYDRUS-1D model.

The estimated spatially distributed groundwater recharge delay in the vadose zone using the Brooks–Corey model ranges from 0 to 110 months, with a spatial mean of 10.3 months. Using the van Genuchten–Burdine model, the delay ranges from 0 to 73 months, with a spatial mean of 6.7 months. The thickness of the vadose zone is the main parameter influencing the spatial distribution of this delay. In regions with shallow groundwater (< 10 m), the groundwater recharge delay is less than 2 months, whereas the delay is up to 110 months for areas with a deep water table (> 40 m).

The delay effect on groundwater drought was analyzed by implementing the delay result of the Brooks–Corey model on the groundwater recharge time series from 1980 to 2013. Groundwater drought characterization features like number, duration, onset, and intensity of drought events were influenced by the delay in the vadose zone.

Finally, from this study, the Brooks–Corey model with a detailed parametrization of the geological layers is recommended to estimate spatially distributed groundwater delay. Besides this, incorporating this delay in groundwater drought delay analysis does affect the timing of groundwater drought significantly. Therefore, combining the delay in the vadose zone with drought propagation in the hydrological cycle is recommended for future studies. The applicability of the findings and methodology of this research depends on the nature of

the vadose zone. In this paper, the method is applied and tested in low land areas. The applicability of the method in mountain catchments needs further investigation.

2.8 References

Abdollahi, K., Bashir, I., Verbeiren, B., Harouna, M., van Griensven, A., Huysmans, M., Batelaan, O., 2017. A distributed monthly water balance model : formulation and application on Black Volta Basin. Environ. Earth Sci. 76(5), 1–18. doi:10.1007/s12665-017-6512-1

Batelaan, O., De Smedt, F., 2007. GIS-based recharge estimation by coupling surface-subsurface water balances. J. Hydrol. 337, 337–355. doi:10.1016/j.jhydrol.2007.02.001

Batelaan, O., DeSmedt, F., 2001. WetSpass: a flexible, GIS based, distributed recharge methodology for regional groundwater modelling, in: Proceedings of a Symposium Held during the Sixth IAHS Scientific Assembly (Impact of Human Activity on Groundwater Dynamics). IAHS-AISH, Maastricht, The Netherlands, pp. 11–17.

Beven, K., 2012. Evolution of Rainfall–Runoff Models: Survival of the Fittest?, in: Rainfall-Runoff Modelling. John Wiley & Sons, Ltd: Chichester, UK, pp. 25–50. doi:10.1002/9781119951001.ch2

Beyene, B. S., Van Loon, A. F., Van Lanen, H. A. J., Torfs, P. J. J. F., 2014. Investigation of variable threshold level approaches for hydrological drought identification. Hydrol Earth Syst Sci Discuss. 12765–12797. doi:10.5194/hessd-11-12765-2014

Brooks, R.H., Corey, a T., 1964. Hydraulic properties of porous media. Hydrology Papers; Colorado State University: Fort Collins, CO, USA, 3 (3), 27 pgs. doi:citeulike-article-id:711012

Brooks, R.H., Corey, A.T., 1966. Properties of Porous Media Affecting Fluid Flow. J. Irrig. Drain. Div. Am. Soc. Civ. Eng. 92, 61–88.

Burdine, N.T., 1953. Relative permeability calculations from pore size distribution data. J. Pet. Technol. 5, 71–78. doi:10.2118/225-G

Charbeneau, R.J., 1999. Groundwater hydraulics and pollutant transport. Prentice Hall: Upper Saddle River, NJ, USA, p. 593. ISBN 0-13-975616-7.

Charbeneau, R.J., 1984. Kinematic Models for Soil Moisture and Solute Transport. Water Resour. Res. 20, 699–706. doi:10.1029/WR020i006p00699

Cools, J.; Meyus, Y.; Batelaan, O.; De Smedt, F., 2002. A large-scale hydrogeological database and groundwater model for Flanders: a tool for integrated groundwater management, In Proceedings of the Hydrology Days 2002 (Twenty Second Annual American Geophysical Union), Colorado State University, Fort Collins, CO, USA, pp. 46–55.

Cosby, B.J., Hornberger, G.M., Clapp, R.B., Ginn, T.R., 1984. A Statistical Exploration of the Relationships of Soil Moisture Characteristics to the Physical Properties of Soils. Water Resour. Res. 20, 682–690. doi:10.1029/WR020i006p00682

Fernandez-Illescas, C.P., Rodriguez-Iturbe, I., 2001. The Ecohydrological Importance of Soil Texture in Water-Limited Ecosystems. Water Resour. Res. 37, 2863–2872.

doi:10.1029/2000WR000121

Germann, P.F., Beven, K., 1985. Kinematic Wave Approximation to Infiltration Into Soils With Sorbing Macropores. Water Resour. Res. 21, 990–996. doi:10.1029/WR021i007p00990

Grismer, M.E., 2013. Estimating agricultural deep drainage lag times to groundwater: Application to Antelope Valley, California, USA 393, 378–393. doi:10.1002/hyp.9249

Hazen, A., 1914. Storage to be provided in impounding reserviors for municipal water supply. Am. Soc. Civ. Eng. 39, 1943–2044.

Hocking, M., Kelly, B.F.J., 2016. Groundwater recharge and time lag measurement through Vertosols using impulse response functions. J. Hydrol. 535, 22–35. doi:10.1016/j.jhydrol.2016.01.042

Kollet, S.J., Maxwell, R.M., 2008. Capturing the influence of groundwater dynamics on land surface processes using an integrated, distributed watershed model. Water Resour. Res. doi:10.1029/2007WR006004

Kollet, S.J., Maxwell, R.M., Woodward, C.S., Smith, S., Vanderborght, J., Vereecken, H., Simmer, C., 2010. Proof of concept of regional scale hydrologic simulations at hydrologic resolution utilizing massively parallel computer resources. Water Resour. Res. 46, 1–7. doi:10.1029/2009WR008730

Lighthill, M.J., Whitham, G.B., 1955. On Kinematic Waves. I. Flood Movement in Long Rivers. Proc. R. Soc. A Math. Phys. Eng. Sci. 229, 281–316. doi:10.1098/rspa.1955.0088

Mattern, S., Vanclooster, M., 2010. Estimating travel time of recharge water through a deep vadose zone using a transfer function model. Environ. Fluid Mech. 10, 121–135. doi:10.1007/s10652-009-9148-1

Miller, J.E., 1984. Basic Concepts of Kinematic-Wave Models. U.S. Geological Survey Professional Paper 1302; U. S. Geological Survey: Alexandria, VA, USA.

Ministerie Vlaamse Gemeenschap, 2004. Departement Leefmilieu en Infrastructuur, Administratie Milieu-, Natuur-, Land- en Waterbeheer, Afdeling Water. Ontwikkelen van regionale modellen ten behoeve van het Vlaams Grondwater Model (VGM) in GMS/MODFLOW 2004a. Perceel nr. 1: Centraal Kempisch Model. Publisher: Ministerie Vlaamse Gemeenschap, Bruxelles, Belgium.

Ministerie Vlaamse Gemeenschap, 2004. Departement Leefmilieu en Infrastructuur, Administratie Milieu-, Natuur-, Land- en Waterbeheer, Afdeling Water. Ontwikkelen van regionale modellen ten behoeve van het Vlaams Grondwater Model (VGM) in GMS/MODFLOW 2004b. Perceel nr. 3: Brulandkrijt Model. Publisher: Ministerie Vlaamse Gemeenschap, Bruxelles, Belgium.

Mirzaei, R. and Sakizadeh, M.: Comparison of interpolation methods for the estimation of groundwater contamination in Andimeshk-Shush Plain, Southwest of Iran, Environ. Sci. Pollut. Res., 23(3), 2758–2769, doi:10.1007/s11356-015-5507-2, 2016.

Mualem, Y., 1978. Hydraulic conductivity of unsaturated porous media: Generalized macroscopic appraoch. Water Resour. Res. 14, 325–334. doi:10.1029/WR014i002p00325

Nimmo, J.R., 2005. Unsaturated zone flow processes. Encycl. Hydrol. Sci. 24. doi:10.1002/0470848944

Peters, E., 2003. Propagation of drought through groundwater systems Illustrated in the Pang (UK) and Upper-Guadiana (ES) catchments. Ph.D. Thesis, Wageningen University, Wageningen, The Netherlands. 221 pp.

Peters, E., Bier, G., van Lanen, H.A.J., Torfs, P.J.J.F., 2006. Propagation and spatial distribution of drought in a groundwater catchment. J. Hydrol. 321, 257–275. doi:10.1016/j.jhydrol.2005.08.004

Peters, E., Torfs, P.J.J.F., van Lanen, H.A.J., Bier, G., 2003. Propagation of drought through groundwater - A new approach using linear reservoir theory. Hydrol. Process. 17, 3023–3040. doi:10.1002/hyp.1274

Peters, E., van Lanen, H.A.J., 2003. Propagation of drought in groundwater in semi-arid and sub-humid climatic regimes. In Proceedings of the International Symposium of Hydrology of the Mediterranean and Semi-Arid Regions, Montpellier, France, 278, pp. 312–317.

Rasmussen, T.C., Baldwin, R.H., Dowd, J.F., Williams, A.G., 2000. Tracer vs. Pressure Wave Velocities through Unsaturated Saprolite. Soil Sci. Soc. Am. J. 64, 75. doi:10.2136/sssaj2000.64175x

Rossman, N.R., Zlotnik, V.A., Rowe, C.M., Szilagyi, J., 2014. Vadose zone lag time and potential 21st century climate change effects on spatially distributed groundwater recharge in the semi-arid Nebraska Sand Hills. J. Hydrol. 519, 656–669. doi:10.1016/j.jhydrol.2014.07.057

Sargent, R.G., 2011. Verification and validation of simulation models. Proc. 2011 Winter Simul. Conf. 2194–2205. https://doi.org/10.1109/WSC.2011.6148117

Scaini, A., Audebert, M., Hissler, C., Fenicia, F., Gourdol, L., Pfister, L., Beven, K.J., 2017. Velocity and celerity dynamics at plot scale inferred from artificial tracing experiments and time-lapse ERT. J. Hydrol. 546, 28–43. doi:10.1016/j.jhydrol.2016.12.035

Sisson, J.B., Ferguson, A.H., 1980. Simple Method for Predicting Drainage from Field Plots 1 Soil Sci. Soc. Am. J. 44, 1147–1152.

Smith, R.E., 1983. Approximate Soil Water Movement by Kinematic Characteristics1. Soil Sci. Soc. Am. J. 47, 3. doi:10.2136/sssaj1983.03615995004700010001x

Tricot, C., Debontridder, L., Van de Vyver, H., Vandiepenbeek, M., Dewitte, S., De Backer, H., Malderen, R., Vannitsem, S., Roulin, E., 2015. Oog voor het Klimaatt/Vigilance climatique. Royal Meteorological Institute of Belgium: Bruxelles, Belgium.

van Genuchten, M.T., 1980. A Closed-form Equation for Predicting the Hydraulic Conductivity of Unsaturated Soils1. Soil Sci. Soc. Am. J. 892. doi:10.2136/sssaj1980.03615995004400050002x

van Genuchten, M.T., Pachepsky, Y.A., 2011. Hydraulic properties of unsaturated soils. In Encyclopedia of Earth Sciences Series. Springer Netherlands, pp. 368–375. doi:10.1007/978-90-481-3585-1_69

Van Lanen, H.A.J., 2006. Drought propagation through the hydrological cycle, In climate variability and change—Hydrological impacts. In Proceedings of the Fifth FRIEND World Conference held, Havana,Cuba, Volume 308, pp. 122–127.

van Loon, A.F. Van, 2013. On the propagation of drought How climate and catchment characteristics influence hydrological drought development and recovery. Ph.D. Thesis,

Wageningen University, Wageningen, The Netherlands. Available online: http://edepot.wur.nl/249786 (accessed on 11 June 2019).

Vandersteen, K., Gedeon, M., 2013. Hydrogeology of North-East Belgium; External Report of Belgian Nuclear Research Centre, SCK•CEN-ER-236; SCK CEN: Mol, Belgium.

Verbeiren, B., Huysmans, M., Tychon, B., Jacquemin, I., Canters, F., Vanderhaegen, S., Engelen, G., Poelmans, L., De Becker, P., Tsakiris, G., Vangelis, H., Batelaan, O., 2013. Drought-related vulnerability and risk assessment of groundwater resources under temperate conditions. In Proceedings of the 13th International Conference on Environmental Science and Technology, Athens, Greece, p. 10.

VMM, 2008. Grondwater in Vlaanderen: Het Brulandkrijtsysteem. Publisher: Flanders Environmental Agency, Aalst, Belgium.

Yao, X., Fu, B., Lü, Y., Sun, F., Wang, S. and Liu, M.: Comparison of Four Spatial Interpolation Methods for Estimating Soil Moisture in a Complex Terrain Catchment, PLoS One, 8(1), doi:10.1371/journal.pone.0054660, 2013.

Yevjevich, V., 1967. An objective approach to definitions and investigations of continental hydrologic droughts. Hydrology Papers; Colorado State University: Fort Collins, CO, USA, 1967; Volume 23, p. 25.

Chapter 3

3 Groundwater drought propagation in the hydrological cycle in temperate climate regions

Based on: Wossenyeleh, B. K., Worku, K. A., Verbeiren, B., and Huysmans, M.: Drought propagation and its impact on groundwater hydrology of wetlands: a case study on the Doode Bemde nature reserve (Belgium), Nat. Hazards Earth Syst. Sci., 21, 39–51, doi:10.5194/nhess-21-39-2021, 2021.

Wossenyeleh, B. K., Verbeiren, B., and Huysmans, M.: Drought propagation in temperate climate regions: A case study on the Dijle river catchment and parts of the Demer and Zenne basins (Belgium), Hydrogeology journal, in preparation, 2021

3.1 Abstract

Drought can be described as a temporary decrease in water availability over a significant period and affects both surface and groundwater resources. Droughts propagate through the hydrological cycle and may impact vulnerable ecosystems such as rivers and wetlands fed by groundwater. This chapter investigates drought propagation in the hydrological cycle and assesses its impact on a groundwater-fed wetland ecosystem. Meteorological drought indices were used to analyze meteorological drought severity. Besides, a method for assessing groundwater drought and its propagation in the aquifer was developed and applied. Groundwater drought was analyzed using the variable threshold method. Furthermore, meteorological drought and groundwater recharge drought were compared to investigate drought propagation in the hydrological cycle. This research is carried out in the Dijle river catchment and parts of the Demer and Zenne basins in central Belgium.

The results of this research show that droughts are attenuated in the groundwater system. The number and severity of drought events of groundwater discharge to river and wetlands were smaller than for groundwater recharge. However, the onset of both groundwater drought events occurred with a short delay, indicating a quick response of the groundwater system to hydrological stresses. In addition, drought propagation in the hydrological cycle indicated that not all meteorological droughts result in groundwater drought. Furthermore, this drought propagation effect was also observed in the Doode Bemde wetland in the Dijle catchment.

3.2 Introduction

Drought can be described as a temporary decrease in water availability over a significant period and caused by deficient precipitation and/or high evapotranspiration. Droughts propagate through the hydrological cycle and affect both surface and groundwater resources (Bloomfield and Marchant, 2013; Calow et al., 1997; Mishra and Singh, 2010; Wilhite, 2000).

If drought concerns groundwater, it is called groundwater drought. Groundwater drought can be defined as a temporary decrease in groundwater availability over a significant period (Peters and van Lanen, 2003). Groundwater drought results in decreased groundwater levels and discharges to surface water bodies (Peters, 2003a). As groundwater systems are often slowly responding to drought, groundwater drought is often characterized by long recovery periods (Calow et al., 1997). Groundwater drought and its impacts have been less studied than other aspects of drought (Verbeiren et al., 2013; Wilhite and Glantz, 1985).

During drought propagation, meteorological drought may result in decreased water input for the hydrological system such as streams, soil moisture storages, and groundwater. That means that meteorological drought may cause hydrological drought but not every meteorological drought results in an equally severe hydrological drought (Van Lanen, 2006). Conversely, a series of minor meteorological droughts can turn into a severe hydrological drought (Van Lanen, 2006; van Loon et al., 2011). This drought propagation in the hydrological cycle is controlled by catchment characteristics and the climate's nature and seasonality (Eltahir and Yeh, 1999; Van Loon and Van Lanen, 2012; van Loon, 2013; Peters et al., 2003). Moreover, in drought propagations, the drought characteristics such as duration, severity, and onset behave differently in different drought types.

In the context of Belgium, Tricot et al. (2015) have shown that meteorological drought periods have not intensified during the last century. The meteorological drought periods were defined as the number of consecutive days without significant precipitation (less than 0.5 mm) for the six hottest months of the year. However, the authors suggest that their findings do not apply to all forms of drought. For instance, when investigating groundwater drought, precipitation deficits over longer periods (seasons to years) need to be investigated (Tricot et al., 2015). Furthermore, climate change projections for Belgium predict drier summers for the coming century, causing drought conditions (Hoyaux et al., 2016; Tabari et al., 2015).

Like other drought types, groundwater droughts can have severe socio-economic and environmental impacts (Verbeiren et al., 2013). Streams fed by groundwater may run dry if the groundwater system feeding them is affected by drought. These droughts may have significant implications on water supply, agriculture, and ecology. For example, droughts such as the one experienced in the summer of 2018 may significantly impact the groundwater discharge that is feeding wetlands and streams (Ridder et al., 2020). Therefore, investigating groundwater drought is a crucial step towards groundwater management.

Groundwater drought can be assessed by investigating groundwater recharge, groundwater level, and groundwater discharge with a high spatial and temporal resolution (Van Lanen and Peters, 2002). Although data on the groundwater levels (H) are typically available with a high temporal resolution, this is usually not the case for groundwater recharge (R) and groundwater discharge (Q) data. Therefore, numerical models are used to simulate these hydrological variables with high temporal and spatial resolution.

Numerical groundwater models are useful for simulating groundwater head and discharge if the necessary data are available and if proper boundary conditions are defined and implemented. Temporal and spatial variations of these variables can be obtained so that further analyses could be performed to identify drought periods. The effect of groundwater abstraction on the occurrence of groundwater drought can also be assessed by incorporating it into the models. Some previous studies (Peters, 2003a; Peters et al., 2006) have used groundwater models to simulate groundwater level and discharge in spatial and temporal scales and investigate groundwater drought using a constant threshold value method. In this thesis, variable threshold value methods and standardized groundwater index (SGI) were combined with groundwater modeling to investigate groundwater drought in the aquifer.

This chapter aims to investigate drought propagation in the hydrological cycle by developing and applying a method for simulating meteorological drought, groundwater drought, and its propagation in the aquifer. The method combines a water balance model and a groundwater flow model with a threshold method to determine groundwater drought and its effect on groundwater discharge. Moreover, its impact on wetlands and surface water bodies were also investigated.

3.3 Methodology

3.3.1 Study area and data

The study area consists of the Dijle catchment and parts of the Demer and Zenne basins in central Belgium and has a surface area of 1825 km^2 (Figure 3.1). The most important aquifer in this catchment is the Brussels Sands aquifer, and the land surface elevation ranges between 10 m and 110 m. Belgium has a temperate climate with a long-term average annual rainfall of around 800 mm and an average temperature of approximately 10 ^oC (RMI, 2020).

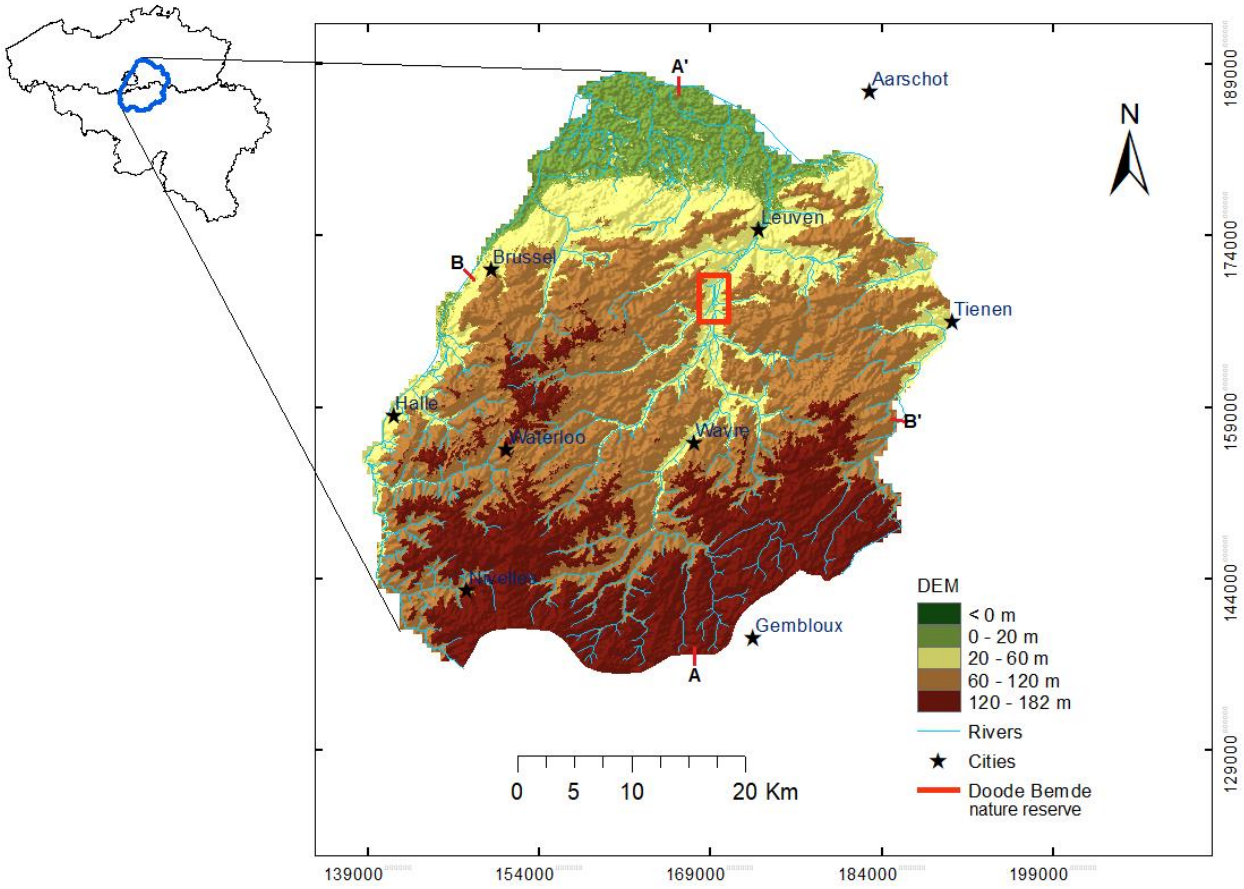


Figure 3.1: Location of the study area, the digital elevation model (DEM) in Belgium

In the middle of the study area, the Dijle river has cut through the surrounding hills to form a 1 km wide and 40 m deep north-south oriented valley (De Becker et al., 2006). The hills are situated in the western and eastern parts of the study area

The land cover in the area is predominantly grassland in the western and arable lands in the eastern part of the study area. Around 70% of the soil in the study area is silty loam, and the area has a gentle slope that varies between 0.00^{o} to 19.34^{o}.

Hydrogeological studies on the Dijle catchment show that the top aquifers are unconfined with thicknesses ranging from 0 to 120 m. The Dijle river has cut into the sandy tertiary formations of Lede (Ld), Brussel (Br), and the clayey formation of Kortrijk (Ko). During the Quaternary, a relatively thick layer of loam was deposited in the central valley. A successive deposition of Quaternary deposits near the river further shaped the valley due to repetitive inundations (Figure 3.2).

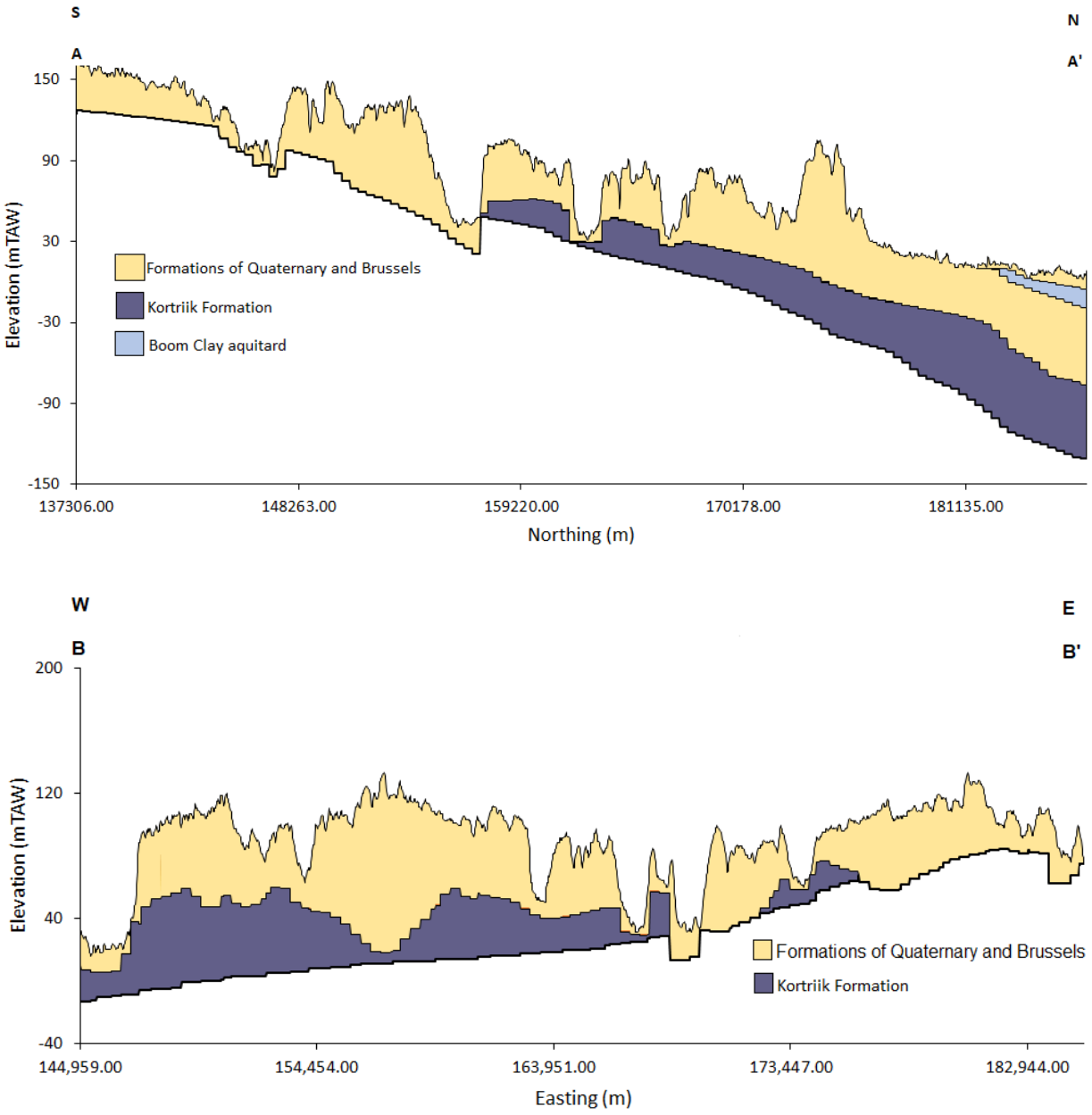


Figure 3.2: Hydrogeological S-N (top) and W-E (bottom) cross-sections through the study area. The location of the cross-section is indicated in Figure 3.1 A-A' and B-B', respectively. The elevation is measured from a Belgian referencing system for elevation called TAW ("Tweede Algemene Waterpassing")

Spatially distributed groundwater recharge generated in the GroWaDRISK (Drought-related vulnerability and risk assessment of groundwater resources in Belgium) project funded by the Belgian Federal Science Policy Office (BELSPO) was used. This project was aiming for the development of a drought-related vulnerability and risk assessment strategy for sustainable management of groundwater resources under temperate conditions (Verbeiren et al., 2013).

In the GroWaDRISK project, a monthly averaged spatially distributed groundwater recharge time series from 1980 to 2013 was estimated using the WetSpass-M model. WetSpass is a physically-based model for estimating spatially distributed surface runoff, actual evapotranspiration, and groundwater recharge (Batelaan and De Smedt, 2001). This model accounts for spatially distributed land use, soil type, slope, elevation, monthly average groundwater depth, and meteorological conditions as an input (Abdollahi et al., 2017; Batelaan and De Smedt, 2007). However, since the recharge obtained from WetSpass corresponds to the infiltration at the bottom of the root zone, it did not take into account the delay of recharge in the unsaturated zone between the root zone and the groundwater table. Therefore, a delay estimated using Brooks_Corey model was implemented on the recharge extracted from the WetSpass model to account for the time it takes for water to reach the groundwater table from the root zone (Chapter 2, Wossenyeleh et al., 2020). Therefore, every month of the original groundwater recharge is shifted based on the amount of the delay calculated for the every particular period.

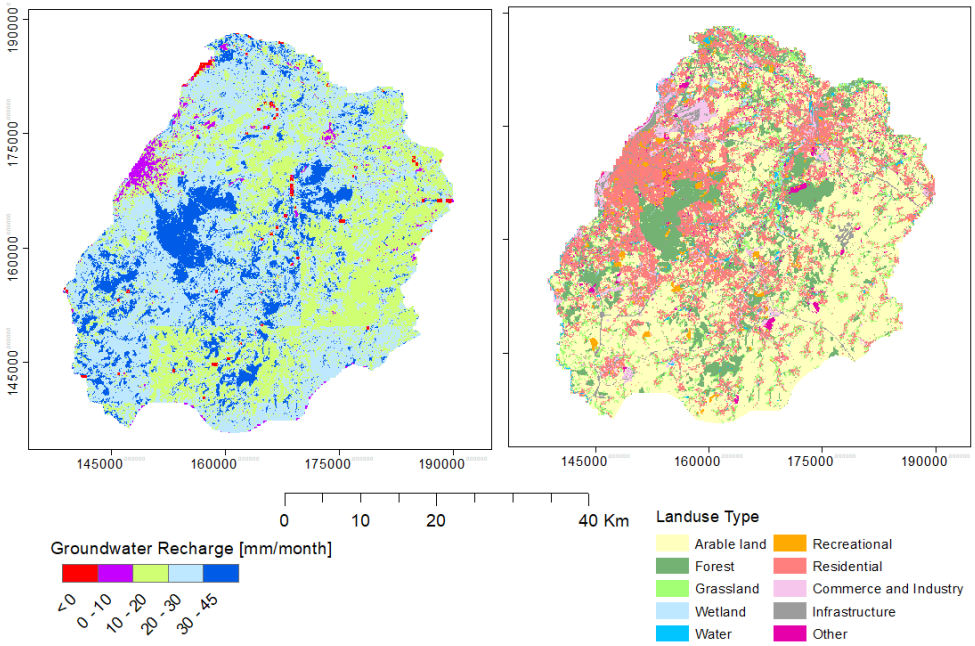


Figure 3.3: Monthly averaged delayed groundwater recharge from 1980 to 2013 of the study area, estimated using WetSpass (left) and land cover class (right)

The estimated groundwater recharge is larger than 10 mm/month in most of the study area, and the spatial average is 23.12 mm/month (Figure 3.3). The zones indicated in red have very shallow groundwater levels (abundant water availability) might resulting in high evapotranspiration rates exceeding infiltration or excess surface runoff or drainage and leading to a "negative" net recharge.

3.3.2 Methods

The study was divided into three parts; meteorological drought analysis, groundwater modeling, and groundwater drought analysis (Figure 3.4).

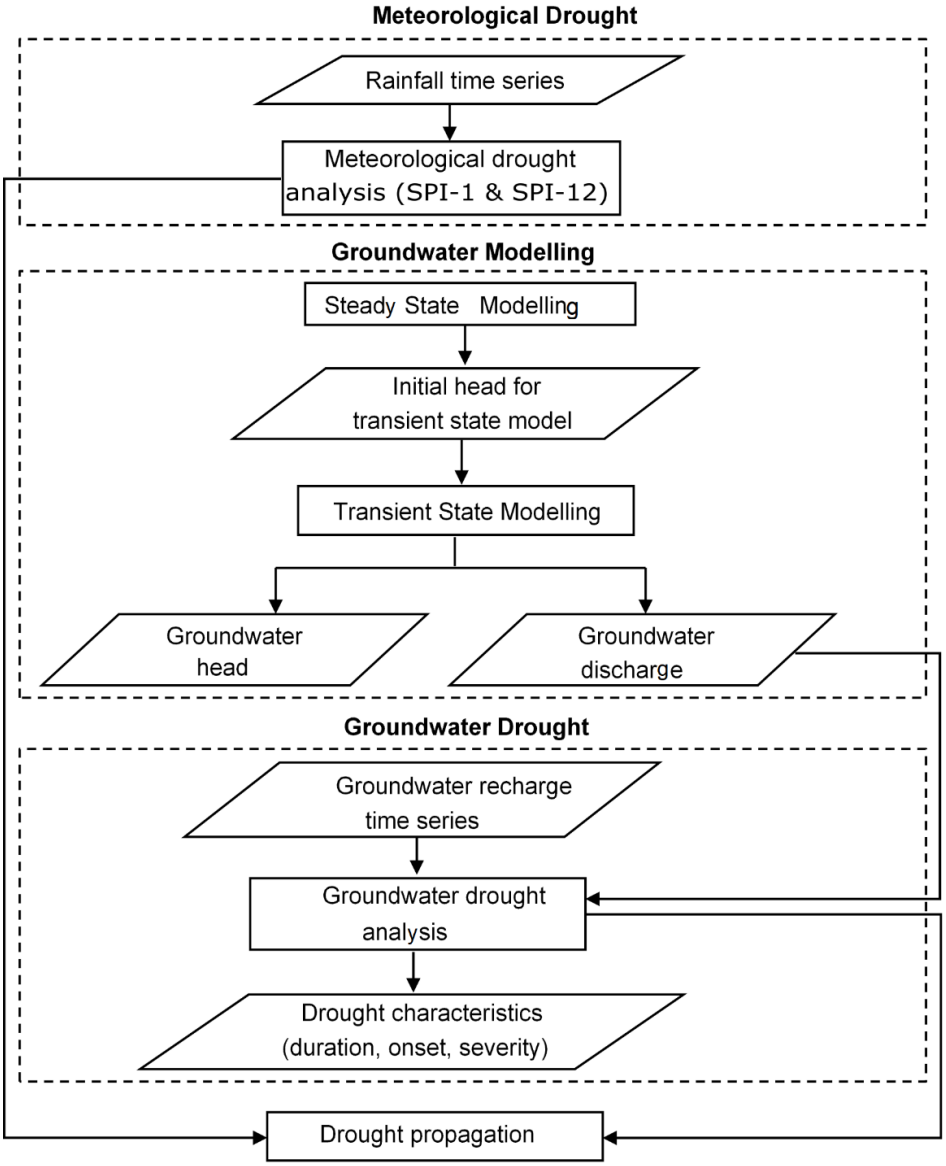


Figure 3.4: Conceptual framework of the study

First, meteorological drought analysis was conducted to investigate drought based on precipitation time series. A transient state groundwater flow model was then built to acquire temporally and spatially distributed simulated hydraulic head and groundwater discharge. Groundwater drought analysis was performed on simulated groundwater discharge and monthly groundwater recharge time series. Finally, drought analysis was conducted to investigate drought propagation in the hydrological cycle. This was done by comparing groundwater drought to meteorological drought.

3.3.2.1 Meteorological drought analysis

The meteorological drought severity and spatial and temporal extent of the drought were determined using the standardized precipitation index (SPI; McKee et al., 1993). Thirty-one years of monthly averaged precipitation were obtained from the Royal Meteorological Institute (RMI) of Belgium at the Uccle station for the period 1981 to 2011, which was used to calculate SPI and identify meteorological drought events and severity.

As McKee et al. (1993) stated, SPI is based on the probability distribution of long-term rainfall on different time scales. In this study, the SPI values for one month, three months, six months and twelve months were calculated to investigate the long-term meteorological drought severity. This drought index was used to analyze the propagation of drought from meteorological to groundwater drought.

The long-term rainfall is fitted to a probability distribution, which is then transformed into a normal distribution so that the mean SPI for the location and desired period is zero (Edward and McKee, 1997). The gamma distribution is used to normalize the rainfall time series (Thom, 1958). Positive SPI values indicate greater than median precipitation, and negative values indicate less than median rainfall. Accordingly, a moderate drought event occurs when the index reaches an intensity of -1.0 or less (Table 3.1). The event ends when the SPI becomes positive.

According to McKee et al. (1993), drought intensity categories based on the SPI value are defined as shown in Table 3.1.

Table 3.1: Drought intensity categories based on SPI values (McKee et al., 1993)

SPI. Values	Drought category
0.0 and more	No
0.0 to -0.99	Mild
-1.0 to -1.49	Moderate
-1.5 to -1.99	Severe
-2.00 and less	Extreme

3.3.2.2 Groundwater modeling

Groundwater modeling was performed using the groundwater modeling software MODFLOW-2000 (Harbaugh et al., 2000). First, a steady-state groundwater model for the study area was set up and ran to obtain initial heads for the transient state model, which was built and ran subsequently.

3.3.2.2.1 Conceptual model setup

The conceptual model shown in Figure 3.5 was developed based on geology, hydrogeology, and hydrology. The model has an area of 1824 km^2 and contains the Dijle catchment and parts of the Demer and Zenne basins and the groundwater extraction wells operating in the study area. The model is discretized by a single aquifer layer with a varying thickness between 1.5 m and 122 m and a rectangular grid with a grid cell size of 100 m X 100 m.

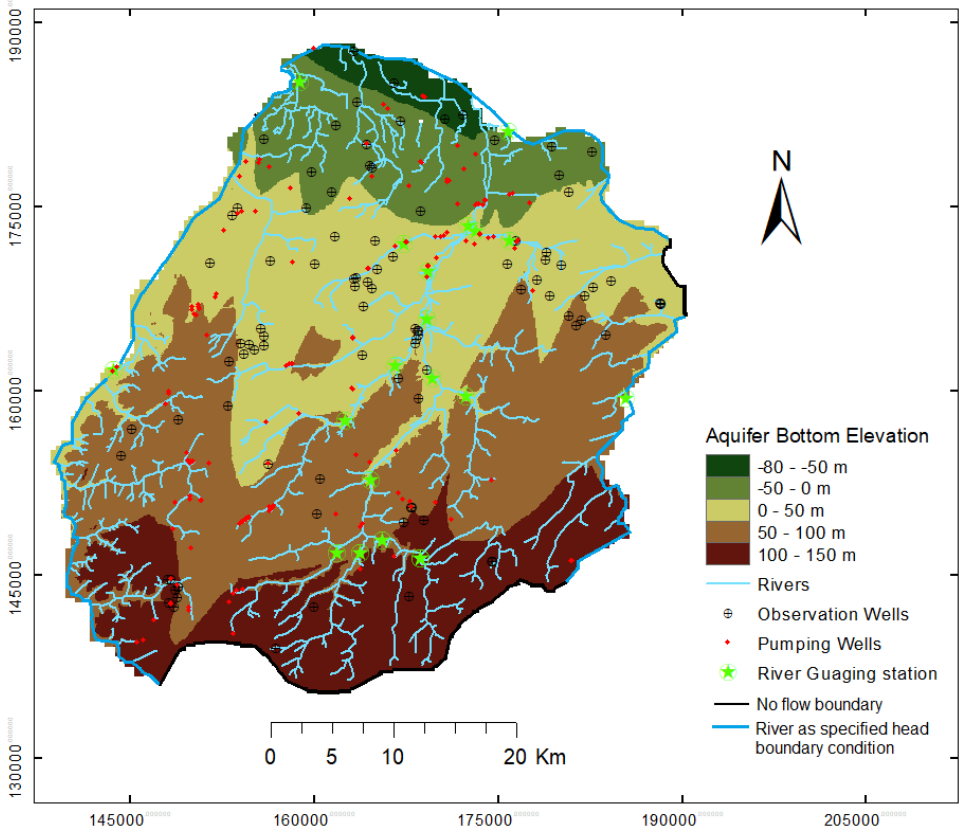


Figure 3.5: Conceptual model setup, showing boundary conditions and aquifer bottom elevation

The idea of the study area conceptual model setup was derived from Peeters (2010). The clayey formation of Kortrijk shown in Figure 3.2 was taken as the impervious model bottom due to its much lower hydraulic conductivity than the Brussels Sands formation and Quaternary loam. Huysmans and Dassargues (2006) reported that the average vertical hydraulic conductivity of the Eocene Ypresian clays, which includes the Kortrijk formation, is 2.1 X 10^{-8} m/d. The Brussels sand formation and Quaternary loam were represented as a one-layer phreatic aquifer system with heterogeneous hydraulic conductivity zones. According to Huysmans et al. (2008), Peeters (2010), and Possemiers et al. (2012), the pumping test results show that the study area's hydraulic conductivity is heterogeneous; values vary from 0.86 m/d to 64.16 m/d. The spatially varying hydraulic conductivity map made by Peeters

(2010), using stochastic conditional simulation, is used as the initial value. However, in the river valleys where the Brussels Sands is eroded, and the alluvial deposits consist of silts, peats, and clay with some coarser sediments near the bottom, a lower value of 1 m/d replaces the simulated hydraulic conductivity as initial value (Peeters, 2010). These initial values of hydraulic conductivities are later optimized during calibration of the model.

Figure 3.5 shows that most of the model area is bounded by the rivers found in the study area that are bound most of the model area. Therefore, these rivers are chosen as the natural boundaries of the model; the Zenne river and tributaries in the west, Dijle and Demer in the north, and Gete and tributaries in the east. In the south, due to scarcely observed groundwater levels and no clear natural boundaries, a no-flow boundary is chosen as a model boundary corresponding to the superficial drainage divide between the Meuse and Schelde basin. According to the groundwater level map done by Moens and Rouhart, 1978, this superficial drainage divide coincides with the groundwater divide. Along the eastern border, which is perpendicular to the equipotential lines obtained through a regional groundwater model for the Bruland-Krijt groundwater system (VMM, 2008), a local no-flow boundary is assumed to bound the model domain.

For this study, the average river stage and river bottom elevation were interpolated from measurement data obtained at a few locations within the study area (Flemish Water Authorities, 2019). According to Peeters (2010), most riverbed sediments in the study area consist of Pleistocene sands and gravels. Hence, the spatially distributed riverbed conductance varies from 0.25 m^2/d to 304.5 m^2/d, derived from a regional groundwater model for the Bruland-Krijt groundwater system (VMM, 2008). In the Dijle catchment, numerous springs occur at the base of the hilltops and the alluvial valley floors (Peeters, 2010). Therefore, for every active cell that was not modeled as a river within the study area's boundary, a drain condition was specified to incorporate springs and seepage zones in the model and prevent the overestimation of simulated heads. From the study of groundwater flow modeling of three wetland ecosystems in river valleys in Flanders by Batelaan et al. (2003), an average drain elevation 0.2 m below topography and a drain conductance of 100 m^2/d was assumed in the present study. Two hundred fifty groundwater extraction wells with an average pumping rate of 448 m^3/d are also present in the study area and the model.

To see the monthly dynamics of the groundwater system, the transient state model with 108 stress periods of one month from 2002 till 2011 was modeled. Calculated spatially

distributed monthly delayed groundwater recharge values were used as input for each stress period. Figure 3.6 shows the seasonal dynamics of groundwater recharge in the study area.

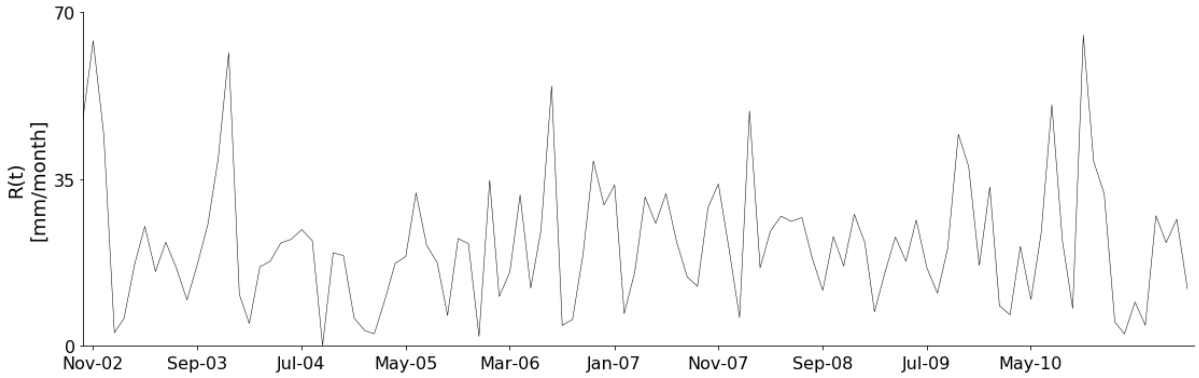


Figure 3.6: Average monthly delayed groundwater recharge

Average observed hydraulic heads between Oct-2002 and Sep-2011 from 97 observation wells in the study area were used to calibrate the steady-state model. Two-weekly observed hydraulic heads from 29 observation wells between Oct-2004 and Sep-2008 were used to calibrate the transient state model. Afterward, the model was validated using observed hydraulic heads between Oct-2008 and Sep-2011. The variance of the differences between observed and simulated heads was used as a quantitative measure of the "success" of the calibration and validation.

3.3.2.2.2 Sensitivity analysis

Since manual calibration does not quantify the statistical uncertainties of model outputs, a sensitivity analysis is required to indicate the uncertainty or reliability of model simulations (Anderson et al., 2015). The relative sensitivity of the simulated heads to changes in model parameters such as hydraulic conductivity (HK), specific yield (S_y), riverbed conductance (C_{riv}), and drain conductance (C_{drn}) was calculated. The relative sensitivity was calculated at six locations with different geological settings. The relative sensitivity is given by:

$$(S_r)_{ij} = \frac{\Delta h_{si}}{h_{si}} / \frac{\Delta P_j}{P_j} \qquad (3.1)$$

Where;

Δh_{si} is the change in simulated head observed at a certain location for a change in the parameter value ΔP_j; h_{si} is the simulated head at a certain location before the change in parameter value; P_j is the original parameter value.

3.3.2.2.3 Groundwater drought analysis

A groundwater drought analysis was performed on the calculated groundwater recharge (R(t)) time series of 34 years (1980-2013) and the modelled groundwater discharge (Q(t)) time series of 10 years (2020-2011) to investigate the propagation of drought in the aquifer. The threshold level method introduced by Yevjevich (1967), with a variable threshold value (Beyene and Van Loon, 2014), has been previously used for investigating hydrological drought in different geo-climatic conditions. In this study, the variable threshold value was used to determine groundwater drought events for both variables, recharge and discharge.

First, a separate frequency analysis was conducted for each of the 12 months. Each month's threshold level was determined as the 80^{th} percentile of the probability of exceedance of monthly recharge in that month in the 34-year series (1980-2013). This threshold level is within the 70^{th}-95^{th} percentile of the probability of exceedance range used for most drought studies (Van Loon, 2013). For each month of the year, the monthly recharge and discharge values in the time series were ranked from highest to lowest. For each month, the 80^{th} percentile of recharge and discharge were then calculated.

After the separate analysis of drought on groundwater recharge and discharge, the two analyses were combined to characterize groundwater drought events, gain insight into the propagation of drought in the aquifer and assess the groundwater system's response to drought. The groundwater drought events were investigated in terms of the number of droughts, duration, and severity (cumulative volume deficit from the threshold level) (Peters, 2003a).

Moreover, a standardized groundwater drought index (SGI) and standardized precipitation index (SPI) were used to analyze drought propagation in the hydrological cycle, from meteorological drought to groundwater drought. The Standardized Groundwater drought Index (SGI) introduced by Bloomfield and Marchant (2013) was used to analyze groundwater level drought. In this research, SGI was calculated from delayed groundwater recharge by applying appropriate normalization procedures. The long-term delayed groundwater recharge time-series was normalized by fitting to a gamma distribution. Then, like SPI, the standardized groundwater drought index (SGI) was calculated for the spatially averaged monthly delayed groundwater recharge time series from 1981 to 2011.

3.4 Results and discussion

3.4.1 Meteorological drought

The meteorological drought severity based on monthly SPI (SPI-1) and annual SPI (SPI-12) in the Uccle station between 1980 and 2011 is shown in Figure 3.7. As can be seen, there is a difference in severity and frequency between them. Based on the SPI-1 value (Figure 3.7A), the drought categories vary from extreme to no drought. In contrast, the SPI-12 value (Figure 3.7B) shows less severe drought categories, ranging from severe to no drought.

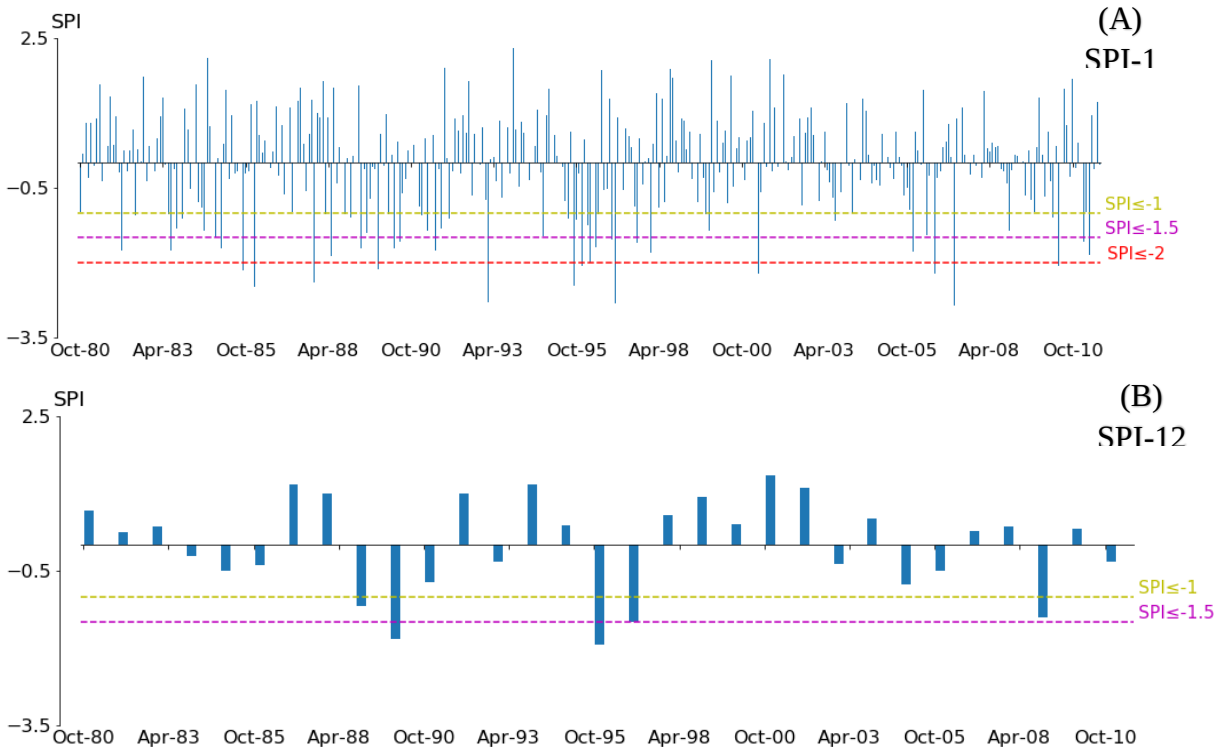


Figure 3.7: Meteorological drought severity for the Uccle station based on (A) SPI-1 value and (B) SPI-12 value between the hydrological year of 1980 and 2011

Within the analysis period, twelve extreme meteorological droughts at a monthly scale are identified using SPI-1. However, two severe meteorological droughts are identified using SPI-12; these occur in 1989-90 and 1995-96. From this result, in a short period of SPI calculation, the meteorological drought is frequent but short, and as the period of SPI calculation increases, the duration of drought increases with lower frequency. Therefore, SPI-1 is more convenient for the study of drought propagation in a quickly responding hydrological system. Cammalleri and Barbosa (2019) also showed a short period SPI calculation is suitable for a quickly responding hydrological system.

Meteorological drought severity is also variable on a spatial scale. For example, Figure 3.8 shows that in the hydrological year of 2008-09, the drought severity categories vary from mild to extreme in the study area. Moreover, Figure 3.8 also shows the spatial distribution of drought severity categories for SPI-3, SPI-6, and SPI-12.

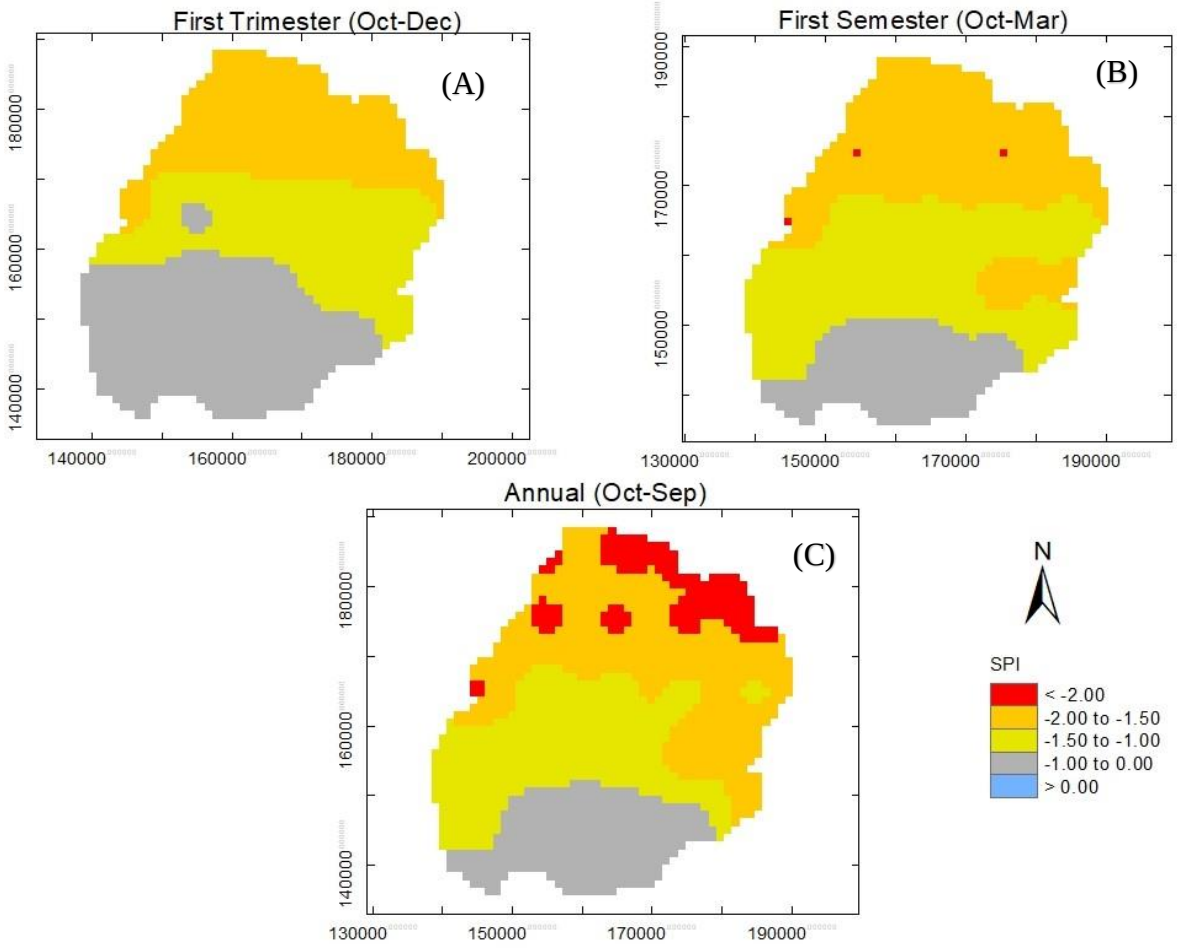


Figure 3.8: Spatially distributed Meteorological drought severity for Dijle catchment and parts of the Demer and Zenne basin based on (A) SPI-3 (Trimester) value, (B) SPI-6 (Semester) value, and (C) SPI-12 (Annual) value for the hydrological year of 2008-09

3.4.2 Groundwater modeling

Relative sensitivities of model parameters at locations in the Brussels Sands show that hydraulic conductivity of the Brussels sand formation (HK1) was the most sensitive parameter (relative sensitivity of 0.026), followed by drain conductance (C_{drn}) (relative sensitivity of 0.008). Specific yield and river conductance had little effect on simulated heads. For the locations within the Quaternary loam, the river conductance was the most sensitive parameter (0.017), followed by hydraulic conductivity HK2 (0.003) and drain conductance (0.001). Storage parameters had little effect on calculated heads.

Generally, the relative sensitivities of the model parameters were small, indicating that the uncertainties of the model parameters have a limited influence on the simulated heads.

Hydraulic conductivities of the Brussels Sands and the Quaternary loam in the valleys were optimized during calibration of the steady-state model. After calibration, the variance amounts to 1.85 m^2. The mean absolute error of the simulated heads was 1.36 m with a percent of bias (PBIAS) of - 0.13. This model performance result indicates that the model overestimates groundwater head.

The resulting spatial groundwater depth distribution is shown in Figure 3.9 and indicates that groundwater depth is up to 75 m in the hills. In the north of the study area and the river valleys, groundwater depths are less than two m. However, in most of the study area, groundwater depth lies between 10 m and 40 m. Generally, the study area has deep groundwater depths below the hills and shallow groundwater depths in the valleys and the northern area.

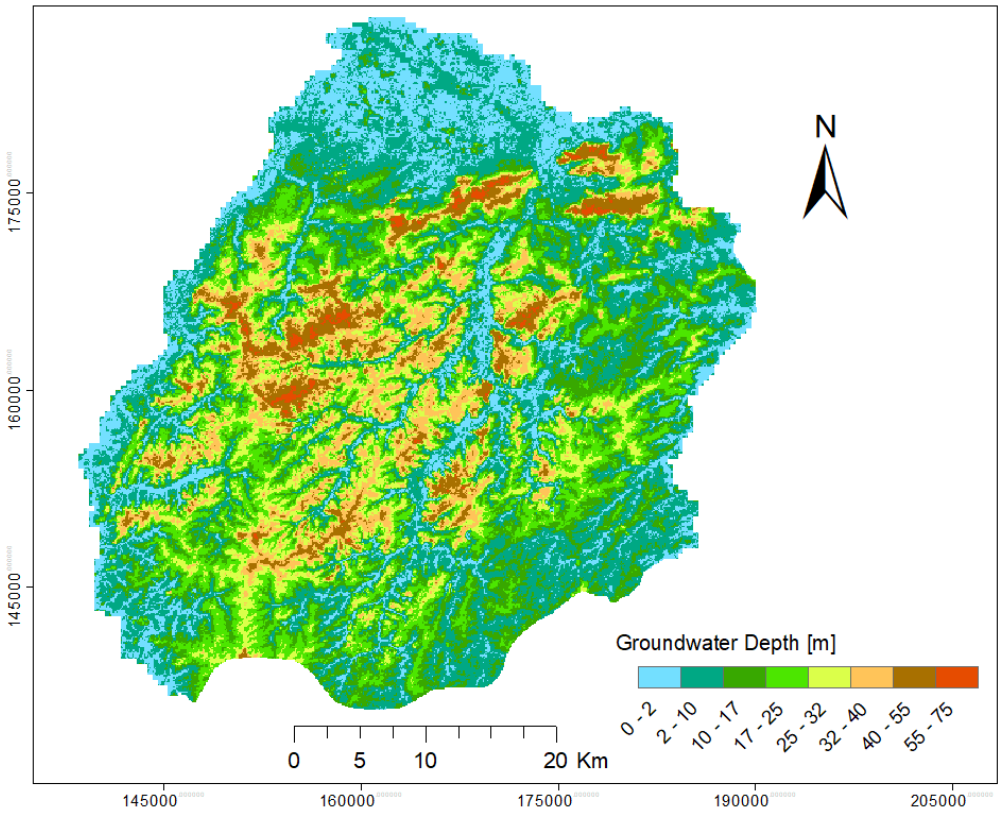


Figure 3.9: Spatial groundwater depth distribution after steady-state groundwater model calibration

The steady-state groundwater balance was calculated to obtain average fluxes in the study area (Figure 3.10). Groundwater recharge constituted around 77 % of the input into the groundwater system. The remaining inflow was from river leakage into the groundwater

system. The largest outflow was groundwater discharge to the rivers, which was around 63 % of the groundwater system's total output. Moreover, groundwater is discharged to the springs represented by drain outflow, and this represents about 30 % of the total flow out of the aquifer. The water balance error was approximately 0.00 %.

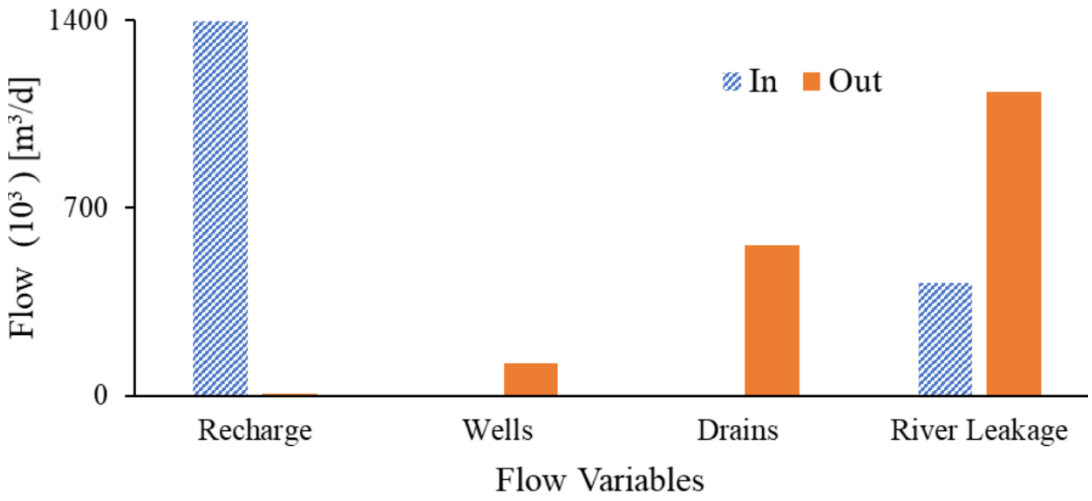


Figure 3.10: Steady state groundwater model water balance

During calibration of the transient model, specific yield was optimized taking into account the geological setting. Table 3.2 shows different statistical coefficients to evaluate the model performance during the calibration and validation period. In both periods, PBIAS was negative, indicating that the model slightly overestimates groundwater head. NSE values are larger than 0.7 in the calibration and validation periods indicating a very good performance of the model. The final calibrated values of the specific yield are 0.15 in the area where the Brussels Sands are the dominant deposits and 0.03 in the area dominated by the Quaternary loam around the river banks. Figure 3.11 shows the hydraulic conductivity distribution before and after the calibration. The final hydraulic conductivity value varies from 2.6 m/d to 66 m/d in the study area.

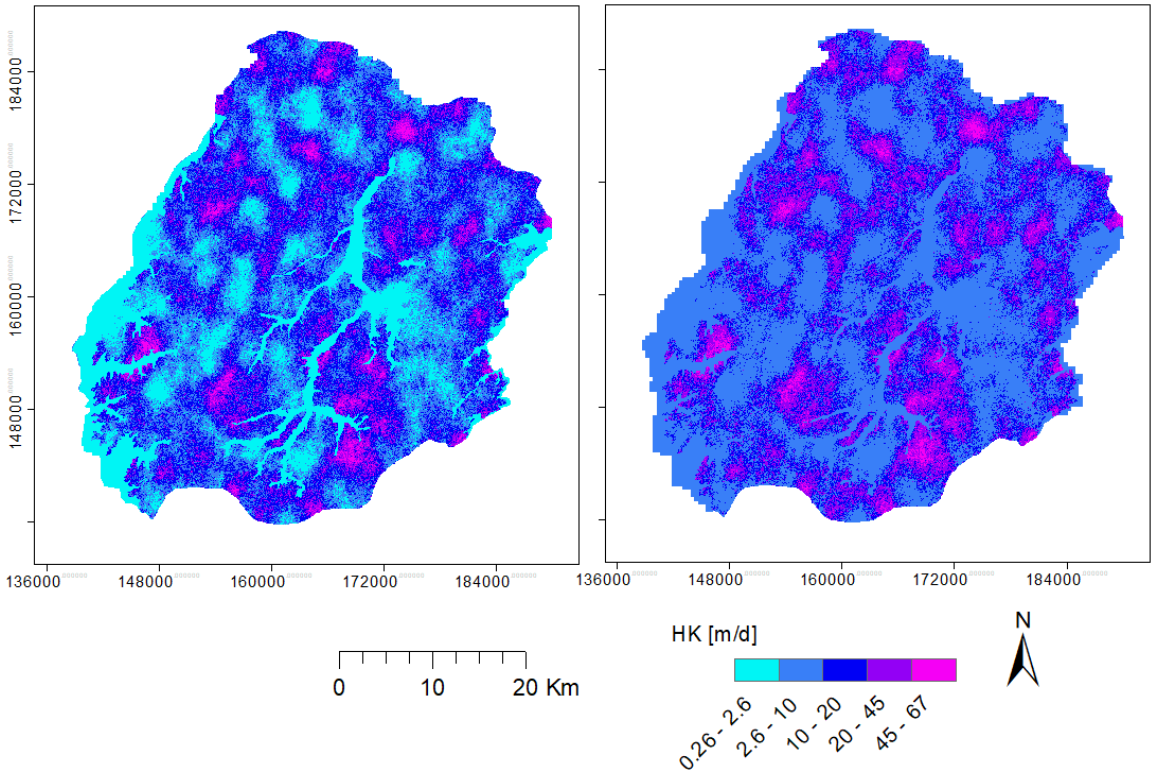


Figure 3.11: Spatially distributed hydraulic conductivity before (left) and after (right) calibration

Table 3.2: Model evaluation statistics for calibration and validation period

Statistical Coefficient	Calibration period	Validation period
RMSE (m)	1.66	1.84
$\sigma^2(m^2)$	2.77	3.23
NSE (--)	0.91	0.84
PBIAS (%)	-1.07	-1.91

Time-series of the observed and simulated head at the observation wells (2-weekly interval) show that the model reasonably captures the dynamics of groundwater head in the study area. As an example, Figure 3.12 shows the temporal variation of observed and simulated groundwater head at observation well DYLP081.

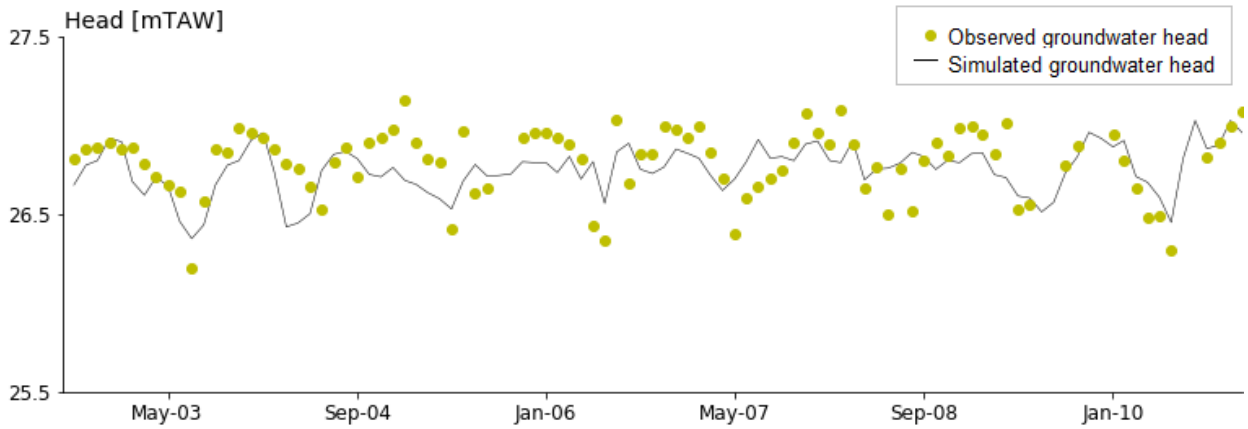


Figure 3.12: Observed and simulated groundwater head at observation well DYLP081 between Oct-2002 and Sep-2011

The simulated spatially average hydraulic head dynamics between 2002 and 2011 are compared to groundwater recharge (Figure 3.13). Average groundwater head and recharge show a strong correlation. Groundwater head is high in winter (Dec-Feb) and low in summer (Jun-Aug), following the seasonality of groundwater recharge. There is also a small systematic delay in the timing of the peaks and lows of the hydraulic head and recharge. This indicates a fast response of the groundwater system to recharge.

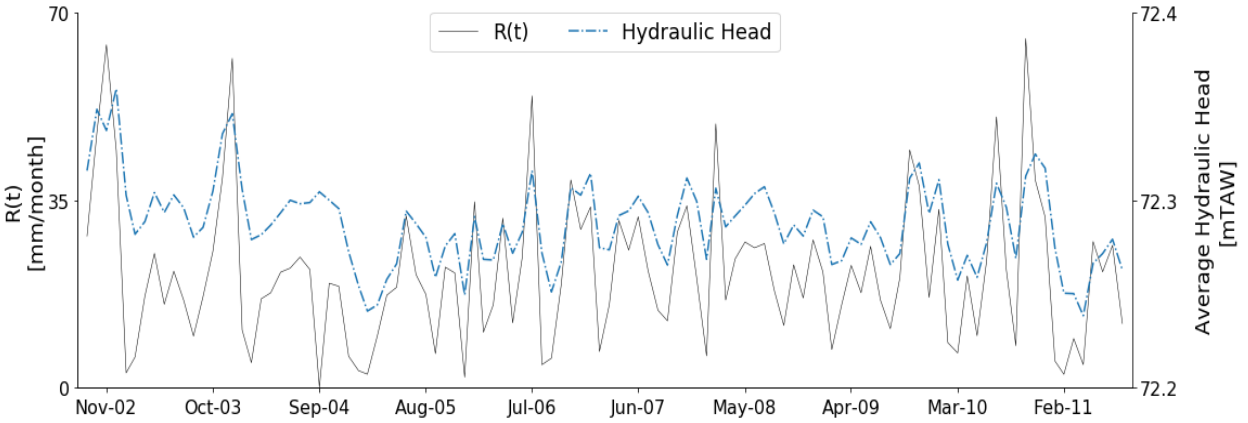


Figure 3.13: Average simulated groundwater head time series and groundwater recharge time series

Simulated total groundwater discharge to the river (Figure 3.14) also shows clear seasonality and a high correlation to recharge; high groundwater discharge in winter (Dec- Feb) and low groundwater discharge in summer (Jun-Aug).

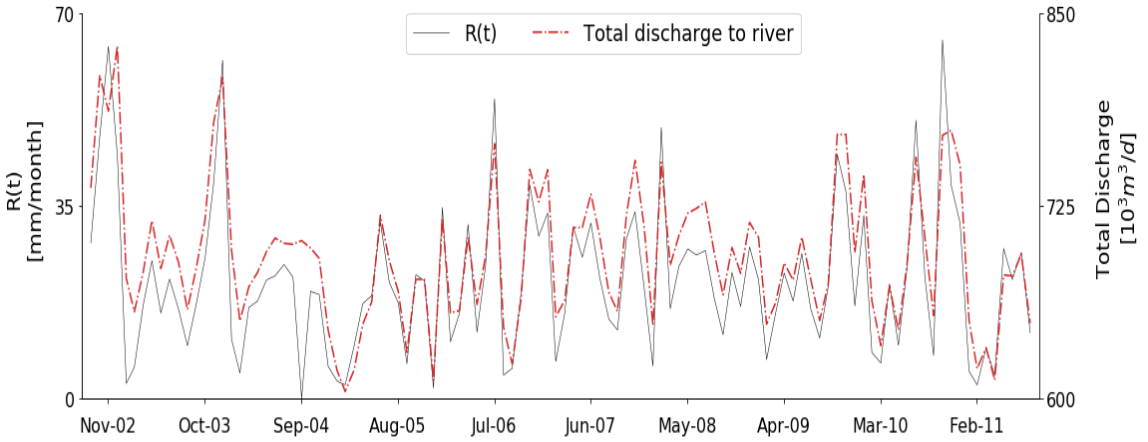


Figure 3.14: Simulated total groundwater discharge and monthly average groundwater recharge

3.4.3 Groundwater drought

3.4.3.1 Groundwater recharge drought

Groundwater recharge deviation from the threshold and groundwater recharge drought events from 2002 to 2011 are shown in Figure 3.15. Five drought events with a severity higher than 2 mm of cumulative deficit recharge were observed during this period. In terms of duration, the drought events had a mean duration of 3 months. The drought with the longest duration was from Jul-2004 to Feb-2005, which lasted for eight months, followed by the drought from Aug-2005 to Dec-2005, which lasted for five months. Droughts with shorter durations were observed in Feb-2003, Feb-04, Sep-2007, Jan-2010, and Sep-2011 (1 month). The severity of the drought events was assessed based on cumulative deficit recharge from the threshold. The most severe drought was from Jul-2004 to Feb-2005 with a cumulative deficit recharge of 62.7 mm, followed by the drought from Aug-2005 till Dec-2005 with a cumulative deficit recharge of 24.3 mm. These severe droughts have a drought volume higher than the average estimated recharge of, 23.12 mm/month.

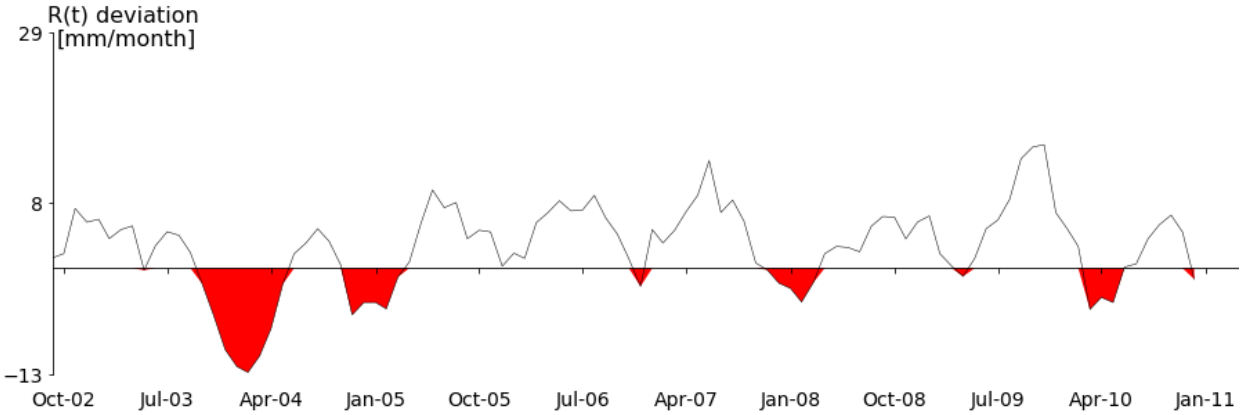


Figure 3.15: Deviation from the threshold value of monthly groundwater recharge. The red color represents the groundwater recharge drought events.

3.4.3.2 Groundwater discharge drought

Deviations of groundwater discharge from the threshold and discharge drought events are shown in Figure 3.16.

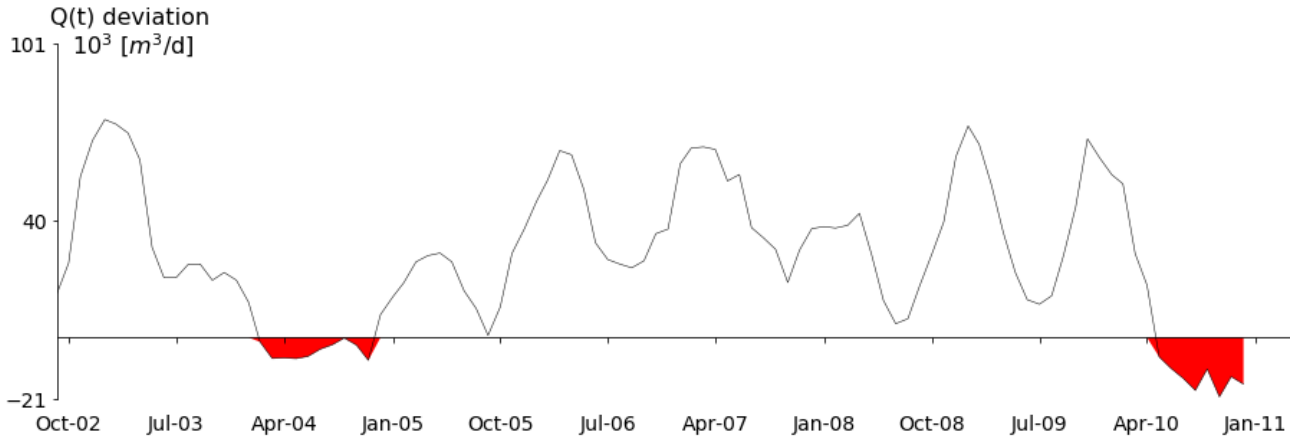


Figure 3.16: Deviation from the threshold value of monthly groundwater discharge to rivers. The red color represents groundwater drought events on discharge.

Two groundwater discharge drought events occurred between 2002 and 2011. The first one was from Nov-2003 to Aug-2005. The second drought event occurred from Feb-2011 to Sep-2011. The drought events lasted for ten months and eight months, respectively, with a mean duration of 9 months. The second drought event from Feb-2011 to Sep-2011was the most severe with a cumulative deficit volume of 110051 m^3. The first drought had a cumulative volume deficit of 46587 m^3.

The average duration of discharge droughts (9 months) is much larger than the mean duration of recharge droughts (3 months). Also, the number of discharge droughts events (2) is much smaller than the number of recharge drought events (5). This was expected as the propagation of recharge drought through an aquifer usually results in a lower number of hydrological droughts (Van Lanen, 2006). Also, recharge drought events were more severe than groundwater discharge drought events (Figure 3.17). This decrease in severity is probably also caused by attenuation in the groundwater system (Peters, 2003a). Another important observation is that the discharge drought events have a delay 2 to 4 months compared to drought events of recharge. This small delay could be attributed to the limited thickness of the aquifer and shallow groundwater levels in most parts of the study area, which results in a quick response to hydrologic stresses.

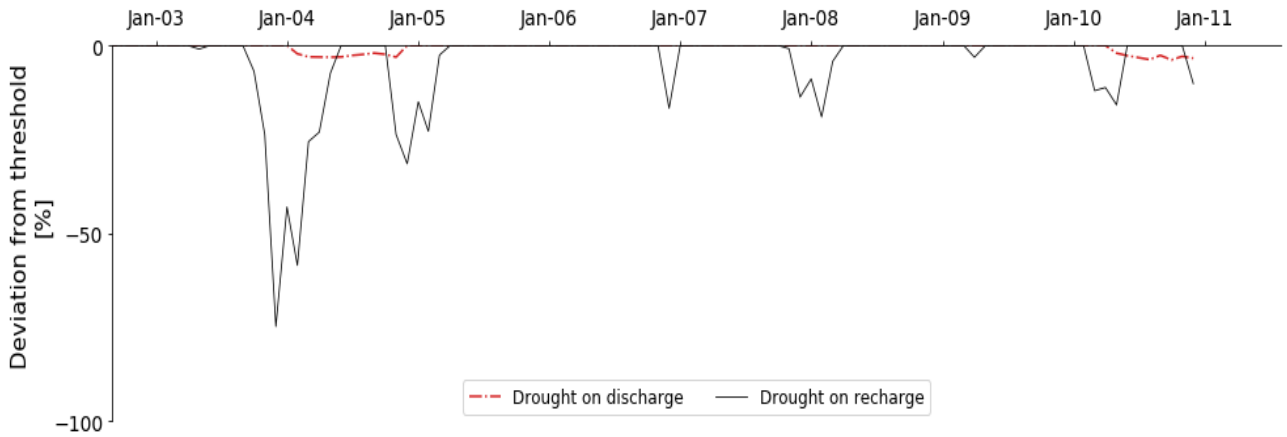


Figure 3.17: Comparison of recharge and discharge drought events as percent deviation from the threshold

3.4.4 Drought propagation from meteorological drought to groundwater recharge

Table 3.3 shows the groundwater drought characteristics between 1980 and 2011 for the major groundwater recharge events calculated using the variable threshold method as shown in Figure 3.18.

Table 3.3: Groundwater recharge drought characteristics (onset, number events, duration, and deficit volume) between Oct-1981 and Sep-2011

Onset	Duration [month]	Number of drought events	Deficit [mm]
Jun-83	2	1	8.34
Nov-84	9	2	2.02
Aug-88	21	2	31.08
Jun-95	30	3	48.06
Feb-03	35	4	84.40
Sep-07	49	5	27.99

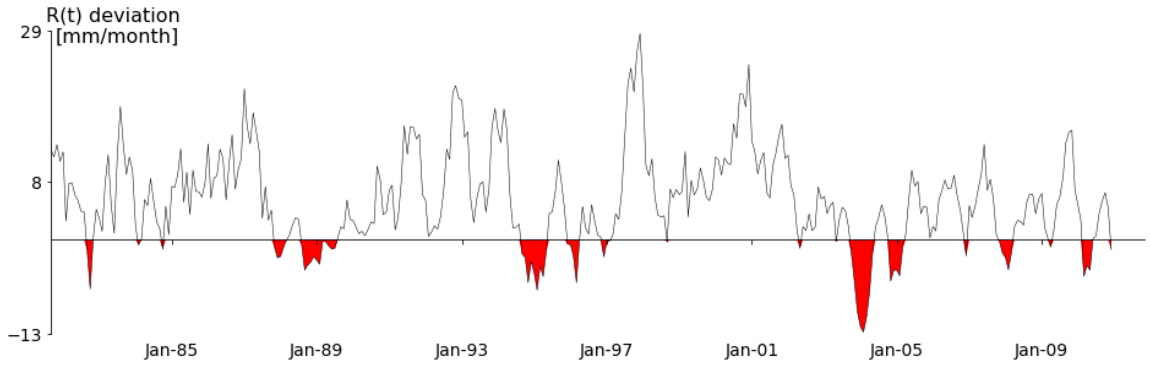


Figure 3.18: Groundwater recharge deviation from the threshold between 1981 to 2011. The red color represents recharge drought events.

The propagation of drought from meteorological drought to groundwater was analyzed using SPI-1 and monthly groundwater recharge SGI. Since not all negative SGI should be considered as groundwater drought, during drought propagation analysis only more severe groundwater recharge droughts, which correspond to the lowest 20 % SGI, are considered. Table 3.4 shows the lag time and the number of meteorological droughts (SPI-1) before the onset of groundwater recharge drought between 1981 and 2011. The lag time was calculated as the time between the start of the meteorological drought and the monthly groundwater recharge SGI. Before every groundwater drought, meteorological drought was observed with different severity ranges.

Moreover, the severity of the meteorological drought had an impact on the deficit volume and duration of groundwater drought, for example, the groundwater droughts that occurred after Aug-1988 (Figure 3.18 and Figure 3.19). In this study area, moderate and severe meteorological drought also propagate to the groundwater, e.g., the minor groundwater drought that started in Jun-1983 and Nov-1984 (Figure 3.18). The lag time in Table 3.4 is the average of the lag of each groundwater drought event based on SGI.

Furthermore, by comparing Figure 3.19 (A) and (B), the propagation of drought from meteorological drought to groundwater recharge can be evaluated. Within the analysis period, meteorological drought is more frequent and observed earlier than groundwater recharge drought. Besides, most of the meteorological droughts propagated to groundwater recharge with an average lag of 2.25 months.

Table 3.4: Onset of SGI groundwater recharge drought between Oct-1981 and Sep-2011 and number of meteorological droughts (SPI-1) ranging from moderate to extreme severity before the onset of groundwater recharge drought with lag time.

Onset	Number of SGI drought events	Number of meteorological drought (SPI-1) before the onset of groundwater drought on Recharge	Lag time [month]
Feb-82	1	2 (1S)	2
Oct-83	2	5 (1S, 4Mo)	7
Feb-85	3	6 (2E,1S,3Mo)	6
Dec-87	1	1 (1E)	2
Nov-89	5	7 (1E,2S,4Mo)	9
Mar-93	1	2 (1E, 1S)	11
Feb-98	7	9 (3E,1S,5Mo)	9
Oct-99	3	3 (1E, 2Mo)	5
Feb-03	2	1 (1E)	2
Oct-04	7	4 (1E, 1S, 2Mo)	12
Feb-11	3	4 (1E, 1S, 2Mo)	15

*E: extreme; S: severe; Mo: moderate

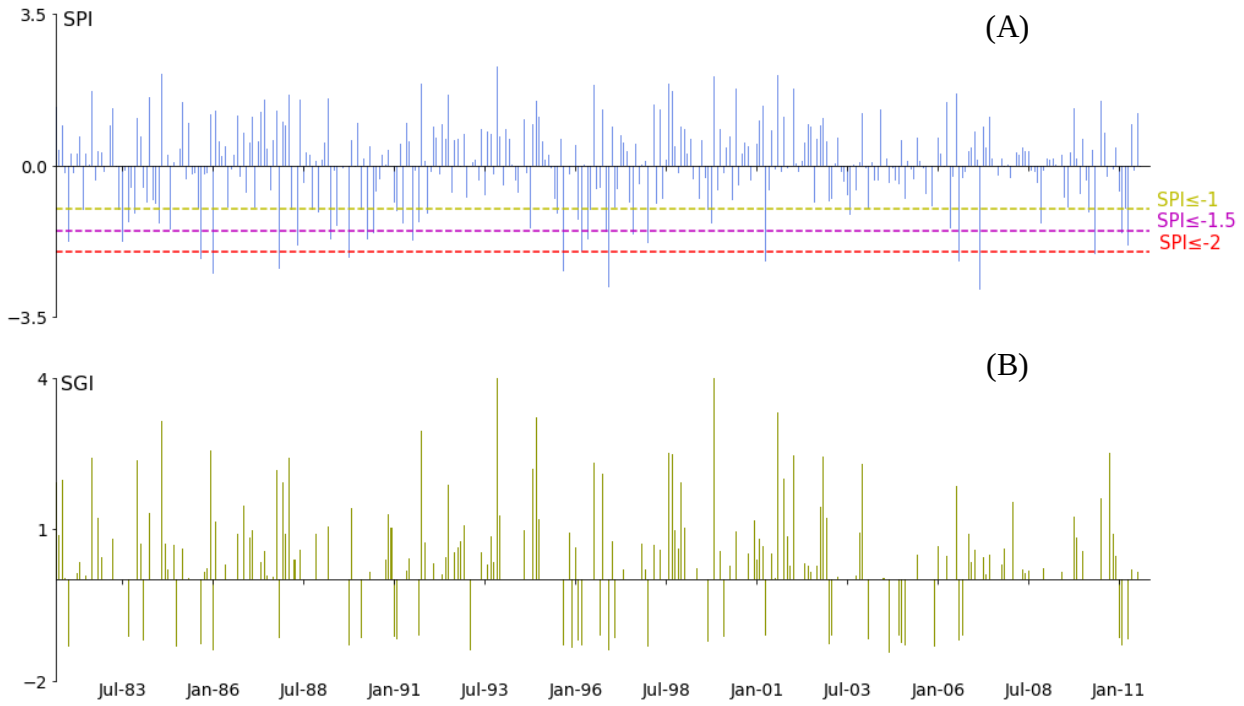


Figure 3.19: Comparison of meteorological drought severity and groundwater recharge drought (A) Monthly SPI value and (B) Groundwater recharge drought using monthly SGI.

3.4.5 Drought propagation and its impact on groundwater hydrology of wetlands

Ecosystems such as wetlands that are fed directly by groundwater discharge are also vulnerable to groundwater drought. Therefore, investigating groundwater drought is especially crucial in nature reserves such as groundwater-fed wetlands. Doode Bemde wetland, found in the Djile catchment (Figure 3.1 and Figure 3.20), is primarily fed by groundwater and an ecologically valuable part of the ecosystem. The propagation of drought in the hydrological cycle from meteorological to groundwater recharge drought and from groundwater recharge to discharge drought was analyzed, and its impact was assessed on this groundwater-fed wetland ecosystem.

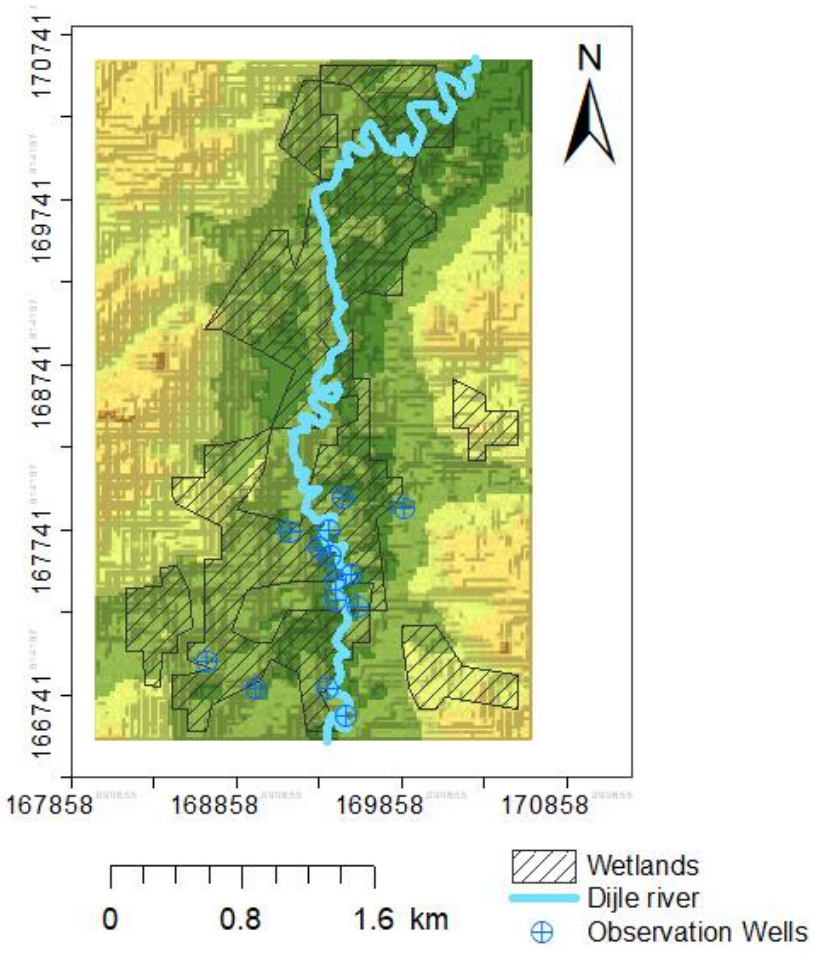


Figure 3.20: Doode Bemde nature reserve with delineated wetland

Figure 3.21 indicates that the average duration of discharge droughts (5.3 months) is slightly larger than the mean duration of recharge droughts (5 months). However, the number of discharge droughts events (3) is smaller than the number of recharge drought events (7). This decrement was expected as the propagation of recharge drought through an aquifer usually results in a lower number of hydrological droughts (Van Lanen, 2006).

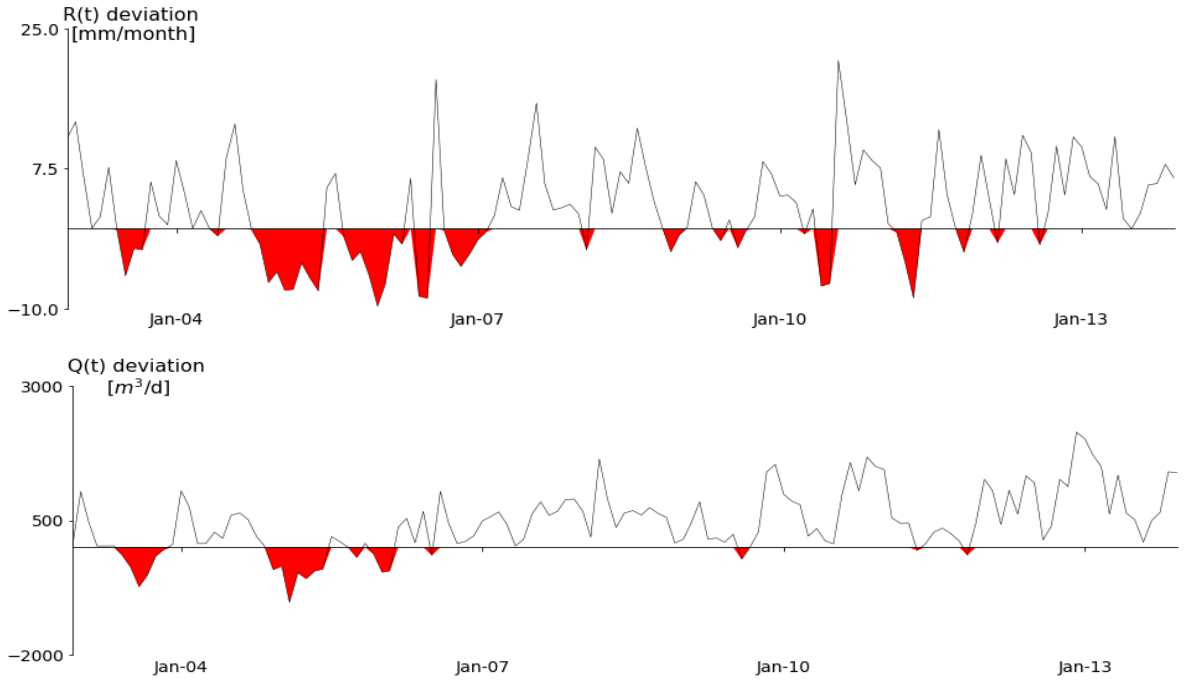


Figure 3.21: Deviation from the threshold value of monthly averaged modelled groundwater recharge of Doode Bemde wetland (top) and monthly total modelled groundwater discharge to wetland (bottom). The red color represents groundwater recharge drought events.

Because of the attenuation in discharge through the groundwater system, recharge drought events were more severe than groundwater discharge droughts to the wetland (Figure 3.22). Another important observation was the absence of any significant shift in drought events. The recharge and discharge drought events seem to occur at approximately the same time. This could be attributed to the limited thickness of the aquifer and shallow groundwater levels in Doode Bemde wetland, which results in a quick response to hydrologic stresses.

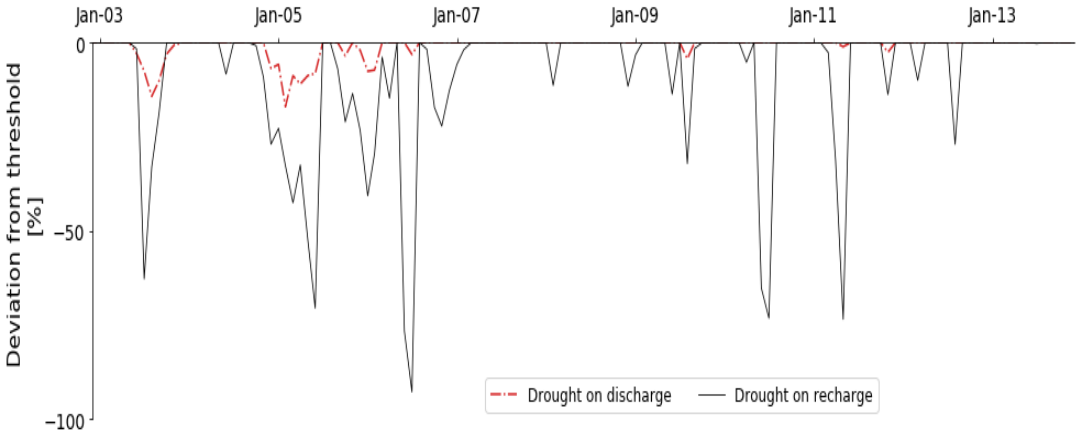


Figure 3.22: Comparison of groundwater recharge and groundwater discharge drought events using the percent deviation from the threshold for the Doode Bemde wetland

Table 3.5 shows the groundwater drought characteristics between 1980 and 2011 for the major groundwater recharge events calculated using the variable threshold method as shown in Figure 3.23.

Table 3.5: Groundwater recharge drought characteristics (onset, number events, duration, and deficit volume) between 1981 and 2010, calculated using variable threshold method.

Onset	Duration [month]	Number of drought events	Deficit [mm]
Dec-83	25	4	9.65
May-89	28	10	32.97
Apr-96	24	6	28.63
Jun-03	45	6	123.26
Feb-08	66	8	45.35

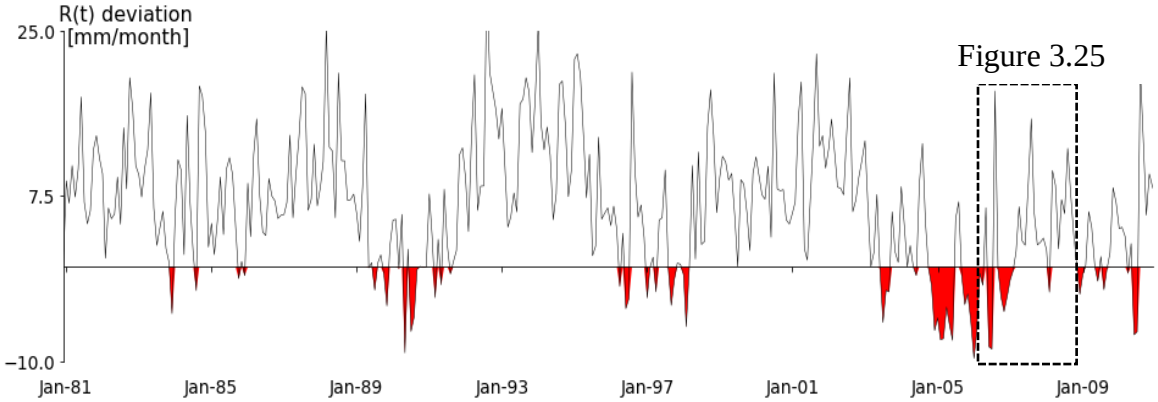


Figure 3.25

Figure 3.23: Groundwater recharge deviation from the threshold between 1981 to 2011. The red color represents recharge drought events.

In the Doode Bemde wetland, the propagation of meteorological drought to groundwater was analyzed by using SPI-1 and monthly groundwater recharge SGI. Since not all negative SGI should be considered as a groundwater drought, during drought propagation analysis only more severe groundwater recharge droughts, which correspond to the lowest 20 % SGI, are considered. Table 3.6 shows the lag time and the number of meteorological droughts (SPI-1) before the onset of groundwater recharge drought between 1981 and 2011. Before every groundwater drought, meteorological droughts of different severities were observed. Moreover, the severity of the meteorological drought impacts the deficit volume and duration of groundwater drought, for example, the groundwater droughts that occurred after May-1989 (Figure 3.23 and Figure 3.24). In this study area, moderate meteorological drought also propagates to the groundwater, e.g., the minor groundwater drought that started in Aug-1984 (Figure 3.23).

Furthermore, by comparing Figure 3.24 (A) and (B), the propagation of meteorological drought to groundwater recharge can be evaluated. Within the analysis period, meteorological drought is more frequent and observed earlier than groundwater recharge drought. Besides, most of the meteorological droughts propagated to the groundwater recharge with an average lag of 1.5 months, which is attributed to the shallow groundwater depth in the wetland.

Table 3.6: Onset of SGI groundwater recharge drought between Oct-1981 and Sep-2011 and number of meteorological droughts (SPI-1) ranging from moderate to extreme severity before the onset of groundwater recharge drought with lag time.

Onset	Number of SGI drought events	Number of meteorological drought (SPI-1) before the onset of groundwater drought on Recharge	Lag time [month]
Jul-84	2	5 (2S, 3Mo)	18
Jul-89	7	11 (4E,3S,5Mo)	9
Jul-95	9	13 (3E,6S,4Mo)	6
Jun-03	10	8 (2E, 6Mo)	8
Jun-09	7	8 (1E,5S,2Mo)	9

*E: extreme; S: severe; Mo: moderate

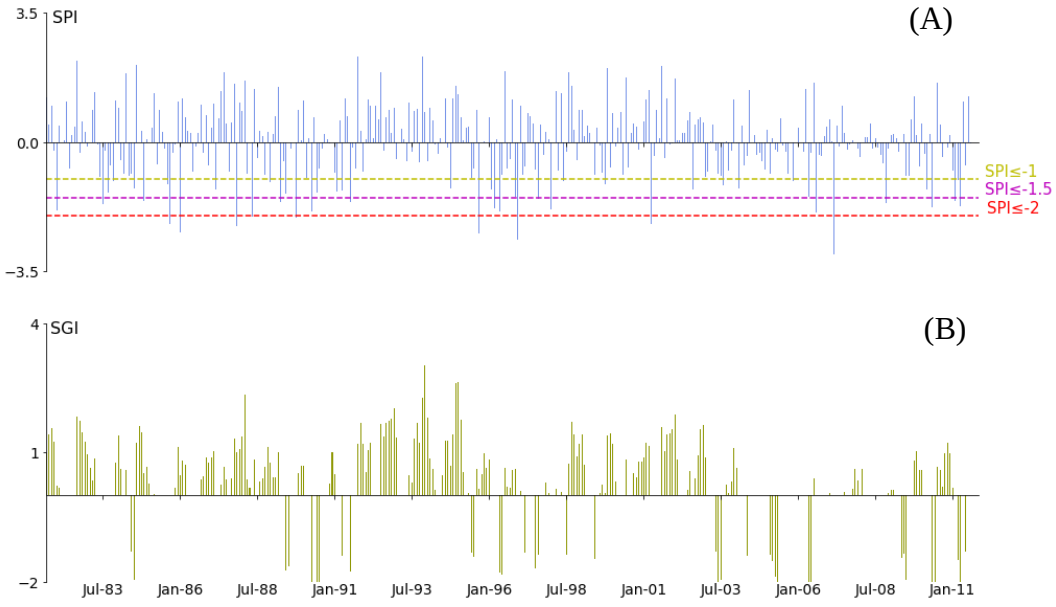


Figure 3.24: Comparison of meteorological drought severity and groundwater recharge drought (A) Monthly SPI value and (B) Groundwater recharge drought using monthly SGI.

This propagation of drought had an impact on the hydrological functioning of the groundwater-fed wetland of Doode Bemde. The monthly box plots in Figure 3.25 show observed groundwater head distribution measured using 14 observation wells mostly found in the wetland. Long-term average groundwater heads (green) show clear seasonal dynamics: highest level in January, lowest in June. The identified groundwater recharge drought (blue)

seems to explain most of the observed deviations between 2006 to 2008. The lower than long-term average groundwater levels measured in the winter (Jan, Feb) and summer (Jun, Jul) of 2006 and the winter (Jan, Feb) of 2008 could be the result of the groundwater droughts that occurred in 2006 and 2008, respectively (Figure 3.25). However, the groundwater drought impact between fall 2006 and winter 2007 was delayed, which is visible in the groundwater level measurements of the spring of 2007. This delay could be because of upland recharge from the Dijle valley.

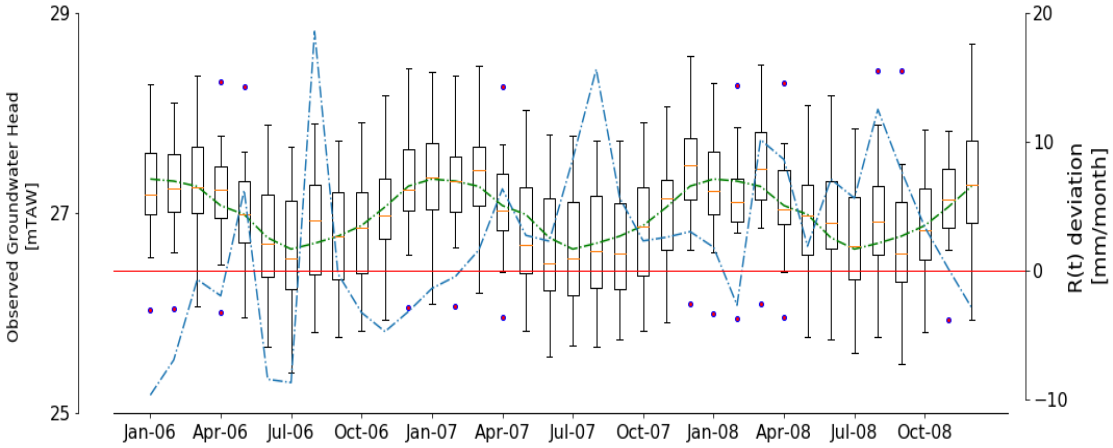


Figure 3.25: Observed groundwater head distribution collected from 14 observation wells (boxplot with monthly timestep), long-term (2003-2013) average monthly observed groundwater head (dotted-green line), and groundwater recharge deviation from threshold value (dotted-blue line) between 2006 and 2008. These observation wells are mainly found in the delineated wetland area (Figure 3.20).

During drought propagation in the hydrological cycle, the multi-year meteorological droughts of 1981 – 2011 propagate to groundwater recharge drought. This propagation continues to the groundwater system. The groundwater drought propagation analysis shows that even though the number and severity of drought events observed in discharge to the wetland are lower than for recharge, the wetland is still vulnerable to groundwater drought. This is also reflected in the lower groundwater level measurements between 2006 and 2008. This vulnerability could be because of the shallow water table and limited thickness of the aquifer in the study area, resulting in a quick response to changes in hydrological stresses such as droughts. The drought propagation towards a wetland studied by Fang and Pomeroy (2008) also showed much lower discharge to the wetland from groundwater and snowmelt runoff developed in drought years. Moreover, Drexler and Ewel (2001) performed a field experiment during the 1997–1998 ENSO-related drought and found that the mean water table level in the wetlands lowered by 12 to 54 cm. This could also be explained by drought propagation from the meteorological to the groundwater system.

3.5 Conclusions

This study proposes a method to investigate the propagation of meteorological drought to groundwater recharge, groundwater levels, and groundwater discharge to a river and wetland. The method combines a water balance model, a transient groundwater flow model, threshold methods, and drought indices. The method is applied to analyze drought propagation in the hydrological cycle, with a focus on groundwater recharge and discharge drought, in the Dijle catchment and parts of the Demer and Zenne basins in central Belgium.

A water balance model (WetSpass) and groundwater model (MODFLOW) were combined to simulate groundwater recharge and groundwater discharge with high temporal and spatial resolution. Moreover, the variable threshold value method was implemented for groundwater drought analysis.

Groundwater drought analysis on groundwater recharge and discharge to the rivers and wetland show that the number of groundwater discharge drought events was smaller than the number of recharge drought events. Not all recharge drought events resulted in discharge drought. This was expected as the number of hydrological droughts normally decreases as the groundwater recharge droughts propagate through the aquifer. When it comes to the onset of the drought events, not much difference was observed between droughts on recharge and discharge to the wetland. The drought events appeared to occur around the same time. However, the discharge drought events to the rivers were delayed by 2 to 4 months compared to recharge drought events. In terms of severity, recharge drought events were more severe than discharge drought events. Attenuation by the groundwater system could have played a role here.

From this study, it is concluded that not all meteorological droughts result in groundwater drought. However, moderate to the extreme of meteorological drought severity range propagates to groundwater and causes groundwater drought. Furthermore, the characteristics of drought, like duration, onset, and deficit, changed during drought propagation in the aquifer, and its impact was also detected on Doode Bemde wetland groundwater level.

3.6 References

Abdollahi, K., Bashir, I., Verbeiren, B., Harouna, M., van Griensven, A., Huysmans, M. and Batelaan, O.: A distributed monthly water balance model: formulation and application on Black Volta Basin, Environ. Earth Sci., 76(5), 1–18, doi:10.1007/s12665-017-6512-1, 2017.

Anderson, M.P., Woessner, W.W., Hunt, R.J.: Applied Modeling Groundwater Simulation of Flow and Advective Transport, Applied Groundwater Modeling, doi.org/10.1016/B978-0-08-091638-5.00013-4, 2015.

Batelaan, O. and De Smedt, F.: WetSpass: a flexible, GIS based, distributed recharge methodology for regional groundwater modelling, in:Proceedings of a symposium held during the Sixth IAHS Scientific Assembly, Maastricht, The Netherlands, July 2001, 269, 11–17, 2001.

Batelaan, O. and De Smedt, F.: GIS-based recharge estimation by coupling surface-subsurface water balances, J. Hydrol., 337(3–4), 337–355, doi:10.1016/j.jhydrol.2007.02.001, 2007.

Batelaan, O., Asefa, T., van Rossum, P. and De Smedt, F.: Groundwater flow modelling of three wetland ecosystems in river valleys in Flanders, Belgium, in: Proceedings of 8th Conference of the European Network of Experimental and Representative Basins (ERB), Ghent, Belgium, 27- 29 September 2000, 1–7, 2003.

Beyene, B. S. and Van Loon, A. F.: Investigation of variable threshold level approaches for hydrological drought identification, Hydrol. Earth Syst. Sci. Discuss, 12765–12797,doi:10.5194/hessd-11-12765-2014, 2014.

Bloomfield, J.P., Marchant, B.P.: Analysis of groundwater drought building on the standardised precipitation index approach. Hydrol. Earth Syst. Sci., 17, 4769–4787, doi:10.5194/hess-17-4769-2013, 2013.

Calow, R. C., Robins, N. S., MacDonald, A. M., Macdonald, D. M. J., Gibbs, B. R., Orpen, W. R.,Mtembezeka, P., Andrews, A. J. and Appiah, S. O.: Groundwater management in drought prone areas of Africa, Int. J. Water Resour. Dev., 13(2), 241–262, doi:10.1080/07900629749863, 1997.

Cammalleri, C., Barbosa, P.: Analysing the Relationship between Multiple-Timescale SPI and GRACE Terrestrial Water 11, 14, doi:10.3390/w11081672, 2019.

De Becker, P., Hermy, M. and Butaye, J.: Ecohydrological characterization of a groundwater-fed alluvial floodplain mire, Appl. Veg. Sci., 2(2), 215–228, doi:10.2307/1478985, 1999.

Drexler, J.Z., Ewel, K.C.: Effect of the 1997-1998 ENSO-related drought on hydrology and salinity in a Micronesian wetland complex. Estuaries 24, 347–356. doi:10.2307/1353237, 2001.

Edward, D. C. and McKee, T. B.: Characteristics of 20th century drought in the United States at multiple time scales, Colorado State University, Fort Collins, Colorado,

Climatology Reports,172 pp., 1997.

Eltahir, E.A.B., Yeh, P.J.F.: On the asymmetric response of aquifer water level to floods and droughts in Illinois. Water Resour. Res. 35, 1199–1217, doi:10.1029/1998WR900071, 1999.

Fang, X., Pomeroy, J.W.: Drought impacts on Canadian prairie wetland snowhydrology. Hydrol. Process. 22, 2858–2873. https://doi.org/10.1002/hyp.7074, 2008.

Flemish Water Authorities: https://www.waterinfo.be/, last access: 20 April 2019.

Harbaugh, A. W., Banta, E. R., Hill, M. C. and McDonald, M. G.: MODFLOW-2000, The U.S. Geological Survey Modular Ground-Water Model - User Guide to Modularization Concepts and the Ground-Water Flow Process, Reston, Virginia, Open-File Report 2000-92, 130pp.,2000.

Hoyaux, J., Verheyden, S., Bogaert, J., Ghelen, Y., Van Leest, M., Annemarie, V. der A. and Squilbin, M.: Belgian National Adaptation Plan (2017-2020), B-1000 Brussels, Belgium, 40pp., 2016.

Huysmans, M. and Dassargues, A.: Hydrogeological modeling of radionuclide transport in low permeability media: A comparison between Boom Clay and Ypresian Clay, Environ. Geol., 50(1), 122–131, doi:10.1007/s00254-006-0191-7, 2006.

Huysmans, M., Peeters, L., Moermans, G., Dassargues, A.: Relating small-scale sedimentary structures and permeability in a cross-bedded aquifer. J. Hydrol. 361, 41–51. doi:10.1016/j.jhydrol.2008.07.047, 2008.

McKee, T. B., Doesken, N. J. and Kleist, J.: A drought climatology for Europe, in: Proceedings of the 8th Conference on Applied Climatology, Anaheim, California, 17-22 January 1993, 179– 183,1993.

Mishra, A.K., Singh, V.P.: A review of drought concepts. J. Hydrol. 391, 202–216, doi:10.1016/j.jhydrol.2010.07.012, 2010

Moens, M., Rouhart, J.: Monografie van het Dijle-bekken, Chapt. Hydrogeologische beschrijving van het Dijle-bekken ten zuiden van Wavre, 1978.

Peeters, L.: Groundwater and geochemical modelling of the unconfined Brussels aquifer, Ph.D. thesis, KU Leuven, Belgium, 128 pp., 2010.

Peters, E.: Propagation of drought through groundwater systems, Ph.D. thesis, Wageningen University, The Netherlands, 221 pp., 2003.

Peters, E., Bier, G., van Lanen, H. A. J. and Torfs, P. J. J. F.: Propagation and spatial distribution of drought in a groundwater catchment, J. Hydrol., 321(1–4), 257–275, doi:10.1016/j.jhydrol.2005.08.004, 2006.

Peters, E., Torfs, P.J.J.F., van Lanen, H.A.J., Bier, G. : Propagation of drought through groundwater - A new approach using linear reservoir theory, Hydrol. Process. 17, 3023–3040. doi:10.1002/hyp.1274, 2003.

Peters, E., Van Lanen, H.A.J.: Propagation of drought in groundwater in semi-arid and sub-

humid climaticregimes, In: Proceedings of the International Symposium of Hydrology of the Mediterranean and Semi-AridRegions, Montpellier, France, 1–4 April, 278, pp. 312–317, 2003.

RMI, 2020. RMI - Temperature. URL https://www.meteo.be/en/weather/forecasts/weather-model-alaro/temperature (accessed 4.5.20).

Ridder, K. De, Couderé, K., Depoorter, M., Liekens, I., Pourria, X., Steinmetz, D., Vanuytrecht, E., Verhaegen, K., Wouters, H., Evaluation of the Socio-Economic Impact of Climate Change in Belgium, 2020.

Tabari, H., Taye, M. T. and Willems, P.: Water availability change in central Belgium for the late 21st century, Glob. Planet. Change, 131, 115–123, doi:10.1016/j.gloplacha.2015.05.012, 2015.

Thom, H. C. S.: A Note on the Gamma Distribution, Mon. Weather Rev., 86(4), 117–122, doi:10.1175/1520-0493(1958)086<0117:anotgd>2.0.co;2, 1958.

Tricot, C., Debontridder, L., Van de Vyver, H., Vandiepenbeek, M., Dewitte, S., De Backer, H.,Malderen, R., Vannitsem, S. and Roulin, E.: Oog voor het Klimaatt/Vigilance climatique, KML,Bruxelles, Belgium, 87 pp., 2015.

Van Lanen, H. A. J.: Drought propagation through the hydrological cycle, in: Proceedings of the Fifth FRIEND World Conference about Climate Variability and Change—Hydrological Impacts, Havana, Cuba, November 2006, 308, 122–127, 2006.

Van Lanen, H. A. J. and Peters, E.: Temporal variability of recharge as an indicator for natural groundwater droughts in two climatically contrasting basins, in: Proceedings of Fourth International Conference on FRIEND 2002 - regional hydrology: bridging the gap between research and practice, Cape Town, South Africa, 101–106, 2002.

Van Loon, A.F., Van Lanen, H.A.J.: A process-based typology of hydrological drought. Hydrol, Earth Syst. Sci. 16, 1915–1946. doi:10.5194/hess-16-1915-2012, 2012.

Van Loon, A.F., van Lanen, H.A.J., Tallaksen, L.M., Hanel, M., Sapriza, G., Koutroulis, A., vam Huijgevoort, M., Hisdal, H.: Propagation of drought through the hydrological cycle. Watch Tech. Rep, 2011.

Van Loon, A. F. Van: On the propagation of drought How climate and catchment characteristics influence hydrological drought development and recovery, Ph.D. thesis, Wageningen University, The Netherlands, 195 pp., 2013.

Verbeiren, B., Huysmans, M., Tychon, B., Jacquemin, I., Canters, F., Vanderhaegen, S., Engelen, G., Poelmans, L., De Becker, P., Tsakiris, G., Vangelis, H. and Batelaan, O.: Drought-related vulnerability and risk assessment of groundwater resources under temperate conditions, in: 13th International Conference on Environmental Science and Technology, Athens, Greece, 5–7 September 2013, 10 pp., 2013.

VMM: Grondwater in Vlaanderen: Het Brulandkrijtsysteem., Aalst, Belgium, 2008.

Wilhite, D.A.: Chapter1 Drought as a Natural Hazard: Concepts and Definitions, Drought A Glob. Assess. 1, 3–18, 2000.

Wilhite, D. A. and Glantz, M. H.: Understanding the drought phenomenon: The role of definitions, Water Int., 10, 111–120, doi:10.4324/9780429301735-2, 1985.

Wossenyeleh, B.K., Verbeiren, B., Diels, J., Huysmans, M.: Vadose zone lag time effect on groundwater drought in a temperate climate. Water 12, 2123, doi:10.3390/w12082123, 2020.

Yevjevich, V.: An objective approach to definitions and investigations of continental hydrologic droughts, Hydrol. Pap. Color. State Univ. Fort Collins CO, 23, 25 pp., 1967.

Chapter 4

4 Differentiating between land use and climate as influencing factors on groundwater recharge drought

Based on: Wossenyeleh, B. K., Verbeiren, B., and Huysmans, M.: Differentiating between land use and climate as influencing factors on groundwater recharge drought, temperate climate context, Journal of Hydrology regional studies, under review, 2021.

4.1 Abstract

Drought is considered an important natural hazard mainly caused by below-normal precipitation for a large area and significant duration that affects both surface and groundwater resources. Natural meteorological variations (climate factor) and human-induced factors, such as land use/land cover (LULC) change, play a role in inducing or intensifying drought. Due to drought propagation, effects of drought can be detected in groundwater recharge, groundwater discharge, and groundwater level. Groundwater recharge forms the primary source for replenishing aquifers. Therefore, reliable estimation of groundwater recharge is crucial. This chapter aims to develop a methodology that enables differentiation in space and time between the effects of LULC change and the climate factor on groundwater recharge estimation and groundwater drought. A water balance model was used to estimate spatially distributed groundwater recharge. A variable threshold value method was implemented for groundwater drought analysis. This research is carried out in a study area encompassing the Dijle river catchment and parts of the Demer and Zenne basins in central Belgium.

This study shows that LULC change and the shift of meteorological variables from the long-term "normal" conditions decreased average groundwater recharge from 1990 to 2013. Drought characteristics such as duration, number, and severity of groundwater drought events are also affected by LULC change and the shift of meteorological variables from long-term "normal" conditions. The study also reveals the effect of each LULC class on groundwater recharge.

4.2 Introduction

Drought is considered an important natural hazard mainly caused by below-normal precipitation for a large area and significant duration. It is a creeping natural threat, in contrast to, for example, flooding, which has a direct and visible effect. Droughts can have significant socio-economic and environmental impacts and endanger environmental resource sustainability (Bloomfield and Marchant, 2013; Calow et al., 1997; Mishra and Singh, 2010; Wilhite, 2000). Drought can affect both surface and groundwater resources. In case the drought affects groundwater bodies, the term groundwater drought is used. Groundwater drought can be defined as a temporary decrease in groundwater availability over a significant period. This drought develops slowly on groundwater recharge, levels, and discharge to the surface (Van Lanen and Peters, 2000b; Mishra and Singh, 2011; Peters and van Lanen, 2003; Tallaksen et al., 2006).

Droughts, particularly groundwater drought, mainly occurs because of natural meteorological variations; however, human-induced factors play a role in inducing or intensifying drought. Van Loon et al. (2016a) reported anthropogenic change plays a significant role in recent droughts in different parts of the world. This anthropogenic change, such as land-use change and increasing water demand because of population growth, alter depletion of groundwater level and groundwater recharge (Jin et al., 2015; Van Lanen and Peters, 2002; Van Loon et al., 2016a, 2016b; Mustafa et al., 2017; Schwartz and Ibaraki, 2011). Therefore, there is a need for an improved understanding of groundwater drought and the human-induced factors influencing the groundwater balance. Besides, due to the focus on natural factors inducing groundwater drought, this field remains poorly studied; hence, it is essential to understand and identify human-induced factors on groundwater drought. This should contribute to an integrated approach that allows tackling adverse effects and safeguarding groundwater resources' sustainability.

Due to drought propagation in the aquifer, low groundwater recharge often results in low groundwater levels and groundwater discharge (Peters, 2003a; Peters et al., 2003, 2006). This means that groundwater drought can be detected in groundwater recharge, groundwater discharge, and groundwater level. Groundwater recharge forms the primary source of water for replenishing aquifers. Therefore, reliable estimation of groundwater recharge in space and time is of utmost importance for sustainable management of groundwater resources and detecting groundwater drought propagation in the aquifer (Bakker et al., 2013; von Freyberg et al., 2015; Jin et al., 2015; Van Lanen and Peters, 2000b; Peters et al., 2006).

Groundwater recharge is affected by precipitation, interception, evapotranspiration, surface runoff, and infiltration (Batelaan and De Smedt, 2007; Savenije, 2004). Bakker et al. (2013) and Scanlon et al. (2002) discussed various groundwater recharge estimation methods. Since groundwater recharge is highly variable in space and time, many methods of groundwater recharge estimation incorporate a spatial and/or temporal variation of hydrometeorology, land-use, and soil texture (e.g., Batelaan and De Smedt, 2007; Best and Lowry, 2014; Eilers et al., 2007; Jyrkama et al., 2002; Jyrkama and Sykes, 2007; Minor et al., 2007). Different models such as SWAT (Arnold et al., 2000), DREAM (Manfreda et al., 2005), WetSpa (Wang et al., 1996), WetSpass (Batelaan and DeSmedt, 2001), etc. have been developed to estimate groundwater recharge in space and time. According to Abdollahi et al.(2017) and Batelaan and DeSmedt (2001), the WetSpass model is suited for areas with shallow groundwater and allows incorporating high variability of land-use change. For example, for Flanders, Belgium,

Zomlot et al. (2015) estimate spatially distributed groundwater recharge using the WetSpass model.

Verbeiren et al. (2013) discussed soil and topographic characteristics, land-use, and climate as influencing factors for groundwater recharge in the Belgian context. Based on the relative change in time, the first two influencing factors are static, and the latter two are dynamic. The change of these factors affects groundwater recharge's Spatio-temporal estimation (Brouyere et al., 2004; Bultot et al., 1990; Price, 2011; Verbeiren et al., 2013). Moreover, these dynamic factors also influence groundwater recharge drought events (Van Loon, 2015). As Van Loon et al. (2016b) stated, natural activities, such as the occurrence of meteorological drought events, and human activities, such as land-use dynamics resulting from extensive urbanization, play a role in changing these influencing factors. Differentiating and quantifying each influencing factor's contribution to groundwater recharge and groundwater drought is challenging, but it is an essential task.

This chapter aims to develop a methodology that enables differentiation in space and time between the effects of land-use and climate on groundwater recharge in a temperate context. Moreover, the potential contribution of land-use and climate on groundwater recharge drought will be identified.

4.3 Methodology

In this study, a combined methodology based on a spatially distributed water balance model and drought analysis using the variable threshold method is developed to differentiate between the main influencing factors (climate and land use/land cover) on groundwater recharge. The study was divided into four parts: (1) Spatio-temporal estimation of groundwater recharge, (2) identifying the influence of land use/land cover (LULC) change on groundwater recharge, (3) identifying the influence of climate on groundwater recharge, and (4) drought analysis on groundwater recharge. First, a water balance model was built and ran several times with varying LULC and meteorological input to acquire spatially distributed simulated groundwater recharge for different scenarios. A thorough analysis of the main influencing factors (climate and LULC) was done to investigate their impact on simulated groundwater recharge. Finally, groundwater recharge drought was analyzed to identify each factor's potential effects on the occurrence and characteristics of drought events in groundwater recharge.

4.3.1 Groundwater recharge estimation

Groundwater recharge is affected by a combination of physical conditions and meteorological factors. All water balance components are simulated at a monthly timestep using the WetSpass-M model (Abdollahi et al., 2017; Batelaan and DeSmedt, 2001; Batelaan and De Smedt, 2007).

4.3.1.1 WetSpass-M Model

The WetSpass model is a physically-based distributed water balance model (Batelaan and DeSmedt, 2001; Batelaan and De Smedt, 2007). Abdollahi et al. (2017) adjusted the model, enabling water balance simulation at a monthly timestep (WetSpass-M) instead of a seasonal timestep (WetSpass). In contrast to the seasonal approach (summer/winter season), the monthly approach enables considering the specific conditions of a study area (e.g., more than two seasons) and considering within-season dynamics, thus, have broader applicability.

4.3.1.2 Study area

The study area consists of the Dijle catchment and parts of the Demer and Zenne basins in central Belgium and has a surface area of 1825 km^2 (Figure 4.1). In this study area, the most important aquifer is the Brussels Sands aquifer, and the land surface elevation ranges between 10 m and 110 m. Belgium has a temperate climate with a long-term average annual precipitation of approximately 800 mm and a mean temperature of around 10 ^oC (Royal Meteorological Institute, 1931).

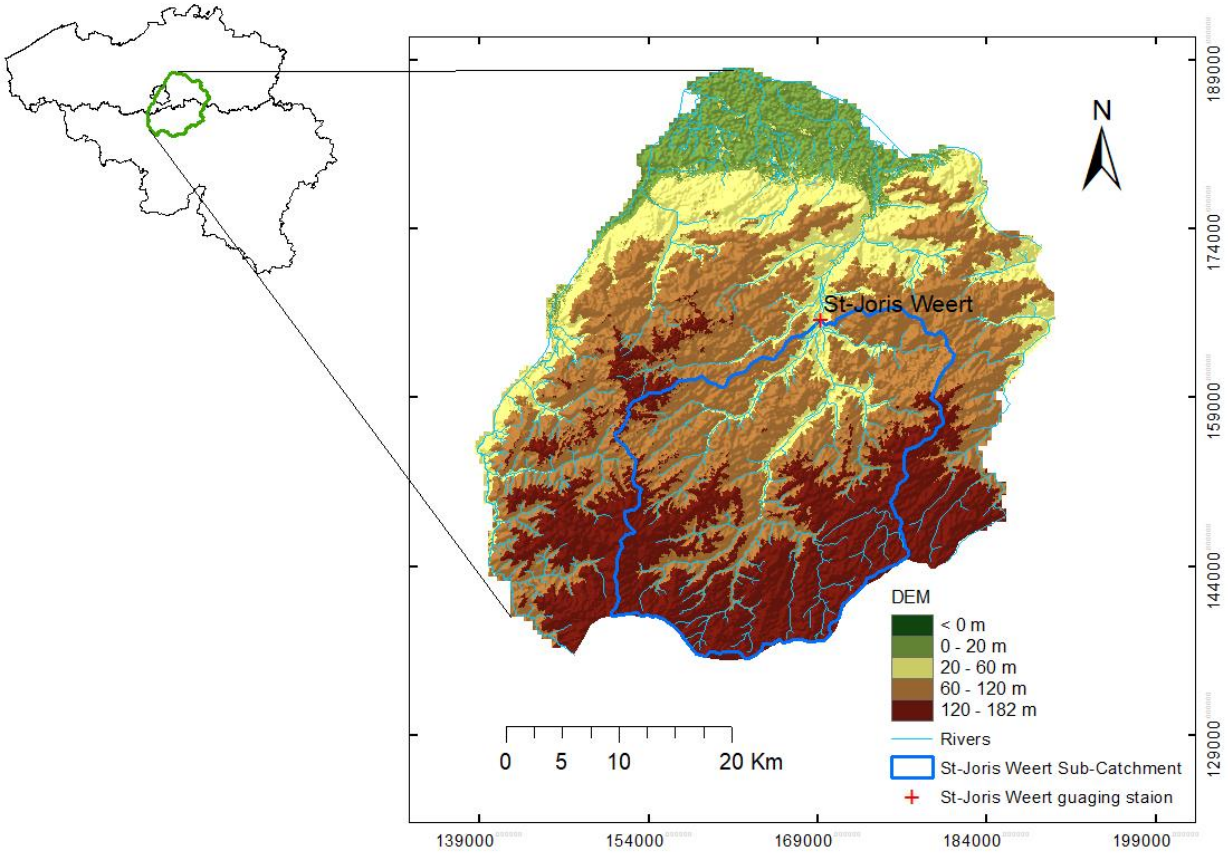


Figure 4.1: Location of the study area, the digital elevation model (DEM) in Belgium

4.3.1.3 Data

The main inputs are spatially distributed maps for land-use, soil, slope, and four meteorological parameters: precipitation, potential evapotranspiration, temperature, and wind speed. All spatially distributed input maps used were generated in the GroWaDRISK project. This project aimed to develop a drought-related vulnerability and risk assessment strategy for sustainable management of groundwater resources under temperate conditions (Verbeiren et al., 2013). The spatial resolution of the land-use, soil texture, and slope maps for WetSpass simulations is 100m, resulting in a monthly time-series of groundwater recharge maps at the same resolution.

4.3.1.3.1 Land-use and land-use change

The distributed LULC map, generated by the GroWaDRISK project and containing 21 land-use classes (Figure 4.2), forms the main and best available input regarding the LULC for the situation 2013. However, one of the major goals of this study is to differentiate the contribution of the changes in each of the influencing factors (climate and LULC) on the occurrence of drought. Historical land-use maps, such as the CORINE Land Cover maps (1990, 2000, and

2006 – 100 m resolution) and VITO land-use map (2013 – 100 m resolution), are also used to assess the influence of land-use and land-use change (especially urban expansion). The CORINE land-cover maps have the advantage of being created in a consistent way; however, CORINE land-cover maps also suffer from some limitations like tending to overestimate urban land-cover (Diaz-Pacheco and Gutiérrez, 2014). The GroWaDRISK project made use of historic urban masks for 1986, 2000, and 2013 (Table 4.1) to overcome this major limitation. The urban masks alter the CORINE land cover maps to make them consistent with the sealed surface proportion maps and the new LULC map (Vanderhaegen et al., 2015). The sealed surface fraction maps account for variability in the degree of imperviousness within the urban masks. Three sealed surface fraction maps (1986, 2000, 2013) were generated by the GroWaDRISK project using LANDSAT imagery for 1986, 2000, and 2013. For years between these dates, the sealed surface fraction is linearly interpolated on a pixel-by-pixel basis. Although sealed cover change (mainly urban expansion or densification) is more likely to be a discrete process (sudden change at a given moment), the assumption of a more gradual change in sealed surface proportion aims at reducing the uncertainty regarding the actual moment of change. LULC dynamics are considered a combination of a series of four LULC maps and continuous sealed fraction maps (Table 4.1).

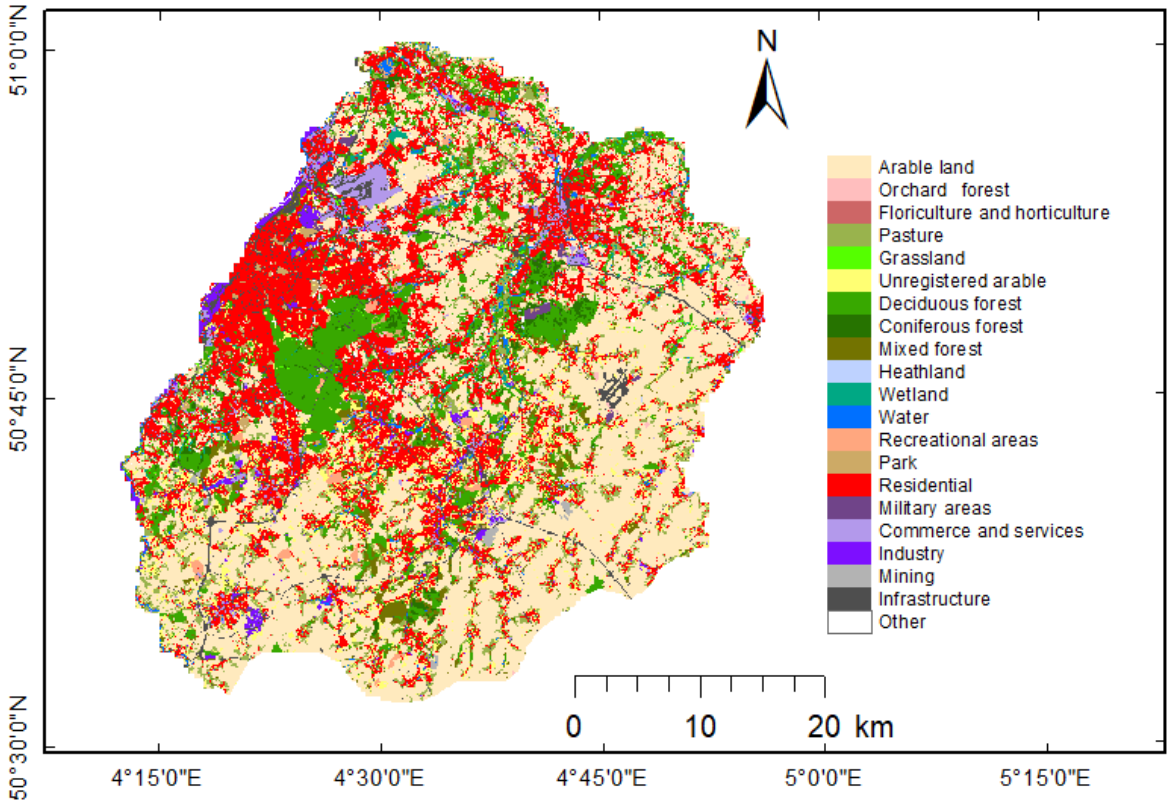
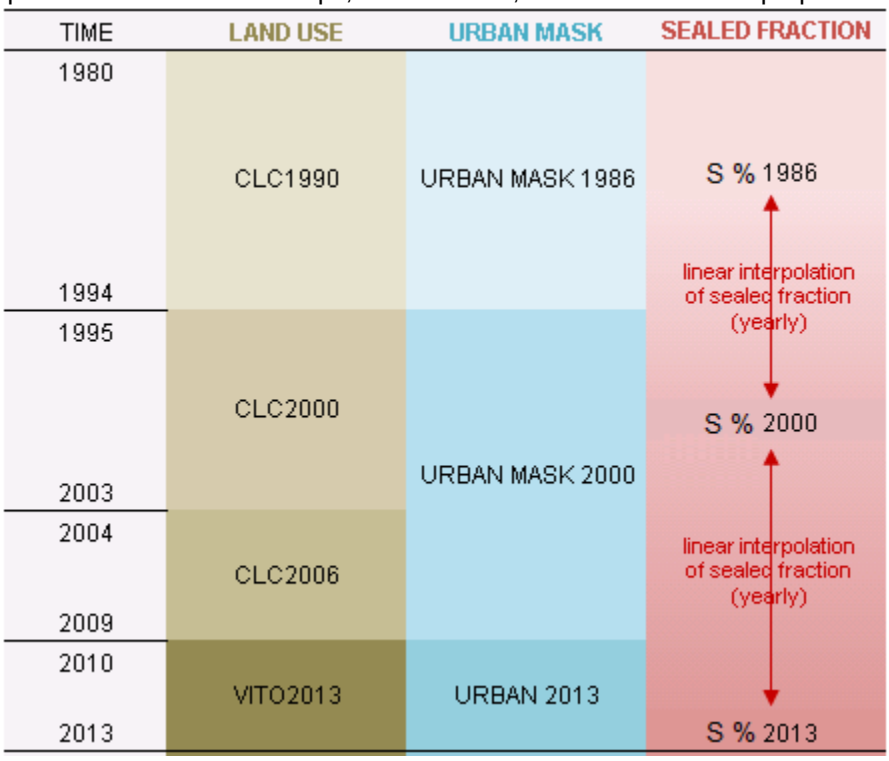


Figure 4.2: Integrated land use map of 2013 (obtained from GroWaDRISk project)

Table 4.1: Period-specific use of land-use maps, urban masks, and sealed surface proportion maps.



4.3.1.3.2 Soil

A regional soil map is available from the GroWaDRISK project, where the Flemish and Walloon region soil maps were combined. The merging of both maps was relatively straightforward, as both maps are based on the Belgian soil classification. WetSpass uses a different soil classification (12 soil texture USDA classes), so the Belgian soil texture classes were converted using the soil texture triangle (Soil Survey Staff, 1951). In the case of missing soil texture information (e.g., in urban areas), the dominant nearby soil texture class was attributed.

4.3.1.3.3 Slope

The spatially distributed slope map is derived from the area-covering digital elevation model developed and used in an earlier study (Batelaan et al., 2007). This DEM combines elevation data from the National Geographic Institute (NGI) and the Flemish Groundwater Model (VGM - Meyus et al., 2005).

4.3.2 Identifying the influence of land use and climate factors on recharge

WetSpass simulations were used to assess the impact of the influencing factors' LULC' and 'climate' with respect to drought effects on the recharge time series. Hereto, WetSpass is run several times with varying LULC and meteorological input. Table 4.2 summarizes the runs

used to identify the separate influence of land use and climate factors. Two static LULC maps and one dynamic LULC map were used to assess the impact of LULC change. In these static LULC maps, the real LULC change was neglected. The dynamic LULC and meteorological maps were derived from the observed LULC and meteorological inputs, respectively.

Table 4.2: WetSpass model runs with varying inputs, enabling to assess the separate effects of the factor' LULC change' and 'climate variability.'

WetSpass Simulations		Run 1	Run 2	Run 3	Run 4
LULC Change	Static (CLC1990)	**X**			
	Static (VITO2013)		**X**		
	Dynamic (1980-2013)			**X**	**X**
Meteo Input	Dynamic (1980-2013)	**X**	**X**	**X**	
	Long-term Average				**X**
Accounting for:		Influence Land-Use Change			Influence Climate Factor

Runs 1 to 3 were used to assess the influence of LULC change on the recharge estimation. By keeping the meteorological input constant and varying the LULC map (static 1990, static 2013, and dynamic), the differences between the resulting monthly recharge time-series (spatially averaged) give a good indication of the effect of the LULC on calculated recharge. Figure 4.3 presents conceptually how the effect of 'LULC change' can be visualized.

Similar, runs 3 and 4 are used to assess the influence of the natural 'climate variability' factor, enabling the assessment of meteorological drought effects on groundwater recharge. The dynamic model simulation (run 3) for 34 years (1980-2013) and at a monthly timestep, using dynamic LULC and meteorological input, is compared to the simulation (run 4) assuming long-term "normal" meteorological conditions.

The dynamic modeling approach of both LULC and meteorological (run 3) enables estimating the combined influence of LULC change and climate at each month or year. This means that this analysis can be made for a period of drought, and the contribution of both can be assessed.

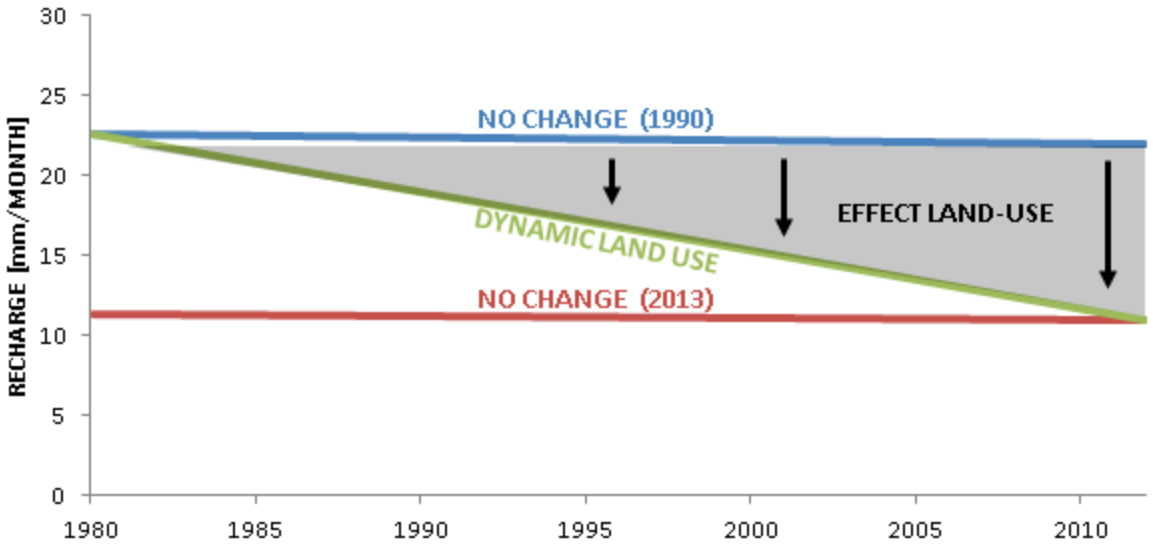


Figure 4.3: Conceptual figure that demonstrates how LULC effects on recharge are assessed, using two static and one dynamic run.

4.3.3 Model calibration

Since the dynamic run (run 3) represents the actual condition, the WetSpass-M model was calibrated based on this run. The model's calibration is based on four global parameters (evapotranspiration parameter (α), surface runoff parameter (LP), interception parameter (a), and average rainfall intensity) and three local weight factors (slope factor, land factor, and soil factor). It was manually optimized according to the goodness of fit between base-flow calculated using equation (1) from the dynamic run of groundwater recharge of Sint-Joris-Weert sub-catchment (Figure 4.1) and the separated base-flow from observed river discharge calculated using WETSPRO (Willems, 2009) at Sint-Joris-Weert gauging station (Figure 4.1) for the year between 1982 and 1983. This period has been chosen deliberately to represent the initial conditions (without LULC change), as one of the main objectives is to assess the impact of LULC change on groundwater recharge and drought.

According to Abdollahi et al. (2017), monthly base-flow is calculated from the groundwater storage of the previous month and groundwater recharge (R_m) in the considered month as follows:

$$Q_{b(t)} = \beta Q_{b(t-1)} + 0.001 N_m (1-\beta) \emptyset R_m \quad (4.1)$$

Where β is a storage parameter [-] between 0 and 1, $Q_{b(t-1)}$ is the base-flow from the previous month [m^3/month], N_m is a number of days per month (≈ 30 days), and Ø [m^2/day] is the recharge contribution parameter to current base flow. For the pixel area A [m^2] with recession index k [day], this parameter would be:

$$\emptyset = \frac{1.15A}{k} \quad (4.2)$$

The result of the calibration should be evaluated both qualitatively and quantitatively. The Nash Sutcliffe Efficiency (NSE) and the coefficient of determination (r^2) are used to express the model's overall efficiency.

The coefficient of determination, r^2, is giving the proportion of the variance (fluctuation) of simulated base flow from groundwater recharge (q_s) and the filtered base flow (q_f):

$$r^2 = \left(\frac{\sum_{i=1}^{n}(q_s - \bar{q}_s)(q_f - \bar{q}_f)}{\sqrt{\sum_{i=1}^{n}(q_f - \bar{q}_f)^2}\sqrt{\sum_{i=1}^{n}(q_s - \bar{q}_s)^2}} \right) \quad (4.3)$$

Nash Sutcliffe Efficiency is a normalized statistic that determines the residual variance's relative magnitude compared to the measured data variance (Krause & Boyle, 2005).

$$NSE = 1 - \frac{\sum_{i=1}^{n}(q_f - q_s)^2}{\sum_{i=1}^{n}(q_f - \overline{q_f})^2} \quad (4.4)$$

Where n is the number of months

4.4 Results and Discussion

4.4.1 Model calibration

An initial flow value of 2.13 m^3/s, one filter step, a recession constant of 31 days and a wf-parameter filter of 0.35 was used for base-flow separation. The optimized β value of 0.25 was adapted by matching simulated and filtered base-flow. Besides, an optimized recharge contribution parameter of 0.0032 m^2/sec is calculated using *Equation 4.2*. Figure 4.4 compares simulated baseflow from the dynamic run recharge and monthly filtered base-flow separated from river discharge using WETSPRO (r^2=0.91, Nash-Sutcliffe efficiency coefficient =0.74).

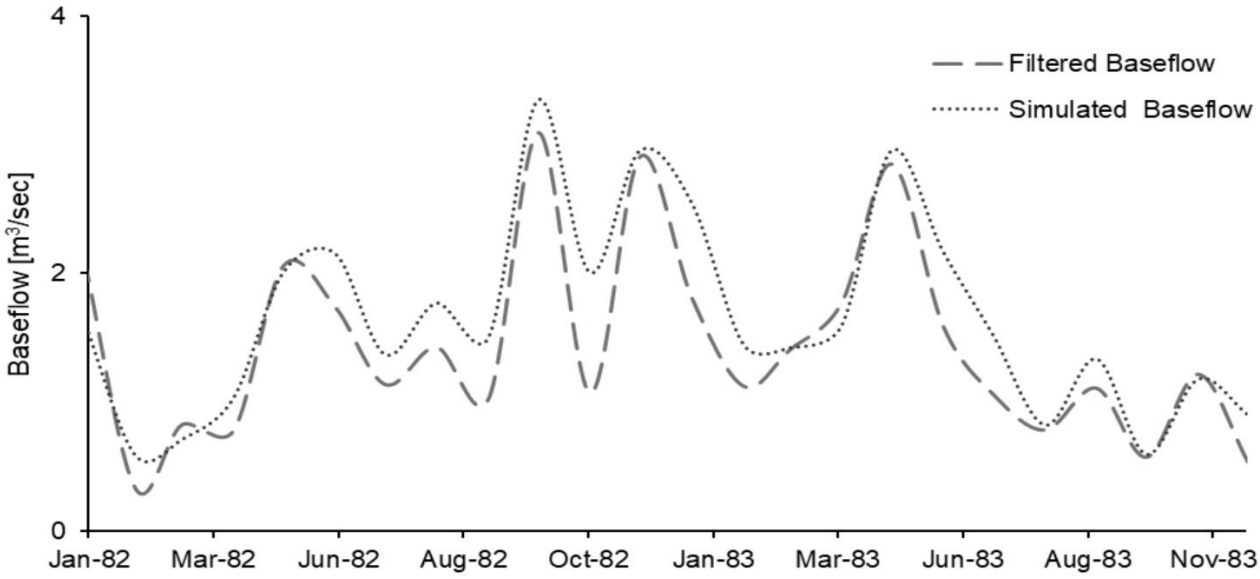


Figure 4.4: Simulated baseflow calculated from dynamic run (run 3) recharge of Sint-Joris-Weert sub-catchment vs. monthly filtered base-flow from flow measurement at Sint-Joris-Weert station.

Table 4.3: Calibrated parameter values after calibration

Categories	Parameter	Final value
Global Parameters	α	1.8
	LP	0.9
	a	4.5
	Average intensity [mm/hr]	2
Local weight factors	Slope factor	0.2
	Land factor	0.3
	Soil factor	0.5

4.4.2 Groundwater recharge

Four WetSpass-M model simulations were done to assess the influence of climate and LULC change on groundwater recharge by considering different meteorological and LULC inputs. The first three runs were used to identify the effect of LULC change. The last two runs were

used to identify the climate factor on groundwater recharge. Figure 4.5 shows the spatial distribution of the calculated monthly averaged groundwater recharge between 1980 to 2013 for all runs. A spatial and temporal average groundwater recharge of 25.6 mm/month, 25.45 mm/month, 24.19 mm/month, and 26.09 mm/month was estimated for run 1, run 2, run 3, and run 4, respectively. Simulated groundwater recharge depends strongly on the land use/ land cover. This means that the simulated groundwater recharge values are higher in forest areas and lower in areas with high impervious surfaces such as industries, residential, and commercial areas. Moreover, simulated groundwater recharge in the study area shows strong seasonal dynamics of (Figure 4.6): high in winter and low in summer.

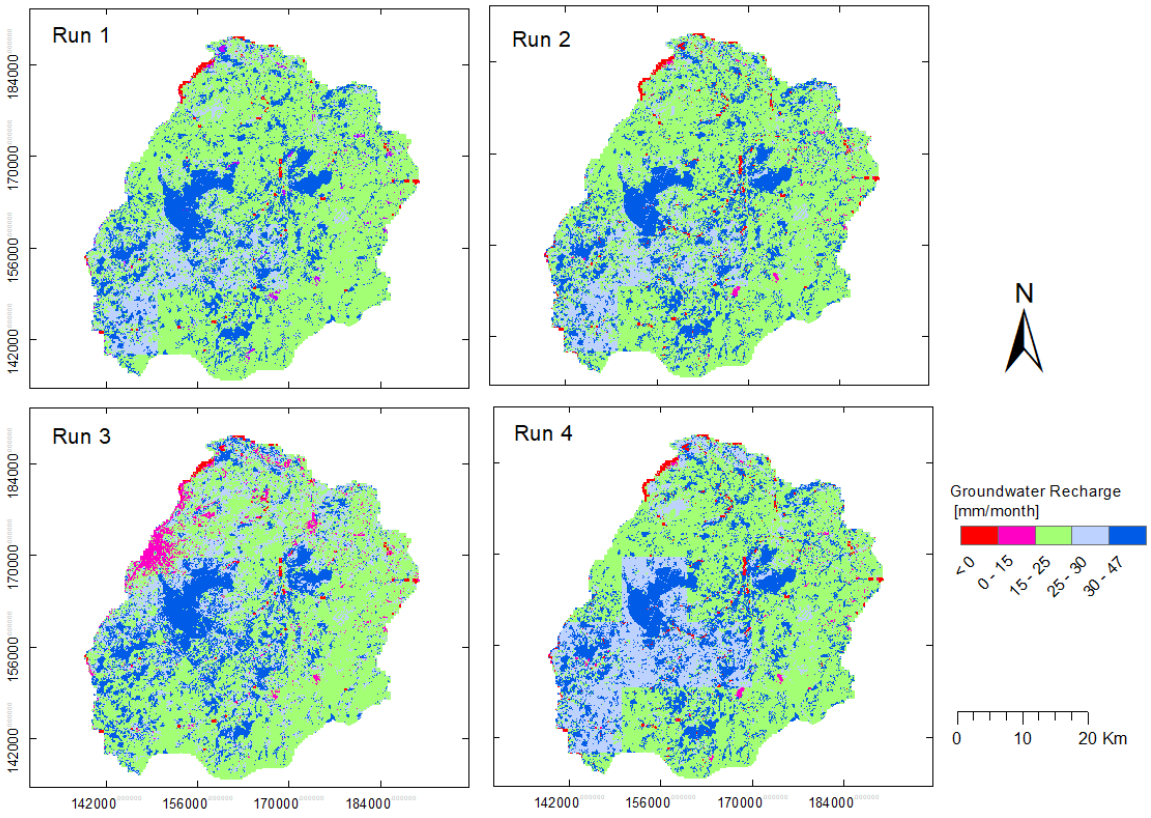


Figure 4.5: Monthly averaged groundwater recharge from 1980 to 2013 of the study area for the four different model runs, estimated using WetSpass-M.

In places where the water table is near the surface, such as wetlands and in areas near ponds and rivers, total evapotranspiration is higher than infiltration, and the estimated groundwater recharge values are negative.

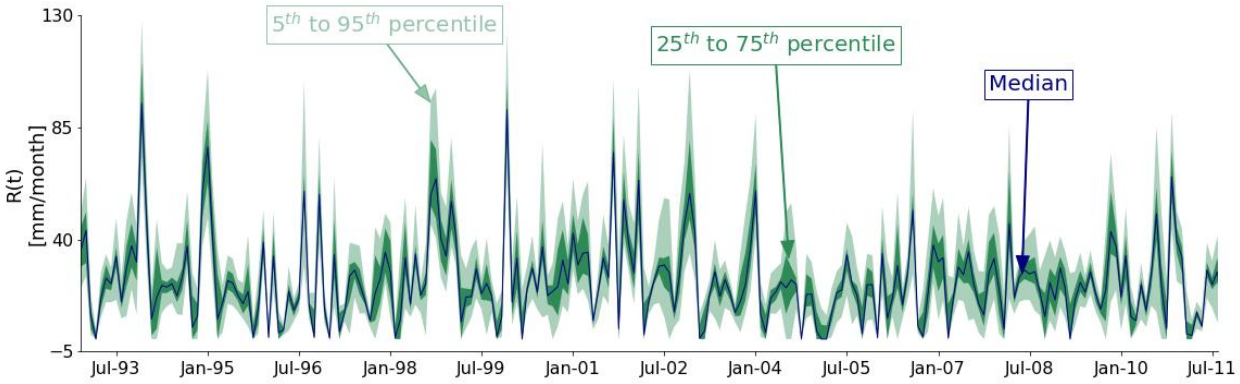


Figure 4.6: Estimated groundwater recharge of the dynamic run (run 3) to show the temporal variation. The dark blue line is the median curve (50th percentile) and shows the median groundwater recharge value for each month. The green shadow area represents the interquartile range (IQR). The light green shaded area represents the lowest and highest 5 % of each month's groundwater recharge values.

4.4.3 Influence of land use/land cover change on groundwater recharge

Run 1, run 2, and run 3 were used to investigate the LULC change contribution on simulated groundwater recharge. Figure 4.7 (left) indicates that groundwater recharge estimated using the two static simulations (run 1 and run 2) gives the same value in the cells without LULC change between the maps of 1990 and 2013, which is the majority of cells in the study area (Figure 4.7 (right)).

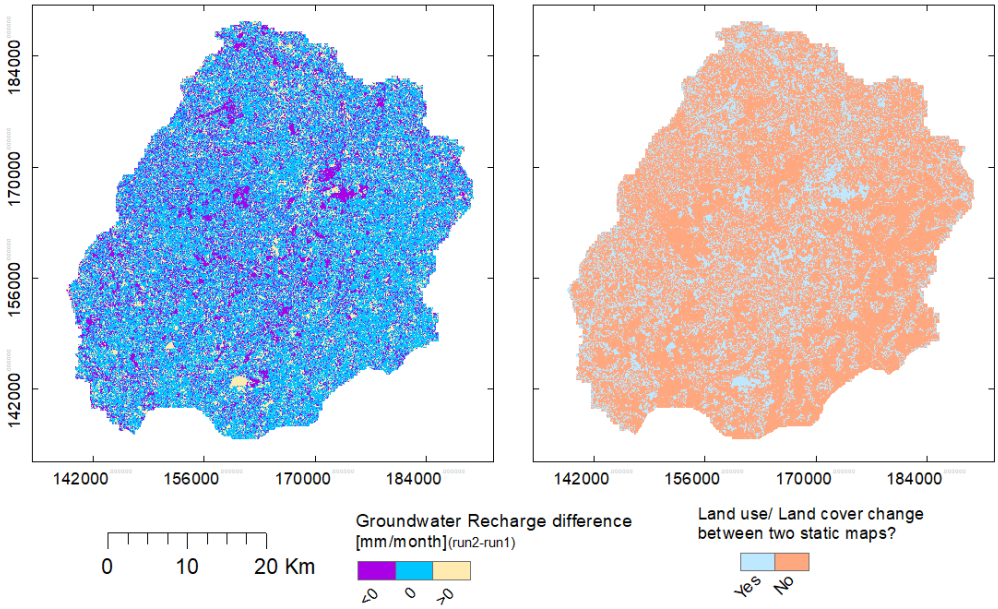


Figure 4.7: Monthly averaged groundwater recharge difference between run 2 and run 1 (left) (run2-run1), and LULC changed places between static land use/cover map of 1990 and 2013 (right).

Moreover, as Figure 4.7 (left) shows, some of the LULC changes result in higher groundwater recharge values, others in lower estimated groundwater recharge values.

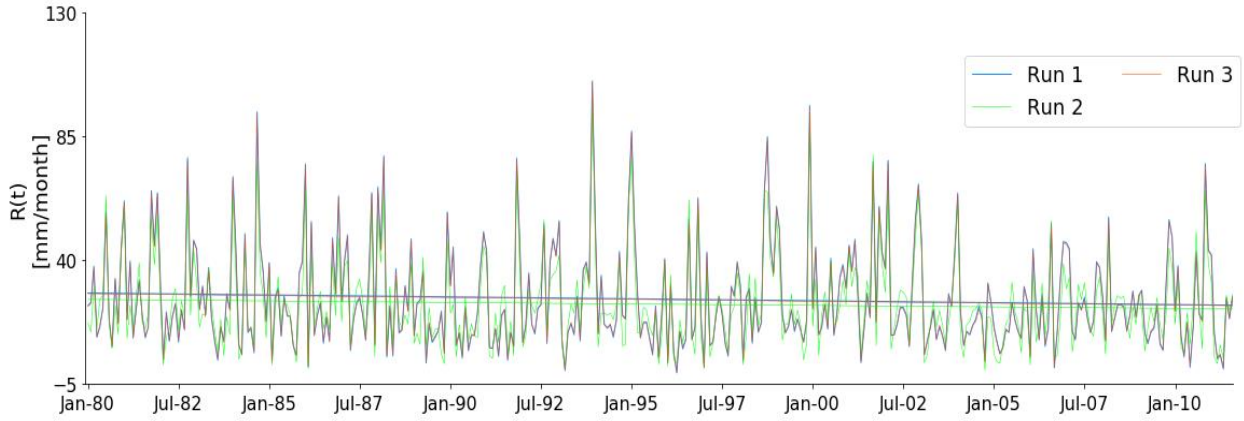


Figure 4.8: Spatially monthly averaged groundwater recharge for the first three runs with their linear regression line.

Figure 4.8 shows that it is difficult to compare the differences between the three runs because of averaging calculated groundwater recharge in space. Therefore, to identify the effect of LULC change on groundwater recharge, only the places which have experienced land use/cover change between the static land use maps of 1990 and 2013 ((Figure 4.7 (right)) are considered in the following analysis. Not all LULC changes have the same effect on simulated groundwater recharge. The effect of these LULC changes on simulated groundwater recharge can be split into two types of cells, where:

I. Land use/land cover change leads to higher simulated groundwater recharge
II. Land use/land cover change leads to lower simulated groundwater recharge

4.4.3.1 Land use/land cover changes that decrease groundwater recharge estimation

Figure 4.9 and Figure 4.10 show the change of LULC between 1990 and 2013. The main changes are conversions of arable land, pastures, forest or infrastructures into residential, industrial, and commercial and service areas. Therefore, the impervious surface area is higher in the LULC map of 2013 than in the LULC map of 1990.

Figure 4.11 shows that spatially monthly averaged groundwater recharge estimated using the LULC map of 2013 is lower than the estimate calculated using the LULC map of 1990. The difference in impervious surface area can explain this difference. Moreover, the estimated dynamic groundwater recharge (run 3) shown in Figure 4.11 indicates a higher gradual decrease in groundwater recharge from 1990 to 2013 than the statistic runs. This dynamic modeling approach (run 3) shows the influence of gradual LULC changes on groundwater recharge through time.

By comparing the groundwater recharge estimated using the dynamic run (run 3) and the static run (run 1), it can be quantified that, on average, groundwater recharge in the areas that have experienced LULC change resulting in decreasing recharge between 1980 and 2013 was 2.95 mm/month lower than it would have been without LULC changes.

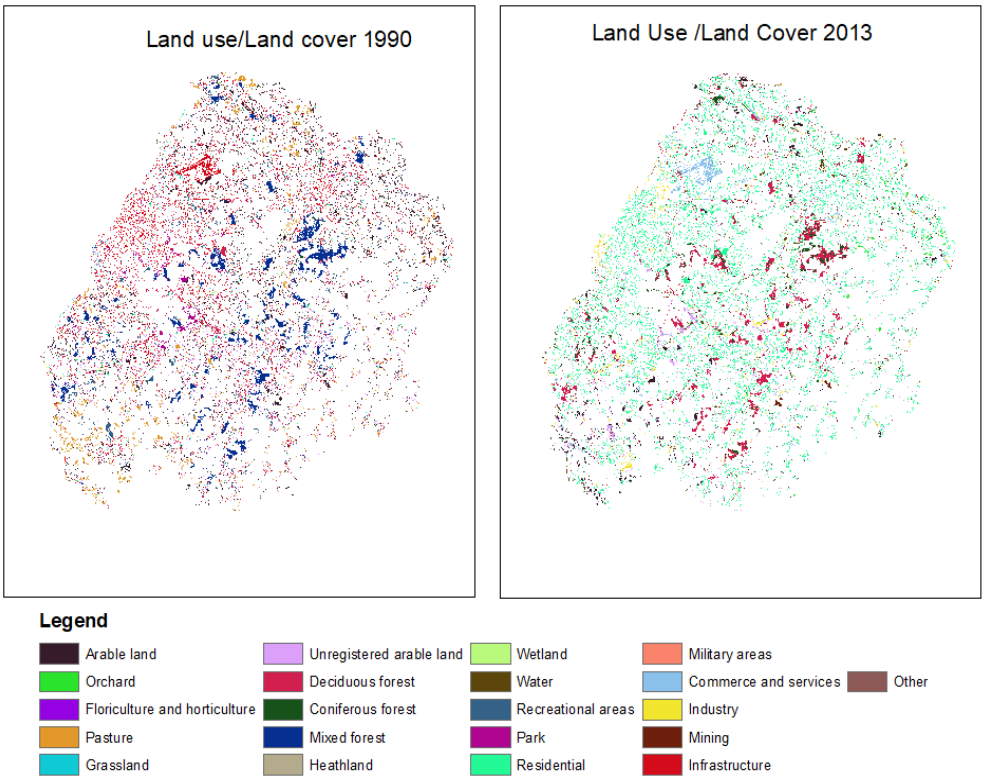


Figure 4.9: Static land use/land cover map of 1990 (left) and 2013 (right) for the places where simulated groundwater recharge has decreased

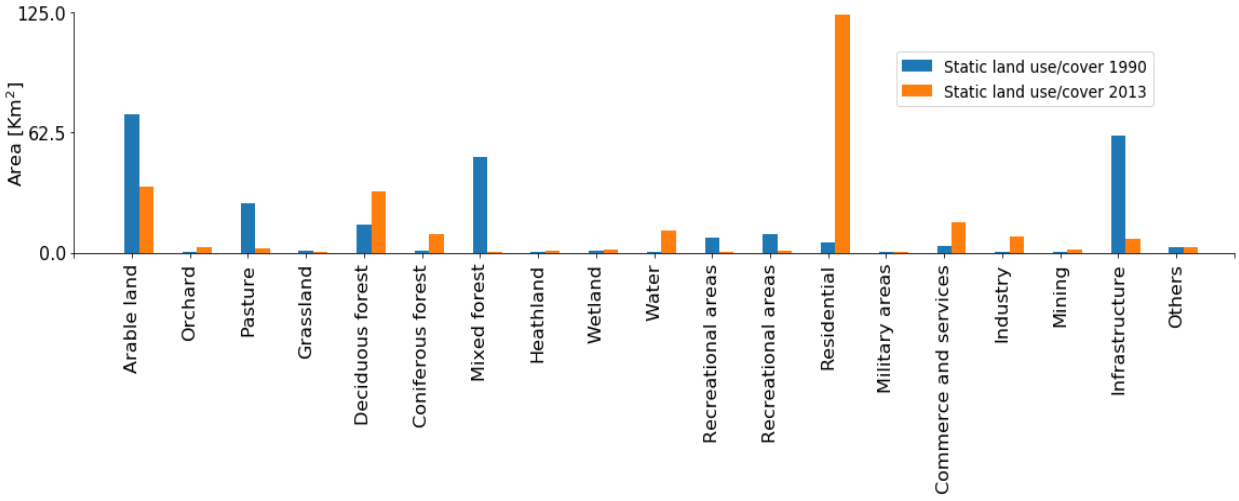


Figure 4.10: Area of each land use/land cover for the places where simulated groundwater recharge has decreased

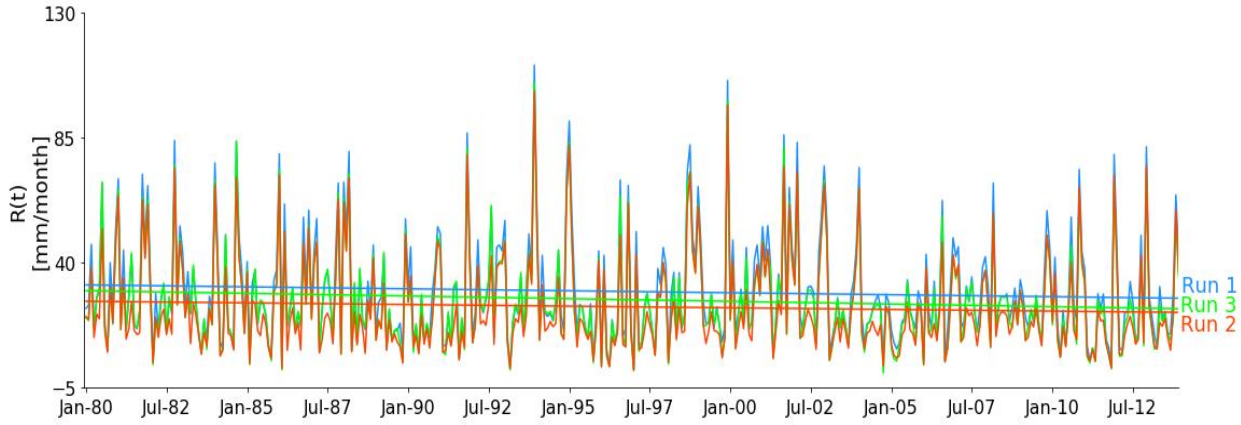


Figure 4.11: Spatially monthly averaged groundwater recharge for the first three runs with their linear regression line, for the places where simulated groundwater recharge has decreased.

4.4.3.2 Land use/land cover changes that increase estimated groundwater recharge

Figure 4.12 and Figure 4.13 show the change of LULC between 1990 and 2013 in locations where estimated groundwater recharge has increased. These cells are mostly arable land that is changed into the pasture, grassland, wetlands, and mixed forests. Moreover, some of the residential areas have also changed into infrastructure. This type of LULC changes may increase the infiltration capacity of the surface and/or decrease evapotranspiration.

Figure 4.14 shows that spatially monthly averaged groundwater recharge in cells with such LULC changes increases between 1990 and 2013. This difference could be explained by the difference in infiltration capacity of the surface or evapotranspiration from each LULC. Moreover, the estimated dynamic groundwater recharge (run 3) shown in Figure 4.14 indicates a gradual slight increase of groundwater recharge from 1990 to 2013 in those cells.

By comparing the groundwater recharge estimated using the dynamic run (run 3) and static run (run 1), it can be quantified that, on average, groundwater recharge in the areas that have experienced LULC change resulting in increasing recharge between 1980 and 2013 was 0.25 mm/month higher than it would have been without LULC changes.

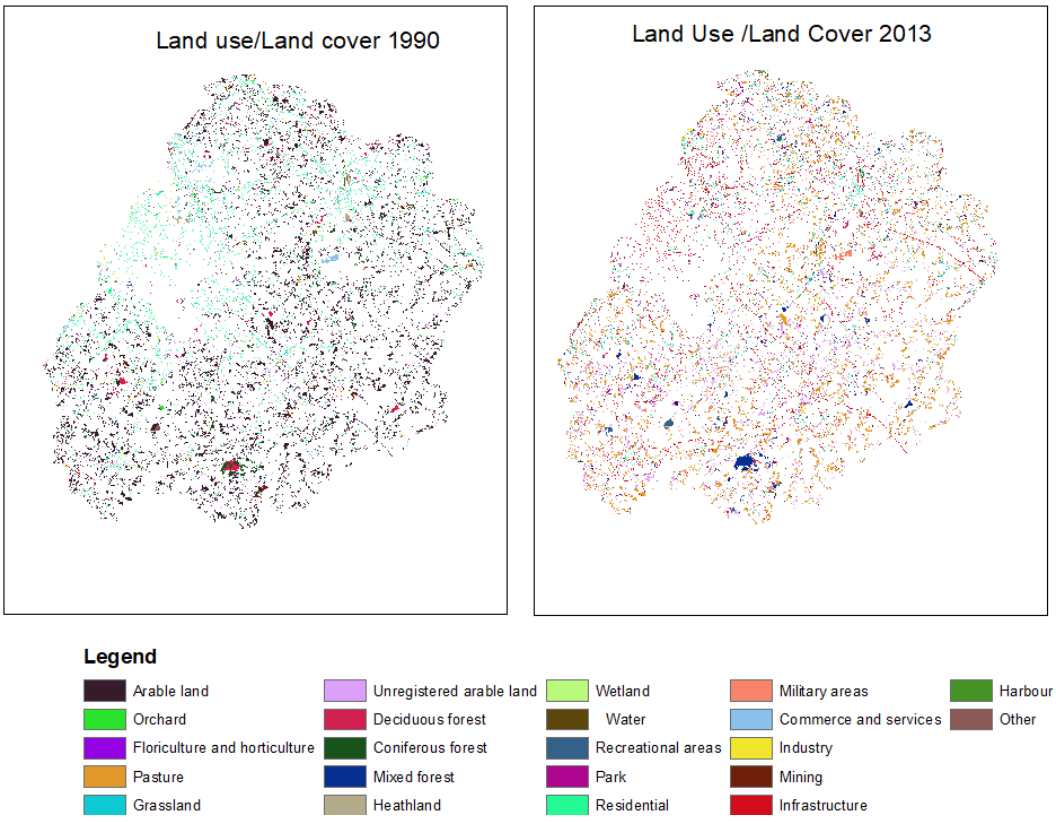


Figure 4.12: Static land use/land cover map of 1990 (left) and 2013 (right) for the places where simulated groundwater recharge has increased.

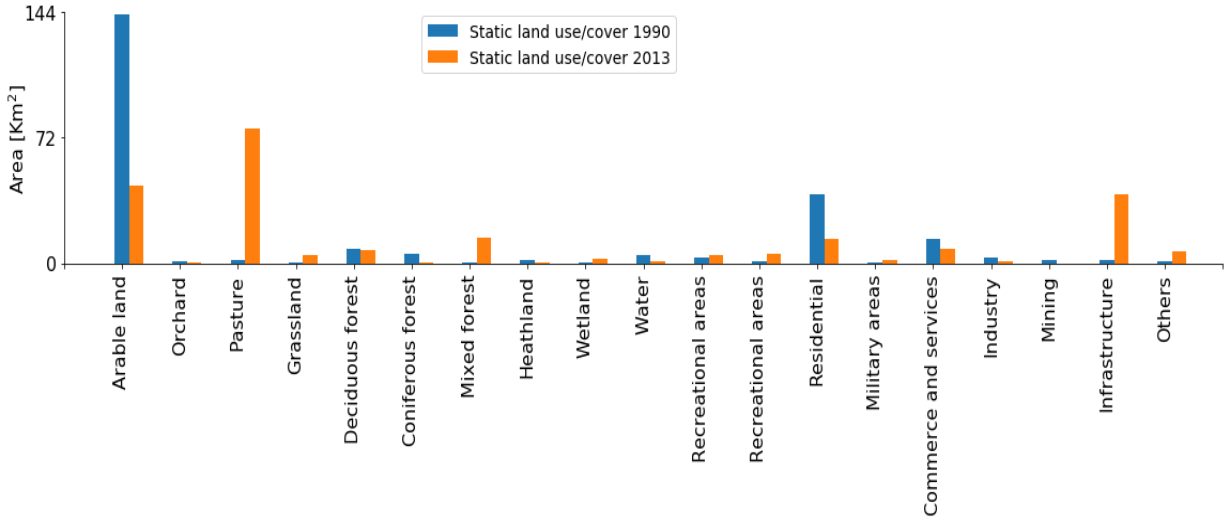


Figure 4.13: Area of each land use/land cover for the places where simulated groundwater recharge has increased.

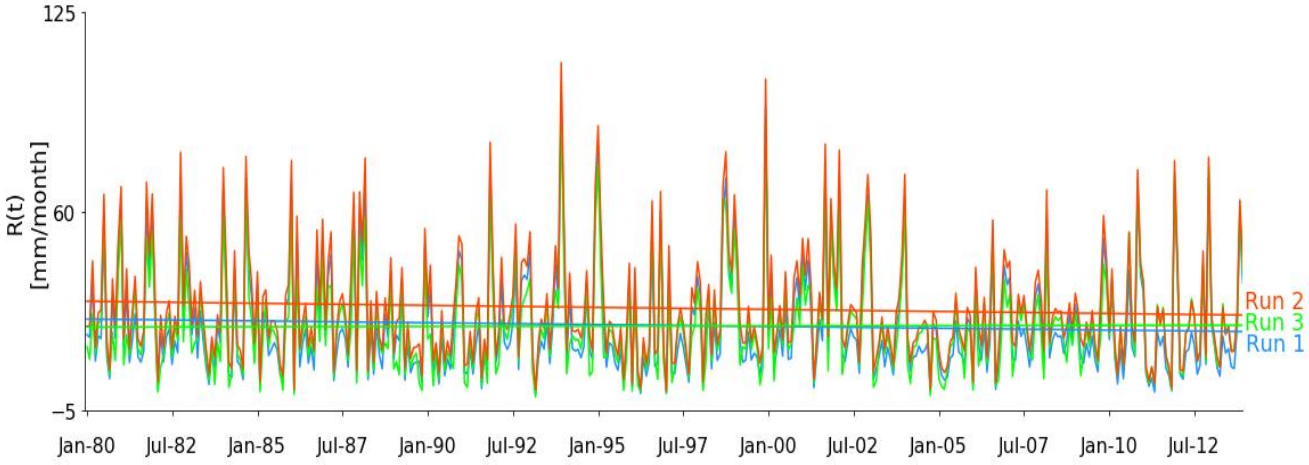


Figure 4.14: Spatially monthly averaged groundwater recharge for the first three runs with their linear regression line, for the places where simulated groundwater recharge has increased.

4.4.3.3 Groundwater recharge drought

Groundwater recharge deviations from a threshold value in time for the dynamic simulation (run 3) and static simulation of 2013 (run 2) from 1980 to 2013 are shown in Figure 4.15. Negative anomalies indicate groundwater drought. A cumulative deficit volume of groundwater recharge of 226 mm with an average drought duration of 3.2 months is observed for the dynamic run. In the static simulation of 2013, a cumulative deficit volume of 361 mm and an average drought duration of 3.7 months is observed.

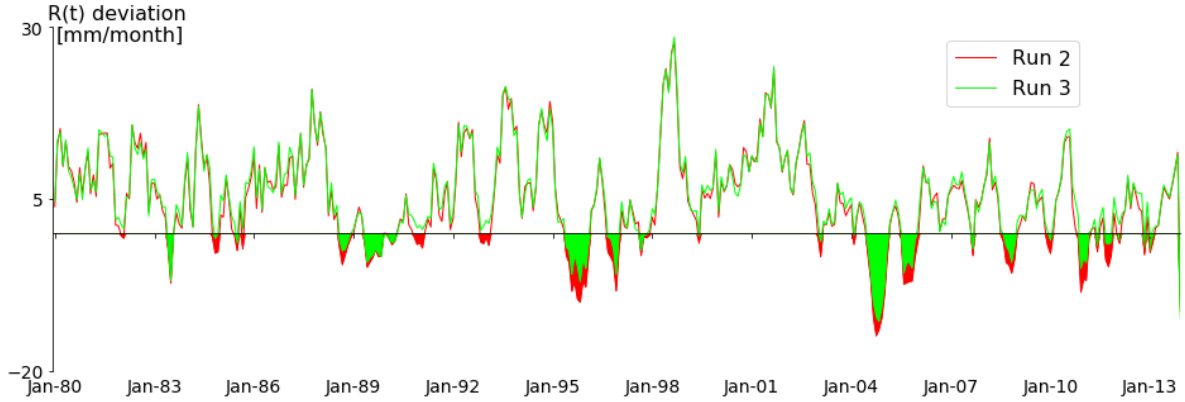


Figure 4.15: Deviation from a threshold value of monthly groundwater recharge based on a 6-month moving average aggregation based on the static LULC of 2013 (run 2, red) and the dynamic run (run 3 lime). The shaded areas represent groundwater drought.

This analysis shows that drought severity increases by a deficit volume of 135 mm if the static LULC map of 2013 is used instead of dynamic LULC. Furthermore, drought duration also slightly increases.

4.4.4 Influence of climate factor on groundwater recharge

Comparing long-term "normal" meteorological conditions (run 4) with dynamic modeling approaches allows to investigate the climate factor contribution on groundwater recharge. The groundwater recharge difference shown in Figure 4.16 indicates that the climate factor influences estimated groundwater recharge in the study area.

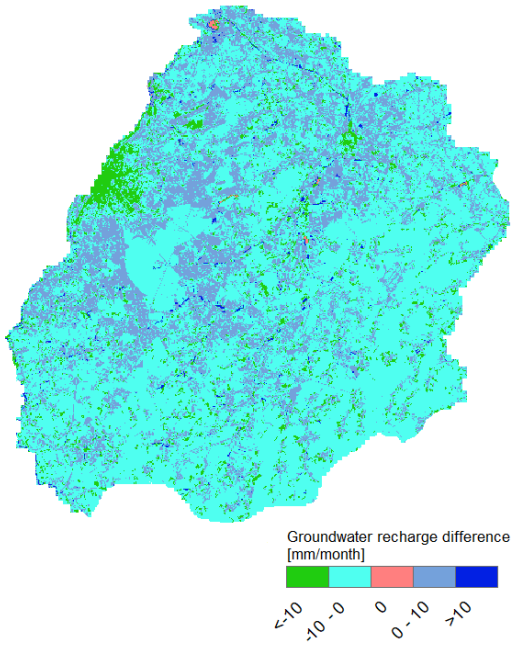


Figure 4.16: Monthly averaged simulated groundwater recharge difference between dynamic (run 3) and long-term average (run 4) meteorological input.

Figure 4.17 shows that spatially monthly averaged groundwater recharge estimated using a dynamic modeling approach (run 3) gives lower groundwater recharge values than using the long-term meteorological average modeling approach (run 4). The recent increasing global temperature trend could explain this difference, as rising temperature increases evapotranspiration (European Environmental Agency, 2020; Hansen et al., 2010). Moreover, the estimated dynamic groundwater recharge (run 3) shown in Figure 4.17 indicates a gradual decrease in groundwater recharge from 1990 to 2013.

By comparing the groundwater recharge estimated using the dynamic (run 3) and the long-term "normal" (run 4) meteorological input, it can be quantified that, on average, 2.06 mm/month groundwater recharge was lost because of the shift of meteorological variables from long term average.

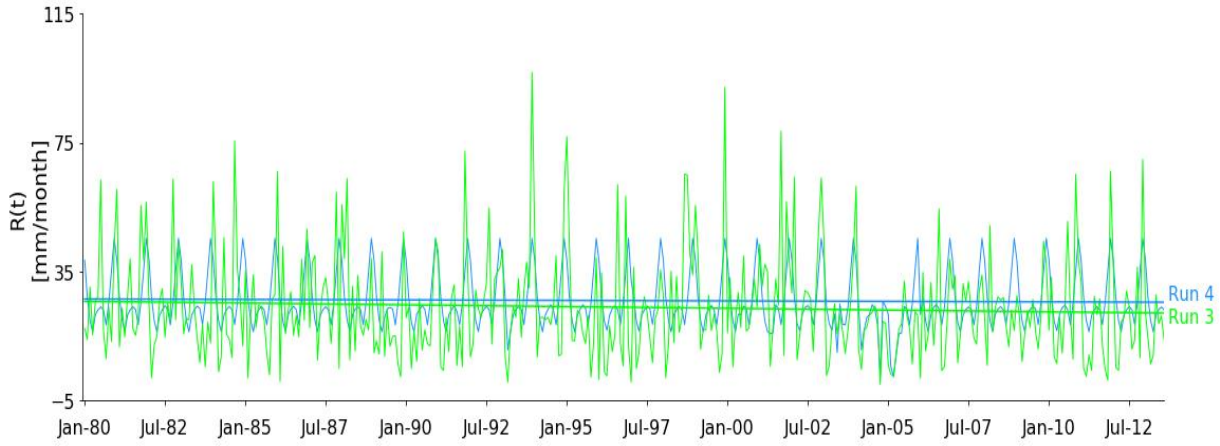


Figure 4.17: Spatially monthly averaged groundwater recharge for dynamic (run 3) and long-term "normal" (run 4) meteorological conditions with their linear regression line.

4.4.4.1 Groundwater recharge drought

Figure 4.18 shows the groundwater recharge deviation from a threshold value in time for the dynamic (run 3) and long-term "normal" (run 4) meteorological conditions from 1980 to 2013. Negative anomalies indicate groundwater drought. The calculated cumulative deficit volume of groundwater recharge is 226 mm with an average drought duration of 3.2 months for the dynamic run. In the long-term meteorological average simulation, the cumulative deficit volume is 215 mm, and the average drought duration is 5 months. As a result, drought severity has increased because of the changes in the meteorological variables between 1980 and 2013.

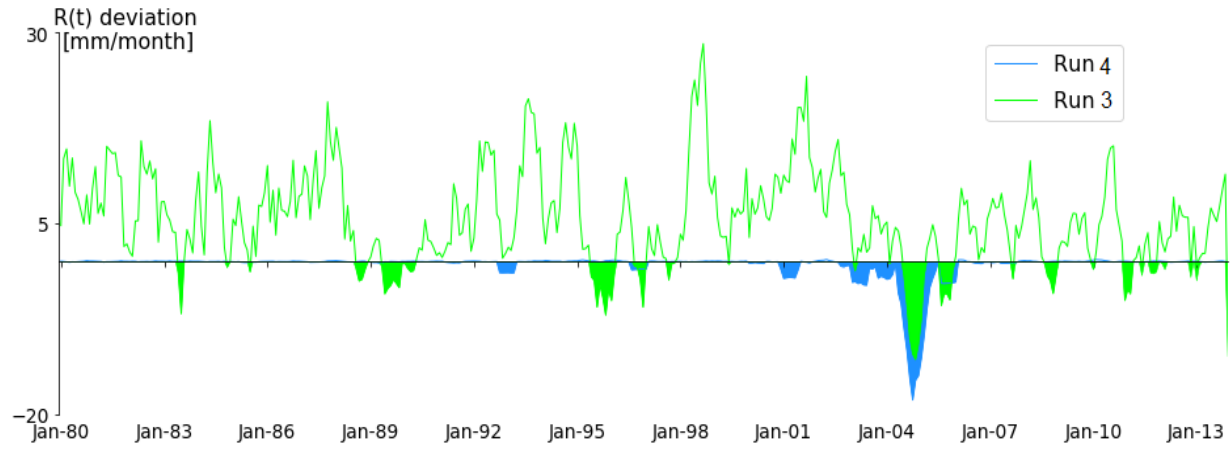


Figure 4.18: Deviation from a threshold value of monthly groundwater recharge based on a 6-month moving average aggregation based on the dynamic run (run 3 lime) and long-term "normal" meteorological conditions (run 4 blue). The shaded areas represent groundwater drought.

4.4.5 Discussion

This study's modeling approach allows quantifying the separate influence of LULC changes and climate on groundwater recharge. The results show that groundwater recharge and groundwater drought being influenced by LULC change and climate factors.

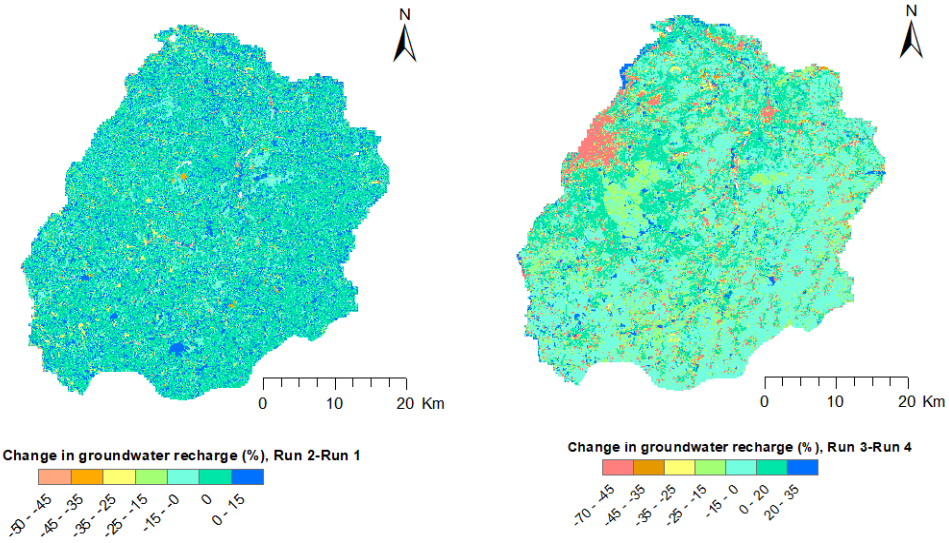


Figure 4.19: Spatial pattern of estimated monthly averaged groundwater recharge difference at pixel scale for run 2 minus run 1 (left); run 3 minus run 4 (right).

The change in estimated groundwater recharge based on the static LULC maps of 2013 and 1990 ranges from -50 % to 15% at the pixel level, with a spatial average of -0.72 % (Figure 4.19 (left)). This finding confirms the finding of Zomlot et al. (2017), showing that spatially averaged change in groundwater recharge between 1990 and 2013 ranges between -0.4 % and -0.8 % for the Dijle and Demer catchment. The most significant decrease of groundwater recharge (-50 % to -45 % at pixel level) occurs mainly in areas that have changed from the deciduous forest into residential areas. Moreover, according to Vanderhaegen and Canters (2016), within Flanders between 1976 till 2013, the sealed surface cover has increased by 82 %. From this increase of sealed surface cover, nearly half of the change occurred in residential areas. Therefore, urbanization plays a significant role in the strongest growth of sealed surface cover and then results in decreased groundwater recharge. In contrast, the largest increase in groundwater recharge due to LULC changes is observed in the areas that have changed from arable land to pasture.

Changes in meteorological variables also play a role in the change in estimated groundwater recharge. At the pixels level, the change in groundwater recharge between the dynamic and long-term "normal" meteorological conditions ranges from -70 % to 35 %, with a spatial

average of - 9.5 % (Figure 4.19 (right)). This finding might result from the increasing temperature trend in the last decades shown in European Environmental Agency (2020).

4.5 Conclusion

This study proposes a modeling approach to investigate the impact of land use/land cover change and climate factors on groundwater recharge estimation and groundwater recharge drought. The approach uses a water balance model to estimate spatially distributed groundwater recharge in the Dijle catchment and parts of the Demer and Zenne basins in central Belgium. Moreover, a variable threshold value method was implemented for groundwater drought analysis.

The modeling was conducted by combining the static land use/cover of 1990 and 2013 with the dynamic meteorological variables from 1980 to 2013 to investigate the impact of land use/cover change on groundwater recharge and groundwater drought. Additionally, a combination of dynamic and long-term average meteorological variables with the dynamic land use/cover from 1990 to 2013 is used to investigate climate factors' impact.

The results show the impact of land use/cover change and climate factors on spatially distributed groundwater recharge. Land use/cover change decreases groundwater recharge by 0.72 % on spatial average in the period between 1980 to 2013 in the whole study area. At the pixel level, decreases of groundwater recharge up to 50% but also increases up to 15% because of LULC change are calculated. Moreover, changes in meteorological variables from the long-term average lead to a spatial average decrease of groundwater recharge by 9.5%.

Groundwater drought was analyzed, and drought comparisons between the modeling approaches were made using the calculated groundwater recharge time series from 1980 to 2013. Groundwater drought characterization features such as the number, duration, and intensity of drought events are influenced by changes in land use/land cover and climate factors. Based on the analysis of the pixels where the LULC change was observed, the land use/cover change effect on groundwater drought severity was higher than the effect from the shift of meteorological variables from the long-term average.

This study concludes that this modeling approach allows the individual contributions of LULC change and climate factors on groundwater recharge estimation and groundwater drought on a spatial and temporal scale. The recharge time-series resulting from all runs will be used as input for the groundwater flow model to analyze further the LULC change and climate factor impact on groundwater resources.

4.6 References

Abdollahi, K., Bashir, I., Verbeiren, B., Harouna, M., van Griensven, A., Huysmans, M. and Batelaan, O.: A distributed monthly water balance model: formulation and application on Black Volta Basin, Environ. Earth Sci., 76(5), 1–18, doi:10.1007/s12665-017-6512-1, 2017.

Arnold, J.G., Muttiah, R.S., Srinivasan, R., Allen, P.M.: Regional estimation of base flow and groundwater recharge in the Upper Mississippi river basin, J. Hydrol. 227, 21–40, doi:10.1016/S0022-1694(99)00139-0, 2000.

Bakker, M., Bartholomeus, R.P., T.P.A., F.: "Groundwater recharge: processes and quantification," Hydrol. Earth Syst. Sci. 17, 2653–2655, doi:10.5194/hess-17-2653-2013, 2013.

Batelaan, O. and De Smedt, F.: GIS-based recharge estimation by coupling surface-subsurface water balances, J. Hydrol., 337(3–4), 337–355, doi:10.1016/j.jhydrol.2007.02.001, 2007.

Batelaan, O. and De Smedt, F.: WetSpass: a flexible, GIS based, distributed recharge methodology for regional groundwater modelling, in:Proceedings of a symposium held during the Sixth IAHS Scientific Assembly, Maastricht, The Netherlands, July 2001, 269, 11–17, 2001.

Batelaan, O., Meyus, Y., De Smedt, F.: De grondwatervoeding van Vlaanderen, Tijdschr. Water 64–71, 2007.

Best, L.C., Lowry, C.S.: Quantifying the potential effects of high-volume water extractions on water resources during natural gas development: Marcellus Shale, NY, J. Hydrol. Reg. Stud. 1, 1–16, doi:10.1016/j.ejrh.2014.05.001, 2014.

Bloomfield, J.P., Marchant, B.P.: Analysis of groundwater drought building on the standardised precipitation index approach. Hydrol. Earth Syst. Sci., 17, 4769–4787, doi:10.5194/hess-17-4769-2013, 2013.

Brouyere, S., Carabin, G., Dassargues, A.: Climate change impacts on groundwater resources: modelled deficits in a chalky aquifer, Geer basin, Belgium, Hydrogeol. J. 12, doi:10.1007/s10040-003-0293-1, 2004.

Bultot, F., Dupriez, G.L., Gellens, D.: Simulation of land use changes and impacts on the water balance - A case study for Belgium, J. Hydrol. 114, 327–348, doi:10.1016/0022-1694(90)90064-5, 1990.

Calow, R. C., Robins, N. S., MacDonald, A. M., Macdonald, D. M. J., Gibbs, B. R., Orpen, W. R.,Mtembezeka, P., Andrews, A. J. and Appiah, S. O.: Groundwater management in drought prone areas of Africa, Int. J. Water Resour. Dev., 13(2), 241–262, doi:10.1080/07900629749863, 1997.

Diaz-Pacheco, J., Gutiérrez, J.: Exploring the limitations of CORINE Land Cover for monitoring urban land-use dynamics in metropolitan areas, J. Land Use Sci. 9, 243–259, doi:10.1080/1747423X.2012.761736, 2014.

Eilers, V.H.M., Carter, R.C., Rushton, K.R.: A single layer soil water balance model for estimating deep drainage (potential recharge): An application to cropped land in semi-arid North-east Nigeria, Geoderma 140, 119–131, doi:10.1016/j.geoderma.2007.03.011, 2007.

European Environmental Agency: Global and European temperatures — European Environment Agency, URL https://www.eea.europa.eu/data-and-maps/indicators/global-and-european-temperature-10/assessment (accessed 2.8.21), 2020.

Hansen, J., Ruedy, R., Sato, M., Lo, K.: Global Surface Temperature Change, Rev. Geophys. 48, RG4004, doi:10.1029/2010RG000345, 2010.

Jin, G., Shimizu, Y., Onodera, S., Saito, M., Matsumori, K.: Evaluation of drought impact on groundwater recharge rate using SWAT and Hydrus models on an agricultural island in western Japan, IAHS-AISH Proc. Reports, 371, 143–148, doi:10.5194/piahs-371-143-2015, 2015.

Jyrkama, M.I., Sykes, J.F.: The impact of climate change on spatially varying groundwater recharge in the grand river watershed (Ontario), J. Hydrol. 338, 237–250, doi:10.1016/j.jhydrol.2007.02.036, 2007.

Jyrkama, M.I., Sykes, J.F., Normani, S.D.: Recharge Estimation for Transient Groundwater Modeling, Gr. Waterwater, 40, 638–648, doi:10.1111/j.1745-6584.2002.tb02550.x, 2002.

Krause, P., Boyle, D.P.: Advances in Geosciences Comparison of different efficiency criteria for hydrological model assessment, Adv. Geosci. 5, 89–97, doi:10.5194/adgeo-5-89-2005, 2005.

Manfreda, S., Fiorentino, M., Iacobellis, V.: DREAM: A distributed model for runoff, evapotranspiration, and antecedent soil moisture simulation. Adv. Geosci. 2, 31–39. doi:10.5194/adgeo-2-31-2005, 2005.

Meyus, Y., Cools, J., Adyns, D., Zeleke, S.Y., Woldeamlak, S.T., Batelaan, O., Smedt, F. De: Hydrogeologische detailstudie van de ondergrond in Vlaanderen, 2005.

Minor, T.B., Russell, C.E., Mizell, S.A.: Development of a GIS-based model for extrapolating mesoscale groundwater recharge estimates using integrated geospatial data sets, Hydrogeol. J. 15, 183–195, doi:10.1007/s10040-006-0109-1, 2007.

Mishra, A.K., Singh, V.P.: Drought modeling - A review, J. Hydrol. 403, 157–175, doi.org/10.1016/j.jhydrol.2011.03.049, 2011.

Mishra, A.K., Singh, V.P.: A review of drought concepts, J. Hydrol. 391, 202–216, doi:10.1016/j.jhydrol.2010.07.012, 2010

Mustafa, S.M.T., Abdollahi, K., Verbeiren, B., Huysmans, M.: Identification of the influencing factors on groundwater drought and depletion in north-western Bangladesh, Hydrogeol. J. 25, 1357–1375, doi:10.1007/s10040-017-1547-7, 2017.

Peters, E.: Propagation of drought through groundwater systems, Ph.D. thesis, Wageningen

University, The Netherlands, 221 pp., 2003.

Peters, E., Bier, G., van Lanen, H. A. J. and Torfs, P. J. J. F.: Propagation and spatial distribution of drought in a groundwater catchment, J. Hydrol., 321(1–4), 257–275, doi:10.1016/j.jhydrol.2005.08.004, 2006.

Peters, E., Torfs, P.J.J.F., van Lanen, H.A.J., Bier, G. : Propagation of drought through groundwater - A new approach using linear reservoir theory, Hydrol. Process. 17, 3023–3040. doi:10.1002/hyp.1274, 2003.

Peters, E., Van Lanen, H.A.J.: Propagation of drought in groundwater in semi-arid and sub-humid climaticregimes, In: Proceedings of the International Symposium of Hydrology of the Mediterranean and Semi-AridRegions, Montpellier, France, 1–4 April, 278, pp. 312–317, 2003.

Price, K.: Effects of watershed topography, soils, land use, and climate on baseflow hydrology in humid regions: A review. Prog. Phys. Geogr. 35, 465–492, doi:10.1177/0309133311402714, 2011.

Royal Meteorological Institute: Weather Belgium - RMI, URL https://www.meteo.be/en/belgium (accessed 2.9.21) , 1931.

Savenije, H.H.G.: The importance of interception and why we should delete the term evapotranspiration from our vocabulary, Hydrol. Process. 18, 1507–1511, doi:10.1002/hyp.5563, 2004.

Scanlon, B.R., Healy, R.W., Cook, P.G.: Choosing appropriate techniques for quantifying groundwater recharge, Hydrogeol. J. 10, 18–39, doi:10.1007/s10040-0010176-2, 2002.

Schwartz, F.W., Ibaraki, M.: Groundwater: A resource in decline, Elements 7, 175–179. doi:10.2113/gselements.7.3.175, 2011.

Tallaksen, L.M., Hisdal, H., Van Lanen, H.A.J.: Propagation of drought in a groundwater fed catchment, the Pang in the UK, IAHS-AISH Publ. 128–133, 2006.

Van Lanen, H. A. J. and Peters, E.: Temporal variability of recharge as an indicator for natural groundwater droughts in two climatically contrasting basins, in: Proceedings of Fourth International Conference on FRIEND 2002 - regional hydrology: bridging the gap between research and practice, Cape Town, South Africa, 101–106, 2002.

Van Lanen, H.A.J., Peters, E.: Definition, Effects and Assessment of Groundwater Droughts, Springer Netherlands, pp. 49–61, doi.org/10.1007/978-94-015-9472-1_4, 2000.

Van Loon, A.F.: Hydrological drought explained. Wiley Interdiscip, Rev. Water 2, 359–392. doi:10.1002/wat2.1085, 2015.

Van Loon, A.F., Gleeson, T., Clark, J., Van Dijk, A.I.J.M., Stahl, K., Hannaford, J., Di Baldassarre, G., Teuling, A.J., Tallaksen, L.M., Uijlenhoet, R., Hannah, D.M., Sheffield, J., Svoboda, M., Verbeiren, B., Wagener, T., Rangecroft, S., Wanders, N., Van Lanen, H.A.J.: Drought in the Anthropocene, Nat. Geosci. 9, 89–91, doi:10.1038/ngeo2646, 2016a.

Van Loon, A.F., Stahl, K., Di Baldassarre, G., Clark, J., Rangecroft, S., Wanders, N., Gleeson, T., Van Dijk, A.I.J.M., Tallaksen, L.M., Hannaford, J., Uijlenhoet, R., Teuling, A.J., Hannah, D.M., Sheffield, J., Svoboda, M., Verbeiren, B., Wagener, T., Van Lanen, H.A.J.: Drought in a human-modified world: Reframing drought definitions, understanding, and analysis approaches, Hydrol. Earth Syst. Sci. 20, 3631–3650, doi:10.5194/hess-20-3631-2016, 2016b.

Vanderhaegen, S., De Munter, K., Canters, F.: High resolution modelling and forecasting of soil sealing density at the regional scale, Landsc. Urban Plan. 133, 133–142, doi:10.1016/j.landurbplan.2014.09.016, 2015.

Vanderhaegen, S. and Canters, F.: Use of earth observation for monitoring soil sealing trends in Flanders and Brussels between 1976 and 2013, Belgeo, (2), 0–23, doi:10.4000/belgeo.18025, 2016.

Verbeiren, B., Huysmans, M., Tychon, B., Jacquemin, I., Canters, F., Vanderhaegen, S., Engelen, G., Poelmans, L., De Becker, P., Tsakiris, G., Vangelis, H. and Batelaan, O.: Drought-related vulnerability and risk assessment of groundwater resources under temperate conditions, in: 13th International Conference on Environmental Science and Technology, Athens, Greece, 5–7 September 2013, 10 pp., 2013.

von Freyberg, J., Moeck, C., Schirmer, M.: Estimation of groundwater recharge and drought severity with varying model complexity, J. Hydrol. 527, 844–857, doi:10.1016/j.jhydrol.2015.05.025, 2015.

Wang, Z.M., Batelaan, O., De Smedt, F.: A distributed model for water and energy transfer between soil, plants and atmosphere (WetSpa), Phys. Chem. Earth 21, 189–193, doi:10.1016/S0079-1946(97)85583-8, 1996.

Wendt, D. E., Van Loon, A. F., Bloomfield, J. P. and Hannah, D. M.: Asymmetric impact of groundwater use on groundwater droughts, Hydrol. Earth Syst. Sci., 24(10), 4853–4868, doi:10.5194/hess-24-4853-2020, 2020.

Wilhite, D.A.: Chapter1 Drought as a Natural Hazard: Concepts and Definitions, Drought A Glob. Assess. 1, 3–18, 2000.

Willems, P.: A time series tool to support the multi-criteria performance evaluation of rainfall-runoff models, Environ. Model. Softw. 24, 311–321, doi:10.1016/j.envsoft.2008.09.005, 2009.

Zomlot, Z., Verbeiren, B., Huysmans, M., Batelaan, O.: Trajectory analysis of land use and land cover maps to improve spatial–temporal patterns, and impact assessment on groundwater recharge, J. Hydrol. 554, 558–569, doi:10.1016/j.jhydrol.2017.09.032, 2017.

Zomlot, Z., Verbeiren, B., Huysmans, M., Batelaan, O., 2015. Spatial distribution of groundwater recharge and base flow : Assessment of controlling factors, Biochem Pharmacol. 4, 349–368, doi:10.1016/j.ejrh.2015.07.005, 2015.

Chapter 5

5 Drought propagation in the hydrological cycle in a semi-arid region: a case study in the Bilate Catchment (Ethiopia)

Based on: Wossenyeleh, B. K., Shuru, A. K., Verbeiren, B., and Huysmans, M.: Drought propagation in the hydrological cycle in a semi-arid region: a case study in the Bilate Catchment (Ethiopia), Hydrogeology Journal, under review, 2021.

5.1 Abstract

Drought is a temporal decrease in water availability and occurs in all climatic regions. Semi-arid environments regularly experience low water availability since the mean annual potential evapotranspiration is two to five times the mean annual precipitation. Droughts propagate through the hydrological cycle, e.g., meteorological drought propagates to groundwater recharge drought. This chapter investigates drought propagation in the hydrological cycle in a semi-arid context. Meteorological drought severity was determined using a standardized precipitation index (SPI). A variable threshold method and standardize groundwater drought index (SGI) were implemented to investigate groundwater recharge drought. Combining these drought assessment methods helps to assess drought propagation in the hydrological cycle. For drought analysis, time-series of rainfall and groundwater recharge need to be available with high spatial and temporal resolution. Therefore, for this study, daily rainfall time-series were collected from eleven meteorological stations, and water balance modeling was used to estimate temporally and spatially distributed groundwater recharge. This research is carried out in the Bilate river catchment in the rift valley basin of Ethiopia.

This research shows that meteorological droughts were observed before every groundwater recharge drought and propagate to groundwater recharge drought. Furthermore, analysis of the drought propagation indicates that not all meteorological droughts propagated. The analysis also shows that a combination of mild to severe meteorological droughts can propagate to groundwater recharge and result in a major groundwater recharge drought event.

5.2 Introduction

Droughts are regional, and regional climatic parameters govern their occurrence. Semi-arid environments regularly experience low water availability since the mean annual potential evapotranspiration is two to five times the mean annual precipitation (Pandey and Ramasastri, 2002; Ponce et al., 2000; Schwabe et al., 2013a; Stahl and Hisdal, 2004; WMO, 1975). In consequence, droughts in semi-arid regions may have a large impact on the poverty rate, health, ecosystem services, and economic development (Schwabe et al., 2013b).

During a meteorological drought period, water scarcity may affect agricultural activities, leading to reductions in agricultural production and productivity, i.e., agricultural drought is developed (Das et al., 2003; Pandey et al., 2008; Todmal, 2019). In semi-arid regions, particularly in Ethiopia, meteorological drought, agricultural drought, and food security have

been studied. However, the impact of drought on groundwater resources, i.e., groundwater drought, hasn't received much attention.

Regardless of its surface water and groundwater resource potential, Ethiopia has been facing drought at an increasing frequency throughout the past decades (Edossa et al., 2010; Zewdie, 1994). Severe drought was recorded in the country throughout human history. The drought frequency used to be once in five years in Ethiopia based on the recent records (Edossa et al., 2010). However, all these studies are based on meteorological, surface water, or agricultural data. Therefore, the country needs to investigate its potential for groundwater resources due to its reliability, particularly in periods of drought.

The water security of the country during meteorological, hydrological (only surface water), and agricultural drought is highly dependent on groundwater availability, access to groundwater, and demand for groundwater (MacDonald et al., 2001). Furthermore, Godfrey and Hailemichael (2017) and Thomas et al. (2019) indicated that groundwater is the only available water resource in drought-affected parts of the country. Hence, managing and developing groundwater is an essential option for the sustainable development of the country. However, studies about groundwater resource management related to drought propagation and characterization have not been conducted for the study area. Consequently, future studies about groundwater drought are essential for the sustainable use of groundwater during drought in Ethiopia.

Estimation of reliable groundwater recharge plays a significant role in groundwater resources management. Precipitation is the main source of groundwater recharge in Ethiopia, particularly in the central rift valley catchment. Rainfall is, however, variable in space and time throughout the country, and as a result, groundwater recharge is also variable. In the northcentral and southwestern plateau of the country, where rainfall is high, higher groundwater recharge occurs than in the rest (Tamiru, 2006). Chernet (1993) estimated the mean annual groundwater recharge varies between 0 to 400 mm/year for the major river basins by assuming that the annual base flow separated from the total runoff is equal to the groundwater recharge in the catchment at which the discharge gauge station is found. Like rainfall, groundwater recharge varies geographically in the country; the southwest and north-central plateau of the country have the highest groundwater recharge (Kebede, 2013). Moreover, the mean annual weighted groundwater recharge over the country is estimated at 39 mm/year using baseflow separation methods for individual basins and global remote sensing data (Döll and Fiedler, 2008). Other studies in semi-arid climate regions of Ethiopia,

such as Gebremeskel and Kebede (2017), Kahsay et al. (2019), Teklebirhan et al. (2012), Gebreyohannes et al. (2013), and Tilahun and Merkel (2009), used the WetSpass model for groundwater recharge estimation incorporating a spatial-temporal variation of hydrometeorology, land use/land cover, and soil texture variables.

In Ethiopia's central rift valley catchment, meteorological drought frequency and intensity have increased in the past decades (Seboka Tura, 2017). This drought might propagate from meteorological to groundwater drought affecting groundwater recharge, groundwater levels, and groundwater discharge. Additionally, according to Thomas et al. (2019), groundwater demand increases in the region during drought periods. This may worsen groundwater drought intensity and frequency.

Drought propagation in the hydrological cycle can be assessed by comparing drought events of different drought types (Van Lanen, 2006; Van Loon and Van Lanen, 2012; van Loon, 2013; Tallaksen et al., 2006; Wossenyeleh et al., 2021). Groundwater recharge drought events can be investigated using threshold value methods (Peters, 2003a; Yevjevich, 1967). However, groundwater recharge is variable in space and time. Therefore, spatially distributed numerical water balance models are used to simulate groundwater recharge. In this study, the WetSpass model (Abdollahi et al., 2017; Batelaan and De Smedt, 2007) was used to simulate groundwater recharge with high temporal and spatial resolution. On the other hand, rainfall and evapotranspiration are used to investigate meteorological drought severity in space and time. Various studies have used SPIE and SPI drought indexes in Ethiopia's rift valley to investigate meteorological drought severity distribution in the region (Bekele et al., 2019; Moloro, 2018; Nasir et al., 2021). In this study, SPI is used to investigate the drought propagation in the hydrological cycle and drought distribution.

This chapter aims to investigate drought propagation in the hydrological cycle of semi-arid climate regions by applying a method for simulating meteorological drought and groundwater drought on recharge. The method developed in the Wossenyeleh et al. (2021) study that combines a water balance modeling, a variable threshold method to determine groundwater drought, and drought indices for meteorological drought was used. Moreover, drought propagation from meteorological to groundwater drought was also investigated.

5.3 Study area and data

The study area consists of the Bilate river catchment in Ethiopia's central rift valley basin and has a surface area of 5419 km^2 (Figure 5.1). The main perennial river in the catchment, Bilate

river, flows from the north to south and outflows to Lake Abaya. The catchment is characterized by the rift, transitional escarpment, highlands, and wide valleys with small and large streams and narrow flatlands between valleys caused by the following processes: volcano-tectonic, rifting, erosion, deposition, and land-use practices (Ayenew et al., 2008). The land surface elevation ranges from 3,331 m above sea level (a.s.l) in the north and 1,174 m a.s.l at the most southerly part of the catchment. Moreover, based on the Thornthwaite climate classification, the catchment is classified as a semi-arid climate zone (Walker, 2003).

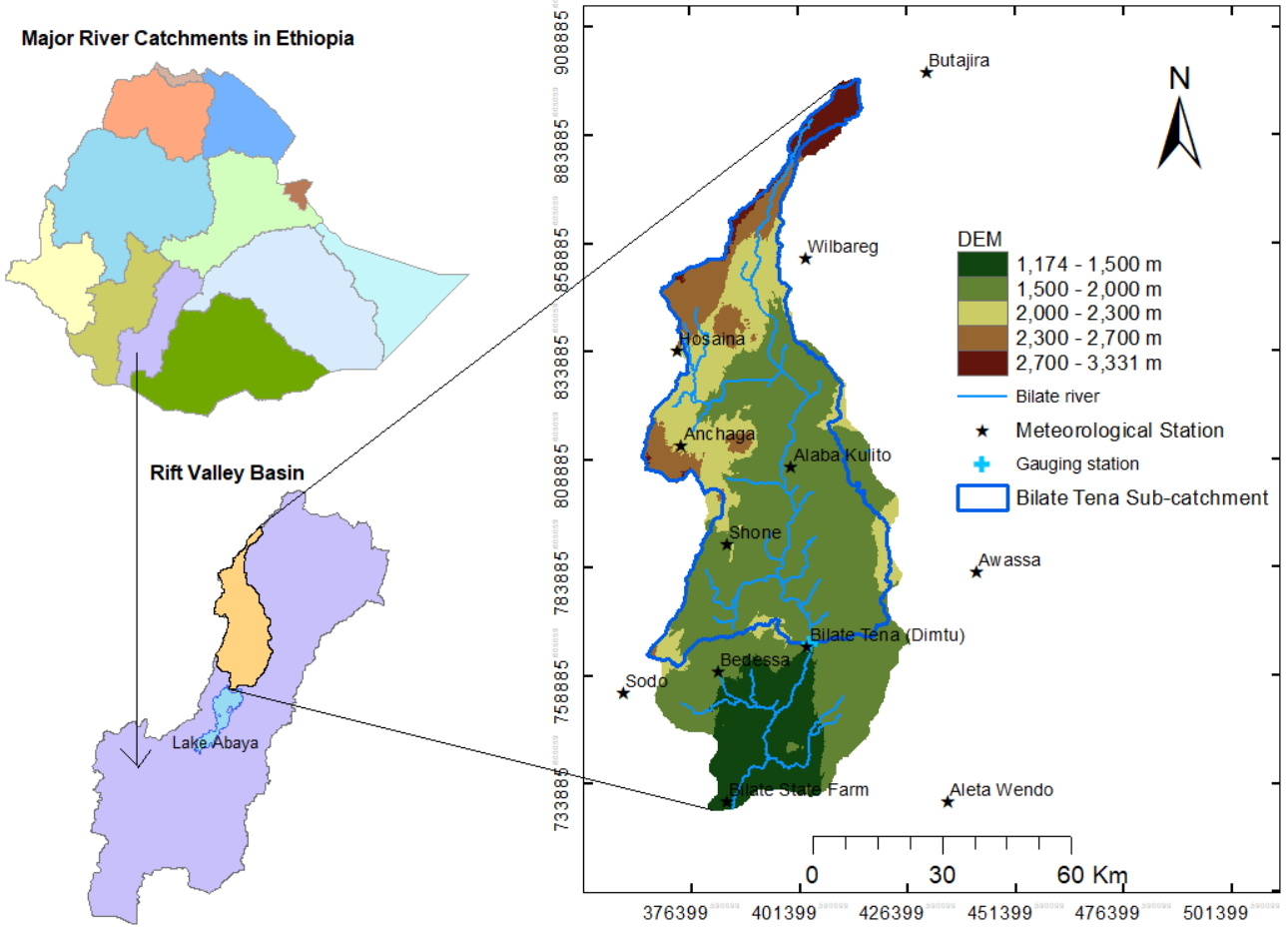


Figure 5.1: Location and Digital Elevation Model (DEM) of the study area

5.3.1 Meteorological Data

Thirty-four years (1980-2013) of meteorological data were collected from the Ethiopian Meteorological Agency (EMA) from 11 meteorological stations shown in Figure 5.1. The stations are reasonably distributed within and around the catchment area at different elevations recording daily rainfall, temperature (maximum, minimum), wind speed, and other climatic data. Missing data were filled using linear interpolation and Ordinary Least Squares

(OLS) methods. Potential evapotranspiration (PET) was calculated using the FAO Penman-Monteith equation from observed meteorological data.

Figure 5.2 shows the seasonal variation of rainfall. The summer periods, which are June, July, August, and September, are considered rainy months in the catchment. The yearly mean of rainfall between 1980 and 2013 varies from 900 mm to 1500 mm. Moreover, the monthly average temperature recorded during the analysis period is 18 ^{o}C. The spatial average yearly total potential evapotranspiration is ranging from 876 mm to 2550 mm in the study area.

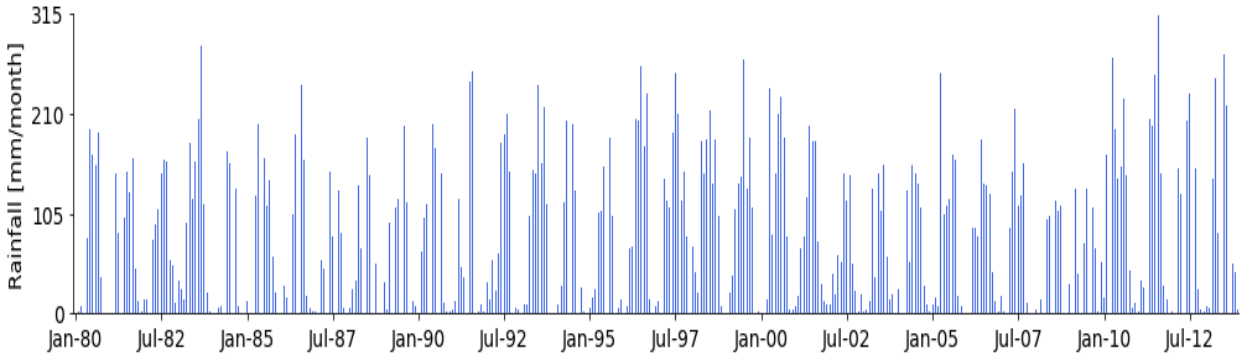


Figure 5.2: Average monthly total rainfall distribution of Bilate catchment using 11 meteorological stations.

Figure 5.3 shows the spatial distribution of the monthly total rainfall in the catchment interpolated using Bayesian kriging of total rainfall in the 11 meteorological stations. Rainfall is high in the north and north-west highlands of the catchment, while rainfall is much lower in the catchment's low land areas.

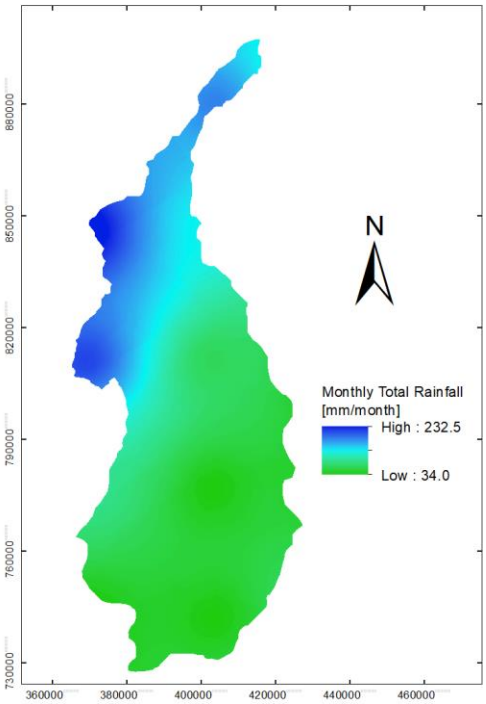


Figure 5.3: Spatial average monthly total rainfall distribution of Bilate catchment using 11 meteorological stations.

5.3.2 Soil and land use/ land cover

Soils in the catchment are classified into four types based on the FAO (FAO, 1998) and USDA soil texture classification (Figure 5.4 (left)). Silty loam and loam dominate the catchment, and soil depths vary between 1.00 and 2.00 m (FAO, 1998).

Since the study area is mainly dominated by state agricultural land and small-scale farm, the land use/land cover map is developed based on the digitized map of 1978 made by the Ethiopian Ministry of Agriculture. The digitized map describes the land use as "state farm", "crop cultivation", "moderately cultivated", "dense woodland/perennial", “bare land”, "grassland", "shrubland", "woodland/forest", and "waterbody". However, in this research, the map was modified based on the land use/land cover classification set up by the WetSpass-M model input guide (Figure 5.4 (right)). Because of state farms and population density in the surrounding cities and towns, most of the catchment is cultivated (Tesfaye Tessema, 2010).

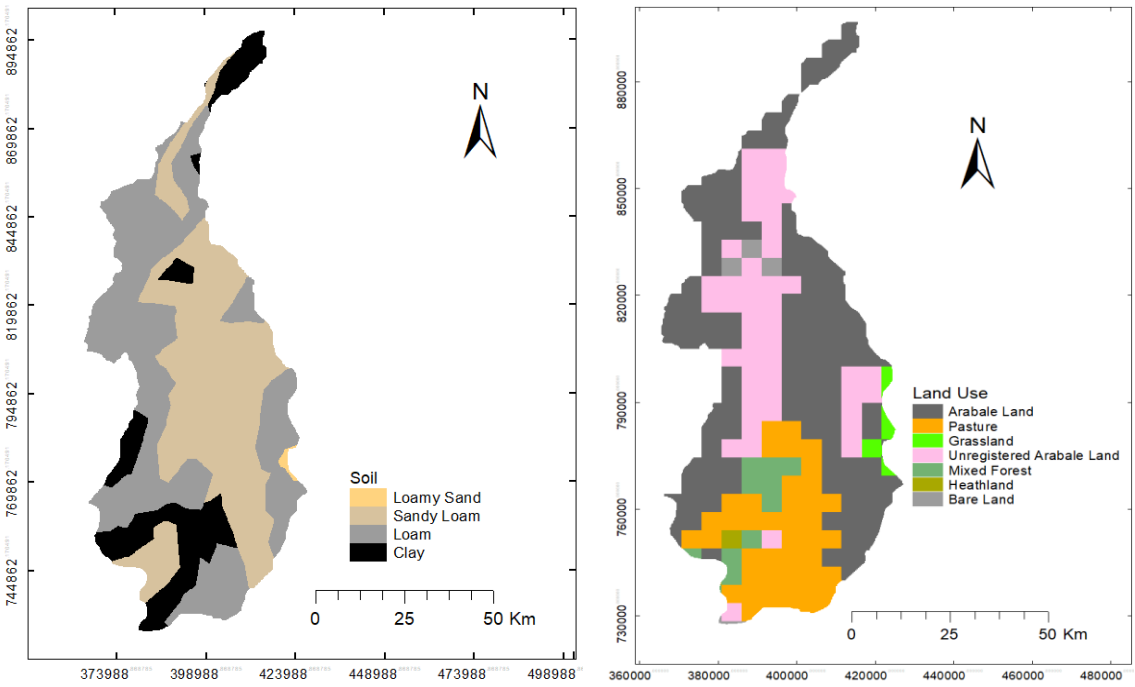


Figure 5.4: Soil texture distribution (left) and land use/land cover classification (right).

5.3.3 Slope

A spatially distributed slope map is derived from the area-covering digital elevation model (Figure 5.5). The catchment slope shows steep slopes are found around the mountainous part of the western edge, and gentle slopes are dominant in the cultivated land of the eastern edge. The slope and elevation variation in the catchment leads to significant erosion and deposition processes (Förch and Althoff, 2009).

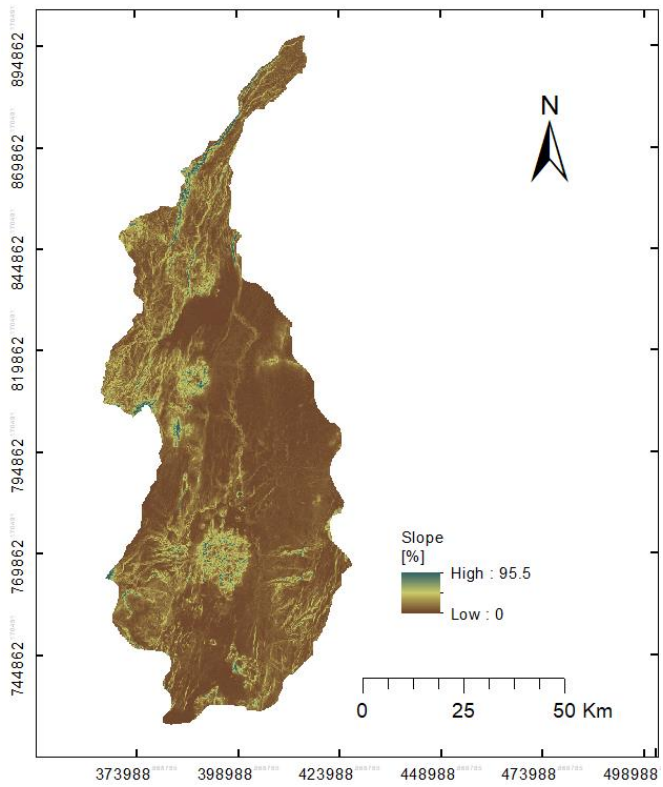


Figure 5.5: Slope distribution of the Bilate river catchment.

5.3.4 Hydrogeology

According to the FAO (1998) geological map, Oligocene-Miocene volcanic rock is dominant in the catchment (Förch and Althoff, 2009). Geological features such faults, fractures, the graben and horst structures play a significant role in groundwater flow. This can be seen from the many springs that discharge groundwater onto the land surface along fault and fracture zone beneath the catchment's mountainous part (Dereje and Nedaw, 2019). These springs discharge shallow groundwater. However, groundwater abstraction wells in the catchment extract water from the deep aquifer (Tesfaye Tessema, 2010).

The average groundwater depth collected by the Southern nations and nationalities water resources regional bureau from 51 boreholes in the catchment is 35 m. Moreover, the observation data indicates that groundwater depth in most of the study area is higher than 5 m. As a result, groundwater depth doesn't influence the water balance calculation of the WetSpass model as no evapotranspiration from groundwater happens in areas with such deep groundwater tables.

5.4 Methodology

The study was divided into three parts: groundwater recharge estimation, meteorological drought analysis, and groundwater drought analysis (Figure 5.6).

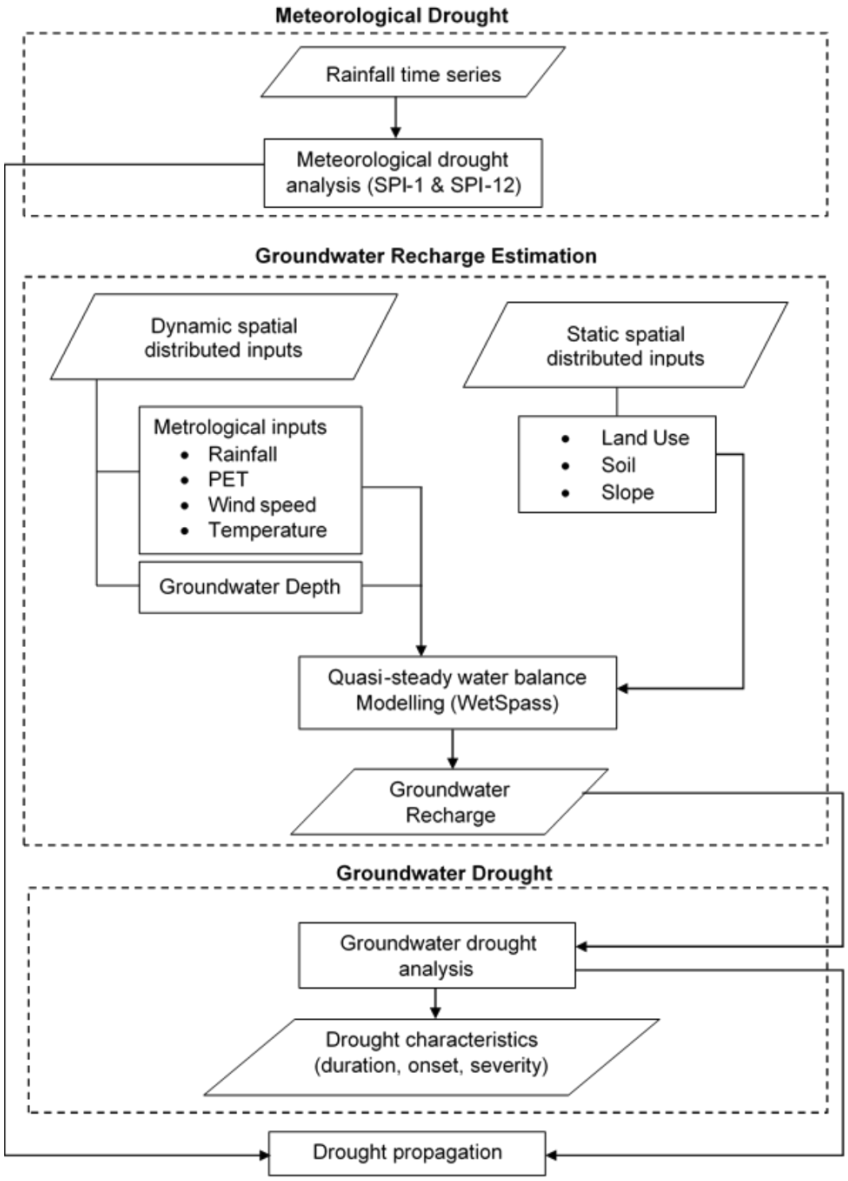


Figure 5.6: Conceptual framework of the study

First, drought severity in rainfall was investigated using meteorological drought analysis. Then, a water balance model was built to estimate temporally and spatially distributed groundwater recharge. Groundwater drought analysis was performed on the calculated time series of groundwater recharge. Finally, drought propagation in the hydrological cycle was

investigated by comparing groundwater recharge drought occurrence, intensity and frequency to meteorological drought.

5.4.1 Meteorological drought analysis

The standardized precipitation index (SPI) is used to determine the spatial and temporal extent of meteorological drought severity (McKee et al., 1993). Thirty-four years of monthly average rainfall (see section 5.3.1) for a period from 1980 to 2013 were used to calculate SPI and identify meteorological drought events and severity.

A long-term rainfall probability distribution was used to calculate SPI on different time scales (McKee et al., 1993). The probability distribution was used to fit the long-term rainfall, and then the fitted distribution is transformed to a normal distribution using the gamma distribution (Thom, 1958). That results in the mean SPI value to zero for the given location and analysis period (Edward and McKee, 1997). The SPI value indicates rainfall deviation from the median rainfall; a positive value means greater than the median, and negative values indicate less than the median. Hence, an extreme drought event occurs when the index reaches the value of -2.0 or less (Table 1). The drought event ends once the SPI becomes positive; this indicates a higher rainfall intensity than the long-term average value. According to McKee et al. (1993), drought severity categories can be defined based on the SPI value as shown in Table 5.1.

Table 5.1: Drought severity categories based on SPI values (McKee et al., 1993)

SPI. Values	Drought category
0.0 and more	No
0.0 to -0.99	Mild
-1.0 to -1.49	Moderate
-1.5 to -1.99	Severe
-2.00 and less	Extreme

In this study, monthly and annual SPI values were used to investigate the long-term meteorological drought severity distribution on a temporal and spatial scale. Moreover, this SPI was used to investigate meteorological drought propagation to groundwater.

5.4.2 Groundwater drought estimation

Physical and meteorological factors govern the estimation of groundwater recharge in a catchment. It is estimated at a monthly timestep using a physically-based distributed water balance model called WetSpass (Batelaan and DeSmedt, 2001; Batelaan and De Smedt, 2007). The model was adjusted to enabling water balance calculation at a monthly timestep instead of a seasonal timestep (Abdollahi et al., 2017). In contradiction to the seasonal

approach (summer/winter season), the monthly approach enables considering the specific conditions of a study area (e.g., more than two seasons) and, thus, has broader applicability.

5.4.2.1 Model inputs

The model inputs are spatially distributed maps for land use/land cover, soil, slope, groundwater depth, and four meteorological parameters: rainfall, potential evapotranspiration, temperature, and wind speed (see section 5.3). The meteorological input parameters were interpolated to the catchment scale using Gaussian kriging. All spatially distributed input maps were prepared in 180 m resolution using a python-based GIS tool and resulting in a monthly time-series of groundwater recharge maps at the same spatial resolution.

The default land use/land cover parameters of the WetSpass model are based on typical land uses and land covers for a humid climate as the software was initially developed for applications in Belgium. For Ethiopia's semi-arid climate, particularly for the Bilate river catchment, some adjustments of the parameters' values are introduced based on Gebreyohannes et al. (2013). The adjustments are made based on the nature of the vegetation, bare-land, and imperviousness of the catchment. Accordingly, for this study, the following adjustments to the default values are made: (a) a 30 % decrease in the value of leaf area index, (b) a 10 to 30 % root depth decrement based on the land use types and (c) a 20 % increment of the bareness of all land use classes.

5.4.2.2 Calibration

Four global parameters (α, LP, a, and average intensity) and three local parameters (slope factor, land factor, and soil factor) of the WetSpass model were calibrated. It was manually optimized according to the goodness of fit between the simulated base-flow from simulated groundwater recharge of Bilate-Tena sub-catchment (Figure 5.1) and the separated base-flow from observed river discharge using WETSPRO (Willems, 2009) at Bilate-Tena gauging station (Figure 5.1) for the years between 1981 and 1985.

Monthly base-flow is calculated from the previous month's storage and groundwater recharge (R_m) in the considered month (Abdollahi et al., 2017). This is expressed as follows:

$$Q_{b(t)} = \beta Q_{b(t-1)} + 0.001 N_m (1-\beta) \emptyset R_m \quad (5.1)$$

Where β is a storage parameter [-] between 0 and 1, Qb(t-1) is the base-flow from the previous month [m3/month], Nm is a number of days per month (≈ 30 days), and Ø [m2/day] is the

recharge contribution parameter to current base flow. For the pixel area A [m2] with recession index k [day], it would be:

$$\emptyset = \frac{1.15A}{k} \qquad (5.2)$$

The result of the calibration should be evaluated both qualitatively and quantitatively. The Nash Sutcliffe Efficiency (NSE) and the coefficient of determination (r^2) are used to express the model's overall efficiency.

5.4.3 Groundwater drought analysis and drought propagation

A groundwater recharge drought analysis was performed on the 34 years (1980-2013) simulated groundwater recharge time-series. A threshold level method with a variable threshold value was used to determine groundwater recharge drought (Beyene and Loon, 2014; Yevjevich, 1967).

In order to do that, first, a separate frequency analysis was conducted for each of the 12 months. For most drought studies, the threshold level is within the 70^{th}-95^{th} percentile range of the probability of exceedance (Van Loon, 2013). Therefore, each month's threshold level value was determined as the 80^{th} percentile of the probability of exceedance of monthly groundwater recharge in that month in the 34-year series (1980-2013). For each month of the year, the groundwater recharge values in the time series were ranked from highest to lowest, and then the 80^{th} percentile of groundwater recharge was calculated for each month. Groundwater recharge drought was characterized in terms of the number of droughts, duration of droughts, and drought severity (cumulative volume deficit from the threshold level) (Peters, 2003a).

Moreover, a Standardized Groundwater drought Index (SGI) were combined with monthly SPI to gain insight into the propagation of drought in the hydrological cycle and assess the groundwater system's response to drought. The Standardized Groundwater drought Index (SGI) introduced by Bloomfield and Marchant (2013) was used to analyze groundwater level drought. In this research, SGI was calculated from delayed groundwater recharge by applying appropriate normalization procedures. The long-term delayed groundwater recharge time-series was normalized by fitting to a gamma distribution. Then, like SPI, the standardized groundwater drought index (SGI) was calculated for the spatially averaged monthly delayed groundwater recharge time series from 1980 to 2013.

5.5 Results and discussion

5.5.1 Model calibration

An initial flow value of 0.75 m^3/s, one filter step, a recession constant of 65 days, and a wf-parameter filter of 0.6 was set for base-flow separation on the WETSPRO. Since the catchment had a thick unsaturated soil zone, manual calibration is used to match the simulated and filtered base-flow; a 3-month groundwater recharge delay gave the best match. This three months delay of groundwater recharge could be related to the nature of the hydrogeology of the catchment or the amount of deep infiltration. However, more detailed modeling or study of the unsaturated soil is needed to estimate the delay time as for the temperate climate case study (Chapter 2). An optimized β value of 0.2 and recharge contribution parameter of 0.0066 m^2/sec is obtained using *Equation 5.1*. The simulated baseflow from the WetSpass recharge and monthly filtered base-flow separated from river discharge using WETSPRO gives a good calibration result with a Nash-Sutcliffe efficiency coefficient of 0.69 and coefficient of determination of 0.86 (Figure 5.7).

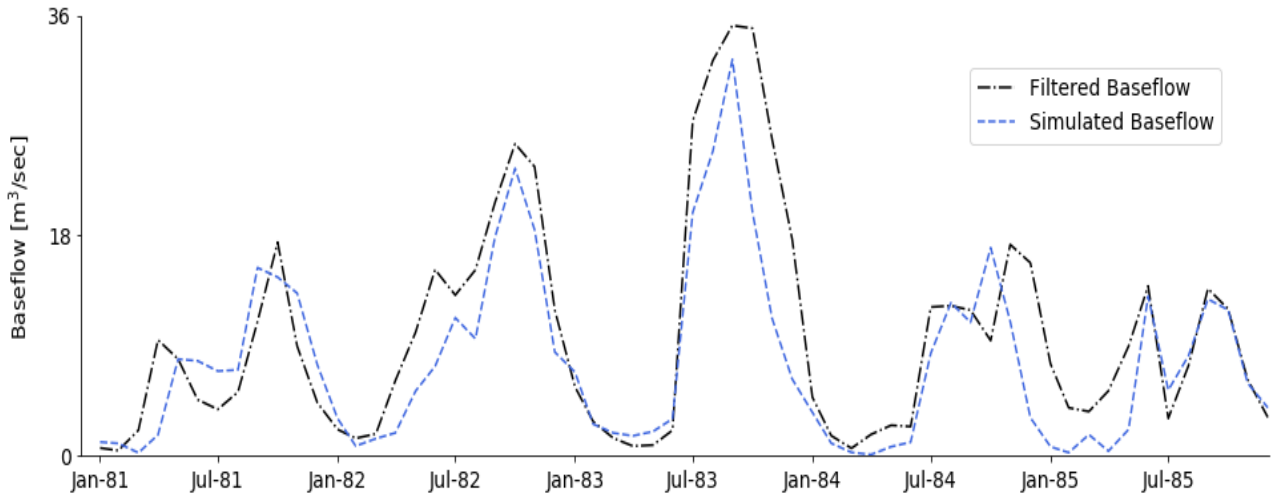


Figure 5.7: Simulated baseflow based on WetSpass output groundwater recharge vs. monthly filtered baseflow from flow measurements at the Bilate -Tena gauging station.

5.5.2 Meteorological drought

Figure 5.8 shows the meteorological drought occurrence and severity between 1980 and 2013 using eleven meteorological stations in the Bilate river catchment. The meteorological drought calculations are based on monthly SPI (SPI-1) shown in Figure 5.8A and annual SPI (SPI-12) shown in Figure 5.8B. The results show that the severity and frequency of drought depend on the calculation period of SPI. The drought severity category varies from extreme to no drought

based on SPI-1 and severe to no drought based on SPI-12. The SPI-12 values show less severe drought categories.

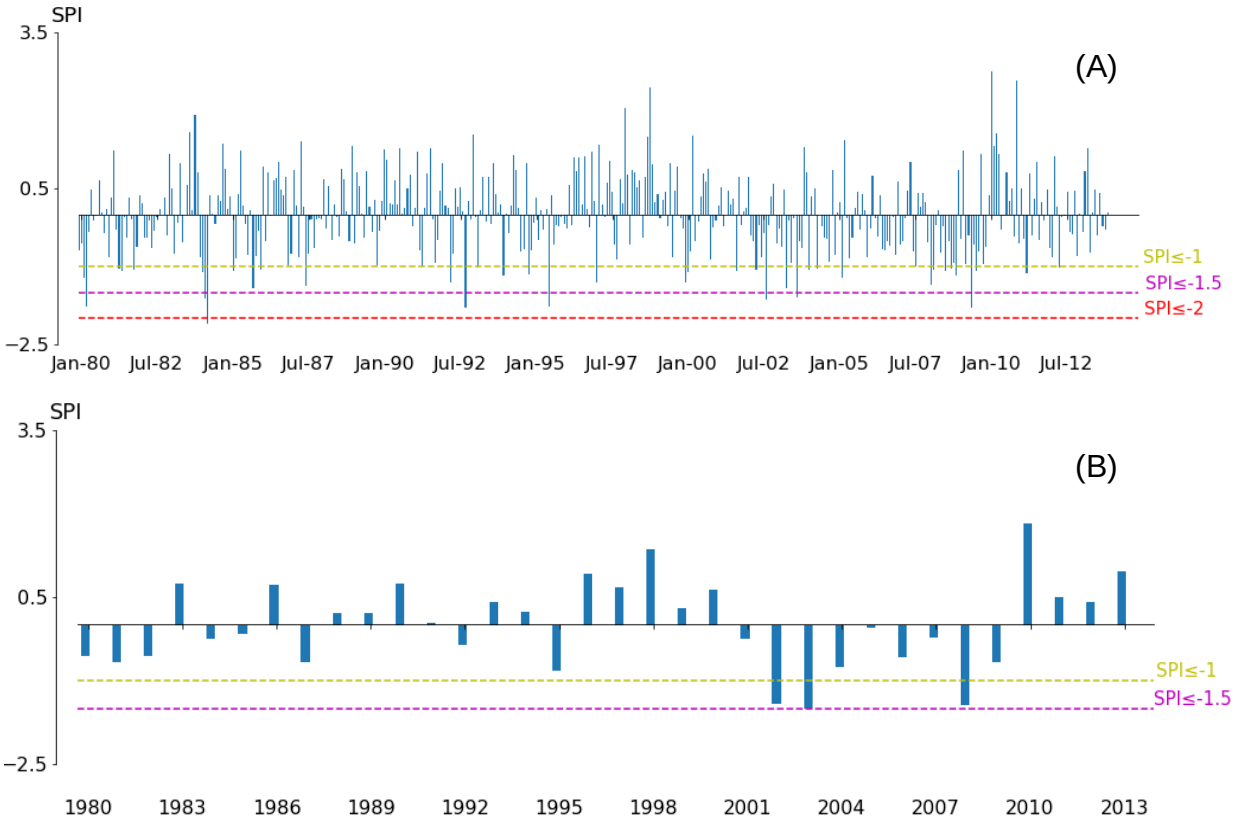


Figure 5.8: Meteorological drought occurrence and severity based on (A) Monthly SPI value and (B) Annual SPI value for 1980 – 2013. The SPI is calculated using the average rainfall of the 11 stations found in the study area.

Between 1980 and 2013, one extreme and eight severe meteorological droughts at a monthly scale are identified using SPI-1. Using SPI-12, only one severe meteorological drought (in 2003-04) is identified. This shows that short meteorological droughts are frequent while longer meteorological droughts occur with lower frequency.

Meteorological drought severity is also variable on a spatial scale. For example, Figure 5.9 shows that in the hydrological year of 2008-09, the drought severity categories vary from no drought to severe in the study area. Moreover, the spatial distribution of the drought severity category is also different for different SPI calculation periods (Figure 5.9 A, B & C). Since July to Oct is the rainy season in the catchment, the first-quarter SPI (SPI-4) drought only varies from no drought to mild. However, two dry months are included in the semester SPI calculation; thus, drought severity increased compared to first quarter SPI. Besides, the

catchment has another rainy season with less rain intensity, i.e., March to June; thus, the annual drought severity is less severe than the semester drought severity.

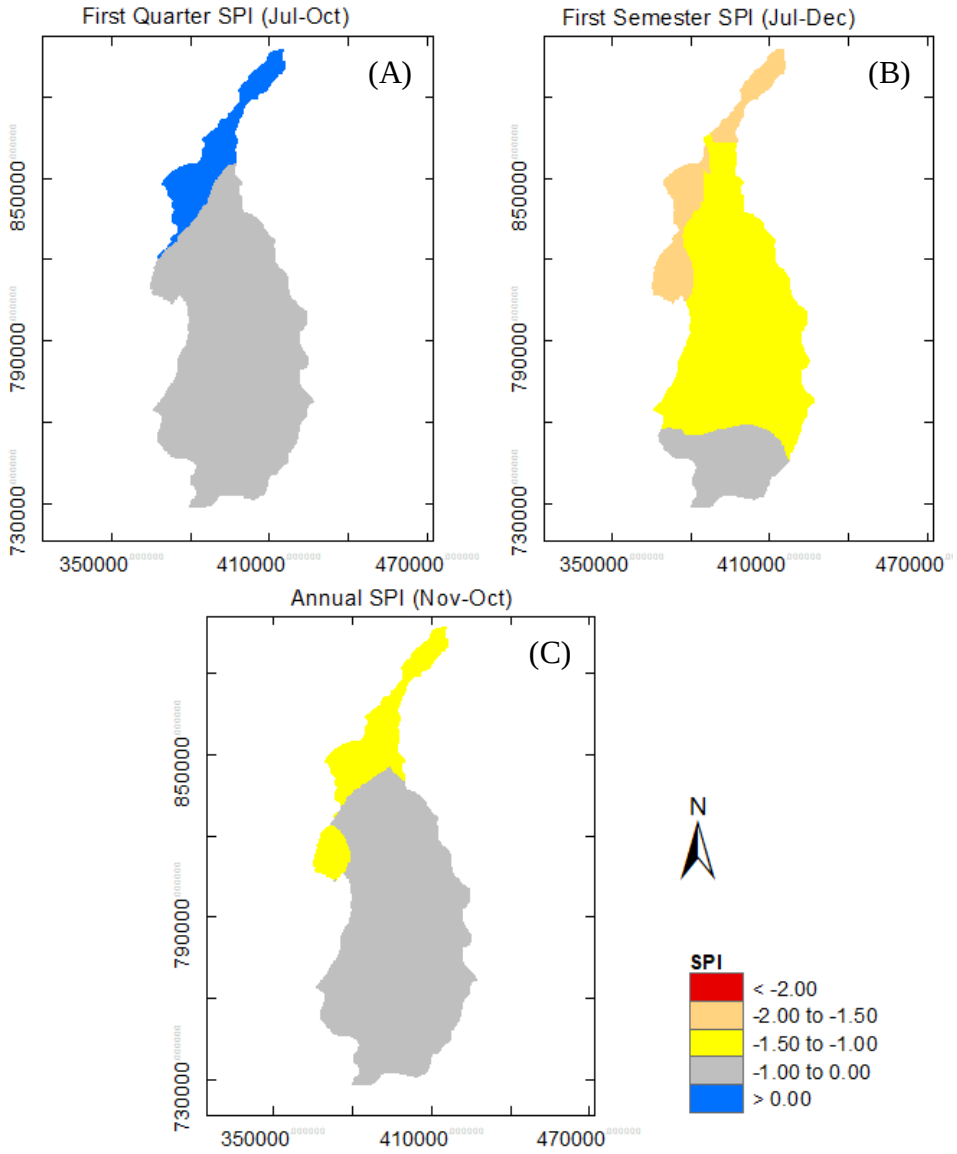


Figure 5.9: Spatially distributed meteorological drought severity based on (A) SPI-4 (Quarter) value, (B) SPI-6 (Semester) value, and (C) SPI-12 (Annual) value for the hydrological year of 2008-09

5.5.3 Groundwater recharge

Figure 5.10 shows the temporal variation of estimated groundwater recharge and total monthly rainfall. The estimated groundwater recharge clearly shows the seasonal dynamics. That means that in the rainy months, July to Oct, calculated recharge is high; while in the dry months, Nov to Feb, a low recharge was estimated. The estimated recharge in most of the

study area is within the 75 percentile range of the distribution; only a few outliers are recorded in some months (Figure 5.11).

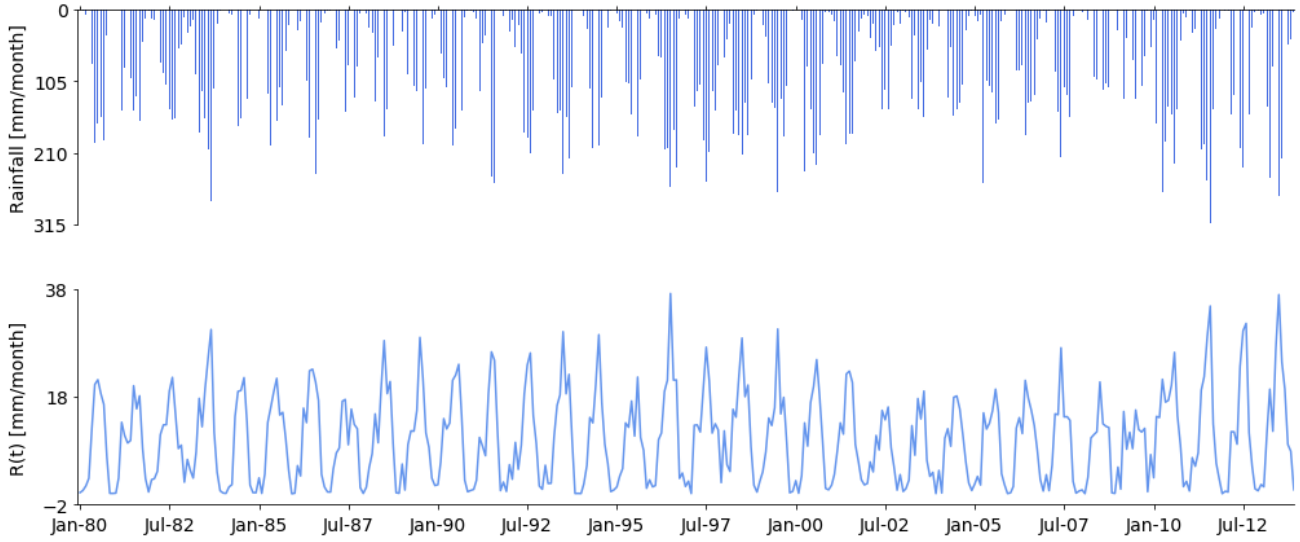


Figure 5.10: Average monthly groundwater recharge distribution and average monthly total rainfall

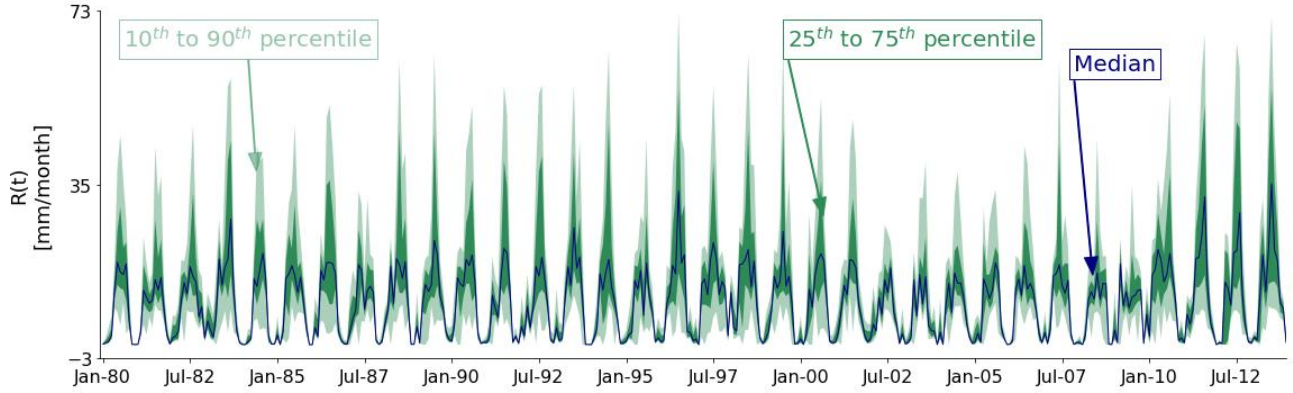


Figure 5.11: Temporal variation of estimated groundwater recharge. The dark blue line is the 50th percentile curve (median) and shows the median groundwater recharge value for each month. The green shadow area represents the interquartile range (IQR). Moreover, the light green shaded area represents the lowest and highest 10 % of each month's groundwater recharge values.

The spatial distribution of groundwater recharge (Figure 5.12) shows that the calculated groundwater recharge ranges from 0 to 37 mm/month with a spatial average of 10.10 mm/month. This result is 9.8 % of the monthly average rainfall of the study area. This estimated groundwater recharge confirms finding of Dereje and Nedaw (2019) for upper Bilate catchment, showing that the average groundwater recharge is 9.4 % of the annual precipitation. The influence of rainfall distribution in the catchment is significantly noticeable in the spatial distribution of groundwater recharge. The north and north-west highlands of the catchment have high groundwater recharge, where rainfall is highest (see Figure 5.3).

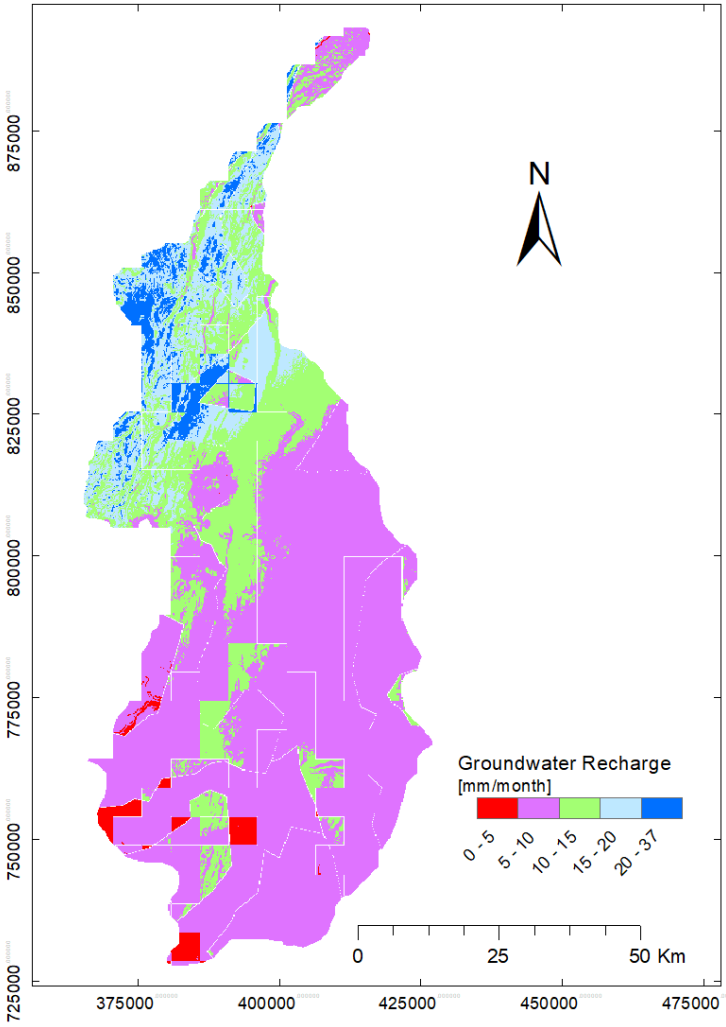


Figure 5.12: Spatial monthly averaged groundwater recharge distribution from 1980 to 2013 in the Bilate river catchment, estimated using WetSpass.

Groundwater recharge is also highly correlated with land use type. High groundwater recharge is estimated in bare land and arable land; this might be because of the dominance of sandy loam and loamy soil types and gentle slopes in those particular areas. In the forest and pasture areas in the southwest of the catchment, groundwater recharge is relatively low.

Table 5.2: Average monthly groundwater recharge based on the land use classes

Land-use type	Groundwater recharge [mm/month]	
	Mean	Standard deviation
Arable land	9.41	4.54
Pasture	6.99	1.48
Grassland	9.41	0.94
Unregistered Arable land	10.44	4.25
Mixed forest	9.51	1.37
Heathland	6.27	1.34
Bare Land	18.70	6.25

5.5.4 Groundwater drought

Figure 5.13 shows the groundwater recharge drought events between 1980 and 2013 calculated using a variable threshold method. Negative anomalies of groundwater recharge deviated from the threshold indicated drought events. Fourteen drought events with a cumulative recharge deficit higher than 5 mm were observed during the analysis. The drought event duration varies from one month to twenty-two months. The drought events with the longest duration were from Dec-2001 to Sep-2003 and from Dec-2003 to Sep-2005, which lasted for twenty-two months. The drought event from Feb-2007 to Aug-2008 lasted for nineteen months. Droughts with shorter durations were observed in Dec-1985, Apr-1989, Jan-1997, Apr-1997, Jan-1999, Nov-2010, Sep-2011, and Sep-2012 (1 month). The drought from Dec-2001 to Sep-2003 with a cumulative deficit recharge of 60.74 mm was the most severe within the analysis period. The drought event from Feb-2007 till Aug-2008 resulted in a cumulative deficit recharge of 36.94 mm. Both severe drought events have a drought volume several times larger than the average estimated recharge of 10.10 mm/month.

Table 5.3 indicates some of the groundwater drought characteristics between 1980 and 2013 for the major groundwater recharge events calculated using the variable threshold method as shown in Figure 5.13. Average duration of groundwater drought in the period between 1980 and 2013 was 6 months. However, most of the droughts occurred between 2001 to 2009, including several severe drought events.

Table 5.3: Groundwater recharge drought characteristics (onset, number events, duration, and deficit volume) between Jan-1980 and Dec-2013.

Onset	Duration [month]	Number of drought events	Deficit [mm]
Dec-80	7	1	13.45
Nov-81	17	2	14.75
Nov-83	18	1	29.71
Sep-86	11	3	16.32
Dec-87	42	5	9.23
Sep-91	17	3	7.85
Oct-93	24	4	22.56
Oct-99	7	1	8.87
Apr-01	30	3	62.62
Dec-03	34	2	40.01
Feb-07	30	2	59.77
Nov-10	23	4	4.89

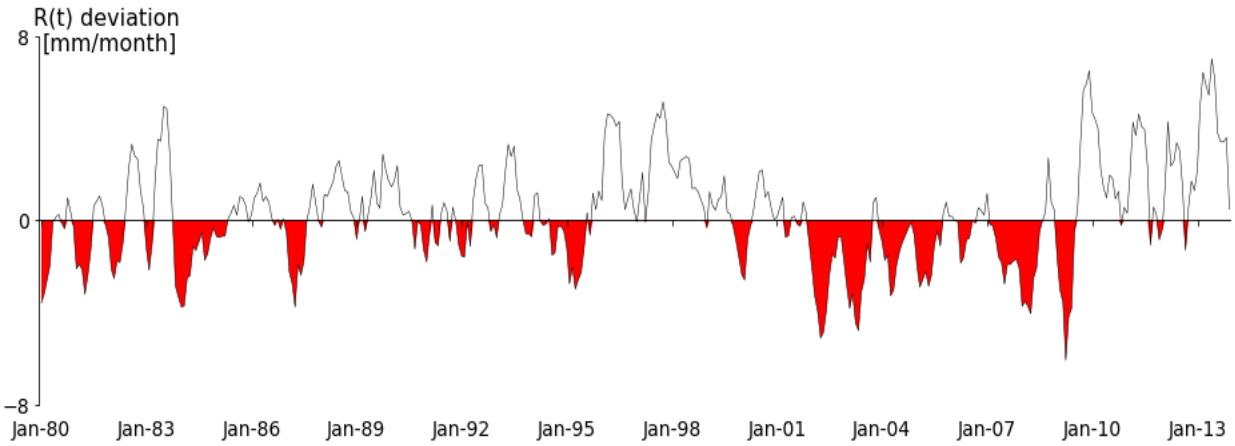


Figure 5.13: Monthly groundwater recharge deviation from the threshold value. The red color indicates groundwater recharge drought events.

5.5.5 Drought propagation in the hydrological cycle

The propagation of drought in the hydrological cycle from meteorological drought to groundwater recharge was analyzed using SPI-1 and monthly groundwater recharge SGI. Since not all negative SGI should be considered as a groundwater drought, during drought propagation analysis only more severe groundwater recharge droughts, which correspond to the lowest 20 % SGI, are considered. Table 5.4 shows the lag time and the number of meteorological droughts (SPI-1) before the onset of groundwater recharge drought between 1980 and 2013. The lag time was calculated as the time between the start of the meteorological drought and the monthly groundwater recharge SGI (Wossenyeleh et al., 2021). Meteorological drought was observed before every groundwater recharge drought with an average lag time of 1.7 months between the beginning of meteorological drought and the beginning of SGI groundwater recharge drought event.

Moreover, a number of different range of severity of meteorological drought (from moderate to severe) happened earlier than the onset of groundwater drought impacted the groundwater drought characteristic for example, the groundwater droughts that occurred after Nov-1983, Apr-2001, Feb-2007 (Figure 5.13 and Figure 5.14). Further findings show that mild and moderate meteorological droughts also propagate to groundwater, e.g., the minor groundwater droughts starting in Nov-1981, Dec-1987, Sep-1991, and Nov-2010.

Figure 5.14 gives insight into drought propagation in the hydrological cycle by comparing groundwater recharge drought to meteorological drought. Frequent meteorological droughts were observed in Figure 5.14 before every groundwater recharge drought.

Table 5.4: Onset of SGI groundwater recharge drought between Jan-1980 and Sep-2013 and number of meteorological droughts (SPI-1) ranging from moderate to extreme severity before the onset of groundwater recharge drought with lag time.

Onset	Number of SGI drought events	Number of meteorological drought (SPI-1) before the onset of groundwater drought on recharge	Lag time [month]
Nov-80	4	5 (1S, 4Mo)	5
Jan-84	5	4 (1E,1S,2Mo)	7
Dec-85	4	2 (2Mo)	4
Dec-87	3	2 (2Mo)	7
Nov-90	2	2 (2Mo)	2
Nov-93	4	5 (1S,4Mo)	7
Feb-97	5	2 (1S,3Mo)	8
Jan-03	3	6 (2S,4Mo)	9
Dec-05	2	2 (2Mo)	10
Nov-07	5	7 (1S,6Mo)	5
Dec-11	3	1 (1Mo)	4

*E: extreme; S: severe; Mo: moderate

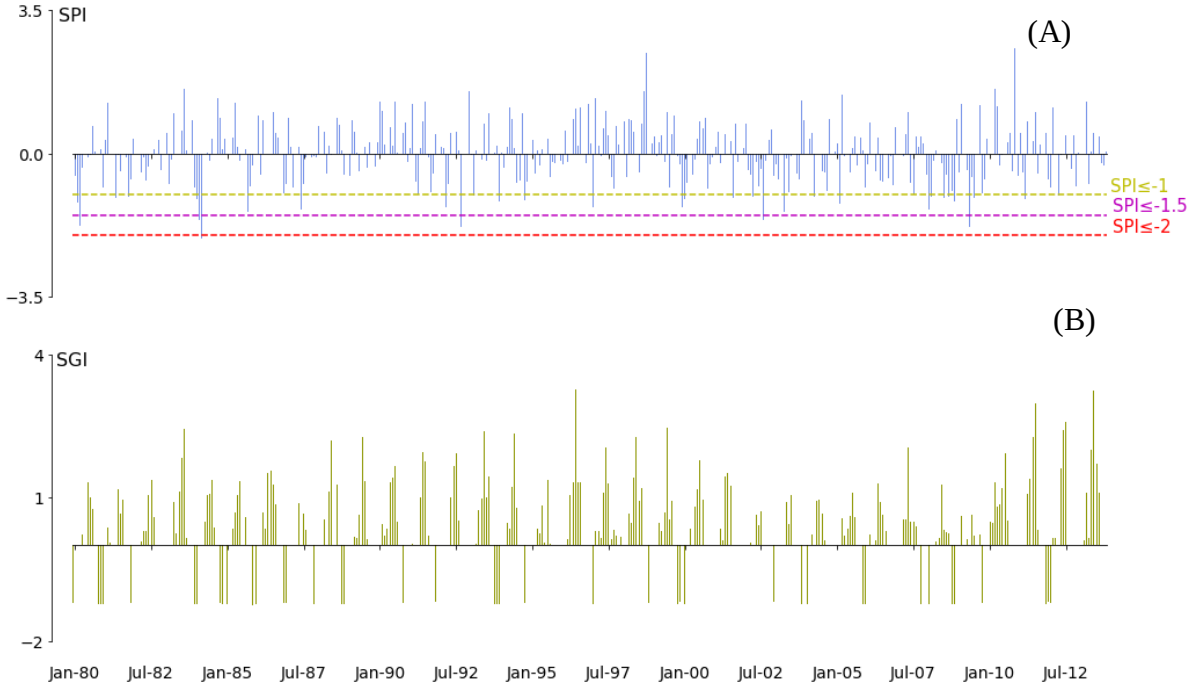


Figure 5.14: Comparison of meteorological drought severity and groundwater recharge drought (A) Monthly SPI value and (B) Groundwater recharge drought using monthly SGI.

The study about temporal and spatial meteorological drought characterization in Ethiopia by Bisrat and Berhanu (2019) indicated that water scarcity occurred in the hydrological year of 2001-02 and 2008-09 of meteorological drought. The result of this study also confirmed that more frequent meteorological droughts happened in these hydrological years. Additionally,

most meteorological droughts are observed in the months of November, December and January.

In this study, the unsaturated soil zone's delay effect is only incorporated in the calibration but not in the whole groundwater drought analysis. Accordingly, the 1.7 months average lag investigated in the drought of propagation analysis is too short to see the effect of drought on the groundwater table. Therefore, seeing the impact of meteorological drought propagation on groundwater level and discharge might take longer than the investigated lag time of 1.7 months.

5.6 Conclusion

In this study, drought propagation in the hydrological cycle from meteorological drought to groundwater recharge drought in a semi-arid climate context was investigated. Meteorological drought and groundwater drought were determined separately and compared to analyze drought propagation in the hydrological cycle. Water balance modeling and a variable threshold method were used to assess groundwater recharge drought. Moreover, a standardized meteorological drought index was used to analyze meteorological drought severity. The research was applied in the Bilate river catchment in the rift valley basin of Ethiopia.

Temporally and spatially variable long-term groundwater recharge was estimated using the water balance model WetSpass. The model was calibrated using separated base flow from observed river discharge. As a result, the model gives a good calibration result with a Nash-Sutcliffe Efficiency of 0.69 and a coefficient of determination of 0.86. Subsequently, the groundwater recharge time series was used for drought analysis.

Meteorological drought analysis in the catchment shows that meteorological drought occurs with different severity ranges, i.e., from no drought to extreme drought. Moreover, the hydrological year of 2007-08 is identified as a severe drought period. In the same manner, groundwater recharge drought analysis indicated the occurrence of drought in recharge. Major groundwater recharge drought events were identified based on the cumulative deficit volume of groundwater recharge, such as the drought from Dec-2001 to Sep-2003 with a cumulative deficit recharge of 136 mm.

Meteorological droughts propagate to groundwater recharge. Meteorological droughts were observed before every groundwater recharge drought with an average lag time of 1.7 months. Moreover, a combination of meteorological droughts ranging from mild to severe can result in a major groundwater recharge drought; for example, the major groundwater drought between Dec-2001 and Sep-2003.

This study shows that a comparison of meteorological drought with groundwater drought helps assess the hydrological cycle's drought propagation. It also shows that meteorological drought can propagate to groundwater recharge drought, but not every meteorological drought results in groundwater drought.

5.7 References

Abdollahi K, Bashir I, Verbeiren B, et al (2017) A distributed monthly water balance model : formulation and application on Black Volta Basin. Environ Earth Sci 76:1–18. doi:10.1007/s12665-017-6512-1

Ayenew T, Demlie M, Wohnlich S (2008) Hydrogeological framework and occurrence of groundwater in the Ethiopian aquifers. J African Earth Sci 52:97–113. doi:10.1016/j.jafrearsci.2008.06.006

Batelaan O, De Smedt F (2007) GIS-based recharge estimation by coupling surface-subsurface water balances. J Hydrol 337(3-4):337–355. doi:10.1016/j.jhydrol.2007.02.001

Batelaan O, DeSmedt F (2001) WetSpass: a flexible, GIS based, distributed recharge methodology for regional groundwater modelling. In: Proceedings of a symposium held during the Sixth IAHS Scientific Assembly. Maastricht, The Netherlands, July 2001, 269, pp 11–17

Bekele B, Wu W, Yirsaw E, et al (2019) Climate change and its effect on land use change in the central rift valley of Ethiopia. Appl Ecol Environ Res 17:7693–7713. doi:10.15666/aeer/1704_76937713

Beyene BS, Loon AF Van (2014) Investigation of variable threshold level approaches for hydrological drought identification. Hydrol. Earth Syst. Sci. Discuss 12765–12797. doi:10.5194/hessd-11-12765-2014

Bisrat E, Berhanu B (2019) Drought in Ethiopia : Temporal and spatial characteristics. In: Extreme Hydrology and Climate Variability: Monitoring, Modelling, Adaptation and Mitigation. pp 263–274. doi:10.1016/B978-0-12-815998-9.00021-X

Chernet T (1993) Hydrogeology of Ethiopia and water resources development. Addis Ababa, pp. 222

Das HP, Kore PA, Jadhav VN (2003) An effective method of identification of drought in kharif season. Mausam 54:909–916

Dereje B, Nedaw D (2019) Groundwater Recharge Estimation Using WetSpass Modeling in Upper Bilate Catchment, Southern Ethiopia. Momona Ethiop J Sci 11:37. doi:10.4314/mejs.v11i1.3

Döll P, Fiedler K (2008) Global-scale modeling of groundwater recharge. Hydrol Earth Syst Sci 12:863–885. doi:10.5194/hess-12-863-2008

Edossa DC, Babel MS, Gupta A Das (2010) Drought analysis in the Awash River Basin, Ethiopia. Water Resour Manag 24:1441–1460. doi:10.1007/s11269-009-9508-0

Edward DC, McKee TB (1997) Characteristics of 20th century drought in the United States at multiple time scales. Fort Collins, Colorado

FAO (1998) The Digital Soil and Terrain Map of East Africa (Sea)

Förch G, Althoff I (2009) Water Balance Modelling in the Southern Ethiopian Rift Valley: The Example of the Bilate River Catchment

Gebremeskel G, Kebede A (2017) Spatial estimation of long-term seasonal and annual groundwater resources: application of WetSpass model in the Werii watershed of the Tekeze River Basin, Ethiopia. Phys Geogr 38:338–359. doi:10.1080/02723646.2017.1302791

Gebreyohannes T, De Smedt F, Walraevens K, et al (2013) Application of a spatially distributed water balance model for assessing surface water and groundwater resources in the Geba basin, Tigray, Ethiopia. J Hydrol 499:110–123. doi:10.1016/j.jhydrol.2013.06.026

Godfrey S, Hailemichael G (2017) Life cycle cost analysis of water supply infrastructure affected by low rainfall in ethiopia. J Water Sanit Hyg Dev 7:601–610. doi:10.2166/washdev.2017.026

Kahsay GH, Gebreyohannes T, Gebremedhin MA, et al (2019) Spatial groundwater recharge estimation in Raya basin, Northern Ethiopia: an approach using GIS based water balance model. Sustain Water Resour Manag 5:961–975. doi:10.1007/s40899-018-0272-2

Kebede S (2013) Groundwater in Ethiopia Features, Numbers and Opportunities. Springer-Verlag Berlin Heidelberg, Addis Ababa

MacDonald AM, Calow RC, Nicol AL, et al (2001) Ethiopia: water security and drough

McKee TB, Doesken NJ, Kleist J (1993) A drought climatology for Europe. In: Proceedings of the 8th Conference on Applied Climatology. Anaheim, California, 17-22 January 1993, pp 179–183

Moloro TL (2018) Spatio-Temporal Analysis of Rainfall Variability and Meteorological Drought: A Case Study in Bilate River Basin, Southern Rift Valley, Ethiopia. Int J Environ Sci Nat Resour 14:. doi:10.19080/ijesnr.2018.14.555891

Nasir J, Assefa E, Zeleke T, Gidey E (2021) Meteorological Drought in Northwestern Escarpment of Ethiopian Rift Valley: detection seasonal and spatial trends. Environ Syst Res 10. doi:10.1186/s40068-021-00219-3

Pandey RP, Mishra SK, Singh R, Ramasastri KS (2008) Streamflow drought severity analysis of betwa river system (India). Water Resour Manag 22:1127–1141. doi:10.1007/s11269-007-9216-6

Pandey RP, Ramasastri KS (2002) Incidence of droughts in different climatic regions. Hydrol Sci J 47:S31–S40. doi:10.1080/02626660209493020

Peters E (2003) Propagation of drought through groundwater systems. Ph.D. thesis, Wageningen University, The Netherlands, 221 pp.

Ponce VM, Pandey RP, Ercan S (2000) Characterzation of Drought across Climatic Spectrum. Hydrol Eng 5:222–224. doi:10.1061/(ASCE)1084-0699(2000)5:2(222)

Schwabe K, Albiac J, Connor JD, et al (2013a) Drought in Arid and Semi-Arid Regions. Springer Netherlands, Dordrecht. doi:10.1007/978-94-007-6636-5

Schwabe K, Albiac J, Connor JD, Hassan RM (2013b) Drought in Arid and Semi-Arid Regions, A Multi-Disciplinary and Cross-Country Perspective, Springer Netherlands, Dordrecht, doi:10.1007/978-94-007-6636-5_20

Seboka Tura F (2017) Climate Variability and Drought in the Past 30 Years in Central Rift Valley of Ethiopia. J Nat Sci Res www.iiste.org ISSN 7:18–26

Stahl K, Hisdal H (2004) Hydroclimatology. In: Tallaksen LM, Van Lanen HAJ (eds) Hydrological drought: processes and estimation methods for streamflow and groundwater, 1st edn. Elsevier Ltd, pp 19–51. doi:10.1007/1-4020-3266-8_103

Tallaksen LM, Hisdal H, Van Lanen HAJ (2006) Propagation of drought in a groundwater fed catchment, the Pang in the UK. IAHS-AISH Publ 128–133

Tamiru A (2006) Groundwater occurrence in Ethiopia. Addis Ababa University

Teklebirhan A, Dessie N, Tesfamichael G (2012) Groundwater Recharge, Evapotranspiration and Surface Runoff Estimation Using WetSpass Modeling Method in Illala Catchment, Northern Ethiopia. Momona Ethiop J Sci 4:96. doi:10.4314/mejs.v4i2.80119

Tesfaye Tessema G (2010) Groundwater potential evaluation based on integrated GIS and remote sensing techniques in Bilate river catchment: South Rift Valley of Ethiopia. MSc. Thesis

THOM HCS (1958) A Note on the Gamma Distribution. Mon Weather Rev 86:117–122. doi:10.1175/1520-0493(1958)086<0117:anotgd>2.0.co;2

Thomas EA, Needoba J, Kaberia D, et al (2019) Quantifying increased groundwater demand from prolonged drought in the East African Rift Valley. Sci Total Environ 666:1265–1272. https://doi.org/10.1016/j.scitotenv.2019.02.206

Tilahun K, Merkel BJ (2009) Estimation of groundwater recharge using a GIS-based distributed water balance model in Dire Dawa, Ethiopia. Hydrogeol J 17:1443–1457. doi:10.1007/s10040-009-0455-x

Todmal RS (2019) Droughts and agriculture in the semi-arid region of Maharashtra, western India. Weather Clim Soc 11:741–754. doi:10.1175/WCAS-D-18-0131.1

Van Lanen HAJ (2006) Drought propagation through the hydrological cycle. in: Proceedings of the Fifth FRIEND World Conference about Climate Variability and Change—Hydrological Impacts, Havana, Cuba, November 2006, 308, 122–127,

Van Loon AF, Van Lanen HAJ (2012) A process-based typology of hydrological drought. Hydrol Earth Syst Sci 16:1915–1946. doi:10.5194/hess-16-1915-2012

Van Loon AF Van (2013) On the propagation of drought How climate and catchment characteristics influence hydrological drought development and recovery. Ph.D. thesis, Wageningen University, The Netherlands, 195 pp

Walker S (2003) the Use of Agroclimatic Zones As a Basis for Tailored Seasonal Rainfall Forecasts for the Cropping Systems in the Central Rift Valley of Ethiopia. In:

Insights and Tools for Adaptation: Learning from Climate Variability. Washington D.C., p 8. doi:10.13140/2.1.1709.1522

Willems P (2009) A time series tool to support the multi-criteria performance evaluation of rainfall-runoff models. Environ Model Softw 24:311–321. doi:10.1016/j.envsoft.2008.09.005

WMO (1975) Drought and Agriculture

Wossenyeleh BK, Worku KA, Verbeiren B, Huysmans M (2021) Drought propagation and its impact on groundwater hydrology of wetlands: A case study on the Doode Bemde nature reserve (Belgium). Nat Hazards Earth Syst Sci 21:39–51. doi:10.5194/nhess-21-39-2021

Yevjevich V (1967) An objective approach to definitions and investigations of continental hydrologic droughts. Hydrol Pap Color State Univ Fort Collins CO 23: 25 pp

Zewdie A (1994) Water resources development in Ethiopia: an evaluation of present experience and future planning concepts. Reading (United Kingdom) Ithaca Press, Reading, UK

Chapter 6

6 General conclusions and future perspectives

6.1 Introduction

In this study, a methodology was developed to assess drought propagation in the hydrological cycle, focusing on groundwater drought. This framework was applied in temperate and semi-arid climatic regions. The developed method combines water balance, unsaturated flow, and groundwater flow models with drought quantification techniques. The method was also used to differentiate between land use/land cover and climate as influencing factors on groundwater drought. Groundwater, surface water, geology, and climate data sets were incorporated in this study's hydrological and hydrogeological modeling. The method also allowed quantifying and characterizing meteorological drought and groundwater drought in different climatic regions. Drought propagation in the different parts of the hydrological cycle was characterized in two climatic regions.

In this dissertation, the research started by analyzing the groundwater recharge delay in the unsaturated soil zone to estimate the timing of groundwater recharge reaching the groundwater table of the aquifer and based on the results, the delayed groundwater recharge is estimated. This delayed groundwater recharge was used as an input for groundwater modeling and analysis of drought propagation. Then, propagation of groundwater drought was analyzed by focusing on the delayed groundwater recharge increment/decrement or the relationship between the delayed groundwater recharge, groundwater level, and discharge in the aquifer system. Moreover, drought in the hydrological cycle was investigated using the metrological drought (SPI) and groundwater drought on delayed groundwater recharge (SGI). Besides, the impact of climate and land use/land cover change on delayed groundwater recharge and groundwater drought was analyzed. Finally, the developed method for drought propagation in the hydrological cycle was first implemented in temperate climate then tested in semi-arid climatic regions.

This chapter summarises the key findings on drought propagation in a temperate and semi-arid climate context. The effect of the vadose zone, land use/ land cover, and climate factors on groundwater drought is also summarised. Finally, the limitations of the study and future research directions are given.

6.2 Contribution of the vadose zone on drought propagation

The delay of groundwater recharge in the vadose zone plays a role in the drought propagation from meteorological drought to groundwater drought. In this study, a vadose zone mathematical model was developed under the assumption of deep drainage occurring in

response to rainfall infiltration, steady vertical flow, and isotropic and homogenous soil hydraulic properties. The kinematic wave approximation of Richards' equation was combined with the parametric models of van Genuchten-Burdine and Brooks-Corey to develop the model. The mathematical model was used for estimating the kinematic wave velocity and travel time.

The main findings of this particular study are the following:

1) The kinematic wave velocity or celerity expression was derived in a parametric form using Brooks-Corey and van Genuchten Burdine parametric models. The derived equations are as follows:
    A. The celerity based on the Brooks-Corey parametric equation:

$$c = \frac{K_s(3\lambda+2)S_e^{\frac{3\lambda+2}{\lambda}}}{\lambda(\theta-\theta_r)} \qquad (6.1)$$

    B. The celerity based on the van Genuchten-Burdine parametric equation:

$$c = \frac{K_s S_e}{(\theta_S-\theta_r)}\left[2(1-{S_f}^m) + S_e^{\frac{1}{m}} S_f^{m-1}\right] \qquad (6.2)$$

    where S_f is equal to $1\text{-}S_e^{1/m}$.

2) The van Genuchten-Burdine model gives a higher estimation of soil moisture than the Brooks-Corey model. However, the celerity estimated by the Brooks-Corey model has lower values compared to the van Genuchten-Burdine model.
3) The best validated model result shows that the estimated spatially distributed groundwater recharge delay in the vadose zone ranges from 0 to 110 months.
4) The thickness of the vadose zone is the main parameter influencing the groundwater recharge delay's spatial distribution.
5) Groundwater drought characterization features such as the number, duration, onset, and intensity of drought events are influenced by the groundwater recharge delay in the vadose zone.

Incorporating groundwater recharge delay in groundwater drought delay analysis does affect the timing of groundwater drought significantly. Accordingly, features characterizing drought propagation such as pooling, lag, attenuation, and lengthening, are also influenced by this delay. Therefore, incorporating the delay in the vadose zone in drought propagation in the

hydrological cycle is crucial to tracking drought occurrence in different parts of the hydrological cycle.

The applicability of the findings and methodology of this study depends on the nature of the vadose zone. The developed method is applied and tested in lowland areas. The applicability of the model in other settings such as the mountainous catchments needs further investigation.

6.3 Drought propagation in temperate and semi-arid climatic regions

A series of methods were used to analyze drought in the hydrological cycle for temperate and semi-arid climatic regions. A standardized precipitation index (SPI) was used to investigate temporal and spatial patterns of drought severity in precipitation. Groundwater drought events were analyzed using a variable threshold method and standardized groundwater drought index (SGI). For groundwater drought analysis, time series of groundwater recharge (R) and groundwater discharge (Q) with a high spatial and temporal resolution were simulated using a spatially distributed water balance model (WetSpass) and numerical groundwater flow model (MODFLOW).

Drought propagation in the hydrological cycle was analyzed by comparing the drought characteristics of meteorological drought and groundwater drought. Particularly, groundwater drought on recharge and discharge were compared to investigate groundwater drought propagation in the aquifer. The results from the study of drought propagation in temperate and semi-arid climates in the period between 1980 and 2013 showed that:

A. The estimated groundwater recharge from the water balance model clearly follows the seasonal dynamics of the regions but with delays in the vadose and saturated zone that results in delayed effects of drought in groundwater recharge and discharge.
B. Based on the cumulative deficit volume of groundwater recharge and discharge, minor to major groundwater drought events were detected after meteorological drought.
C. Meteorological drought is more frequent and occurs earlier than groundwater recharge drought. The meteorological droughts propagated to the groundwater recharge in temperate and semi-arid climates with an average lag of 2.25 months and 1.7 months, respectively. In the semi-arid climatic case study, the vadose zone delay is not incorporated during the drought propagation analysis; it is only

incorporated during the calibration of the water balance model, WetSpass. In general, the total lag time is the sum of the delay of groundwater recharge in the vadose zone and lag time investigated from the drought analysis. Therefore, incorporating the delay in the vadose zone for semi-arid climate will significantly change the comparison of the drought propagation with the temperate climate case study.

D. Drought characteristics being changed during propagation in the aquifer. The number and severity of drought events observed in groundwater discharge to rivers and wetlands were smaller than for groundwater recharge. That means droughts are attenuated in the groundwater system.
E. Different severity ranges of meteorological drought, from mild to extreme, propagate to groundwater recharge and causes groundwater drought.

Groundwater drought severity is different in the two climatic regions. Between 1980 to 2011, the total cumulative deficit volume of groundwater recharge was 203 mm, which is 2.2 % of the total recharge, in the temperate climate. In the semi-arid climatic region, 300 mm of total deficit volume of groundwater recharge, which is 7.2 % of the total recharge, is calculated. This indicates that groundwater recharge drought in a semi-arid climate can be much more severe than in a temperate climate. Moreover, the groundwater recharge drought in the semi-arid climate has a longer average drought duration of 6 months compared to the temperate climate average drought duration of 3.5 months.

In both

Finally, this study concluded that combining water balance and groundwater models with drought quantification methods can help the study of drought propagation in the hydrological cycle in both climate regions.

6.4 Land use/ land cover and climate factors as influencing factor on groundwater drought

A water balance modeling method with different land use/land cover and meteorological scenarios is used to investigate the influence of land use/land cover and climate on groundwater recharge estimation and groundwater drought. Two static LULC maps of 1990 and 2013, one dynamic LULC map, dynamic meteorological variables, and long-term average meteorological variables are incorporated as an input for the water balance modeling. The two static runs based on the 1990 and 2013 static LULC maps are compared with the dynamic

run, based on the dynamic LULC, to investigate the LULC influence. To investigate the climate factors' influence, the dynamic run was compared to the long-term average run. For all simulations, groundwater recharge droughts were analyzed using a variable threshold method and were compared to each other to investigate the influence of LULC and climate on drought.

Results show that some of the LULC changes lead to decreasing groundwater recharge. On average, in the study area, the estimated groundwater recharge has decreased in the period between 1980 and 2013 because of LULC change. Based on a pixel level analysis, this study also investigated the significant role of urbanization in decreasing groundwater recharge. Moreover, the deviation of meteorological variables from the long-term average also resulted in a decrease of calculated groundwater recharge in the period between 1980 and 2013.

Groundwater drought features such as the number, duration, and intensity of drought events are also influenced by LULC changes and climate factors. The LULC change effect on groundwater drought severity was higher than the impact from the shift of meteorological variables from the long-term average.

This study showed a well-calibrated water balance model's applicability on identifying the climate and LULC change influence on groundwater recharge estimation and groundwater drought. Moreover, water managers can use this approach to predict the influence of future climate change and urbanization on the groundwater ecosystem.

6.5 Limitations

This study's findings have to be seen in the light of some limitations listed based below. These limitations could be addressed in future research.

Vadose zone delay

Spatially distributed groundwater recharge delay in the vadose zone has been estimated using the gravity-driven kinematic wave approximation of Richards' equation combined with the van Genuchten-Burdine and Brooks-Corey parametric model. The limitations of this approach are:

- ✓ The storage effect of the vadose zone is not considered during the development of the model. Also, the model assumes 1D flow in the vadose zone.
- ✓ The model is calibrated using a comparison of the result with the physically-based flow model Hydrus-1D. However, real-time field measurement of soil moisture content

and lag time of soil moisture content in the vadose zone would help the model to reduce the uncertainty.

Drought propagation in the hydrological cycle

A water balance model has been used for groundwater recharge estimation in both temperate and semi-arid climatic regions. Because of the limited availability of long-term groundwater level time series, model calibration was done using the separated base flow observed river discharge in one of the study areas' sub-catchments. However, measured groundwater recharge or coupling the model with a well-calibrated groundwater model and including the whole catchment groundwater recharge estimation in the calibration would reduce the model uncertainty.

Evapotranspiration plays a significant role in meteorological drought creation, especially in semi-arid climate regions. However, a Standardized Precipitation Index (SPI) has been used in this study to characterize the meteorological drought severity. Therefore, using drought indices that incorporate evapotranspiration, such as the Standardized Precipitation Evaporation Index (SPEI), might improve meteorological drought analysis.

For groundwater drought analysis, long-term groundwater discharge has been simulated using a groundwater model. However, the simulated groundwater discharge is not long enough to accurately analyze groundwater discharge drought because of the limited availability of long-term groundwater level time series.

6.6 Concluding remarks and future research perspectives

The main lesson learned from this research is the nature of drought propagation in the hydrological cycle and the aquifer. Moreover, this study showed the application of a methodology that combines water balance and groundwater flow models and drought quantification indices to analyze each drought type in the hydrological cycle.

Many different research directions and applications have been left for future studies based on this current study. The following future study directions are recommended:

A. The groundwater recharge delay model was developed separately in this study (Wossenyeleh et al., 2020). In future research, incorporating this model into the water balance model (WetSpass-M) would reduce the simulation time and increase the groundwater recharge estimation efficiency.

B. In this study, the developed model for groundwater recharge delay in vadose zone was applied and tested in low-land areas of the temperate clime case study. In future investigation, the applicablity of the developed model in mountain catchments such as the semi-arid climate case should be further investigated.
C. In this study, the drought effect on the wetlands and river ecosystems was analyzed (Wossenyeleh et al., 2021, Chapter 3). The developed methodology was recommended to apply in the sector of agricultural food production to see how drought propagation influences crop production.
D. In the future, there is a climate and land-use change. The methodology developed in the current study (Chapter 4) would help to analyze the future climate and land use impact on groundwater recharge and drought.
E. Coupling our drought propagation method in the semi-arid climate to a groundwater flow model would enable to study the impact of drought propagation in the aquifer.

Finally, this study's findings can be used by policymakers to incorporate the impact of the drought into their policies and drought preparedness strategies.

6.7 References

Wossenyeleh, B.K., Verbeiren, B., Diels, J., Huysmans, M.: Vadose zone lag time effect on groundwater drought in a temperate climate. Water 12, 2123, doi:10.3390/w12082123, 2020.

Wossenyeleh, B.K., Worku, K.A., Verbeiren, B., Huysmans, M.: Drought propagation and its impact on groundwater hydrology of wetlands: A case study on the Doode Bemde nature reserve (Belgium), Nat. Hazards Earth Syst. Sci. 21, 39–51, doi:10.5194/nhess-21-39-2021, 2021.

Appendices

Appendix A: Vadose zone groundwater recharge delay

A1: Aggregated soil texture in 168 soil borehole

Detailed soil characterization of the geological layers was taken from 168 Soil boreholes found in the Demer and Dijle catchments (*Figure 2.1*). In these soil boreholes, soil texture is aggregated using a soil texture triangle, and homogeneous soil texture within the thickness of each borehole was considered.

Soil borehole ID	Aggregated Soil Texture	X	Y
1	loamy sand	238546.00	172158.00
2	loamy sand	238636.00	171853.00
3	sandy loam	183339.00	166624.00
4	loamy sand	155980.06	173190.74
5	sand	237464.50	188289.00
6	sandy loam	177627.00	191232.00
7	loamy sand	237745.65	168936.29
8	loam	237599.64	170152.70
9	loam	200922.60	199699.10
10	sandy clay loam	200229.00	166007.00
11	clay loam	174586.00	165125.00
12	loam	201082.00	170846.00
13	loam	211092.80	200187.22
14	sandy clay	199176.00	201034.00
15	sand	191336.22	195139.48
16	sand	189308.95	198913.20
17	sand	172161.20	202337.58
18	sand	178432.10	204801.92
19	sandy clay	166334.33	196733.66
20	sandy loam	232979.74	168552.28
21	sandy loam	226013.08	178274.46
22	sandy loam	219220.97	163356.05
23	clay	214149.59	165722.62
24	clay	201051.29	158214.86
25	loamy sand	201160.24	161129.65
26	sandy clay	201219.11	163181.41
27	silt	227625.00	154915.00
28	loamy sand	151981.54	208764.21
29	sand	174665.72	173378.33
30	sand	176940.00	170075.00
31	sand	183027.30	210567.60
32	sand	212605.40	201174.40
33	sand	161544.70	179232.90
34	sand	171575.00	194481.00
35	sand	207751.00	195385.30
36	silty clay loam	141718.00	159454.00
37	clay	161647.00	162329.00
38	sand	149739.00	160056.00
39	loam	151117.00	165669.00
40	sandy clay	148209.00	159612.00
41	loam	146943.00	163032.00

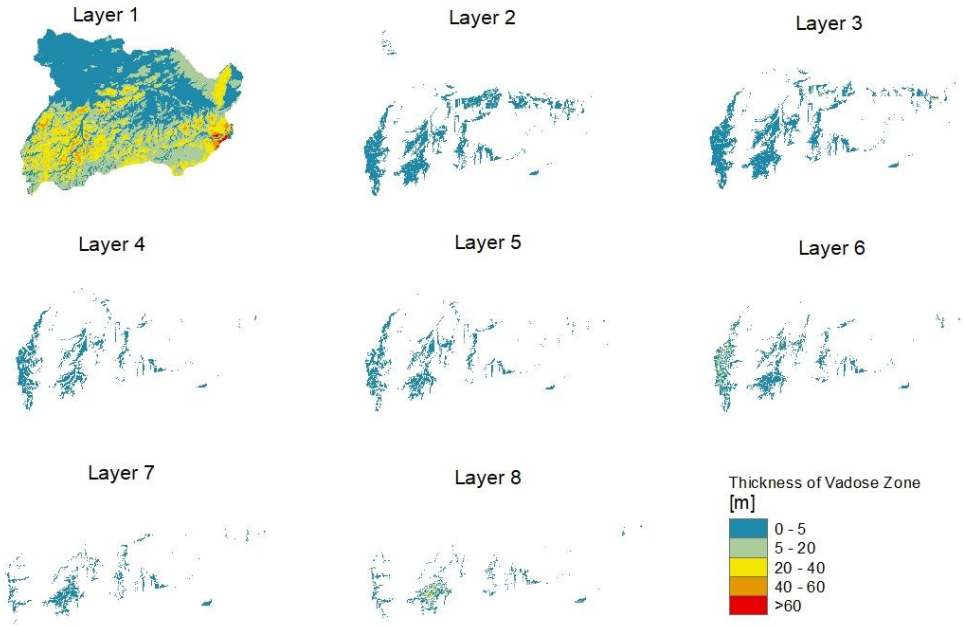
Soil borehole ID	Aggregated Soil Texture	X	Y
42	sand	150944.00	172853.00
43	loam	148214.00	168875.00
44	sandy loam	178376.00	158597.00
45	sandy clay	176940.00	171065.00
46	sand	192390.00	170936.00
47	sandy clay	189875.00	172551.00
48	sand	207757.00	159737.00
49	silt	200863.30	161817.60
50	silt	220220.00	166300.00
51	silt	220232.00	161809.90
52	silt loam	220285.40	170498.90
53	loam	239815.70	160971.30
54	sandy loam	237941.70	162431.60
55	sand	237982.40	175471.60
56	loam	231413.70	170313.60
57	loam	231414.20	173422.90
58	silt	141672.00	157649.00
59	sandy clay	151633.00	158000.00
60	sandy loam	151981.00	154755.00
61	sandy loam	148090.00	154762.00
62	loam	151580.00	156188.00
63	clay loam	190724.00	154505.00
64	sandy loam	159999.00	152805.00
65	loam	195246.27	162138.98
66	sandy caly	195582.83	164617.27
67	sandy loam	184098.26	163359.02
68	Loam	191895.86	164622.08
69	sandy loam	210226.10	162285.69
70	sandy loam	209172.94	166704.07
71	clay	203210.23	163118.61
72	sandy clay	203052.00	175165.60
73	sandy loam	184258.34	169024.55
74	sand	192154.06	173318.09
75	sand	182497.43	174735.98
76	sand	196989.25	182633.49
77	sand	207687.44	191822.74
78	sand	207466.13	185189.91
79	sandy clay	203709.51	194515.46
80	sandy clay	188363.94	188350.22
81	sandy clay	188533.30	180248.20
82	sand	179966.40	183414.00
83	sand	238316.00	170467.00
84	clay	206406.00	170083.00
85	sand	217384.00	200250.00
86	caly	214963.00	170950.00
87	sandy loam	219223.94	177169.37
88	clay loam	175902.00	169756.38
89	loamy sand	165671.85	172901.04
90	sandy clay	176907.07	175029.38
91	sand	169422.67	180118.12
92	clay loam	163584.01	183567.14
93	loamy sand	162035.90	178054.00

Soil borehole ID	Aggregated Soil Texture	X	Y
94	sand	164203.44	188341.78
95	loamy sand	159028.62	207872.73
96	loamy sand	184600.00	170155.00
97	sand	155710.00	212191.00
98	sandy clay	142022.10	157093.30
99	silt loam	162159.00	162161.00
100	sand	151913.00	212226.00
101	loam	143007.00	161353.00
102	clay loam	158369.00	183094.00
103	loamy sand	163428.00	212143.70
104	sand	156875.00	210131.00
105	sandy clay	148417.00	200458.00
106	sandy clay	164132.50	212143.40
107	sand	186123.60	208215.90
108	sand	164969.10	201742.20
109	sand	187623.00	204161.60
110	sand	217329.60	200953.20
111	sand	157582.20	190932.30
112	sand	181555.00	197086.00
113	sandy loam	182311.00	191220.00
114	sand	168871.00	183329.00
115	sandy loam	165767.00	182990.00
116	sandy clay	183797.00	185802.00
117	sandy loam	215660.70	181149.70
118	sand	228887.00	181150.00
119	silt loam	143781.00	159836.00
120	silty clay loam	141601.00	158189.00
121	loamy sand	144268.00	160634.00
122	clay	145385.00	167467.00
123	sand	159282.00	162031.00
124	clay loam	154319.00	162748.00
125	loamy sand	158820.00	160495.00
126	sandy clay	147813.00	160459.00
127	sand	148331.00	169257.00
128	sand	148702.00	172931.00
129	silt clay	150025.00	173123.00
130	silt	174140.00	164480.00
131	clay loam	174295.00	159828.00
132	sandy loam	174452.00	159886.00
133	sand	162434.00	162762.00
134	loam	189328.00	161313.00
135	sandy loam	188066.00	158880.00
136	silt loam	192675.00	158208.00
137	sand	188888.00	162744.00
138	silt	189749.00	158836.00
139	clay	191751.00	165979.00
140	sandy clay	183644.00	166450.00
141	silt clay	179340.00	160375.00
142	clay loam	182303.00	158206.00
143	sandy clay	185623.00	166168.00
144	sandy clay	181230.00	167685.00
145	clay loam	168467.00	172034.00

Soil borehole ID	Aggregated Soil Texture	X	Y
146	loamy sand	190061.00	173140.00
147	sandy clay loam	209877.20	163637.20
148	silt clay	200298.30	159931.40
149	sandy loam	199477.30	159899.60
150	clay	220184.90	161235.20
151	silt loam	220209.50	158180.80
152	clay	215742.90	160343.20
153	loam	217958.90	159870.60
154	clay	205040.00	172010.00
155	clay	240099.70	164511.10
156	loam	168806.00	178293.00
157	sandy clay	233259.00	178349.00
158	sandy clay loam	209894.00	178375.90
159	loam	233322.10	173106.80
160	sandy clay	142514.00	155465.00
161	silt loam	205117.60	155479.40
162	loam	205114.80	155311.60
163	silt clay	206018.90	155241.10
164	silt	200942.10	156992.40
165	silt	215287.00	156508.00
166	silt loam	187861.00	157178.00
167	loam	159226.00	156726.00
168	sandy loam	216939.60	158847.60

A2: Thickness of geological layers in vadose zone

Thickness of geological layers in vadose zone (m) of the study area within 5 color-coded classes, estimated as the difference in 100-m digital elevation model data, base elevation of each geological layers and 34years(from 1980 to 2013) averaged water table digital data. (refer layer type from Table 2.1 *in chapter 2).*



A3: Python Code for Delayed recharge mapping

Workflow

Goal is to construct delayed groundwater recharge map based on Delay result from the model based on Brook_Corey parametric model and Groundwater recharge data

- ✓ Load Delay map file and recharge files as dictionaries of pandas data frames
- ✓ For every `pixel' in every input file check if the value is bigger than the difference between the current_month and the start_month which is equal to 1.
  - Example:
    current_month = 1,
    start_month = 1,
    diff = 0
    —> if value > 0: NaN, else: lookup value
- ✓ If condition is True look up the recharge value for the according month
  - Example:
    current_month = 12,
    start_month = 1,
    value = 6
    —> lookup_month = current_month - value
    —> Lookup_value = value_in_lookup_month

Remarks

- ❖ Change file naming to be consistent with month/(year)
  - 6 = June of first year
  - 23 = November of second year
- ❖ Delay file works with 0-based counting
- ❖ key-pairs work with 1-based counting as this is easier for months

In[1]:

```
import pandas as pd
import numpy as np
import os
```

Data loading

In[2]:

Read in delay file

```
delay = pd.read_csv("Folder location of the Delay Map", skiprows=6, header=None, sep=" ")
```

In[3]:

Read in recharge files

```
rootDir ="Folder location of the original Groundwater recharge Maps"
recharge_dict = {}
```

```
for file in os.listdir(rootDir):
 recharge_dict[int(file.split(".")[0])] = pd.read_csv(rootDir + "/" + file, skiprows=6, header=None,
sep=" ")
 print(file, end=';')
```

In[4]:

- Instead of checking which 'pixels' in the delay file are NaN every
- time in the loop just do it once and save the index pairs in a list

```
indices = [ ]
```
- Create numpy mask with only the grid points that have data

```
for i in range(delay.shape[0]):
   for j in range(delay.shape[1] - 1):
```
- Check for NaN

```
      if delay.iat[i ,j] != -9999:
         #print("NaN")
         indices.append((i, j))
print("Shape of delay matrix:", delay.shape)
print("Number of non NaN values:", len(indices))
```

Functions
In[5]:

```
def create_delayed_recharge_maps_new(delay, recharge, n_months, start_month=1):
   """Create delayed recharge maps for specified number of months
   Parameters:
         Delay data
delay : pd.DataFrame
        Recharge data
   recharge : dict
      Number of months to calculate delayed recharge for
   n_months : int
      Integer to use as starting month
   start_months : int (optinal)
   Returns:
   output_dict : dict
      Delayed recharge maps for requested number of months
   """
```
- Initialize output dictionary

```
   output_dict = {}
   for current_month in range(1, n_months):
```
- Initialize empty output matrix with -9999.0 as values

```
      output = np.full(shape=(delay.shape[0], delay.shape[1] - 1), fill_value=-9999.0, dtype="float64")
```

```
    print("current_month:", current_month, "\n")
    for index_pair in indices:
```

- Look up number of delay months

```
    delay_months = delay.iat[index_pair]
```

- Check if lookup month is not before start_month

```
    if start_month <= current_month - delay_months:
```

- Calculate month to look up recharge data from

```
        lookup_month = current_month - delay_months
```

- Look up recharge data and save in according place in output

```
        output[index_pair] = recharge[lookup_month].iat[index_pair]
    else:
        output[index_pair] = -9999.0
```

- Save generated output in dictionary as value with current month as key

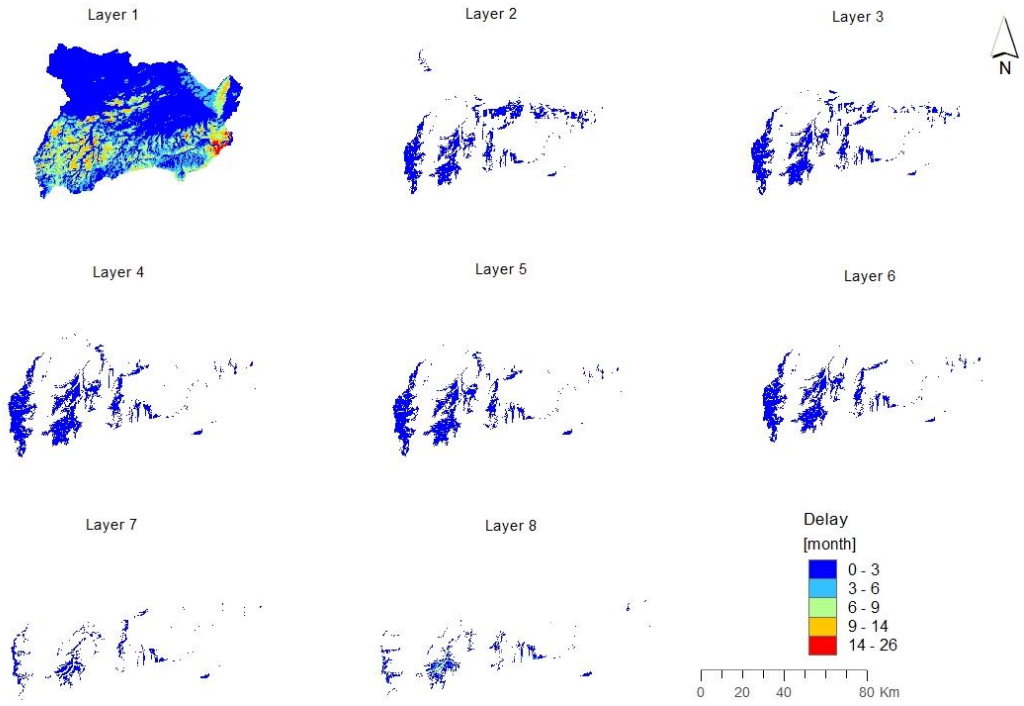
```
    output_dict[current_month] = output
return output_dict
----
```

Calculations

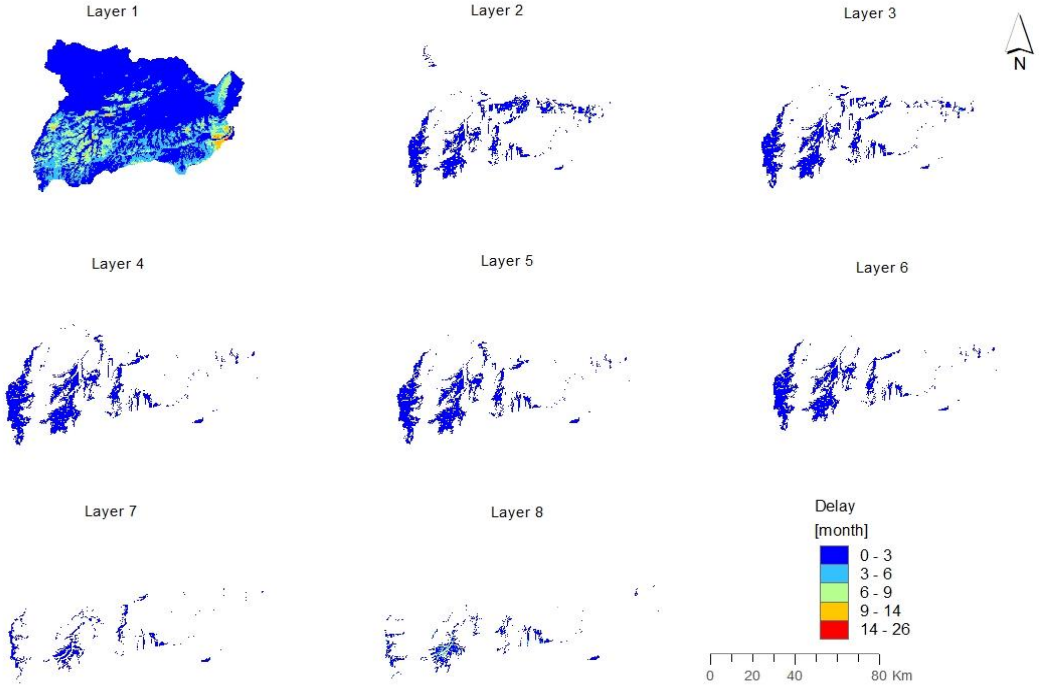
```
In[6]:
----
output_files = create_delayed_recharge_maps_new(delay, recharge_dict, 409)
----
```

A4: Spatially distributed groundwater recharge delay for each geological layers based on Lumped parametrization of geological layers

A4.1: Spatially distributed groundwater recharge delay in each geological layer of the vadose zone using Brooks Corey parametric model

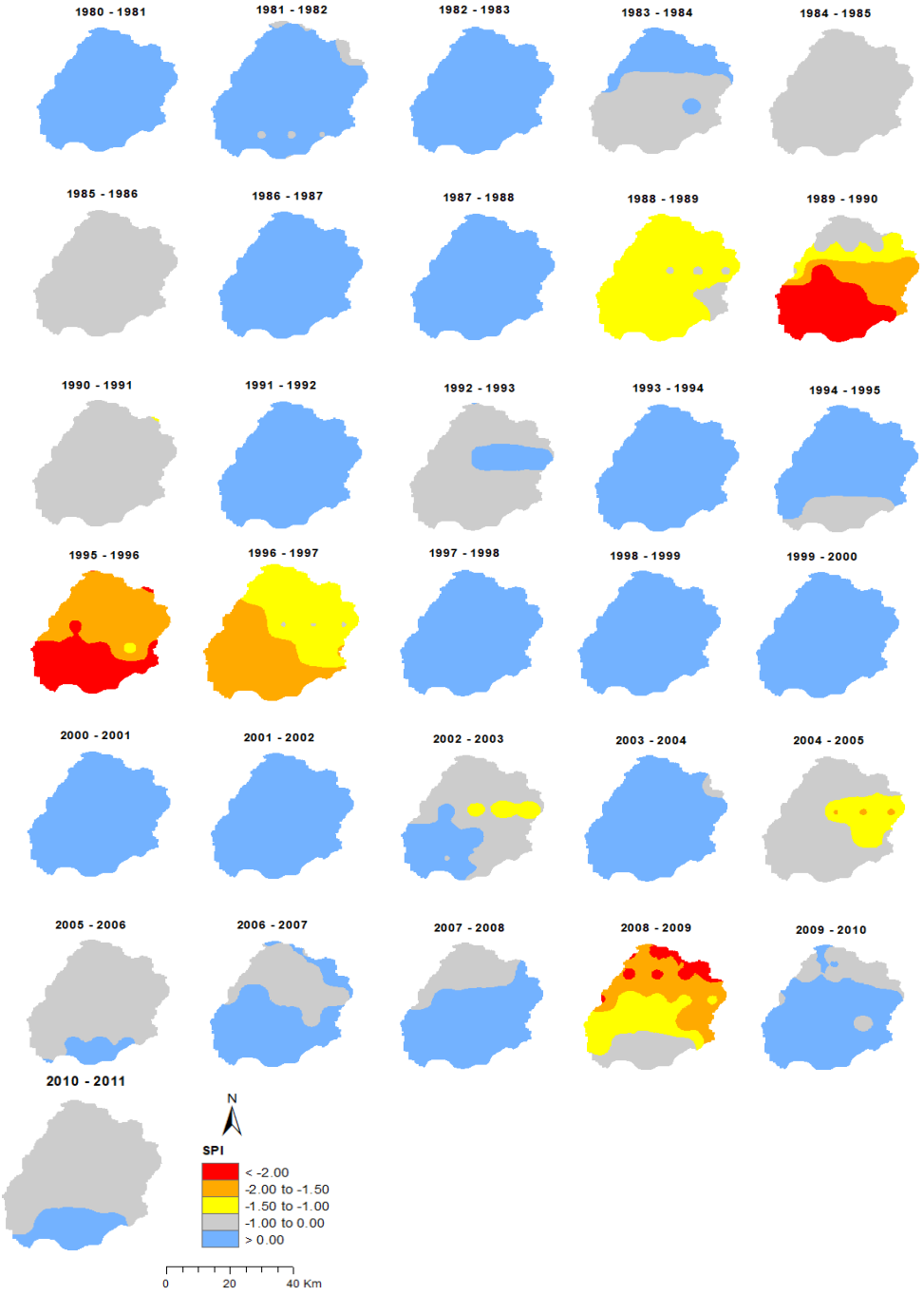


A4.2: Spatially distributed groundwater recharge delay in each geological layer of the vadose zone van Genuchten-Burdine Parametric model

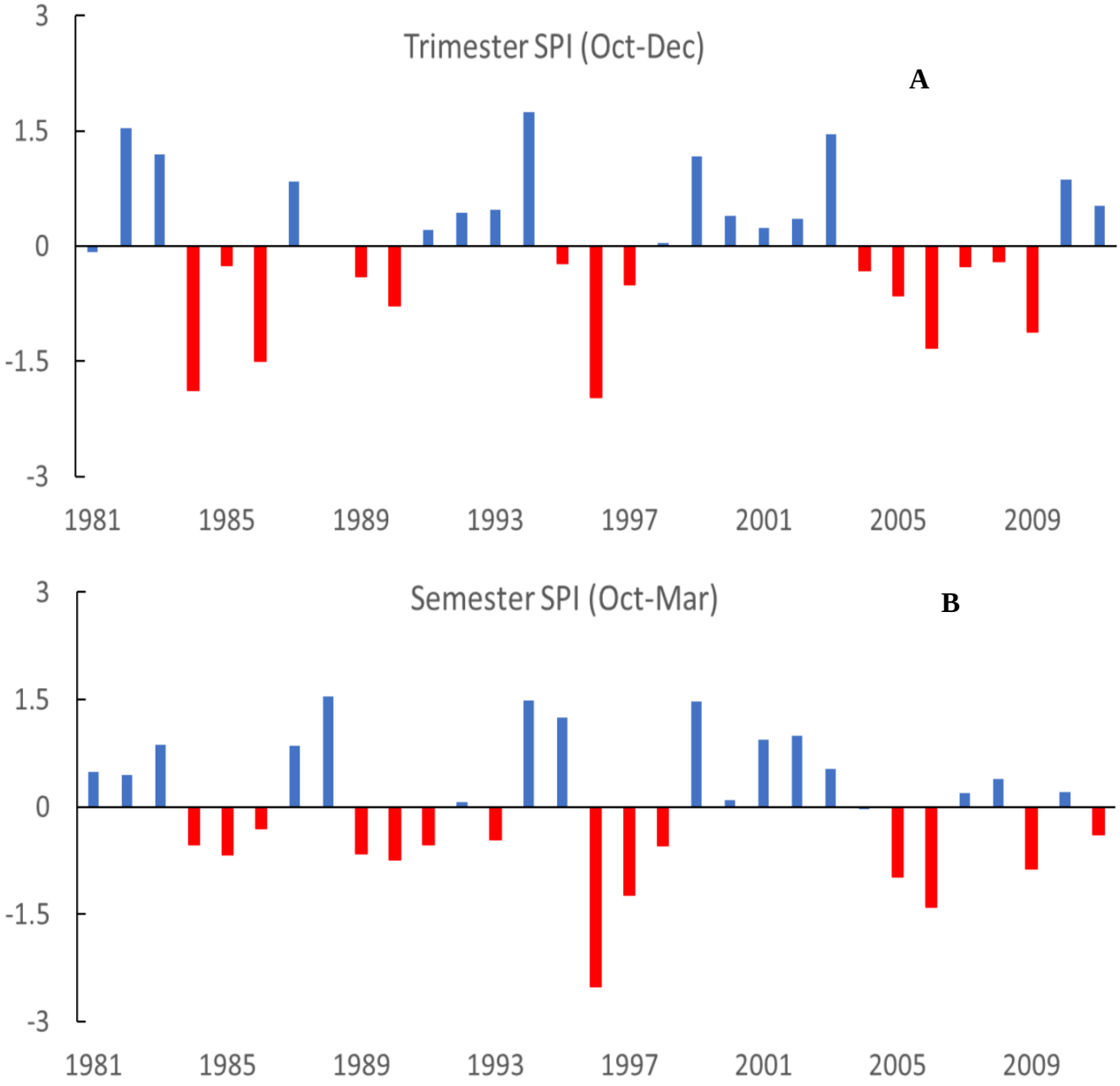


Appendix B: Meteorological drought, groundwater recharge and discharge thresholds values for Dijle and parts of the Demer and Zenne basin

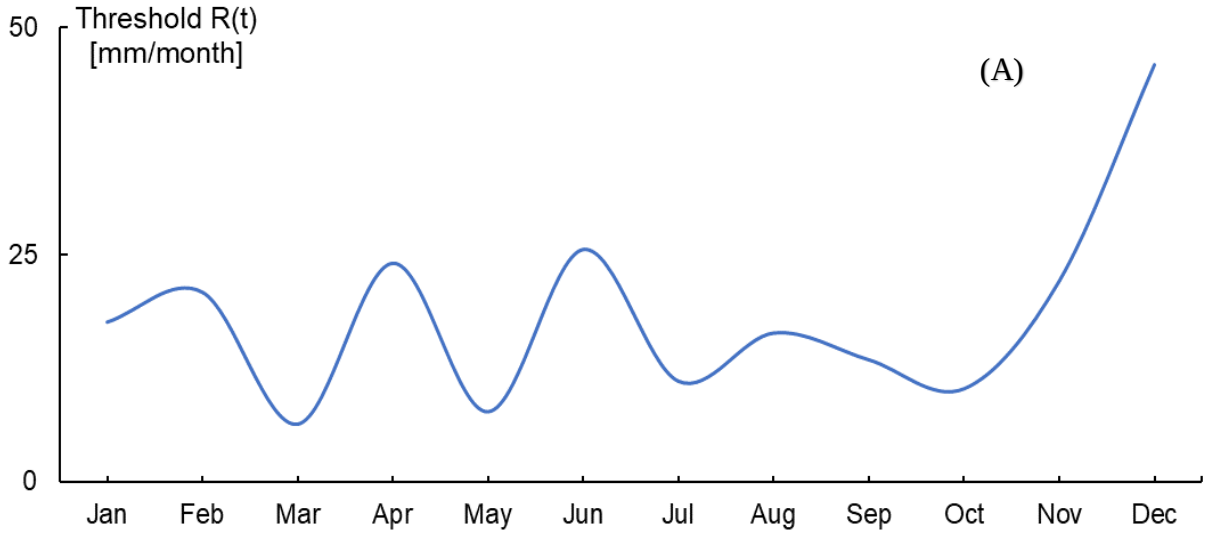
B1: Spatially distributed Meteorological drought severity for Dijle catchment and parts of the Demer and Zenne basin based on SPI-12 (Annual) value for 31 hydrological year

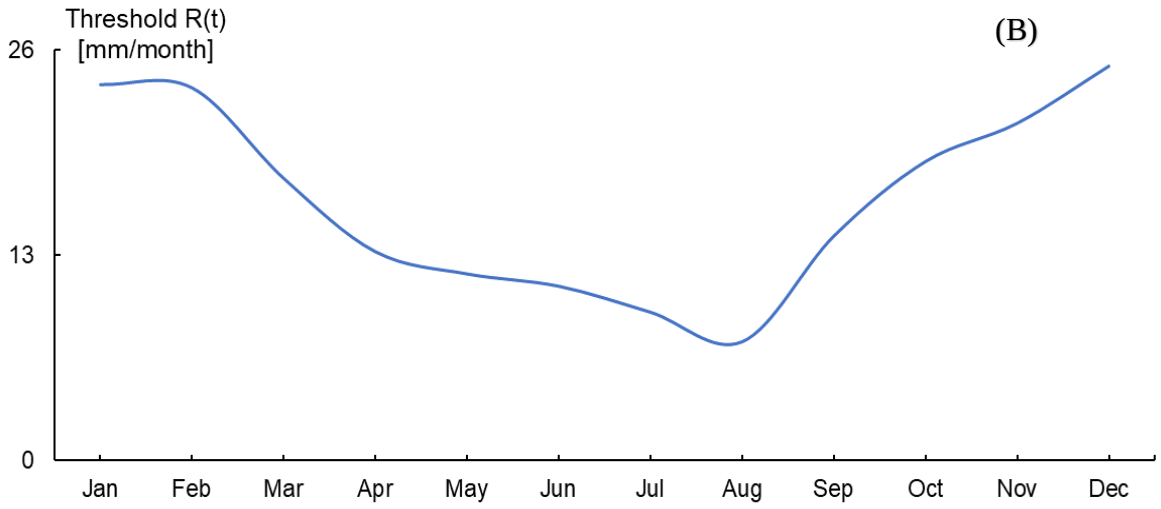


B 2: Meteorological drought severity for the Uccle station based on (A) SPI-3 value and (B) SPI-6 value between the hydrological year of 1980 and 2011

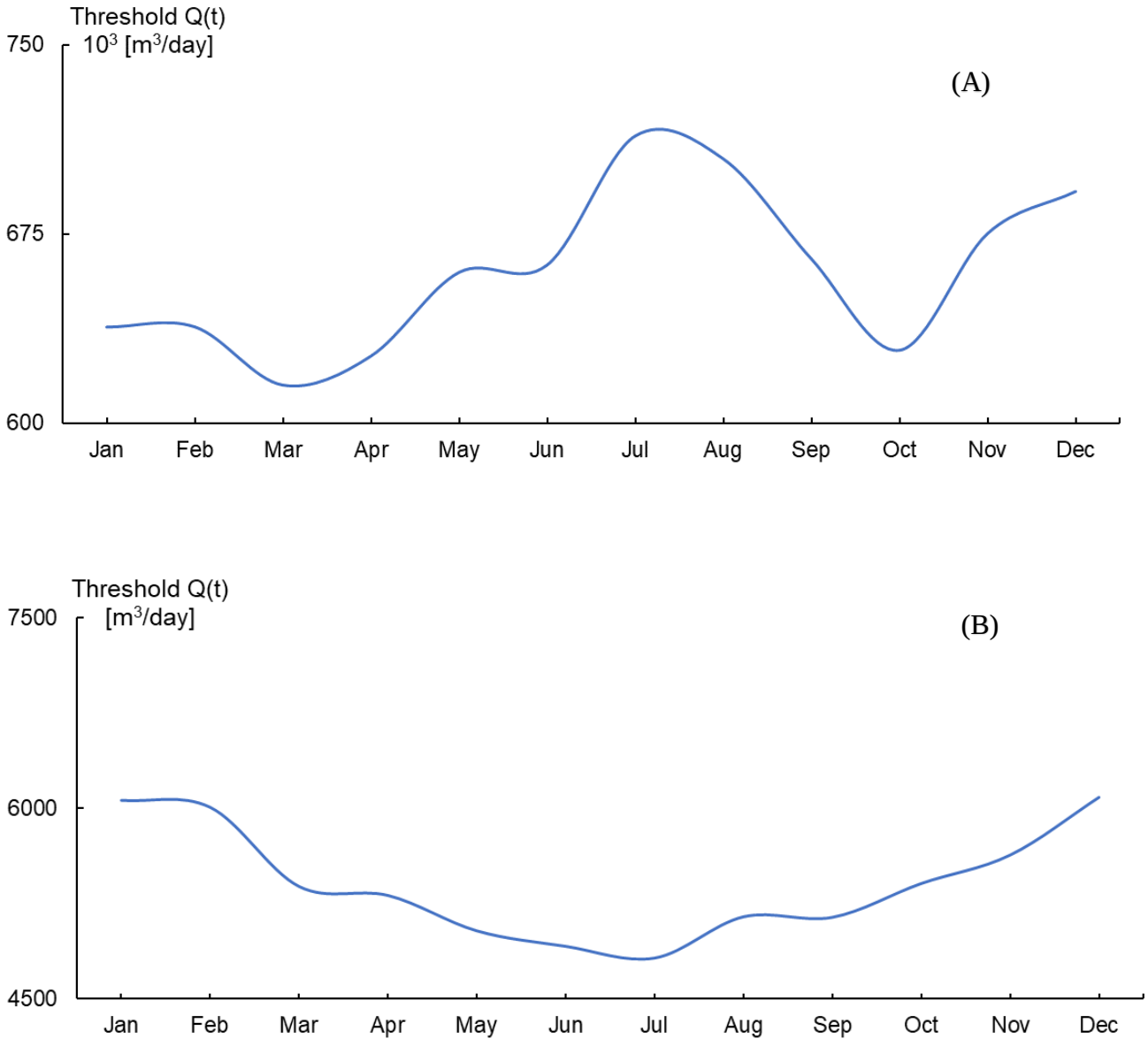


B 3: Variable threshold value of groundwater recharge for (A) Dijle catchment and parts of the Demer and Zenne basin, and (B) Doode Bemede wetland. Each month's variable threshold level was determined as the 80th percentile of the probability of exceedance of monthly recharge in that month in the 34-year series (1980-2013).



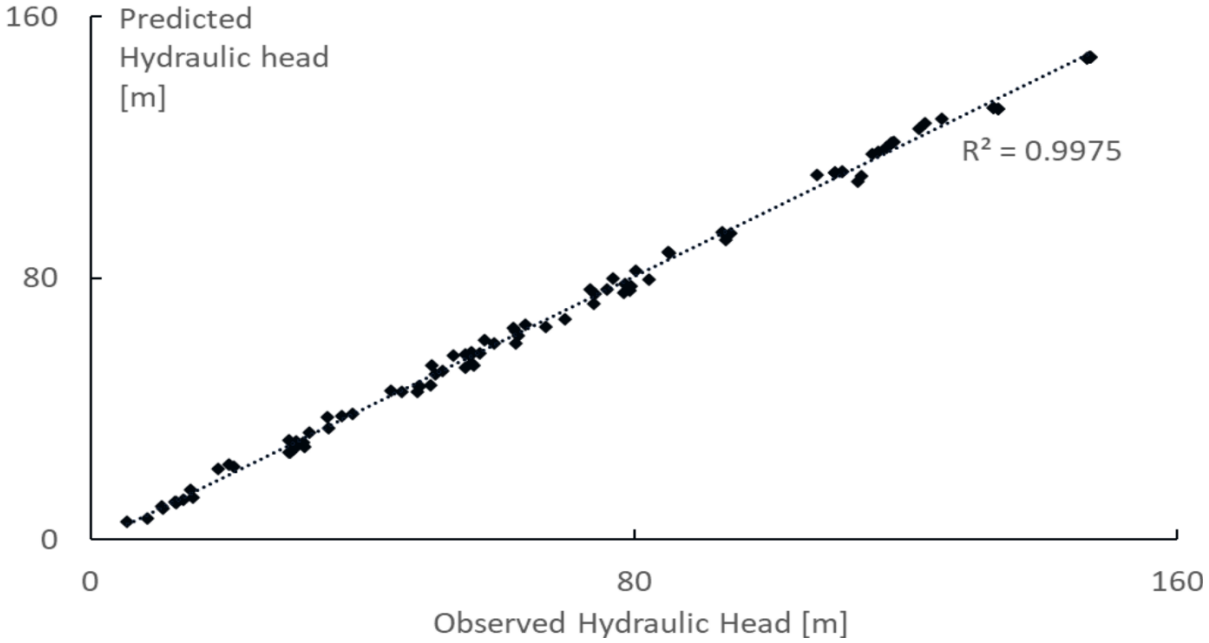


B 4: Variable threshold value of total groundwater discharge for (A) Dijle catchment and parts of the Demer and Zenne basin, and (B) Doode Bemede wetland.



Appendix C: Steady-state groundwater model calibration result

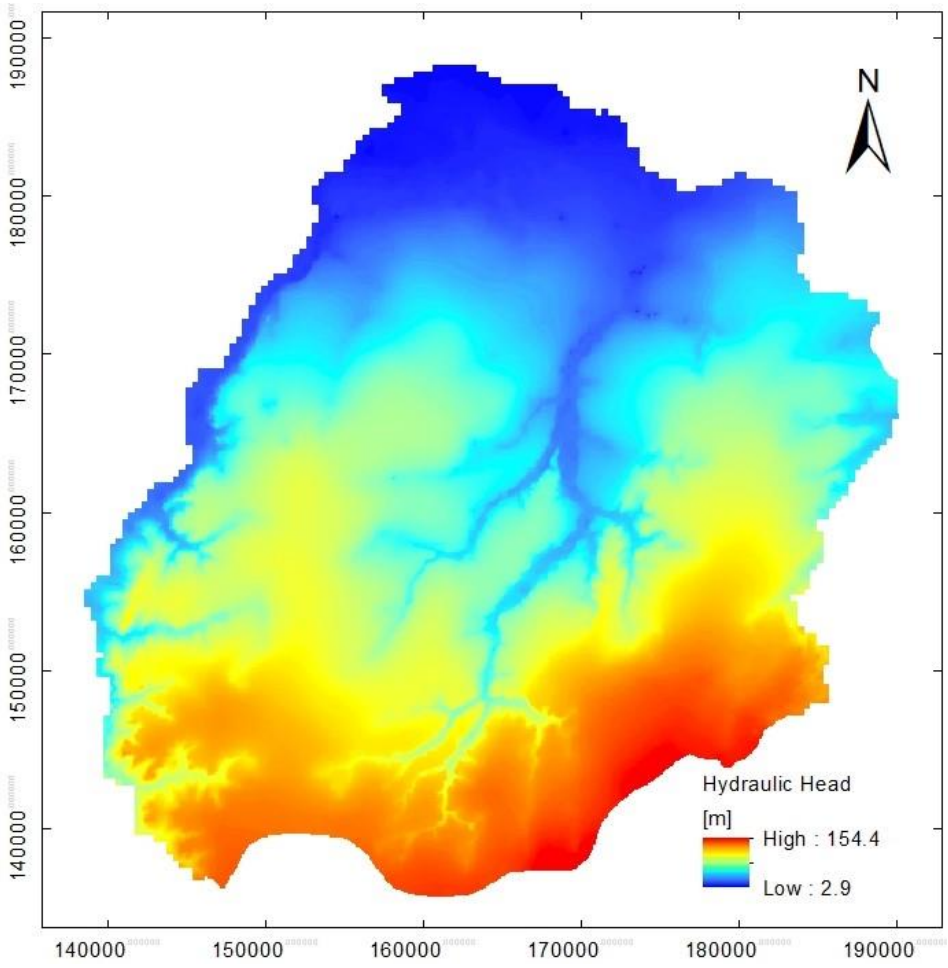
C 1: The hydraulic head comparison between the observed and simulated for steady-state groundwater model of Dijle and parts of the Demer and Zenne basin



C 2: Model evaluation statistics for calibration of steady state groundwater model of Dijle and parts of the Demer and Zenne basin

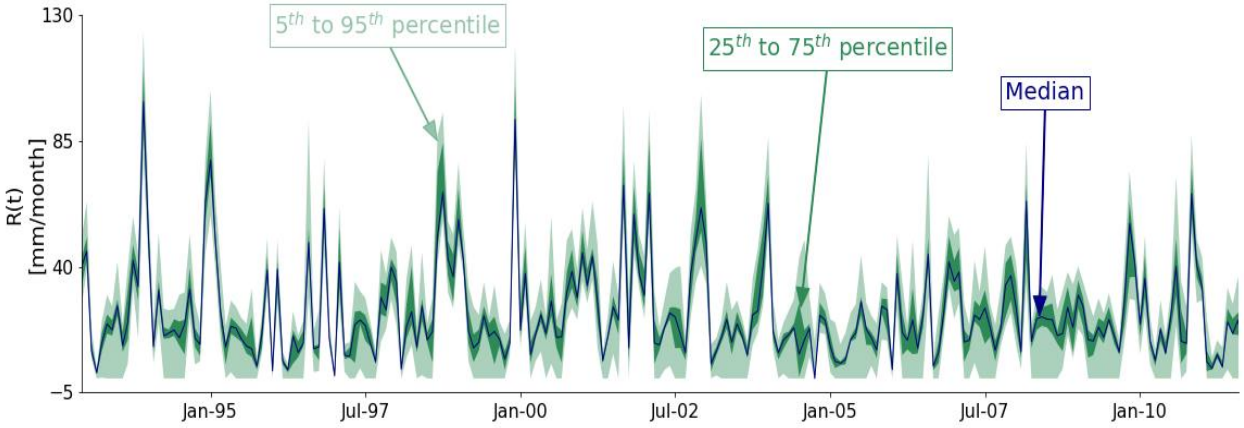
Statistical Indicator	Value
NSE	0.98
RMSE (m)	1.3
PBIAS (%)	-0.13
σ^2	1.85
R^2	0.99

C 3: Steady state groundwater model hydraulic head distribution for Dijle and parts of the Demer and Zenne basin

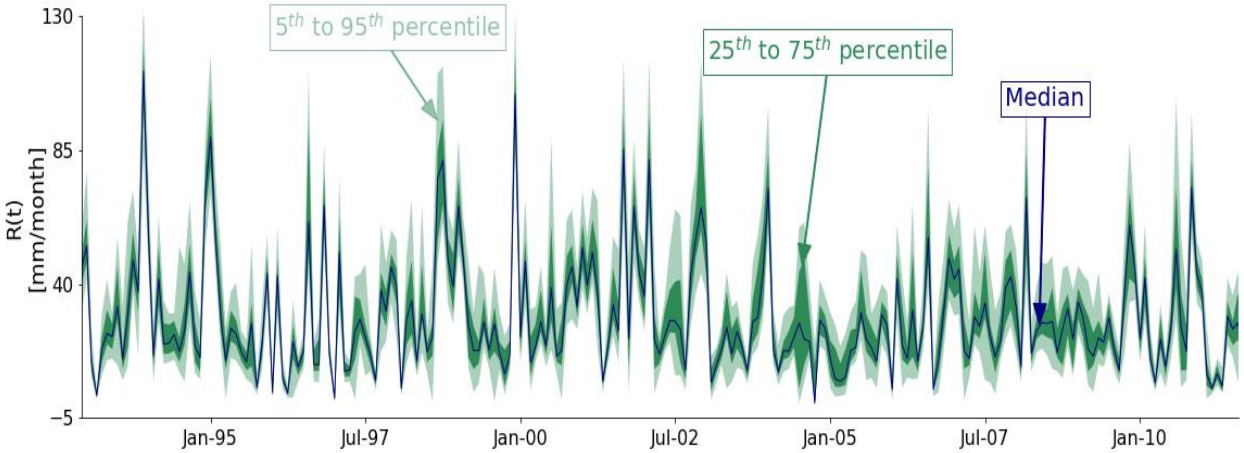


Appendix D: Estimated groundwater recharge of the Static runs

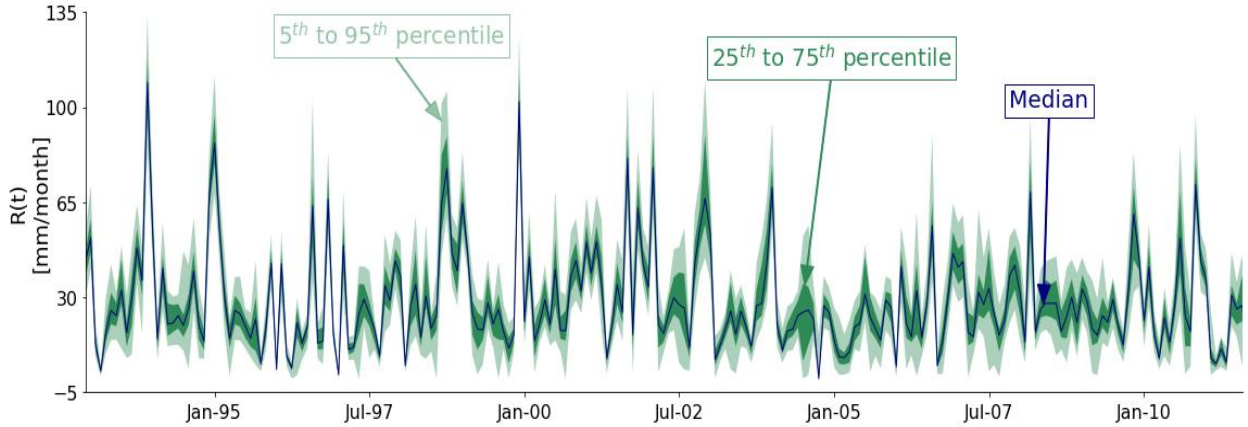
D 1: Estimated groundwater recharge of the 1990 static run (run 1) to show the temporal variation for only the places which decreased the groundwater recharge estimation. The dark blue line is the median curve (50th percentile) and shows the media groundwater recharge value for each month. The green shadow area represents the interquartile range (IQR). Moreover, the light green shaded area represents the lowest and highest 5 % of each month's groundwater recharge values.



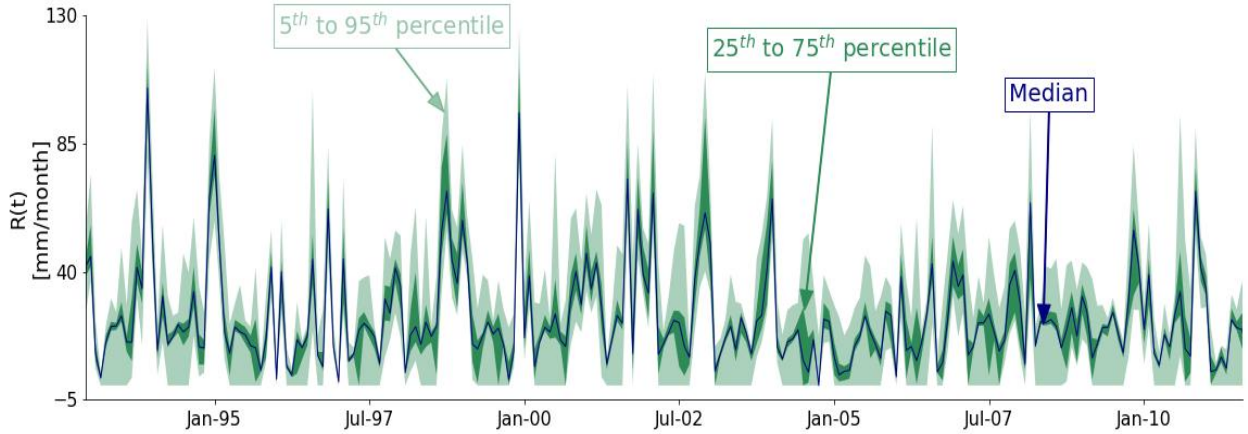
D 2: Estimated groundwater recharge of the 1990 static run (run 1) to show the temporal variation for only the places which increased the groundwater recharge estimation. The dark blue line is the median curve (50th percentile) and shows the media groundwater recharge value for each month. The green shadow area represents the interquartile range (IQR). Moreover, the light green shaded area represents the lowest and highest 5 % of each month's groundwater recharge values.



D 3: Estimated groundwater recharge of the 2013 static run (run 2) to show the temporal variation for only the places which decreased the groundwater recharge estimation. The dark blue line is the median curve (50th percentile) and shows the media groundwater recharge value for each month. The green shadow area represents the interquartile range (IQR). Moreover, the light green shaded area represents the lowest and highest 5 % of each month's groundwater recharge values.

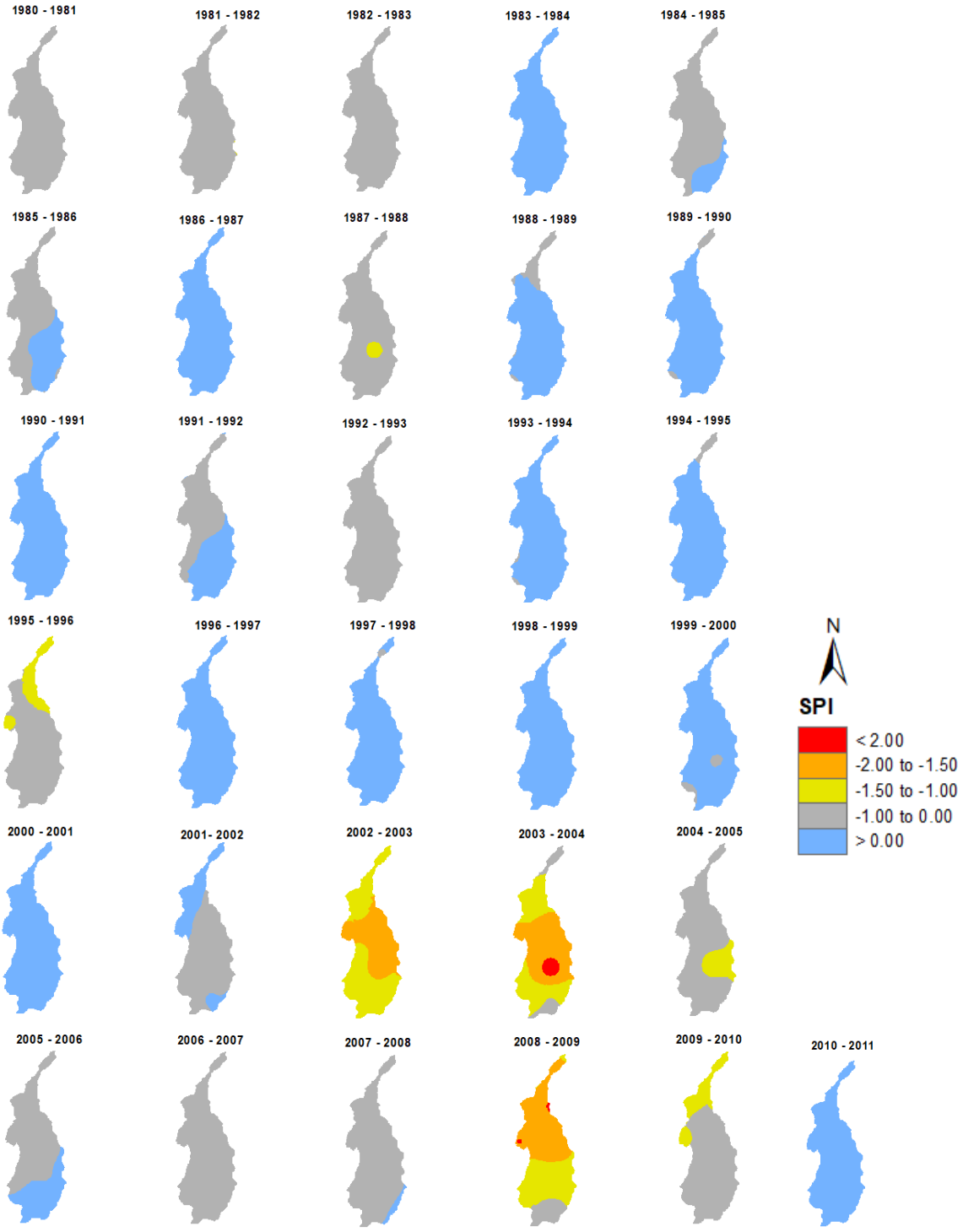


D 4: Estimated groundwater recharge of the 2013 static run (run 2) to show the temporal variation for only the places which increased the groundwater recharge estimation. The dark blue line is the median curve (50th percentile) and shows the media groundwater recharge value for each month. The green shadow area represents the interquartile range (IQR). Moreover, the light green shaded area represents the lowest and highest 5 % of each month's groundwater recharge values.

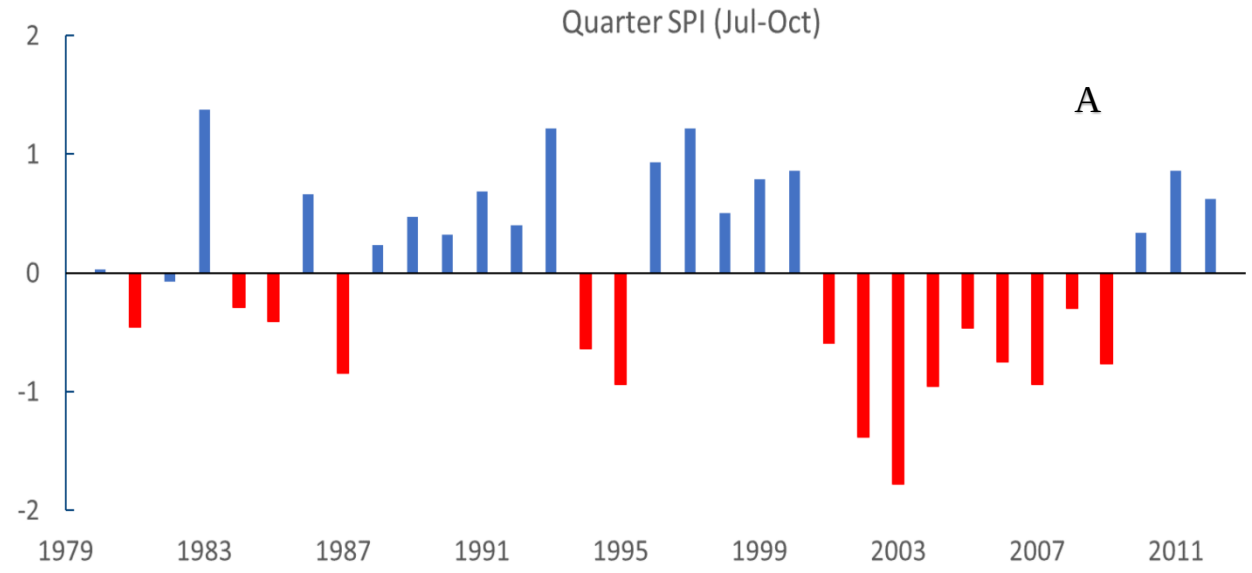


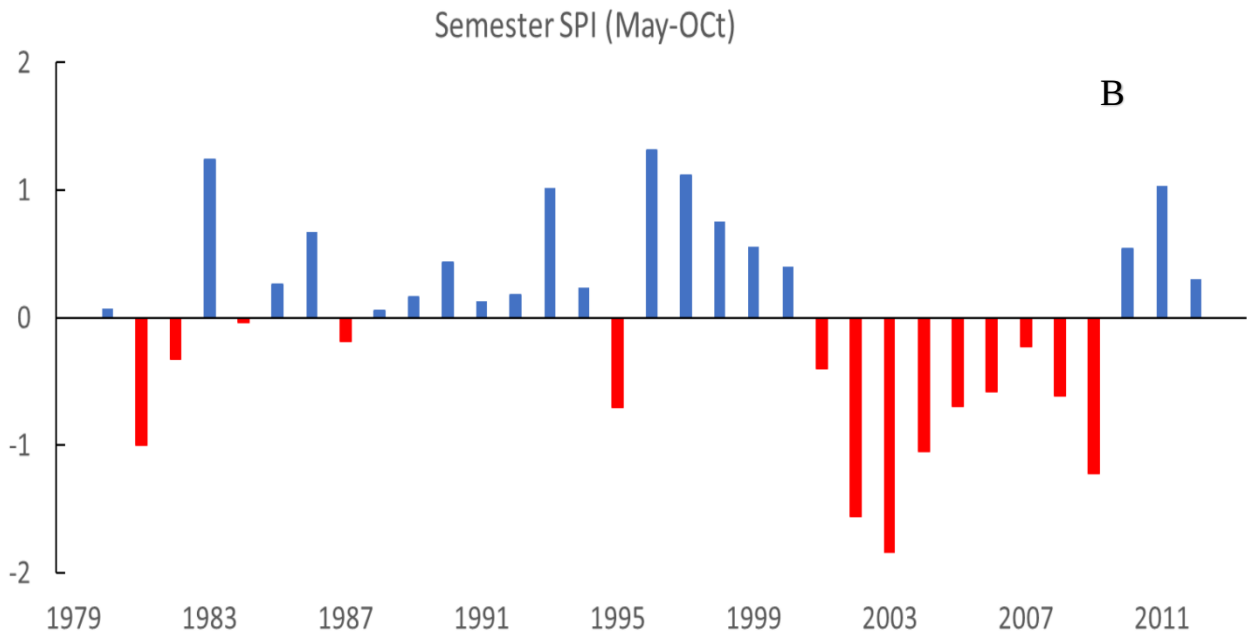
Appendix E: Meteorological drought and groundwater recharge threshold value for Bilate river catchment

E 1: Spatially distributed Meteorological drought severity for Bilate river catchment and parts based on SPI-12 (Annual) value for 31 hydrological year

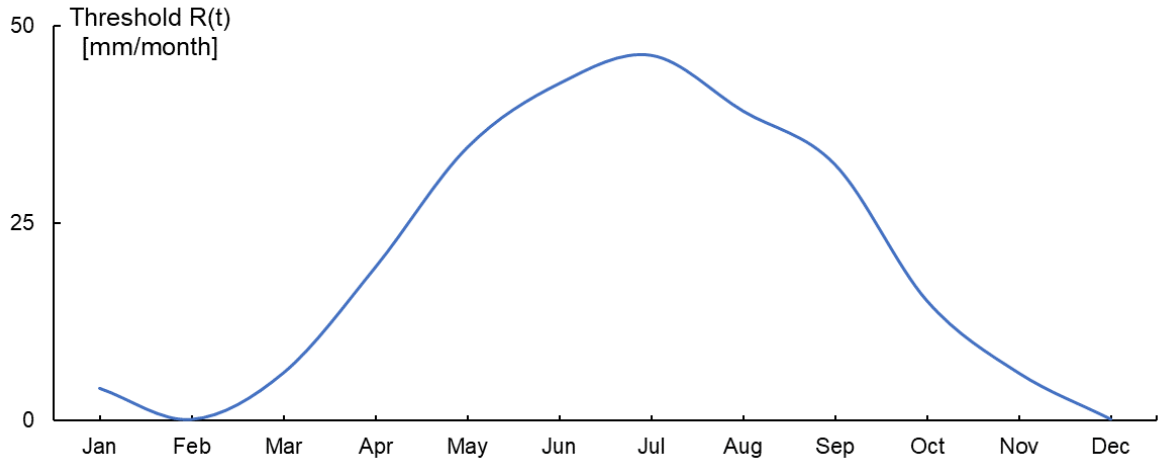


E 2: Meteorological drought severity for Bilate river catchment, based on (A) SPI-4 value and (B) SPI-6 value between the hydrological year of 1980 and 2013





E 3: Variable threshold value of groundwater recharge for Bilate river catchment. Each month's variable threshold level was determined as the 80th percentile of the probability of exceedance of monthly recharge in that month in the 34-year series (1980-2013).



List of publications during the PhD

International peer-reviewed academic journal

Wossenyeleh, B. K., Verbeiren, B., Diels J., and Huysmans, M.: Vadose zone lag time effect on groundwater drought in a temperate climate. Water 12, 2123, doi:10.3390/w12082123, 2020.

Wossenyeleh, B. K., Worku, K. A., Verbeiren, B., and Huysmans, M.: Drought propagation and its impact on groundwater hydrology of wetlands: a case study on the Doode Bemde nature reserve (Belgium), Nat. Hazards Earth Syst. Sci., 21, 39–51, doi:10.5194/nhess-21-39-2021, 2021.

Wossenyeleh, B. K., Verbeiren, B., and Huysmans, M.: Differentiating between land use and climate as influencing factors on groundwater recharge drought, temperate climate context, Journal of Hydrology regional studies, under review, 2021.

Wossenyeleh, B. K., Shuru, A. K., Verbeiren, B., and Huysmans, M.: Drought propagation in the hydrological cycle in a semi-arid region: a case study in the Bilate Catchment (Ethiopia), Hydrogeology Journal, under review, 2021.

Wossenyeleh, B. K., Verbeiren, B., and Huysmans, M.: Drought propagation in temperate climate regions: A case study on the Dijle river catchment and parts of the Demer and Zenne basins (Belgium), Hydrogeology journal, in preparation, 2021.

International Scientific conference

Wossenyeleh, B. K., Verbeiren, B., Diels J., and Huysmans, M.: Vadose zone lag time effect on groundwater drought propagation in a temperate climate. Geopysical reserch abstract, Vol. 21, EGU2019-5103, Vienna, Austria, 7-12 April 2019.

Wossenyeleh, B. K., Verbeiren, B., and Huysmans, M.: Analysis of groundwater drought propagation in temperate climates using a water balance model and groundwater model. 46th IAH Congress, Malaga, Spain, 22-27 September 2019.

Wossenyeleh, B. K., Verbeiren, B., and Huysmans, M.: Contribution of land use/land cover and climate factors on groundwater recharge estimation and groundwater drought in temperate context, 48th IAH Congress, Brussels, Belgium, 06 – 10 September 2021.

Wossenyeleh, B. K., Verbeiren, B., and Huysmans, M.: Groundwater drought propagation in the hydrological cycle and its impact on river discharge: a case study on Dijle river, Belgium. 48th IAH Congress, Brussels, Belgium, 06 – 10 September 2021.

Curriculum Vitae

Buruk WOSSENYELEH

Born in Wollo, Ethiopia

Research interest

Groundwater modelling, Hydro logical extremes, Vadose zone modelling, climate change and Anthropocene effect on drought

Education

KU Leuven — Leuven, Belgium
PhD in Science (Hydrogeology) — Oct 2016 – August 2021 (defense)
Thesis: *Groundwater drought* propagation and distribution in Temperate and Semi-arid climates
Supervisors: Prof. Dr. Ir. Marijke Huysmans, Prof. Dr. Boud Verbeiren

KU Leuven and VUB — Brussels, Belgium
MSc in Water Resources Engineering — Sep 2013 – Jul 2015
Thesis: Characterization and Modelling of Groundwater towards a Public Drinking Water Wellfield
Supervisors: Prof. Dr. Ir. Marijke Huysmans, Dr. Ir. Christian Anibas
Rank: Very Great Distinctions

Arba Minch University — Arba Minch, Ethiopia
BSc in Water Supply and Environmental Engineering — Sep 2006 – Jul 2010
Thesis: GIS application in water quality assessment of Ronne river, Sweden
Mentor: Dr. Hymanot T.
Rank: Very Great Distinctions

Experience

Teaching assistant and PhD researcher — KU Leuven, Belgium, Oct 2016 – Present

Researcher — VUB, Belgium, Oct 2020 – Apr 2021

Lecturer — Haramaya University, Ethiopia, Sep 2015 – Sep 2016

Graduate Lecturer — Haramaya University, Ethiopia, Sep 2010 – Sep 2013